ABSTRACT

Title of Dissertation: NUTRIENT MOVEMENT IN A VEGETATED COMPOST BLANKET AMENDING A VEGETATED FILTER STRIP ON A HIGHWAY SLOPE

Erica Rose Forgione
Doctor of Philosophy, 2022

Dissertation directed by:

Dr. Allen P. Davis
Professor, Department of Civil and Environmental Engineering

Dr. Ahmet Aydilek
Professor, Department of Civil and Environmental Engineering

Dr. Gary Felton
Associate Professor, Department of Environmental Science and Technology

Excess stormwater runoff caused by rapid urbanization and exacerbated by climate change generates many challenges for public safety and the environment. Large runoff volumes contribute to flooding and pollutants in stormwater runoff pose risks to human and environmental health, including toxicity to the aquatic environment caused by heavy metals and nutrient pollution leading to eutrophication, the cause of harmful algal blooms. An effort is being made to improve the efficiency of existing highway stormwater control systems which have limited performance in terms of volume reduction and pollutant removal. To address this issue, amendment of highway Vegetated Filter Strips (VFS) with a Vegetated Compost Blanket (VCB), a layer of seeded compost placed on an established

slope, has been proposed. Compost has high water holding capacity and organic matter content which can immobilize contaminants of concern. However, the high nutrient content of compost poses a threat to net beneficial performance since excess nutrient leaching occurs after application. This research has posed the question: Can a VCB be used as a stormwater control measure (SCM) while avoiding excessive nutrient leaching?

The VCB/VFS system was assessed through lab-scale, greenhouse-scale, and field-scale experiments. Hydrologic performance was evaluated in field and greenhouse experiments through evaluation of dynamic flow modification, event volume storage, and cumulative volume retention. Water quality performance was assessed through analysis of Total Suspended Solids (TSS), Nitrate + Nitrite (NOx), Total Kjeldahl Nitrogen (TKN), Total Nitrogen (TN), Total Phosphorus (TP), filtered and total Copper, and total Zinc concentrations. Nitrogen (N) and phosphorus (P) in compost are naturally transformed from organic to inorganic, soluble forms through the microbially-mediated process of mineralization. Nutrient removal occurs through adsorption as compost leachate passes through the VFS soil layer. To further investigate nutrient movement, small scale laboratory experiments were completed to determine the N and P compost mineralization rates and theoretical soil adsorption capacities. Nutrient data from greenhouse and field experiments were empirically evaluated using the lab-obtained mineralization data. Nutrient release was simulated and compared to experimental field data using a new open-source software, OpenHydroQual, which combines hydraulic and water quality modeling.

VCBs were found to have a significant impact on both flow and volume reduction, though at the highest flowrates, VCBs were unable to significantly reduce flow and instead acted as conveyance. A useful design estimate for representative storage capacity using the saturated moisture content and wilting point of both the VCB and VFS was determined. Significant TSS removal was observed in both the field and greenhouse studies and particulate metals were largely removed; however dissolved copper leaching was observed in the field experiment, as has been observed previously for some compost in stormwater systems. Highly elevated concentrations of nutrients (as high as 100 mg/L TN and 12 mg/L TP) were observed in the effluent of both field and greenhouse experiments, resulting in net nutrient leaching and concentrations above recommended EPA freshwater limits even after 1-2 years. Additionally, mass loading rates at the field site (as high as 41 kg/ac/yr for TN and 14 kg/ac/yr for TP) were 1-2 magnitudes higher than observed influent mass loading rates (~3.8 kg/ha/yr for TN and ~0.47 kg/ha/yr for TP).

Through laboratory mineralization studies, N and P mineralization rates were found to differ between compost batches, with initial nutrient content and age/leaching of compost being important factors. Adsorption experiments indicated increasing P adsorption from compost leachate with increasing soil Al+Fe content. Comparisons to greenhouse and field data showed differences in N speciation, likely due to differences in moisture content and temperature causing differing amounts of nitrification and volatilization. OpenHydroQual modeling showed modest results, with varying levels of accuracy for storm hydrograph simulation and mass release. VCBs are not currently recommended for use due to the risk of nutrient and metals pollution, especially in nutrient and metals sensitive watersheds. However, several impactful factors were identified that may reduce nutrient leaching, including compost composition, compost age/leaching, and VFS soil type.

NUTRIENT MOVEMENT IN A VEGETATED COMPOST BLANKET AMENDING A VEGETATED FILTER STRIP ON A HIGHWAY SLOPE

by

Erica Rose Forgione

Dissertation submitted to the Faculty of the Graduate School of the
University of Maryland, College Park, in partial fulfillment
of the requirements for the degree of
Doctor of Philosophy
2022

Advisory Committee:
Professor Allen P. Davis, Chair
Professor Ahmet Aydilek
Professor Gary Felton
Professor Alba Torrents
Associate Professor Birthe V. Kjellerup
Professor John D. Lea-Cox

© Copyright by
Erica Rose Forgione
2022

Dedication

This work would never have been finished without a stormcloud.

Acknowledgements

I would like to acknowledge the support of the National Cooperative Highway Research Program (NCHRP 14-39), the Maryland Department of Transportation State Highway Administration (MDOT SHA), and the Low Impact Development (LID) Center.

Additionally, I would like to acknowledge additional funding sources including the NRT-INFEWS: UMD Global STEWARDS (STEM Training at the Nexus of Energy, WAter Reuse and FooD Systems) that was awarded to the University of Maryland School of Public Health by the National Science Foundation National Research Traineeship Program, Grant number 1828910, as well as the University of Maryland Graduate School Dean's Fellowship and the University of Maryland Graduate School COVID Delay Fellowship.

Mesocosm and field equipment design and construction support was provided by the University of Maryland Environmental Science and Technology (ENST) Project Development Center, especially Gary Seibel and Les Lorenz. Greenhouse space and equipment were provided by the University of Maryland Research Greenhouse Complex through the College of Agriculture and Natural Resources (AGNR) and the Department of Plant Science and Landscape Architecture (PSLA), especially Sydney Wallace and Meghan Fisher Holbert. Special thanks are also extended to Stancill's Inc. (Perryville, MD) for providing engineered soils, especially Terry Stancill and Otis Harrison, and to the Montgomery County Yard Trim Composting Facility (Dickerson, MD), especially Lonnie Heflin, for providing Leafgro yard waste compost.

Table of Contents

Dedication ii
Acknowledgements iii
Table of Contents iv
List of Tables vii
List of Figures viii
List of Abbreviations x
CHAPTER 1: INTRODUCTION 1
Highway Stormwater Runoff 1
Stormwater Control Measures 3
Compost 4
Vegetated Compost Blankets (VCBs) 7
Research Goal 8
Research Objectives 9
CHAPTER 2: HYDROLOGIC PERFORMANCE OF VEGETATED COMPOST BLANKETS FOR HIGHWAY STORMWATER MANAGEMENT 11
Abstract 11
Introduction 13
Materials and Methods 15
Field Site Layout and Sampling 15
Greenhouse Experiments 19
Compost and Soil Testing 23
Vegetative Cover 24
Data Handling and Statistical Analysis 25
Results and Discussion 28
Observed Storm Event Characteristics 28
Flow and Volume Retention Over Time 29
Volume Reduction 39
Impact of Site and Design Characteristics 50
Media Properties and Vegetative Growth 55
Conclusions 59
Acknowledgements 62

CHAPTER 3: WATER QUALITY PERFORMANCE OF VEGETATED COMPOST BLANKETS FOR HIGHWAY STORMWATER MANAGEMENT 63
Abstract 63
Introduction 65
Materials and Methods 68
Field Site Description 68
Field Sampling 68
Greenhouse Experiments 69
Water Quality Methods and Data Analysis 71
Data Handling and Statistical Analysis 72
Results and Discussion 74
Water Quality Sampling Collection Characteristics 74
Runoff Characteristics 77
Total Suspended Solids (TSS) 89
Heavy Metals 94
Nutrients 103
Pollutant Loads 113
Impact of Design Variations 114
Conclusions 115
Acknowledgements 118
CHAPTER 4: NUTRIENT FATE AND TRANSPORT IN A VCB/VFS SYSTEM 119
Abstract 119
Introduction 121
Materials and Methods 124
Compost and Soil Composition 124
Compost Mineralization Experiment 124
Nutrients Adsorption Experiment 127
Analytical Methods 129
Biomass and Plant Tissue Nutrient Methods 130
OpenHydroQual Model Development 131
Data Handling and Statistics 135
Results and Discussion 136
Compost Mineralization 136
Soil Adsorption 146

Comparison to Large Scale Studies 154
Nutrient Mass Balance 161
OpenHydroQual Model 167
Conclusions 179
Acknowledgements 182
CHAPTER 5: CONCLUSIONS AND NEW RESEARCH QUESTIONS 183
Conclusions 183
New Research Questions 186
APPENDIX 187
REFERENCES 201

List of Tables

Table 2-1: Drainage Areas and Drainage Area Ratios for Field Sampling Locations..... 18
Table 2-2: Synthetic Storm Event Distributions Applied to Greenhouse Experiments..... 21
Table 2-3: Mesocosm Parameters for Greenhouse Experiments Study 1 and Study 2. 23
Table 2-4: Compost and Soil Analyses Conducted and Methods Used. 24
Table 2-5: Field Total Volumes and Storage over the Full Experiment..... 48
Table 2-6: Field Soil Hydraulic Properties and Statistics..... 56
Table 2-7: Comparison of Grass Cover Before and After Greenhouse Experiment. 57
Table 3-1: Chemical Composition of Synthetic Stormwater Used in Greenhouse Experiments. 70
Table 3-2: WSSC Laboratory Methods. 71
Table 3-3: Summary EMC Statistics for Field Experiments. 81
Table 3-4: Summary EMC Statistics for Greenhouse Experiments. 83
Table 3-5: Summary Mass Statistics for Field Experiments. 86
Table 3-6: Summary Mass Statistics for Greenhouse Experiments..... 88
Table 3-7: Compost Composition and Potential Effect on Experiment Results..... 94
Table 3-8: Mass Loads for Field Experiment Contaminants..... 114
Table 4-1: Field Site Biomass Sampling Collection Summary. 131
Table 4-2: Block Parameters for the OpenHydroQual System..... 133
Table 4-3: Compost Composition for Greenhouse and Field Experiments..... 138
Table 4-4: Field Experiment Soil Characteristics Before and After Compost Application. 147
Table 4-5: Greenhouse Experiment Soil Characteristics Before and After VCB Application... 149
Table 4-6: Biomass Plant Tissue Nutrient Content..... 161
Table 4-7: Field Site Nutrient Mass Balance..... 165
Table 5-1: Summary of Nitrogen Mineralization. 194
Table 5-2: Summary of Phosphorus Mineralization..... 195
Table 5-3: Summary of Nitrogen Release. 196
Table 5-4: Summary of Phosphorus Release..... 197

List of Figures

Figure 1-1: Composting Process Phases. 5
Figure 1-2: VCB/VFS System Considered in this Research. 8
Figure 2-1: Map of Field Site Location in Howard County, MD. 16
Figure 2-2: Field Site Vegetated Compost Blankets..... 17
Figure 2-3: Greenhouse Mesocosms and Flow Apparatuses. 22
Figure 2-4: Observational VCB for Vegetation Establishment Monitoring. 25
Figure 2-5: Observed Precipitation-Duration Distributions at Field Site. 29
Figure 2-6: Selection of Field Site Hydrographs. 32
Figure 2-7: Hydrographs from a High Intensity Multiple Peak Storm. 33
Figure 2-8: Peak Flows, Time-to-peak, and Flow Durations Observed at Field Site. 36
Figure 2-9: Flow-Duration Curves for All Flow Data Observed at Field Site. 38
Figure 2-10: Field Normalized Stormwater Discharge Volumes and Statistics. 41
Figure 2-11: Field Inflow Outflow Curves for 3-m and 6-m VCBs. 45
Figure 2-12: Field Storage Volumes and Statistics for 3-m and 6-m VCB Systems..... 49
Figure 2-13: Inflow-Outflow Curves for Greenhouse Experiments. 54
Figure 2-14: Rainfall Applied Until Vegetative Establishment for Field and Greenhouse. 58
Figure 3-1: Rainfall Occurrence and Water Quality Testing Totals. 75
Figure 3-2: Water Quality Event Rainfall-Duration Distribution Compared to Full Dataset..... 77
Figure 3-3: Comparison of Greenhouse and Field Stormwater Influent Concentrations. 79
Figure 3-4: Field and Greenhouse Exceedance Probability for TSS, Total Cu, and Total Zn. 93
Figure 3-5: Copper Partitioning for Influent and Effluent. 98
Figure 3-6: Copper Partitioning and Kd Values for Field Influent and Effluent. 99
Figure 3-7: Four Storm Events Resulting in VCB Effluent from Greenhouse. 101
Figure 3-8: Influential Processes Affecting TSS and Metals Movement in a VCB/VFS..... 102
Figure 3-9: Field and Greenhouse Exceedance Probability for TN and TP. 105
Figure 3-10: Timeseries of Nitrogen and Phosphorus EMCs in the Field and Greenhouse. 108
Figure 3-11: Field and Greenhouse Exceedance Probability for NO_x and TKN. 110
Figure 3-12: Influential Processes Affecting N and P Movement in a VCB/VFS. 112
Figure 4-1: Laboratory Compost Mineralization Experiment Columns and Flow Apparatus. .. 126
Figure 4-2: OpenHydroQual Model Structure for VCB/VFS System. 132
Figure 4-3: Total Nitrogen Release Curves and Best Fit Statistics. 142
Figure 4-4: Total Phosphorus Release Curves and Best Fit Statistics. 145
Figure 4-5: Phosphate Adsorption Isotherms and Langmuir Best Fit Statistics. 152
Figure 4-6: Results from Ammonium Adsorption Experiments..... 154
Figure 4-7: Comparison of Greenhouse and Mineralization Experiment Nutrient Release. 156
Figure 4-8: Laboratory and Field/Greenhouse N Speciation Comparison. 160
Figure 4-9: Field Biomass, Biomass Nitrogen, and Biomass Phosphorus. 163
Figure 4-10: Comparison of Observed Field and Modelled OpenHydroQual Hydrographs..... 169
Figure 4-11: : Comparison of Modelled and Observed Outflow for Field 3-m VCB. 170
Figure 4-12: Total Phosphorus Mass Movement as Predicted by OpenHydroQual. 172
Figure 4-13: Total Nitrogen Mass Movement as Predicted by OpenHydroQual. 174
Figure 4-14: Observed Storm Event Volumes and Mass Compared to Model Output. 176
Figure 4-15: Processes Affecting Nutrient Movement and Transport in a VCB/VFS. 178

Figure 5-1: Laboratory-Scale Sandy Topsoil Mix Description and Textural Parameters. 187
Figure 5-2: Laboratory-Scale Clayey Topsoil Mix Description and Textural Parameters. 188
Figure 5-3: Photos of the Four Mesocosms in Study 1. 189
Figure 5-4: Photos of the Four Mesocosms in Study 2 and Standard from Study 1. 190
Figure 5-5: Field Site Vegetated Compost Blankets After Establishment. 191
Figure 5-6: Nitrogen Mineralization Curves. 192
Figure 5-7: Phosphorus Mineralization Curves. 193
Figure 5-8: Field Site VCB Design Plan Page 1. 198
Figure 5-9: Field Site VCB Design Plan Page 2. 199
Figure 5-10: Field Site VCB Design Plan Page 3. 200

List of Abbreviations

Acronym	Definition
AASHTO	American Association of State Highway and Transportation Officials
BMP	Best Management Practice
CEC	Cation Exchange Capacity
CN	Curve Number
C:N	Carbon to Nitrogen
DA	Drainage Area
DOC	Dissolved Organic Carbon
DOM	Dissolved Organic Matter
DOT	Department of Transportation
EMC	Event Mean Concentration
LID	Low Impact Development
MDOT	Maryland Department of Transportation
NCHRP	National Cooperative Highway Research Program
NO_x	Nitrate + Nitrite (aqueous)
NOAA	National Oceanic and Atmospheric Administration
NPDES	National Pollutant Discharge Elimination System
NRCS	National Resources Conservation Service
OM	Organic Matter
QA/QC	Quality Assurance/Quality Control
RMSE	Root Mean Square Error
RPM	Rotations Per Minute
SCM	Stormwater Control Measure
SHA	State Highway Administration
STDEV	Standard Deviation
TKN	Total Kjeldahl Nitrogen
TMDL	Total Maximum Daily Load
TN	Total Nitrogen
TP	Total Phosphorus
TRB	Transportation Research Board
TSS	Total Suspended Solids
UMD	University of Maryland
USCC	United States Composting Council
USCS	Unified Soil Classification System
USDA	United States Department of Agriculture
USEPA	United States Environmental Protection Agency
VCB	Vegetated Compost Blanket
VFS	Vegetated Filter Strip
WSSC	Washington Suburban Sanitary Commission

CHAPTER 1: INTRODUCTION

Highway Stormwater Runoff

Rapid urbanization has resulted in worsening environmental and public safety issues due to the increased volumes of stormwater and its associated pollutant loadings (National Research Council 2009). This increased volume of stormwater runoff has had a profound effect on the size and frequency of floods (Konrad 2003), is a major contributor to stream channel erosion (Trimble 1997), and changes the natural hydrologic cycle of the surrounding environment (O'Driscoll et al. 2010). Low-income communities and communities of color are often the most vulnerable to these negative effects due to structural/historical inadequacies in critical infrastructure (Hendricks and Van Zandt 2021). Additionally, as climate change continues to worsen these impacts, rapid adaptation of stormwater infrastructure becomes even more critical (Cook et al. 2020; Moore et al. 2016).

While the hydrologic impact is a major concern, urban stormwater is also a major contributor of non-point source pollution. Stormwater runoff is a highly variable and complex matrix which picks up and carries urban pollution as it passes over impervious surfaces. Specific constituents and concentrations vary depending on spatial factors such as climactic region and land use as well as temporal factors such as season and storm size. Research on highway stormwater specifically has shown that runoff concentrations depend on the rainfall amount, storm intensity, antecedent dry period, drainage area, land use, and annual average daily traffic (Kayhanian et al. 2007; Lee et al. 2011). Because of this variability, input stormwater runoff concentrations from a highway may vary greatly among storm events and seasons. These large ranges in concentration are evidenced by a recent assessment of stormwater runoff characteristics

using thousands of data points from the National Stormwater Quality Database and the International Stormwater BMP Database (Pamuru et al. 2021).

One main category of contaminants of concern in stormwater is nutrients (nitrogen and phosphorus) which in large amounts pose a threat to local ecosystems (Carpenter et al. 1998). While nitrogen (N) and phosphorus (P) are necessary elements of life in small amounts, excess N and P in freshwater systems can cause eutrophication (Harper 2012), where overgrowth of plant-life, often algae, removes oxygen from the water, killing aquatic life. While P is often the limiting nutrient in freshwater systems, it has been shown that reducing concentrations of both N and P in water bodies may be vital to mitigating eutrophication (Conley et al. 2009). Additionally, heavy metals in urban stormwater runoff from vehicle wear and atmospheric deposition are a cause for ecological concern (Davis et al. 2001). Introduction of heavy metals to adjoining water bodies can result in toxicity to aquatic life through bioaccumulation (Zeitoun and Mehana 2014) and pose a risk to human health when consumed with aquatic life or through contact with runoff itself (Ma et al. 2016). Heavy metals are often affiliated with the particulate phase in stormwater runoff (Brown and Peake 2006; Djukić et al. 2016), but can undergo complex processes in the aquatic environment that may make them more mobile (Miranda et al. 2021). This particulate fraction can be defined in numerous ways, one of which is by considering particles that remain suspended in water, or Total Suspended Solids (TSS). TSS can originate from vehicle wear, but also pavement/asphalt wear, natural plant matter, and soils (Taylor and Owens 2009); it reduces aquatic water quality by blocking light and temperature changes, and can be a source of both heavy metals and nutrients (Bilotta and Brazier 2008).

Elevated stormwater contaminant concentrations are the focus of national efforts to reduce pollutant loadings from urban areas to the surrounding environment through the National

Pollutant Discharge Elimination System (NPDES) (US EPA 2015b). Managing stormwater from roadways and other impervious areas within Department of Transportation (DOT) jurisdictions is a growing challenge because many state and local jurisdictions are facing TMDL (Total Maximum Daily Load) requirements, where specific pollutant mass load reductions for a specific drainage area must be met. These increasingly stringent environmental regulations have driven many State Departments of Transportation (DOTs) to address these critical environmental issues in transportation infrastructure.

Stormwater Control Measures

Environmental issues resulting from urbanized areas have led to the development of green infrastructure systems (National Research Council 2009). Green infrastructure refers to an array of sustainable engineered alternatives to "gray" infrastructure, i.e., traditional stormwater systems often involving storm drains and pipes that route stormwater away from the location of rainfall impact. These green infrastructure alternatives are engineered systems designed to mimic the behavior of the natural environment by retaining and infiltrating stormwater runoff on or near-site and removing pollutants via various remediation mechanisms, effectively returning the water balance closer to a pre-urbanization state and preventing target pollutants from reaching adjoining water bodies. These systems are highly diverse, including practices such as wetlands, green roofs, rain gardens, swales, and other infiltration practices and are commonly referred to as stormwater control measures (SCMs) or best management practices (BMPs). In this dissertation, the term SCM will be used consistently to refer to green infrastructure systems. These systems have been shown to reduce stormwater volumes and improve water quality (Jaffe et al. 2010) and green infrastructure systems in general (not limited to stormwater systems) offer an array of

social benefits as well including aesthetic, public health, and climate benefits (Coutts and Hahn 2015; Foster et al. 2011). Implementation of green stormwater systems may also play a part in reducing inequity of societal impacts created by stormwater runoff (Hendricks 2017).

In order to address stormwater issues concerning highways, DOTs are focusing on ways to minimize highway stormwater impacts through improvement of existing SCMs such as Vegetated Filter Strips (VFSs) and swales, which have shown limited performance for water quantity and quality goals (TRB 2006).

Compost

In addition to stormwater management, state governments and DOTs increasingly look to achieve sustainability objectives in conjunction with ongoing improvements, including the use (and/or reuse) of recycled and repurposed materials. For this reason, composted materials from various sources in urban areas are being increasingly seen as a valuable, accessible resource that could be used in SCMs, and its use in DOT projects may open a pathway for compliance with sustainability commitments.

Compost is the product of a controlled aerobic process of biological decomposition in which raw organic materials are transformed into a stable, humus-like material (USCC 2001a). Composting consists of several microbially-mediated stages, including a mesophilic, thermophilic, secondary mesophilic, and maturation phase (Figure 1-1). During the thermophilic phase, high heat produced by bacteria kills pathogens, which acts to sanitize the compost, and during the maturation phase non-degradable compounds are formed, which stabilize the compost. Stabilized compost characteristic are determined by temperature and appearance; raw materials (feedstocks) are reduced in volume by 30%-70%, the original organic materials are no

longer recognizable, the compost no longer generates a significant amount of heat, and the material remaining has a dark crumbly appearance with an earthy odor (Diaz et al. 2007; Dunne 2013). Final maturation of compost is also determined by the oxygen uptake, germination efficiency, and C:N ratio. Each of these results are defined differently by each state, organization, county, or other governing body and there is no consistent specification that defines a compost that has reached maturity before application. Therefore, a finished compost will vary in composition and maturity by region, facility, and season but is primarily determined by the original source materials used.

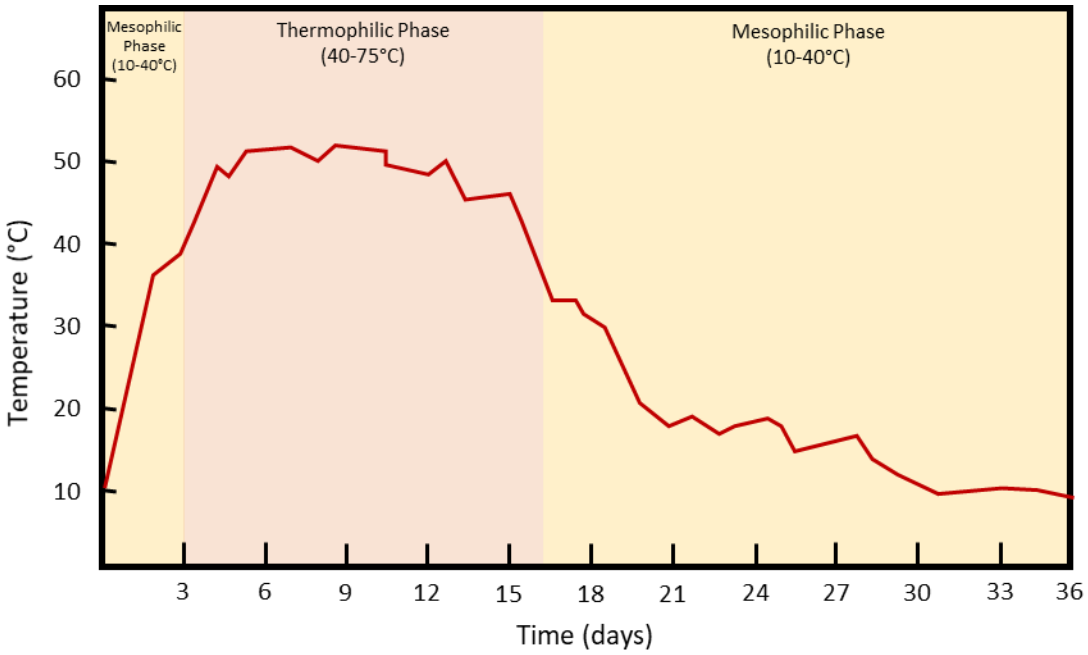


Figure 1-1: Composting Process Phases.
Compost goes through mesophilic, thermophilic, and secondary mesophilic temperature-induced phases. Maturation (also called curing) occurs after second mesophilic phase when compost has cooled (Adapted from Trautmann and Krasny 2014).

The raw materials used to produce compost are referred to as feedstocks, and can include a wide variety of organic waste materials, including agricultural by-products, yard trimmings

(yard waste/green waste), biosolids (sewage sludge) from municipal wastewater processing, food byproducts, industrial byproducts, and municipal solid waste (USCC 2001b). These feedstocks may have a wide range of sizes, chemical makeup, and nutrient availability. The diversity of feedstocks, as well as the variability of the composting process, contribute to a wide range of variability in compost materials. Each feedstock contains a unique blend of macronutrients: carbon, nitrogen, phosphorus, potassium, calcium, magnesium, and sulfur; and micronutrients: copper, zinc, iron, boron, and manganese (Diaz et al. 2007). The feedstock is broken down by bacteria, fungi, and other organisms during the composting process to create a humic material rich in nutrients. The combination of different feedstocks helps determine the quality of the final composted product; i.e., feedstocks high in nitrogen will lead to a final compost that likely has a large amount of nitrogen. Optimal composting occurs with a C:N ratio around 30:1 (Diaz et al. 2007; Rynk 1992); this provides enough available carbon for bacteria and fungi to metabolize the material. If the feedstocks have a ratio much higher than 30:1, organisms might immobilize the nitrogen (Diaz et al. 2007). Other essential elements that lead to quick and complete composting are oxygen, heat, and moisture, facilitated by active management (turning and watering) of compost piles.

A finished compost will impact the physical, chemical, and biological characteristics of the soil media to which it is applied. Compost is biologically active, and its benefits include supplying macro and micronutrients, adding beneficial microorganisms and organic matter, improving soil structure through increased porosity, increasing infiltration, reducing erosion and runoff, improving water holding capacity, stabilizing pH, suppressing plant pathogens, and binding and degrading pollutants (USCC 2001b). Many of these improvements coincide with

stormwater treatment goals, including improved infiltration, reducing erosion, and binding and degrading certain pollutants.

Vegetated Compost Blankets (VCBs)

As a recycled, sustainable material, compost is being considered for use in a Vegetated Compost Blanket (VCB), a layer of surface-applied compost that is placed on an existing hillside or embankment and then seeded. A diagram of a VCB overlaying a VFS as would be applied adjoining a highway is shown in Figure 1-2. Compost benefits include improvement of soil structure, increased infiltration, and increased water holding capacity which improves stormwater volume reduction while the organic matter supplied provides binding sites for certain pollutants (USCC 2001a). The main performance goals of a VCB are enhanced vegetative growth, erosion control, volume reduction, and water quality improvement. To keep costs to a minimum, application involves no major construction or site preparation; existing vegetated sloped areas are covered with a compost blanket and then seeded. Past research has shown that compost blankets can be used effectively as erosion control systems on steep slopes (AASHTO 2010; Bakr et al. 2012; Bhattarai et al. 2011; Faucette 2008; Faucette and Risse 2002; Faucette et al. 2007, 2009b; Fay et al. 2012; Mukhtar 2005); however, there is little research on compost blankets as SCMs.

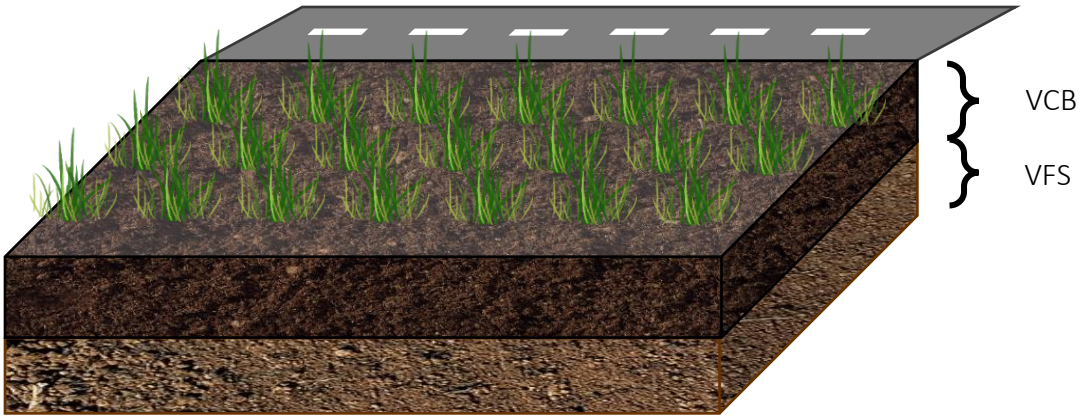


Figure 1-2: VCB/VFS System Considered in this Research.
Compost layer in the form of a Vegetated Compost Blanket (VCB) overlaying a topsoil layer in the form of a Vegetated Filter Strip (VFS).

While there is a potential for compost to absorb nutrients over time, one of the biggest challenges with compost treatments is that compost can release nitrogen and phosphorus in leachate (Ahmad et al. 2008; Brown et al. 2016; Butler and Coale 2005; Confesor Jr et al. 2009; Dietz 2007; Eghball 2003; Hurley et al. 2017; Iqbal et al. 2015; Li et al. 2011; Mullane et al. 2015; Reed et al. 2006; Storey et al. 2006). These recent studies have given reason for caution in recommending the use of compost as a material in SCMs, as there is a potential for negative effects on water quality, mostly from the loss of nutrients (both N and P), through leaching via surface runoff and infiltration.

Research Goal

VCBs are intended to be placed along highway medians, which in total stretch for 264,000 km (164,000 miles) across the United States as of 2014 (FHWA 2014). Because VCBs could be implemented on a large scale, it is imperative that VCBs are researched sufficiently before widespread implementation, especially given the potential issue of nutrient leaching. This

research will be important for use of VCBs in the future, given that there are limited current design guides, but also because future improper use or inefficient design of VCBs resulting in added pollutant loading rather than removal might be avoided.

The intent of this work is to assess the efficacy of using a VCB to improve the effectiveness of a vegetated filter strip (VFS) through stormwater volume reduction and water quality improvement and to quantify the potential impact of VCB compost leaching on receiving waters. Specifically, this work aims to understand and predict nutrient fate and transport through a connected VCB/VFS system on a highway median. This involves evaluation of nutrient release from the VCB and subsequent nutrient removal through the VFS layer and development of a model by which a range of designs can easily be evaluated for composts similar to those in this study (yard waste compost of similar C:N ratio). The ultimate objective is to determine optimal designs for minimization of excess nutrient leaching, and to provide a tool for future research on a VCB/VFS system.

Research Objectives

The objectives of this research project are:

1. To evaluate the hydrologic performance of a VCB/VFS system
    a. Through assessment of experimentally-obtained hydrographs
    b. Through assessment of experimentally-obtained hydrologic mass balance
2. To evaluate the water quality performance of a VCB/VFS system
    a. Through empirical assessment of nutrient fate and transport in a VCB/VFS system
    b. Through empirical assessment of TSS and heavy metals fate and transport in a VCB/VFS system
3. To evaluate nutrient fate and transport in a VCB/VFS system
    a. Through assessment of specific nutrient mechanisms in the compost layer (mineralization) and the soil layer (adsorption)

b. Through comparison of theoretical and empirical nutrient loss using pilot VCB/VFS nutrient data
c. Through computer simulation of nutrient movement through a VCB/VFS system

These objectives will be met by small-scale column studies to separate nutrient movement in the VCB layer from that in the VFS layer, a set of mesocosm boxes in the UMD greenhouse facility, and a field site on a highway median in Howard County, MD. This series of experiments of different scales is proposed to help isolate and understand nutrient movement through both the compost layer and the filter strip. Nutrient movement modeling will use the program OpenHydroQual.

The first experimental scale consists of mini column experiments (Experiment 1) to separate mineralization in the compost layer from adsorption in the filter strip layer. This will provide the mathematical foundation for the interaction of stormwater with a specific compost and the resulting leachate from that compost source with the soil. The second scale is mid-size mesocosm greenhouse experiments (Experiment 2), which includes connected compost and soil layers and vegetation. The results from Part 1 can be expanded to account for more complexity with the controlled greenhouse experiment data. The third scale is a full-scale field experiment (Experiment 3) which experiences seasonality and complex hydrologic conditions. This stage will necessitate the use of statistical methods to compare the results from the highly controlled experiments in Part 1 and 2 with the randomly sampled, highly variable data obtained in the field. By addressing the VCB/VFS system in stages, complexity can be added in parts rather than attempting to fully model a complex real-world system with many unknowns and unpredictable events.

CHAPTER 2: HYDROLOGIC PERFORMANCE OF VEGETATED COMPOST BLANKETS FOR HIGHWAY STORMWATER MANAGEMENT

Erica R. Forgione[1], Gary K. Felton[2], Ahmet H. Aydilek[3], and Allen P. Davis[4]

[1] Graduate Research Assistant, Dept. of Civil and Environmental Engineering, Univ. of Maryland, College Park, MD 20742.
[2] Associate Professor, Dept. of Environmental Science and Technology, Univ. of Maryland, College Park, MD 20742, USA.
[3] Professor, Dept. of Civil and Environmental Engineering, Univ. of Maryland, College Park, MD 20742, USA.
[4] Professor and Charles A. Irish, Sr. Chair in Civil Engineering, Dept. of Civil and Environmental Engineering, Univ. of Maryland, College Park, MD 20742, USA. (corresponding author). E-mail: apdavis@umd.edu

Abstract

Excess stormwater runoff caused by rapid urbanization and exacerbated by climate change generates a host of challenges to public safety and the environment. In an attempt to reduce the impact of stormwater runoff from highways, state Departments of Transportation (DOTs) are exploring ways to improve the existing Stormwater Control Measures (SCMs) adjacent to highways, Vegetated Filter Strips (VFSs) and swales, which have shown limited effectiveness for hydrologic and water quality improvement. Amending existing VFSs with a Vegetated Compost Blanket (VCB) has been proposed to help DOTs meet recent sustainability and stormwater permitting requirements. This study attempts to assess the hydrologic performance of a VCB as a new type of SCM through evaluation of dynamic flow modification, event volume storage, and cumulative performance over the full study period. Because VCBs are applied on top of existing VFSs, assessment considered both layers as a single composite system. Over 2.25 years, 278 rainfall events were observed at a highway median in Howard County, MD for two fully monitored field VCBs of 7.6-cm depth and 30-m width along the highway, one at 3-m length and one at 6-m length perpendicular to the highway.

VCBs were found to have a significant impact for both flow and volume reduction. Flowrates were lowered significantly by the VCBs in comparison to highway runoff, with peak flows reduced by 39% for the 3-m and 72% for the 6-m VCB, based on the median, but the longer flow path (6-m) consistently performed better than the 3-m for the full range of observed flowrates. At the highest flowrates, both VCBs were unable to significantly reduce flow, and instead acted as conveyance. A hockey-stick fit was found to be the most appropriate description of average volume retention performance for inflow-outflow curves, in which a representative storage capacity is reached after which the outflow volume is equal to the inflow volume. A useful design estimate for representative storage capacity using the saturated moisture content and wilting point of both the VCB and VFS was determined. When a rough estimate is needed, the curve number (CN) for a VCB overlaying a VFS was estimated to be 84. Total influent stormwater volume capture over the entire study period was found to be 44% and 55% for the 3-m and 6-m VCBs, respectively. Supplemental investigations in a greenhouse experiment indicated similar performance across a variety of changing site characteristics, but also indicated possible lower volume retention due to compost being applied above grade. Improvements in VFS soil hydraulic properties over the course of the experiment were also observed due to the addition of compost, indicating additional hydrologic improvement indirectly caused by addition of the VCB.

Introduction

Stormwater caused by rapid urbanization coupled with reliance on traditional "gray" stormwater infrastructure has become a major challenge to the resiliency and safety of urban areas (National Research Council 2009). The increase in impervious surfaces produces larger volumes of stormwater runoff that cause an array of environmental and public safety risks (Copeland 2016; Konrad 2003; O'Driscoll et al. 2010). Low-income communities and communities of color are often the most vulnerable to these risks due to structural/historical inadequacies in critical infrastructure (Hendricks and Van Zandt 2021). Additionally, as climate change continues to exacerbate these impacts, rapid adaptation of reliable stormwater infrastructure becomes even more critical (Cook et al. 2020; Moore et al. 2016). Green stormwater infrastructure systems, sustainable engineered alternatives to "gray" infrastructure, have become increasingly utilized in recent decades in an attempt to address the challenges presented by excess stormwater (National Research Council 2009), since they retain, infiltrate, and transpire stormwater on or near-site, effectively returning the water balance closer to a pre-urbanization state. These systems are often referred to as Stormwater Control Measures (SCMs).

In order to address highway stormwater challenges, state Departments of Transportation (DOTs) are finding ways to minimize highway stormwater impacts through improvement of existing SCMs such as Vegetated Filter Strips (VFSs) and swales (TRB 2006). Use of a Vegetated Compost Blanket (VCB) has been proposed as a sustainable, renewable amendment to the VFS systems currently used on highways, as this can help DOTs meet both stormwater and sustainability requirements. VCBs, loosely applied layers of compost placed directly over an existing VFS system, then seeded, have been used successfully as an erosion control method on steep slopes (AASHTO 2010; Bakr et al. 2012; Bhattarai et al. 2011; Faucette 2008; Faucette

and Risse 2002; Faucette et al. 2007, 2009a; Fay et al. 2012; Mukhtar 2005) , but have not yet been evaluated as SCMs. VFS systems have shown limited performance in volume retention when applied to highly compacted soils (Higgins et al. 2016), such as those on highway medians (Davis et al. 2012a). Compost is expected to increase infiltration and water holding capacity, improve soil structure, and increase vegetative growth (USCC 2001a) and, as a blanket evaluated for erosion control, compost has been shown to increase infiltration and reduce runoff volume (Bakr et al. 2012; Beighley et al. 2010; Caltrans 2012; Glanville et al. 2003; Persyn et al. 2004), and increase vegetative cover (Faucette and Risse 2002; Mukhtar et al. 2008; Persyn et al. 2007).

With the possibility of more widespread use of VCBs as stormwater control measures, there is a need to evaluate the hydraulic and hydrologic performance to quantify benefits as a highway SCM. The goal of this study is to evaluate the hydraulic performance of VCBs through assessment of hydrograph characteristics and flow distributions as well as hydrologic performance through assessment of volume storage and compost/soil characteristics. A field study on the median of a four-lane highway in Maryland (USA) was supplemented with a greenhouse mesocosm study and compost/soil characterizations studies to describe the observed hydrologic performance and develop design information.

Materials and Methods

Field Site Layout and Sampling

A large-scale field study was conducted on a median on the eastbound side of Maryland Route 32 in Howard County, MD near a junction with Interstate I-95 (39°08'39.4"N 76°49'12.7"W) (Figure 2-1). This site is the location of a previous VFS/grass swale stormwater study (Davis et al. 2012a; Stagge et al. 2012). Two VCBs were installed, both 7.6-cm (3-in) deep, 30.5-m (100-ft) along the highway, and directly adjacent to edge of pavement. One VCB was 3-m (10-ft) wide perpendicular to the highway and the other 6-m (20-ft) wide perpendicular to the highway, both receiving runoff as sheet flow from the eastbound two-lane highway. At the downstream end of each VCB, a 15-cm (6-in) half PVC pipe was installed to collect effluent flow. Installation was completed on February 27, 2019; yard waste compost was used for the VCB. Design of VCBs was completed by the Low Impact Development Center (LID) Inc. (Beltsville, MD) and installation by DBI Services (Harmans, MD). In compliance with Maryland Department of the Environment (MDE) regulations, a straw matting was placed over the VCB areas after installation and seeded with MDOT SHA approved turfgrass mix (MDOT SHA 705.03.03, (MDOT SHA 2020)). Influent highway runoff was monitored using a 30.5-m (100-ft) section of a preexisting concrete channel from the previous research study on highway swales (Davis et al. 2012a). The highway runoff channel and the two VCBs are shown in Figure 2-2.

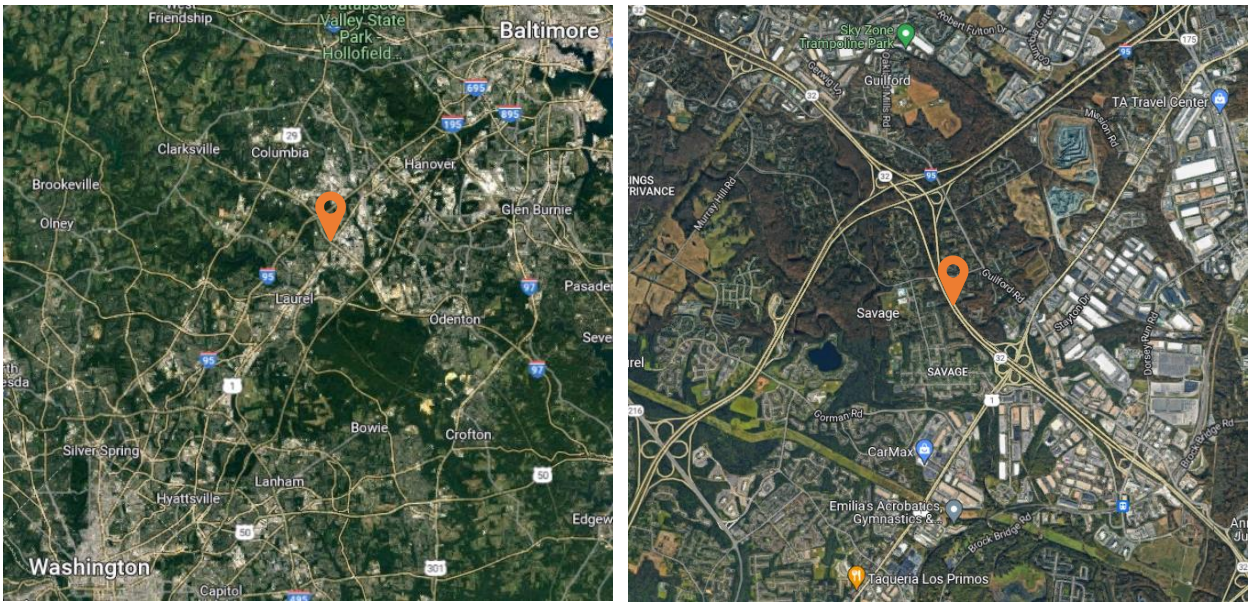


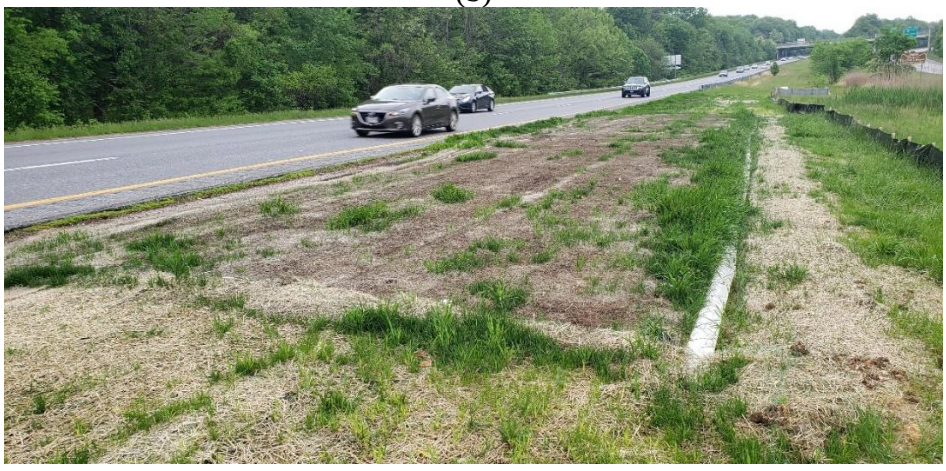
Figure 2-1: Map of Field Site Location in Howard County, MD.
Left: large map; right: zoomed in; balloon indicates the field site location, (39°08'39.4"N 76°49'12.7"W)



(a)



(b)



(c)

Figure 2-2: Field Site Vegetated Compost Blankets.
a) Highway Runoff Channel: 30.5-m (100-ft) along highway; b) 3-m VCB: 30.5-m (100-ft) along highway, 3-m (10-ft) perpendicular to highway; c) 6-m VCB: 30.5-m (100-ft) along highway, 6-m (20-ft) perpendicular to highway; images of VCBs taken on May 04, 2019, 66 days after installation

A pre-construction soil survey classified the VFS media as sandy topsoil (silty sand per USCS Classification, silty or clayey sand per AASHTO Classification) of varied depth (mean = 6.35-cm/2.5-in) overlaying a clay soil (sandy low plastic clay per USCS Classification, clayey soil per AASHTO Classification). The clay soil had a hydraulic conductivity of 2.5 x 10^{-6} cm/s, measured by constant head infiltrometer (van Es et al. 1999), which is within range of compacted clays (Coduto et al. 2011), likely due to compaction during the original construction of the highway. Because the effluent collection pipes were installed below grade into the compacted subsoil layer, VFS effluent flow was limited at the collection pipe, meaning that effluent flow can be considered as including both the VFS and VCB effluents. The acronym VCBS is used as shorthand for both of these layers hereafter.

Although each collection area collected runoff from 30.5-m (100-ft) along the highway, the drainage areas differed slightly. A summary of drainage areas and ratios for the highway runoff channel, as well as the 3-m (10-ft) and 6-m (20-ft) VCBs is shown in Table 2-1. Highway runoff drainage area was estimated using a rainfall-runoff relationship and 3- and 6-m VCB drainage areas were found using mapping estimations from construction specifications.

Table 2-1: Drainage Areas and Drainage Area Ratios for Field Sampling Locations.

	Highway Runoff	3-m VCB	6-m VCB
VCB Area m^2 (ft^2)	0	136 (1460)	251 (2700)
Highway Area m^2 (ft^2)	446 (4796)	338 (3640)	374 (4025)
Total Area m^2 (ft^2)		474 (5100)	625 (6725)
Highway Drainage Area Ratio		**2.49**	**1.49**
Total Area Ratio		**3.49**	**2.49**

The half 15-cm (6-in) PVC pipes on the downstream edge of each VCB for effluent collection were fed downward through manholes into subsurface pipes exiting at a concrete pad

for monitoring. For the highway runoff channel, a custom stainless steel sheet metal weir insert was installed with a 15-cm (6-in) PVC pipe to collect and measure flow. For all three systems, hydrologic data was collected using Teledyne ISCO 6712 autosamplers connected to 15-cm (6-in) Thelmar weirs in each effluent pipe. Two-minute rainfall data was collected using a Teledyne ISCO 674 rain gauge connected to the highway runoff autosampler at the site. Two-minute level data was collected by ISCO 730 bubbler flow meters connected to each effluent weir and converted to flowrate with the weir rating curve. In some instances, flowrates were observed that exceeded the Thelmar weir maximum, and data from a laboratory flume experiment were used to estimate over-limit values.

Greenhouse Experiments

Mesocosm boxes were made of an aluminum-reinforced sloped wooden base and lined with an inert (NSF-ANSI 61 certified drinking water safe) pond liner overlaid with an inert plastic window screen to disrupt preferential pathway formation. A porous plastic insert was attached to the downslope end of the box to prevent soil loss while allowing effluent to be collected. A 10-cm (4-in) layer of engineered topsoil (loamy sand per USDA Classification) was placed as the VFS layer following MDOT SHA specifications for furnished topsoil (MDOT SHA 920.01.02, (MDOT SHA 2020)). A turf grass mixture of 95% tall fescue and 5% Kentucky bluegrass (MDOT SHA 920.06.07, (MDOT SHA 2020)) was then applied according to MDOT SHA specifications (MDOT SHA 705.03.03, (MDOT SHA 2020)) at a rate of 224 kg/ha (200 lb/acre). Grasses were watered on a Mon/Wed/Fri schedule and allowed to establish for 2.5 months, emulating field conditions where a VCB would be applied to an already established VFS. After vegetation establishment, yard waste compost (Leafgro obtained from The Montgomery County

Yard Trim Composting Facility near Dickerson, Maryland) was placed on top of the VFS layer and again seeded according to MDOT SHA specifications.

Rainfall and runoff were both applied: for rainfall, a gentle flow watering can was used to apply deionized water over the top of the mesocosms at equal intervals over the course of the storm duration; for runoff, a synthetic stormwater was pumped to the top of the box as sheet flow at a constant flow rate. The rainfall depth and drainage area ratio dictated the rainfall and runoff volumes and resulting flowrates which were applied. For example, mesocosms with a 3:1 drainage area ratio experiencing a 2.5-cm (1-in) rainfall event received the equivalent volume of 2.5-cm (1-in) of deionized water over the mesocosm surface area applied at equal time intervals, plus the equivalent volume of 7.6-cm (3-in) of synthetic stormwater over three times the mesocosm surface area pumped to the top of the box to represent highway runoff. Synthetic stormwater was prepared in a 600-L polypropylene tank and pumped to the top of each mesocosm box using a Masterflex L/S Precision Variable-Speed Drive fitted with two Masterflex L/S Easy-Load® II 2-Channel Pump Heads. Large storm events necessitated use of a Masterflex I/P Variable Speed Console Drive fitted with a Masterflex I/P Easy-Load® Pump Head. Applied storm event size and duration for each study is shown in Table 2-2. Mesocosms tested with each study are outlined in Table 2-3.

Table 2-2: Synthetic Storm Event Distributions Applied to Greenhouse Experiments.

Study 1

Rain (mm)	Duration (hr)	Intensity (mm/hr)	Date
Compost Applied			12/18/2018
12.7	6.00	2.1	12/19/2018*
12.7	1.00	12.7	01/02/2019*
25.4	1.00	25.4	01/09/2019*
12.7	1.00	12.7	02/19/2019
25.4	3.00	8.47	03/13/2019
25.4	6.00	4.23	04/17/2019
12.7	0.50	25.4	06/07/2019
12.7	6.00	2.12	07/10/2019
25.4	6.00	4.23	07/25/2019
50.8	1.00	50.8	09/04/2019
25.4	0.25	101.6	10/10/2019
38.1	0.25	152.4	03/03/2020

Study 2

Rain (mm)	Duration (hr)	Intensity (mm/hr)	Date
Compost Applied			10/15/2020
12.7	6.00	2.12	10/19/2020
25.4	0.25	101.6	11/10/2020
25.4	1.00	25.4	12/14/2020
25.4	6.00	4.23	01/21/2021
12.7	1.00	12.7	02/23/2021
50.8	1.00	50.8	04/19/2021
25.4	4.00	6.35	07/15/2021

** Not tested for water quality.*

[1] Mesocosm with 2x drainage area was tested in Study 2 and received twice the runoff.

[2] Topsoil layer vegetative establishment occurred over 2.5 months prior to compost application.

A custom inflow apparatus was built to evenly distribute synthetic stormwater to the top of the box from the pump tubing. In order to separate effluent exiting the VFS layer and VCB layer, a custom outflow apparatus was installed to collect effluent from the VCB layer alone. Separate plastic containers were used to collect outflow from each layer so that the total volume for each could be measured. Mesocosm boxes and flow apparatuses are shown in Figure 2-3.

Several operational parameters were tested in the greenhouse, including a range of compost depths, VFS topsoil types, slopes, and drainage area ratios. A summary of the tested mesocosms and variables is shown in Table 2-3.



Figure 2-3: Greenhouse Mesocosms and Flow Apparatuses.
top left: mesocosm boxes prepared for a storm event; top right: pump system with influent apparatuses; bottom right: influent synthetic stormwater sheet flow distributor apparatus during a storm event; bottom left: outflow runoff collection apparatuses.

Table 2-3: Mesocosm Parameters for Greenhouse Experiments Study 1 and Study 2.

Mesocosm	Study	Slope	Compost Depth	Drainage Area Ratio	Topsoil Texture
Mesocosm A (Standard)	*1*	*5:1*	*3″*	*3:1*	*loamy sand (USDA)*
Mesocosm A-2 (Standard)	*2*	*5:1*	*3″*	*3:1*	*loamy sand (USDA)*
Mesocosm B	1	5:1	1″	3:1	*loamy sand (USDA)*
Mesocosm D	2	5:1	3″	6:1	*loamy sand (USDA)*
Mesocosm E	1	8:1	3″	3:1	*loamy sand (USDA)*
Mesocosm F	2	3:1	3″	3:1	*loamy sand (USDA)*
Mesocosm G	2	2:1	3″	3:1	*loamy sand (USDA)*

Compost and Soil Testing

A pre-installation field soil survey was conducted in summer of 2018 and a post-installation survey was conducted in summer 2021 to evaluate changes in media over the period of study. Parameters and the methods used are shown in Table 2-4. Particle size distribution and plasticity were measured for field topsoil and subsoil to determine soil classification. Laboratory tests of bulk density, moisture content, and saturated moisture content were performed for soils and compost to evaluate changes in soil physical properties. Infiltration tests were conducted in the field to determine time to ponding and saturated hydraulic conductivity but were limited by the underlying compacted subsoil layer. These tests were augmented with constant head permeameter tests for saturated hydraulic conductivity in the laboratory for soils and compost.

Table 2-4: Compost and Soil Analyses Conducted and Methods Used.

Soil Analysis	Method (Source)	Field Pre	Field Post
Particle size distribution	Sieve analysis (ASTM D6913 / D6913M – 17)	✓	*
Plasticity	Atterberg limits (ASTM D4318 - 17e1)	✓	*
Bulk density	Soil core method (ASTM F3013 - 13(2018))	✓	✓
Moisture content	Oven drying method (ASTM D2216 – 19)	✓	✓
Saturated moisture content	Vacuum saturation via weighable pressure cell (Klute 1965)	✓	✓
Time to ponding (field)	Miniature rain simulator (Ogden et al. 1997)	✓	✓
Saturated hydraulic conductivity (field)	Constant head infiltrometer (van Es et al. 1999)	✓	✓
Saturated hydraulic conductivity (laboratory)	Constant head permeameter (ASTM D5856 – 15)	✓	✓

**Not expected to change significantly over the course of the experiment, so not tested post-experiment.*
1 Particle size distribution and plasticity were only tested for soils for classification.

Vegetative Cover

At the field site, in addition to the fully monitored VCBs, a third observational VCB (Figure 2-4) was installed for monitoring of vegetative growth, with compost depths of 2.54-cm (1-in), 5.08-cm (2-in), and 7.62-cm (3-in). Brinno TLC Time Lapse cameras (http://www.brinno.com/) were installed and programmed to capture one image per day, with data downloaded during site visits. In the greenhouse, images of mesocosms were taken weekly using a Nikon D7100 HDSLR and processed using an image analysis code written in Matlab (2018b) (Owen et al. 2020). The program operates through two steps: first, manual cropping of images by the user to find the area of interest, and second, machine learning processes which determine the number of pixels belonging to each category: grass, straw, and soil. This is done through evaluations of color, texture, and oriented gradient. Any uncategorized pixels are considered unknowns and any images producing greater than 5% unknowns were not used in analyses.



Figure 2-4: Observational VCB for Vegetation Establishment Monitoring. Observational VCB is divided into three sections outlined by flags: furthest section is 10-cm (4-in)), middle section is 5-cm (2-in), and closest section is 2.5-cm (1-in).

Data Handling and Statistical Analysis

For field site data, the open-source programming software R was used to clean rainfall and flow datasets and conduct QA/QC. Observed field flowrates below the level of detection (0.009 m^3/hr) were excluded from analysis and any values above the maximum of 16 m^3/h were set as the maximum. During QA/QC any storm events identified to exhibit evidence of equipment malfunction (ex. missing data due to batteries dying) were excluded from the analysis. A code was created to separate datasets into individual storm events (defined by a 6-hr break in rainfall) and calculate total storm event volumes for influent and effluent. Total volumes were found through taking the area under the curve for each hydrograph (multiplying the 2-min duration by flowrate at each timestep and summing per storm. The total volume (V) is calculated as:

Equation 2-1

$$V = \int_0^{T_d} Q\ dt$$

where Q is the measured stormwater flowrate at each two-min interval and T_d is the event duration.

Influent volumes for the two field VCBs were not directly measured and were estimated by multiplying the rainfall depth with drainage area. This was found to be an acceptable method based on validation of estimations of drainage area based on lane widths. For the section of 2-lane highway draining to the VCBs width is estimated at 11-m (3.7-m per lane, 3.4-m shoulder, 0.3-m edge), which for a 30-m length results in a 334-m^2 drainage area and is within 1-12% of the 338-m^2 and 374-m^2 highway areas estimated through mapping (Table 2-1). For the highway runoff channel collection area, this section of highway expands to an extra lane (3 total) for an on-ramp, with width estimated at 15-m (3.7-m per lane, 3.4-m shoulder, 0.3-m edge), resulting in a 446-m^2 highway drainage area. Adding ~19-m^2 for the channel itself results in 465-m^2 drainage area, similar (within 4%) to the 446-m^2 estimated by the rainfall-runoff relationship for the highway runoff channel. Storm events for which calculated outflow exceeded estimated inflow (4.6% of 3-m VCB storms and 2.0% of 6-m VCB storms), storage was assumed to be 0 and outflow was set equal to inflow. Storage volume for each storm event was calculated by subtracting the total effluent volume from the total estimated influent volume.

Peak flow, time-to-peak, and flow duration were collected from individual storm hydrographs. Peak flow was considered as the highest flowrate observed at a two-minute interval for each site location over the duration of each storm event. Time-to-peak was calculated as the time from the start of rainfall until the peak flow rate. Flow duration was considered as the time

that flow began to the time that flow ended in each collection area. For a better comparison of VCB performance, peak flows were normalized by drainage area to the highway runoff by multiplying them by the ratio of highway runoff drainage area to VCB drainage area.

Flow-duration curves were created by ranking all measurable 2-min interval flow data for the study period (normalized by drainage area) in descending order and plotting against the cumulative duration (sequentially summing 2 minutes for every data point), allowing for comparison of the range of flowrates experienced by each treatment and the length of time they were observed to occur.

Exceedance probability plots for comparisons of flow and volume data were created by ranking data in descending order, with probability of exceedance for each datapoint calculated as:

Equation 2-2

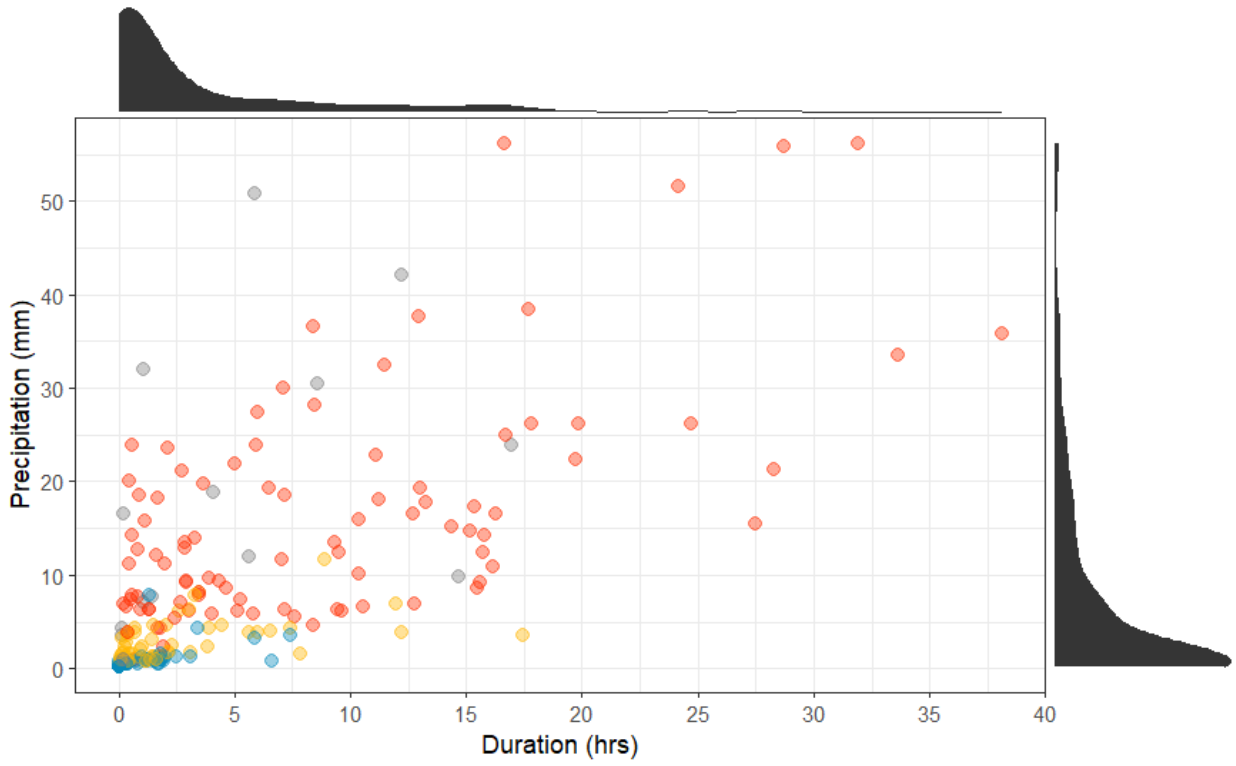
$$p = \frac{i - \alpha}{(n + 1 - 2\alpha)}$$

where i is rank and n is the total number of observations, with a value of 3/8 used for alpha for a normal distribution, as has been used previously (Davis 2007). Student's t-test was used to make statistical comparisons based on mean and evaluated at a 5% significance level, although values of p are also given.

Results and Discussion

Observed Storm Event Characteristics

Between April 2019 and June 2021, 278 rainfall events were observed. Observed rainfall depth and duration are plotted in Figure 2-5 and separated based on volume capture categories; precipitation and duration distributions are plotted on the edges of the plot as well for comparison. Rainfall depth over this period ranged from 0.25-mm (0.01-in) to 56-mm (2.21-in) with a median depth of 1.78-mm (0.07-in) and a mean of 7.23-mm (0.28 in). Rainfall durations ranged from 0.03-hr to 38-hr with a median of 1.1-hr and mean of 4.0-hr. 109 events had so little rainfall (most of these ~0.25- mm (0.010-in) and ~2-min) that no measurable highway runoff was observed. This totals 39% of rainfall events, which is comparable to the 30% of rainfall events with depth between 0.254-2.54 mm (0.01-0.1 inches) and duration of 0-1 hour as previously reported for Maryland (Kreeb 2003). An additional 22% of events were large enough to produce highway runoff but were completely absorbed by both VCBs, totaling 61% of events producing no effluent flow. Rainfall events which exceeded ~10-mm depth and ~15-hr duration consistently produced VCB effluent, with only two storms just outside this range being fully captured. 33% of rainfall events produced runoff, exceeding the volumetric storage capacity of the VCBs, resulting in some amount of discharge volume. The 61% of fully captured storm events only comprised a total of 11% of total rainfall depth, with storms exceeding the storage capacity totaling 75%. While capture of the smallest storms is still significant, emphasis on performance during larger rainfall events is considered to be much more important to evaluating the VCB system performance.



Precipitation Event Type	# of Events	Event %	Rain (mm)	Rain %
all storms	278		2010	
storms not resulting in highway runoff	109	39%	62	3%
storms resulting in highway runoff but not VCB effluent	61	22%	161	8%
storms resulting in VCB/VFS effluent	93	33%	1526	75%
unknown due to missing effluent data	15	5.4%	261	13%

Figure 2-5: Observed Precipitation-Duration Distributions at Field Site. Top) precipitation and duration correlation in center with individual frequency distributions shown on plot margins; Bottom) top plot legend and event statistics, colors shown in precipitation event type align with dataset in the top plot.

Flow and Volume Retention Over Time

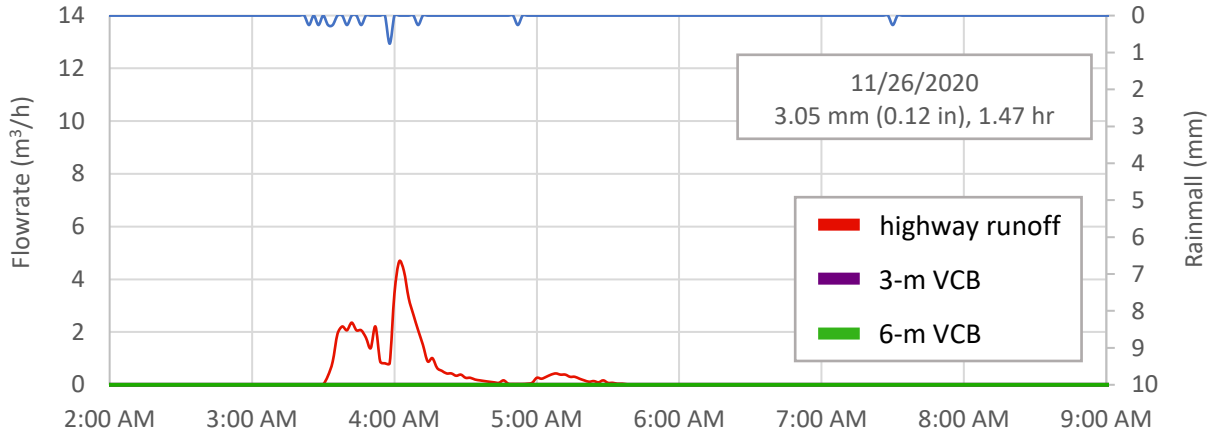
In the VCB systems, flow reduction and volume retention are expected to occur primarily through slowing of flow through the addition of roughness offered by the compost and vegetation as well as pore water storage. As stormwater enters the system as direct rainfall and

highway runoff, available storage (dependent on the antecedent moisture condition) should be filled to some extent in both the VCB and VFS layers. Infiltration below these layers should be insignificant during the period of the storm event, given the compacted subsoil beneath. The retention of stormwater volume is also expected to be dependent on the antecedent moisture condition, rainfall intensity, and duration, as well as seasonality.

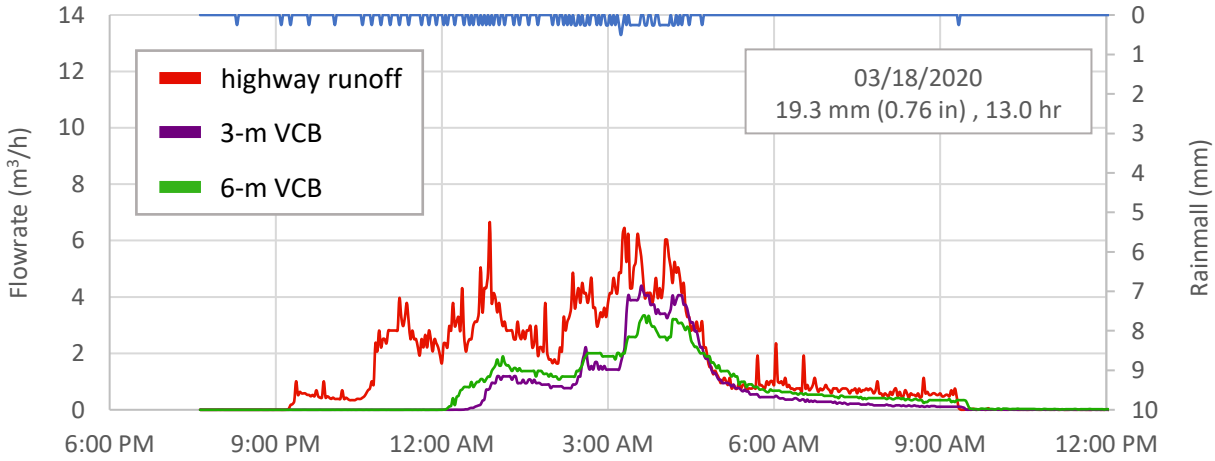
The dynamic performance of VCB treatments over the course of a storm event was compared through a select set of hydrographs (Figure 2-6). For a small storm event (Figure 2-6a) (3.05-mm (0.12-in) 1.47 hr), all incoming volume is totally stored, resulting in no effluent flow from either VCB system. During larger storm events (Figure 2-6b and c), storage in the system starts to fill, until some effluent flow begins. At this stage while effluent is being released, the flashiness seen in the highway runoff hydrograph is considerably smoothed in the effluent hydrographs, and effluent flows are still lower than influent, indicating some additional storage during conveyance. In Figure 2-6b, a 19.3-mm (0.76-in) 13.0 hr storm, the VCB systems were able to dampen peaks and retain stormwater volume through the full storm event. Additionally, while peak flows for the 6-m VCB are lower than for the 3-m VCB at the highest intensity interval of the storm, they are similar for the rest of the event. This indicates that the majority of storage was filled during the first part of the storm event, resulting in little difference between treatments later in the storm when conveyance became dominant.

In comparison, a large storm event is shown in Figure 2-6c at 55.8-mm (2.20-in) and 28.7 hr. During this storm event, similar flowrate reductions and volume retention were observed through most of the storm event, however, during the highest intensity rainfall (~8:00 AM) the hydrographs for highway runoff and both VCB systems are almost indistinguishable. At this point, it appears that the available VCB storage has been exceeded and the flowrates are no

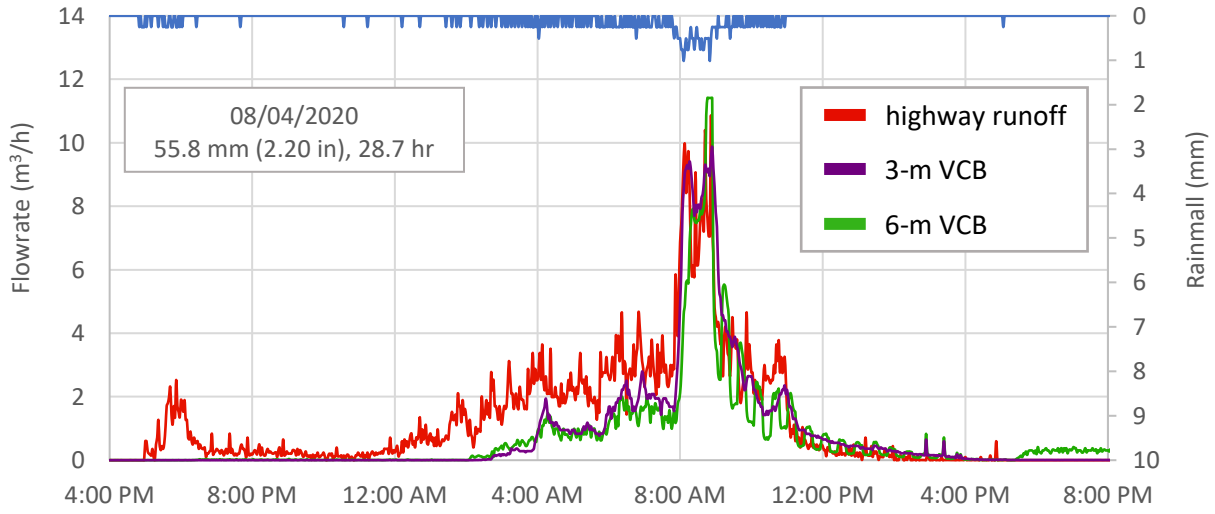
longer reduced through the treatments. Thorough assessment shows that the 6-m system was able to attenuate the first peak at 8:00AM but not the one approximately an hour later, while the 3-m was unable to mitigate either peak. Similar to Figure 2-6b, while some of the higher peaks are reduced by treatments after the high intensity period, significant volume retention no longer occurs. For all three storm events, retention at the start of the storm events shows that some storage was available in the system, while other hydrographs observed during the study period showed little to no volume retention, indicating a high antecedent moisture condition, and therefore very little available storage.



(a)



(b)



(c)

Figure 2-6: Selection of Field Site Hydrographs.
(A) small storm event, (B) moderate storm event, and (C) large storm event.

It is important to note that storms with high intensity peaks resulted in different behavior than storms with consistent, long periods of precipitation. An example is shown in Figure 2-7. At the start of the event, a large pulse of rain results in the first large flow peak for the highway runoff, which is largely reduced by the 6-m VCB but not the 3-m. Subsequent high intensity peaks show that the highest runoff peaks (generally above 10 m^3/h) are not greatly mitigated by the 3-m system, while the 6-m system was able to dampen all peaks a significant amount. This demonstrates a better performance of the 6-m system during high intensity rainfall events. However, the 3-m system does not appear to have filled all storage space during the highest pulses since later peaks at or below 10 m^3/h are also reduced significantly by the 3-m system, indicating volume retention. Instead, this suggests that conveyance could be forced during high intensity pulses (for example, as surface flow over the VCB) which bypasses storage in the VCB/VFS. While some storage still occurs later in the 3-m system, this gives credit to longer flow paths as better protection against high intensity storm events.

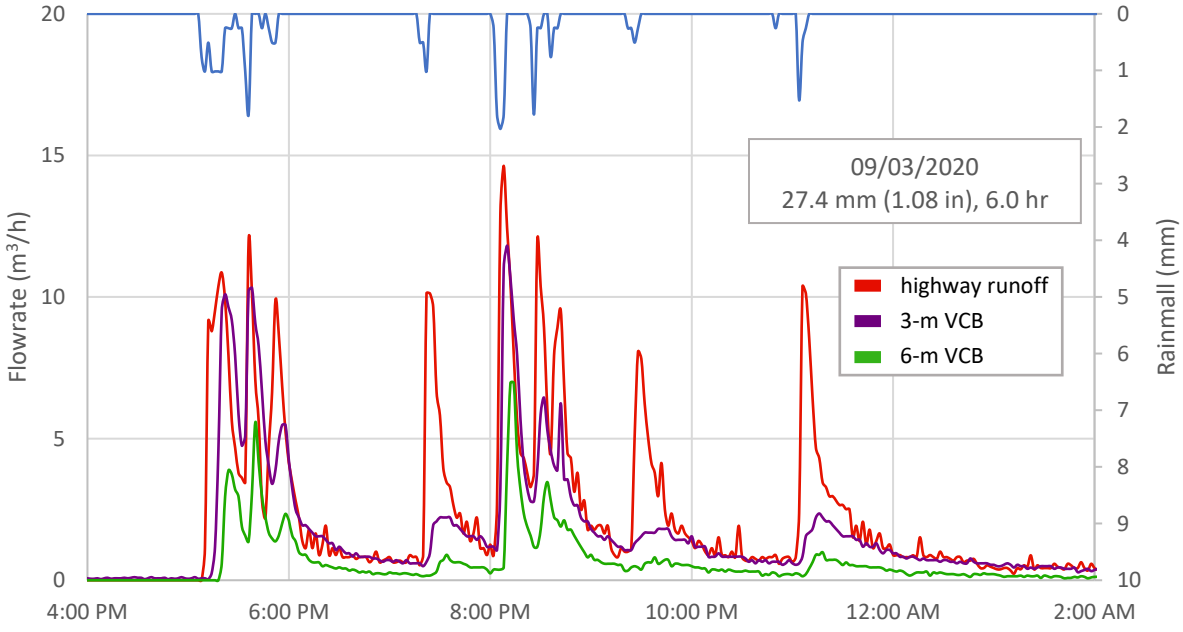
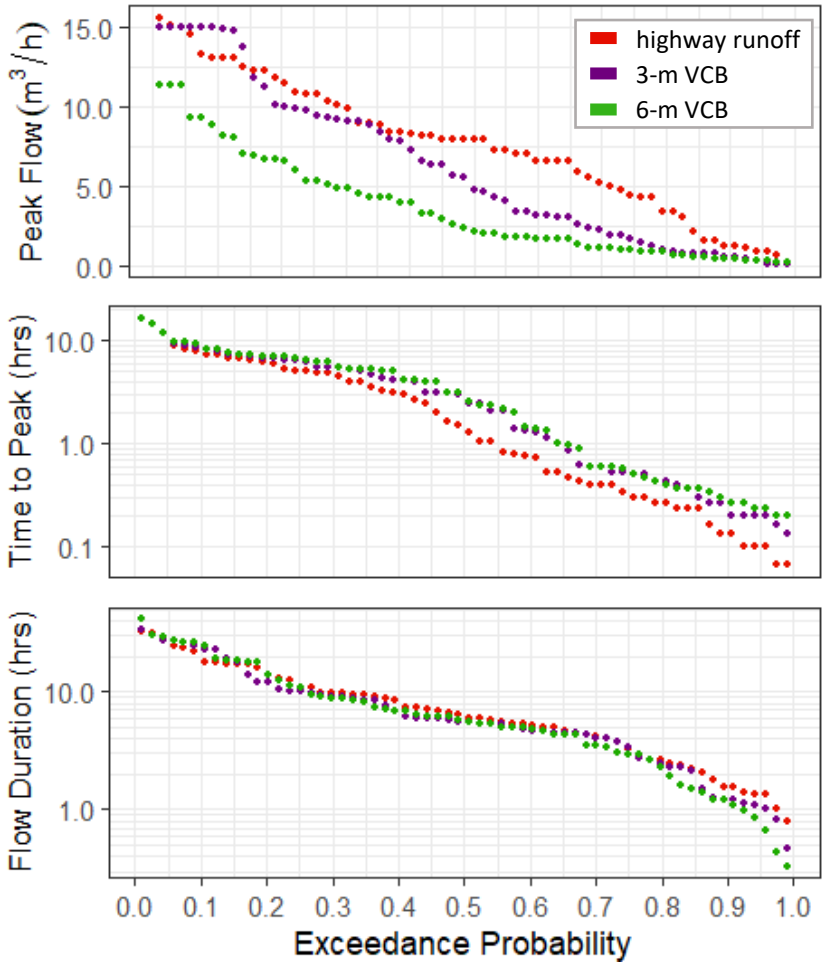


Figure 2-7: Hydrographs from a High Intensity Multiple Peak Storm.

Peak flows, time-to-peak, and flow duration were compared for those storm events where hydrographs were collected at all three sites (this biases towards larger storm events, median = 12.6 mm (0.50 in)). Normalized peak flows were greatly reduced by VCBs based on the median by 39% for the 3-m VCB, which is similar to the 43% peak runoff rate reduction previously found for a 3.75-cm depth, 4.8-m long compost blanket (Faucette et al. 2007), and 72% for the 6-m VCB (Figure 0-7). Both systems reduced high probability flowrates (>50% exceedance), while the 6-m system greatly reduced peak flows over the full probability range. At higher peak flows, 3-m discharges exceed highway runoff flows, which may be attributable to inconsistencies in estimation of drainage areas used in normalizing datasets and/or unaccounted influent volume. Similar difficulty in accurately estimating the real contributing areas was previously experienced at the same location on an earlier research project (Davis et al. 2012a). At the highest peak flows, datapoints for the 3- and 6-m VCBs plateau at the maximum measurable flowrate (15 and 11.4 m3/h for the normalized 3- and 6-m systems, respectively), making it possible that higher flowrates may have occurred, and eliminating ability to make conclusions about system performance at the largest flowrates.

Time-to-peak was nearly doubled for VCB systems based on the median, increasing by 94% and 97% for the 3- and 6-m systems, respectively (Figure 0-7). As expected, for longer peak delays the same level of benefit is not observed, as the systems reach saturation during long storm events (~5-hrs peak delay and longer) any additional attenuation is minimized, and surface flow may also potentially occur. Flow duration, measured as the time from start of flow to the end of flow for each site, shows little difference between treatments. Although SCMs are generally expected to prolong event duration, median durations for the 3-m and the 6-m VCB instead decreased by 10% and 9% compared to the highway runoff (Figure 0-7). Because the

systems do not experience significant infiltration, they perform mainly as storage at the beginning of the storm event until reaching saturation, after which they mainly function as a conveyance. The most significant delay in flow occurs immediately after rainfall, with little delay in flow occurring late in the rainfall event to the end as observed in Figure 2-6. Because of this, flow duration was not significantly extended, but rather a small decrease was found for both systems.



m^3/h	Runoff	3-m	6-m
geomean	5.84	3.57	2.25
mean	7.58	6.16	3.59
median	7.94	4.82	2.23
stdev	4.17	4.97	4.43
n	61	61	61

hr	Runoff	3-m	6-m
geomean	1.24	1.83	1.99
mean	3.11	3.71	3.92
median	1.42	2.75	2.80
stdev	3.65	3.71	3.79
n	60	60	60

hr	Runoff	3-m	6-m
geomean	6.12	5.58	5.34
mean	8.85	8.57	8.84
median	6.12	5.48	5.57
stdev	7.66	8.16	8.89
n	62	62	62

Figure 2-8: Peak Flows, Time-to-peak, and Flow Durations Observed at Field Site. Peak Flow (m3/h) is normalized to highway runoff drainage area

Evaluation of hydraulic performance over the full study period can be done through a flow-duration curve, which was also normalized by drainage area (Figure 2-9). As expected, the 6-m system has the lowest cumulative duration of flow, followed by the 3-m system, and then the highway runoff, indicating that the larger the VCB, the less time high flow was being released. For the highest flowrates the 3-m system consistently exceeds the highway runoff. This counterintuitive result is likely due to differences between actual and estimated drainage area, to which data was normalized, as was discussed for peak flow results (Figure 2-8). The 6-m system had consistently lower flowrates than the highway runoff and a much steeper curve towards the highest flowrates, indicating good performance throughout the majority of its operation. Only at the highest flowrates (~10 m3/hr and higher), is no difference found between the highway runoff and the 6-m system, indicating that only during the highest intensity periods of rainfall is flow not appreciably reduced. This is similar to observations made during the large storm event (Figure 2-6), where a period of high intensity after a long period of volume retention resulted in similarly sized peak flows for the highway runoff and the treatments.

While it is difficult to make conclusions about the 3-m system in comparison to the highway runoff, some insights can still be derived. The 3-m system is much less able than the 6-m system to reduce higher flowrates, though some success in reducing flows is found at the lowest flowrates (< 0.5 m^3/hr). It is likely that for the 3-m system the shorter flow path and the reduced storage capacity result in faster saturation and less flow attenuation in comparison to the 6-m system. Additionally, it is possible that the 3-m system is reaching saturation and unable to offer additional flow reduction at higher flowrates, making it much more similar to the highway runoff curve at high flows, though it cannot be confirmed without a more precise dataset.

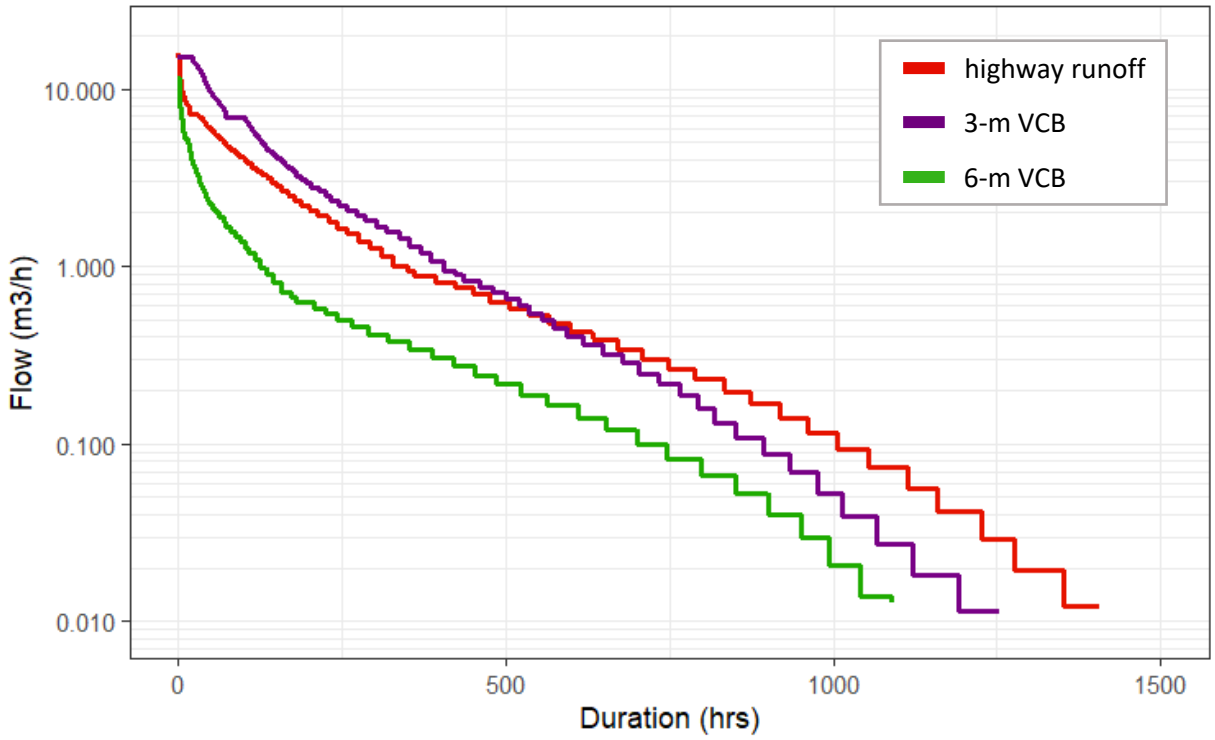


Figure 2-9: Flow-Duration Curves for All Flow Data Observed at Field Site. Flow is normalized by drainage area.

Flowrates for each sampling location can be compared as specific discharge (equivalent rainfall per time over the entire drainage area). For the highway runoff site, the maximum flowrate observed (16-m3/h was the maximum limit for field measurement) is equivalent to 861 mm/day, which is similar to pavement drainage areas evaluated previously: 933 mm/day (Olszewski and Davis 2012) and 638 mm/day from the previous study site (Davis et al. 2012a). Maximum highway runoff discharge is ~10x higher than the maximum observed for a Maryland forested watershed stream (88 mm/day) from (Olszewski and Davis 2012). When considering the median of all peak discharges (Figure 2-8) observed for each site, (427 mm/day highway runoff, 260 mm/day 3-m VCB, 120 mm/day 6-m VCB), VCB/VFS systems have a sizable impact on peak discharge reduction, with 39% and 72% reduction, respectively. In comparing the median

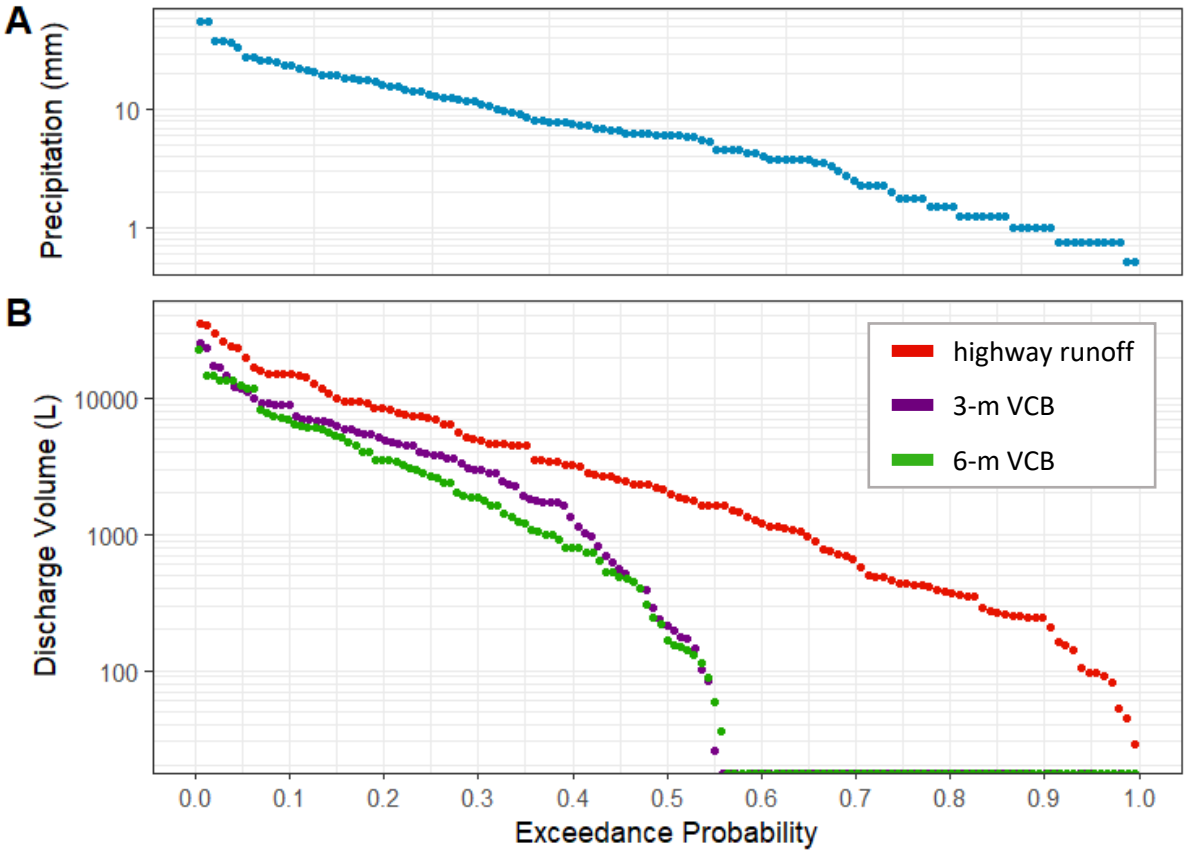
flowrate using all flow data, highway runoff discharge is 18.5 mm/day, which is of the same magnitude of 10.6 mm/day found for the previous study site (Davis et al. 2012a). In comparison, median discharge for the 3- and 6-m VCB/VFS systems were found to be 19.5 mm/day and 8.8 mm/day, respectively. While the 3-m VCB is not an improvement over highway runoff based on median flow (+6%), the 6-m VCB provided improvement (-52%). Median discharges for VCBs are also much closer to the range of values for a forested watershed stream near Baltimore MD (1-5 mm/day) (Davis et al. 2012a). The longer flow path had an improved performance for both peak discharge reduction (largest flows) and median discharge (overall performance) indicating better flow attenuation at the full range of storm sizes and a greater return to predevelopment hydrologic balance.

Volume Reduction

Normalized event volumes for events where highway runoff, 3-m VCB, and 6-m VCB data were all collected was compared on an exceedance probability basis (Figure 2-10b). For comparison, the rainfall distribution for the same subset of data is also presented (Figure 2-10a). Median rainfall for this dataset was 6-mm (0.24-in), near the point in exceedance where effluent begins for both VCB treatments. The 3-m and 6-m treatments produced no discharge for a large portion of events (~45%), and for those which produced effluent, a sizable gap was noted between VCB treatment volumes and highway runoff volume. This indicates a benefit in volume reduction by both VCB treatments.

The 3- and 6-m systems converge at low and high volumes, while in the center increased performance is noted for the 6-m system over the 3-m in volume reduction. It is possible that for events with a high antecedent moisture content, both systems have little remaining storage

capacity (for example, with back-to-back storm events) and therefore less difference in volume retention is found between the two treatments for some portion of storm events. A gap between treatments can be observed from ~10-45% exceedance; this indicates that for events producing effluent from the VCB systems, the 6-m system releases less volume based on the median. By taking a subset of this data for only volumes greater than 0, the 6-m system has a lower (by ~43%) median volume than the 3-m (3475 L for 3-m and 1983 for the 6-m).



C

	Precipitation (mm)	Runoff Volume (L)	3-m VCB Volume (Normalized) (L)	6-m VCB Volume (Normalized) (L)
median	6.1	2070	125	74
mean	9.5	4990	2470	1840
min	0.51	28	0	0
1st quartile	1.8	435	0	0
3rd quartile	13	7090	3630	1950
max	56	35700	25000	22600
n	124	124	124	124

Figure 2-10: Field Normalized Stormwater Discharge Volumes and Statistics. Observed for Runoff Inflow, 3-m VCB, and 6-m VCB.

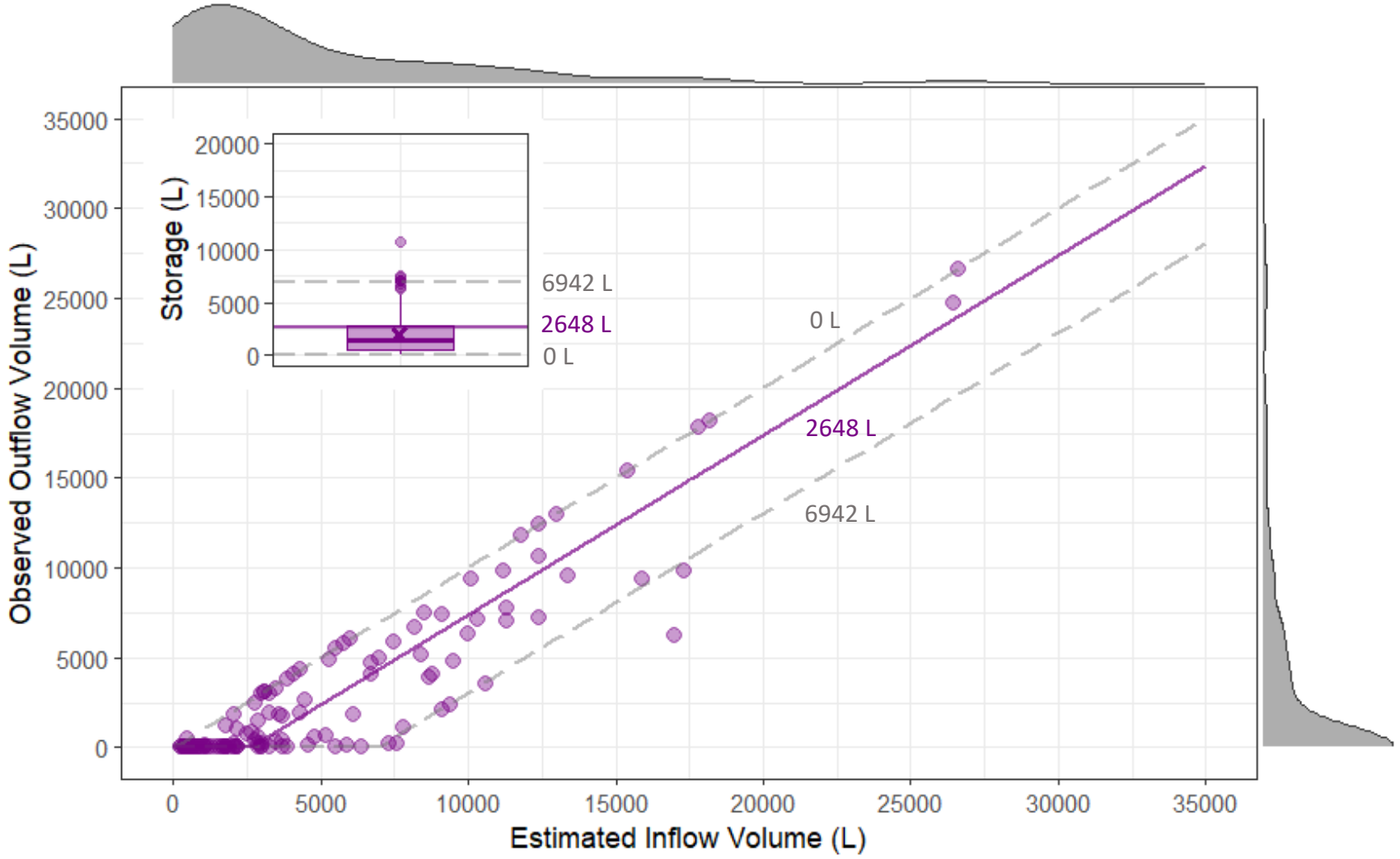
Comparison between inflow and outflow volumes for each event provide an overall summary of hydrologic performance in addressing both storm size and storage volume. Influent

and effluent volumes for each event was compared (Figure 2-11), excluding events where rainfall was so low that no influent highway runoff occurred. For each datapoint (individual storm event), storage is found as the perpendicular distance from the 1:1 correlation line. For additional comparison, the distributions for each variable are plotted at the edges of the main plot as well as an inset boxplot showing the storage values for the same dataset (found by subtracting outflow volume from inflow volume for each event). Because the highway drainage area for the 6-m system was only ~13% higher than for the 3-m, the data in these plots was not normalized.

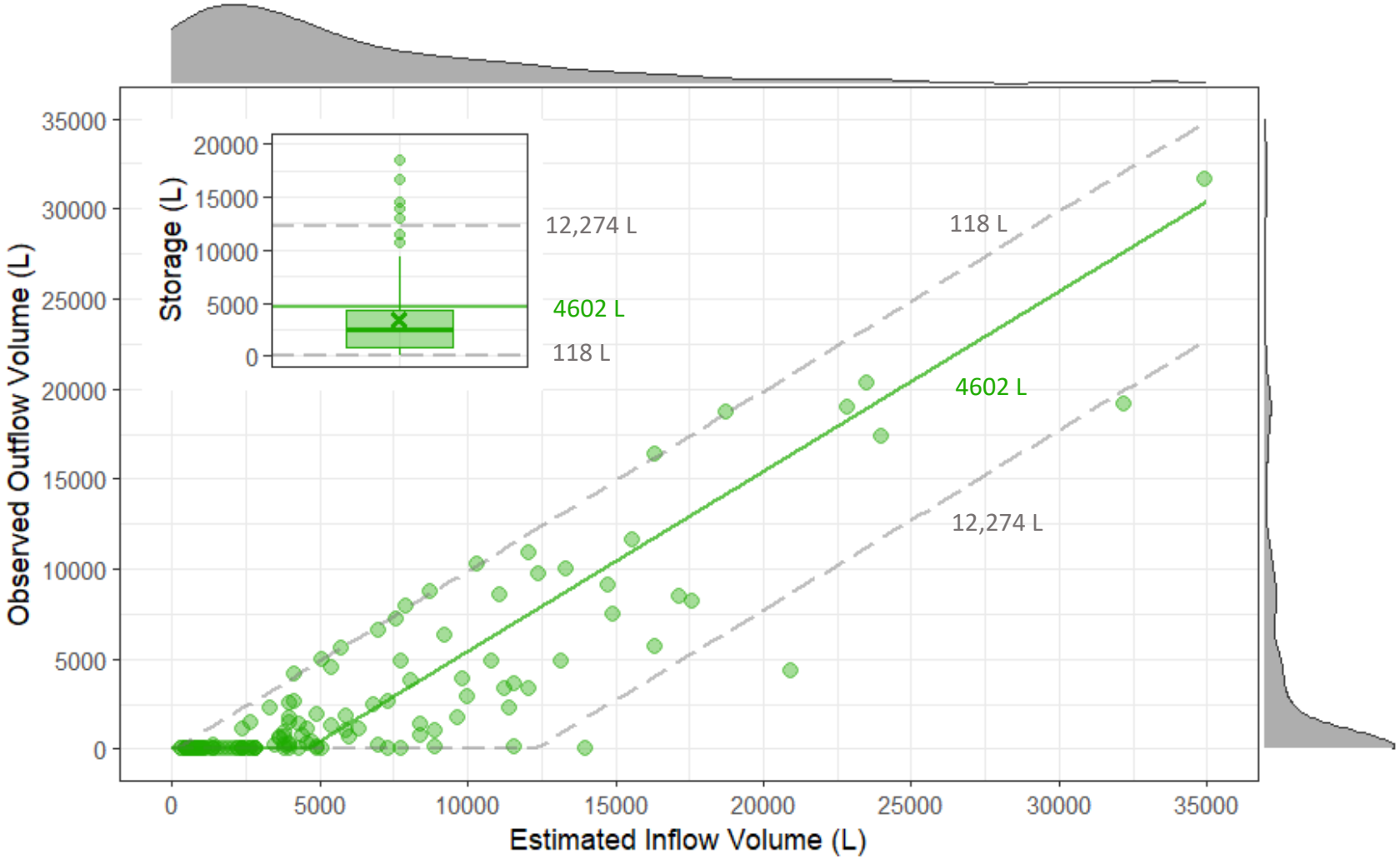
For both VCB systems (Figure 2-11) outflow volume frequency distributions (along the axes) have peaks much closer to 0 and are much narrower in comparison to the inflow volume distributions, indicating more frequent lower discharge volumes for the outflow over the inflow. Many storm events were completely captured by the VCB system, evidenced by the points on the x-axis. The best fit of the system was determined as a hockey-stick fit, where a fixed storage capacity is reached after which the outflow volume would be equal to the inflow volume (slope = 1). This best fit was chosen through assumption that storage in the compost and soil layers was the main means of volume retention, since infiltration was found to be nonsignificant due to compacted clay soils under the VCB/VFS system. These fits are shown in the plots as solid, colored lines. Similar attempts utilizing an initial storage or abstraction volume to describe stormwater control measures have been done previously for bioretention (Davis et al. 2012b) and for greenroofs (Fassman-Beck et al. 2016).

Linear best-fit was found through minimizing the sum of the squares of the residuals between the predicted data and the observed dataset. The average initial storage value using this method was 2648 L for the 3-m system (RMSE = 1964 L, R^2 = 0.8012) and 4602 L for the 6-m system (RMSE = 3215 L, R^2 = 0.7128). The 5^{th} and 95^{th} percentile storage values (dashed lines

in Figure 2-11) were also plotted using the same hockey-stick fit to indicate the storage values within which 90% of events fall. Conceptually, this accounts for the variability of available storage space prior to the rain event as well as the storm size, since many storm events will be completely captured but will not fill all available storage space due to their size (approximately 45% from Figure 2-10, as shown by the datapoints on the x-axis above 55% exceedance). By fitting the majority of the completely captured events to the "blade" of the hockey-stick and remaining events to the "shaft" of the hockey-stick, this method accommodates for small events not reaching storage capacity while also estimating a representative storage value for larger events which exceed storage capacity. The fit is further grounded by the RMSE (1964 L for 3-m and 3215 L for 6-m) which is similar to the storage volume dataset standard deviations for the 3- and 6-m systems (2071 L and 3117 L, respectively) (Figure 2-12b). Boxplots inset in Figure 2-11 (a and b) show the hockey-stick mean (3-m = 2648 L, 6-m = 4602 L) falling near the 3rd quartile for each system (2823 L for 3-m and 3602 for 6-m (Figure 2-12b)), further supporting using the hockey-stick mean as a representative initial storage over the mean or median storage, which would underestimate performance. As discussed previously, the volume retained for each particular storm event will depend on the storm size, duration, intensity, rainfall pattern, antecedent moisture content, and seasonal changes (vegetation, temperature, etc.), making this specific fit most appropriate for regions with similar rainfall distributions to Maryland and conditions most similar to this study.


Observed Outflow Volume (L)
Estimated Inflow Volume (L)
Storage (L)
6942 L
2648 L
0 L
0 L
2648 L
6942 L
0
5000
10000
15000
20000
25000
30000
35000

(a)



(b)

Figure 2-11: Field Inflow Outflow Curves for 3-m and 6-m VCBs.
(a) 3-m VCB/VFS system; (b) 6-m VCB/VFS system; hockey-stick best fit shown in solid line; 95% confidence intervals shown in dotted lines; inset plot shows storage (inflow – outflow) with the storage values labeled; frequency distributions for individual datasets shown on plot margins.

A comparison of the distribution of storage volumes along with summary statistics is shown in Figure 2-12. The 6-m storage volumes trend 43% higher than the 3-m, based on the mean. Determining a storage volume for VCB/VFS design may be approached similarly to previous attempts utilizing a Bioretention Abstraction Volume (BAV) for bioretention SCMs (Davis et al. 2012b). However, unlike in bioretention, there is no bowl storage for a VCB/VFS system nor is the lower media expected to remove a significant volume of stormwater due to the highly compacted subsoil. For the VCB/VFS, only the storage in the VCB and VFS layers should be considered influential. For a VCB/VFS the difference between Saturated Moisture Content (Sat MC) and Wilting Point Moisture Content (WP MC) of the compost is considered as an average upper volumetric storage threshold since this would be the available storage after a long dry period. This difference is considered as the low threshold for volume retention in bioretention (Davis et al. 2012b). Based on behavior of the VCB/VFS storage, many storm events result in little to no storage, making 0 storage a conservative lower threshold.

The VCB/VFS design storage volume is obtained by:

Equation 2-3

$$Volume = \frac{(Volume_{VCB}) * (Sat\ MC - WP\ MC)_{VCB} + (Volume_{VFS})(Sat\ MC - WP\ MC)_{VFS}}{2}$$

where Sat MC is the volumetric saturated moisture content, WP MC is the volumetric wilting point moisture content, VCB indicates the compost layer, and VFS indicates the topsoil layer.

Using this equation, wilting point estimates previously found for a leaf compost (WP MC = 44%) and a topsoil (WP MC = 8%) (Duzgun et al. 2021), and measured saturated MC found

through a vacuum saturation test in the laboratory (compost Sat MC = 75%, topsoil Sat MC = 48%) result in design storage values of 2018 L for the 3-m and 4036 L for the 6-m VCB/VFS (using field media depths of 6.4-cm (2.5-in) for topsoil and 7.6-cm (3-in) for compost. These storage volumes are 23.8% and 12.3% less than the average storage estimated by the hockey-stick method (3-m = 2648 L, 6-m = 4602 L), making this conservative but fairly accurate. Due to the ease of estimation of both Sat MC and WP MC, this can be a simple estimation of average storage performance for a VCB/VFS system, as long as the expected range of storage is contextualized to be approximately from 0 storage to the Sat MC and VCB lengths and drainage area ratios do not deviate largely from those in this research. To obtain the hockey-stick fit, the following two-part equation can be used:

Equation 2-4

1) $for\ Volume_{inflow} \leq design\ volume; \qquad Volume_{outflow} = 0$

2) $for\ Volume_{inflow} > design\ volume; \qquad Volume_{outflow} = Volume_{inflow}$

where inflow volume can be calculated as precipitation*total drainage area, and the design volume is calculated using Equation 2-3.

The cumulative inflow and outflow volumes for each VCB for the field experiment were calculated over the entire study, including the events which did not produce highway runoff (Table 2-5). Due to missing VCB data caused by equipment issues and quality control, the number of events used in this assessment are less than the 278 total observed storm events. Although the VCB/VFS is thin (~14-cm (5.5-in)), relatively short in length (3- and 6-m (10- and 20-ft)), and little to no significant infiltration is expected to occur in the subsoil layer over the

course of a storm event, the 3-m VCB system captured 44% of influent stormwater volume and the 6-m captured 55%. These reductions are similar to those found previously for compost blankets of 3.75-cm depth and 4.8-m length (50-60%) (Faucette et al. 2005, 2007). The addition of the VCB to the VFS improved volume capture performance, with larger volume reductions attained at shorter flow paths, as evidenced by total volume reductions observed previously for a VFS alone of 36% for an 8-m length and 59% for a 20-m length (Knight et al. 2013) and 20-40% for a 2-5-m length and 62-70% for a 8-15-m length (CVC and TRCA 2010).

Table 2-5: Field Total Volumes and Storage over the Full Experiment.

		Rainfall	
3-m VCB	Volume (m^3)	(mm)	(in)
Inflow	703	1484	58
Outflow	392	827	33
Retained	311	656	26
Retained		***44%***	
n		***248***	

		Rainfall	
6-m VCB	**Volume (m^3)**	**(mm)**	**(in)**
Inflow	952	1524	60
Outflow	425	680	27
Retained	527	844	33
Retained		***55%***	
n		***249***	



C

	Observed 3-m VCB Storage Volume (L)	Observed 6-m VCB Storage Volume (L)	Symbol
hockey-stick fit	***2648***	***4602***	
mean	1974	2825	
median	1444	2024	
stdev	2071	3117	
min	0	0	
5th percentile	0	118	
1st quartile	481	693	
3rd quartile	2823	3602	
95th percentile	6942	12274	
max	10724	19978	
n	137	142	
Storage Volumes Estimated from Compost/Soil Laboratory Testing			
Sat MC	7905	15810	
Sat MC – WP MC	4036	8073	
Estimated mean	2018	4036	

Figure 2-12: Field Storage Volumes and Statistics for 3-m and 6-m VCB Systems. (a) 3-m VCB/VFS system; (b) 6-m VCB/VFS system, (c) observation statistics and comparison to laboratory estimations; Saturated Moisture Content (Sat MC), Wilting Point Moisture Content (WP MC), and the estimated mean storage are presented for comparison.

The SCS curve number approach (NRCS 1986) is often used for describing the hydrologic benefit of SCMs (Davis et al. 2012b; Fassman-Beck et al. 2016; Olszewski and Davis 2012), including an attempt previously on compost blankets used for erosion control (Beighley et al. 2010). A composite curve number (CN) that includes the surface area of the highway and each VCB, was found through linear best fit for each system. For the 3-m system the composite CN was determined to be 97 (RMSE = 1767 L, R^2 = 0.8227) and 95 for the 6-m system (RMSE = 2533 L, R^2 = 0.7667). Separating the CN for the VCB areas alone resulted in a CN of 85 for the 3-m and 83 for the 6-m system, resulting in a mean CN of 84. This value is comparable to CNs found previously for compost blankets on steep slopes used in erosion control (Beighley et al. 2010), where blankets of depth 5.0-cm (2-in) over a 4:1 slope resulted in a CN of 80-82 during rainfall simulation experiments (in this field study blankets were 7.6-cm (3-in) depth and ~10:1 slope).

A CN is a widely used tool in stormwater design and implementation, however, has certain drawbacks for use in this particular system. The NRCS method was intended for use at the watershed level, making it less accurate for small systems and it does not account for the flow path of the system, rather estimating a percent runoff over the entire surface area. In reality, highway runoff flows into the VCB area before exiting, making a more complex system in series not accounted for by the CN. When possible, the hockey-stick method (Equation 2-4) with the representative volume storage value should be used.

Impact of Site and Design Characteristics

Because field site slope, drainage area ratio, and compost depth were fixed, a series of greenhouse mesocosm experiments were used to supplement field observations and better

understand VCB system performance over a range of possible site conditions. For each synthetic storm event, the inflow volume consisted of the sum of rainfall and runoff volume, and outflow volume was collected and measured at the end of the event. The inflow-outflow curves for these experiments is shown in Figure 2-13 along with best fit statistics. The best fit for mesocosms was also determined as a hockey-stick fit, with linear best-fit determined through minimizing the sum of the squares of the residuals between the predicted data and the observed dataset. Best fit storage is presented as volume (L) and also normalized as volume per VCB surface area (L/m^2) to account for differences in VCB length for comparison with field storage best fit storage. Using Equation 2-3 and the same values for Sat MC and WP MC to estimate the design volume for the mesocosm boxes (1.8-m length, 0.46-m width, 7.6-cm compost depth, 10-cm soil depth), results in a value of 26.87 L for the hockey-stick fit design value, which is on the upper end of the storage found through regression for all mesocosms (15.29-28.69 L) but the 2x DA (which is discussed more later). The fit is likely an overestimate for some mesocosms due to higher slopes and differing conditions than the field site (greenhouse experiments had steady flow rates applied instead of fluctuating hydrographs). However, field storage in L/m^2 (24.77 L for the 3-m and 28.50 L for the 6-m VCB) is more comparable to the design storage value, and field performance should be used over greenhouse studies for a more accurate estimate of performance. Differing field conditions should have an impact on the average storage performance, but for an estimate of average storage performance, Equation 2-3 should still be appropriate.

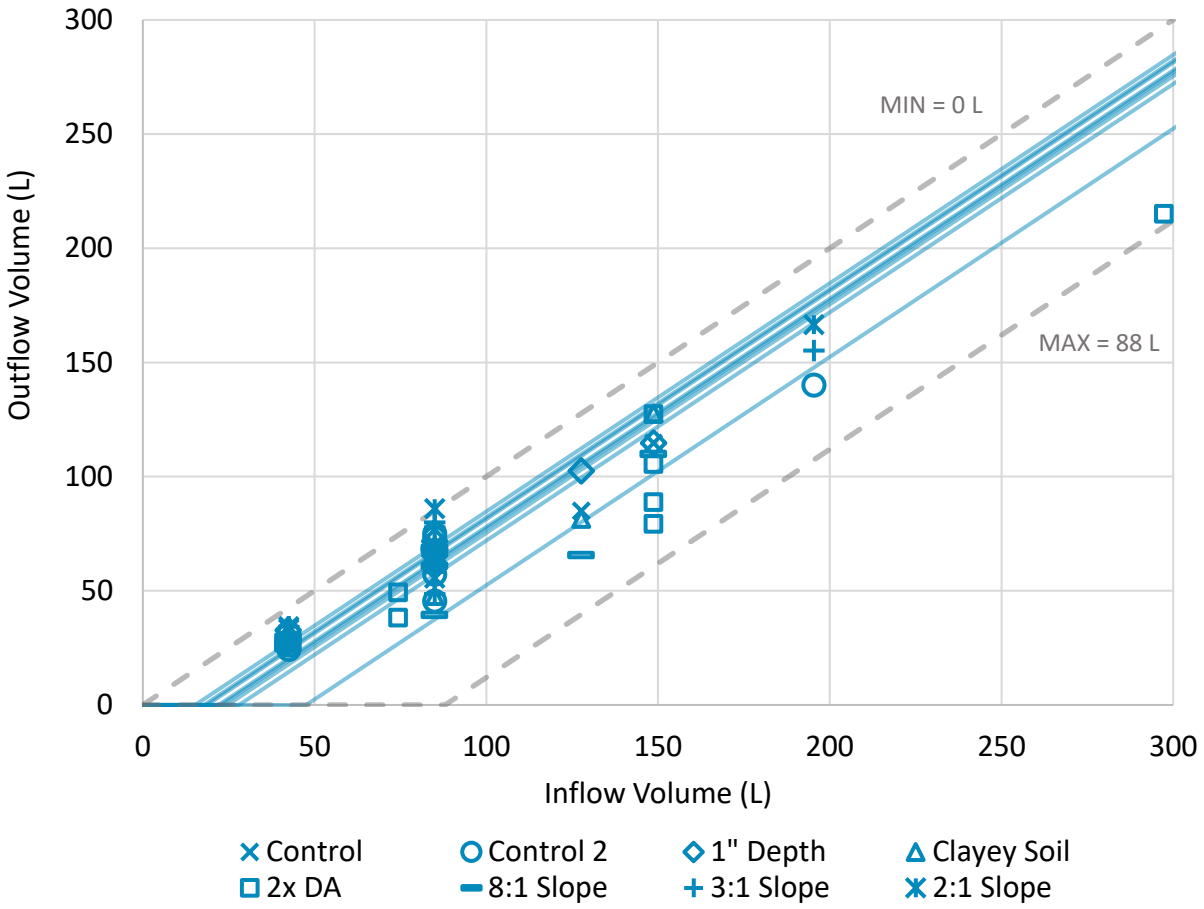
While mean storage was found to decrease with increasing slope, as expected, this result was not found to be statistically significant, which shows that VCB systems can be effective for volume retention for slopes between 20:1 (field site) to 2:1, which is the maximum permitted by Maryland Department of Transportation State Highway Administration (MD DOT SHA). For

compost depth, there was also no significant difference found in mean storage, suggesting that a thinner layer of compost (2.5-cm (1-in)) may achieve similar results to a 7.6-cm (3-in) layer. However, this also further supports evidence that for many storm events, all storage space is not utilized. This result may in part be due to storm characteristics, however, observations in the greenhouse showed that compost was often not saturated over the full length of the mesocosm during low flow events. Because compost was installed above grade (over the existing VFS) and also because the system is sloped, larger volume attenuation for some storm events may be prevented, especially those producing lower highway runoff flows, as water is more likely to move downward to the VFS layer and be transported downslope.

Comparison of differing drainage area ratio mesocosms further supports the idea that all storage space may not be utilized. One system experienced twice the runoff (representing twice the highway drainage area at 6:1 DA ratio) and was the only mesocosm to be found statistically significantly improved ($p \sim 0.05$) by 94% increased storage over the standard (3:1 DA ratio) based on the mean. All other factors, including rainfall over the top of the mesocosm remained the same, isolating the runoff flowrate as the driver for increased storage (and this improvement can be seen in Figure 2-13A). Greater runoff flow rates from the highway should force a taller wetting front in the compost layer, which is above grade. This is further supported by the behavior observed in the high intensity hydrographs in Figure 2-7. During this event, large flowrates were observed before all storage space was filled, with rainfall starting and stopping several times allowing for subsequent peaks to be attenuated and additional volume to be stored. In the greenhouse, however, flowrates remained constant through the storm event; this may allow for steadily increasing storage throughout the event, as the system is continuously inundated. Both datasets give some credit to the theory that higher runoff flowrates (whether

they are caused by a larger highway drainage area or a higher intensity storm event) result in greater contact of highway runoff flows with the compost layer (which has a much higher volumetric saturated moisture content than the topsoil: 76% vs 44%), resulting in increased total storage.

Even though water storage increases, however, the net result was not improved for the 2x DA (6:1 DA ratio) greenhouse system over the standard (3:1 DA ratio). While the mean storage increased from 24.64 L to 47.57 L, the total outflow volume (over the full experiment) increased from 447 L to 703 L (not shown), making the utilization of available storage more efficient, but the overall stormwater volumetric performance much less successful. Finding ways to increase stormwater runoff contact with the compost layer while still maintaining lower drainage area ratios could improve storage efficiency.



Mesocosm	RMSE (L)	R^2	Best Fit Storage (L)	Best Fit Storage (L/m^2)
Standard 1	9.58	0.9269	22.09	26.42
Standard 2	15.4	0.8872	24.64	29.47
1 in Depth	7.11	0.9597	18.69	22.35
2x DA	21.31	0.9041	47.57	56.89
8:1 Slope	16.27	0.7890	28.03	33.52
3:1 Slope	13.41	0.9198	17.84	21.34
2:1 Slope	10.41	0.9517	15.29	18.29
hockey-stick design (Equation 2-3)			26.87	32.14
3-m VCB				28.50
6-m VCB				24.77

Figure 2-13: Inflow-Outflow Curves for Greenhouse Experiments. With best-fit statistics; lines indicate hockey-stick best fit for each mesocosm; max storage for the 1-in compost depth mesocosm is 54 L and for all others is 88 L; Best Fit Storage refers to the x-axis intercept of the best-fit line, which can be considered an estimate of the representative storage value.

Media Properties and Vegetative Growth

Soil testing done before VCB installation and at the end of the experiment (~2.25 years) provided evidence that compost properties as well as its effect on underlying soil structure was influential in increased hydraulic performance. Comparison pre- and post-VCB installation included bulk density, saturated moisture content (porosity), and saturated hydraulic conductivity (Table 2-6). Number of observations differs within tests due to safety limitations and other practical considerations at the field site. At the end of the field experiment (2.25 years) bulk density decreased (26%) though not significantly ($p\sim0.075$), saturated moisture content significantly increased (29% ($p\sim0.009$)), and saturated hydraulic conductivity increased by approximately an order of magnitude ($p\sim0.005$) in the topsoil, all expected positive benefits of compost (USCC 2001b), as has been observed previously (Duzgun et al. 2021; Khaleel et al. 1981; Kirchhoff et al. 2003). However, subsoil characteristics were not changed except for saturated hydraulic conductivity, which significantly increased by an order of magnitude ($p<0.001$). Despite this increase, hydraulic conductivity measurements should be assessed with caution due to the high spatial variability, and even for one order of magnitude difference, this still places the subsoil in the range of a compacted clay soil with low infiltration (Coduto et al. 2011). Improvements in topsoil properties over the course of the study period would allow for increased moisture retention in the VFS layer in addition to the improvements offered by the VCB alone.

Table 2-6: Field Soil Hydraulic Properties and Statistics.
Bulk Density, Saturated Moisture Content, and Saturated Hydraulic Conductivity.

		Field Pre-Condition			Field Post-Condition		
		Compost	Topsoil	Subsoil	Compost	Topsoil	Subsoil
Bulk Density (g/cm^3)	mean	0.286	1.226	1.654	0.360	0.977	1.636
	stdev	0.0086	0.049	0.059	0.058	0.187	0.056
	n	3	3	3	10	4	9
Saturated Moisture Content (Θ) (%)*	mean	75.5	44.38	35.40	60.7	62.9	33.4
	stdev	1.06	2.35	2.53	6.39	9.38	4.82
	n	3	3	3	11	4	9
Saturated Hydraulic Conductivity (cm/s)	mean	7.87E-02	1.62E-02	2.53E-06	1.32E-02	2.04E-01	1.61E-05
	stdev	1.57E-02	9.70E-03	3.10E-06	1.93E-02	8.25E-02	1.06E-05
	n	3	5	30	6	4	12

**Volume basis*

Hydrologic performance and soil media changes should also be attributable in large part to a significant improvement in vegetative establishment by compost, which offered increased rooting depth, added nutrients, and higher moisture retention all contributing to improved growing conditions for turfgrasses. VCB treatments were observed to have statistically significantly improved establishment of MD DOT SHA turfgrasses over a VFS (topsoil) alone in greenhouse experiments through assessment of living grass cover ($p < 0.001$) and total cover (living grass and residue) ($p < 0.001$) over the study period (Table 2-7). Images of greenhouse turfgrass growth over the experiment period are also shown in the Appendix. In all greenhouse mesocosm experiments, compost placed over vegetated topsoil increased living vegetative cover between ~30-90%, with compost treatments reaching 90 to >99% total cover (living and residue) by the end of the monitoring period (~ 1 yr) compared to 30-75% for a VFS alone. Because all mesocosm variations made an improvement in vegetative cover over topsoil alone, VCBs should

improve vegetative establishment for a range of site slopes (8:1 to 2:1), compost depths (2.5-cm (1-in) to 7.6-cm (3-in)), and drainage area ratios (3:1 to 6:1).

Table 2-7: Comparison of Grass Cover Before and After Greenhouse Experiment.

Mesocosm	Living Grass (%)			Living Grass + Residue (%)		
	Pre-Compost	End of Experiment	diff	Pre-Compost	End of Experiment	diff
Standard	31	92	*+61*	39	98	*+60*
1" Depth	28	61	*+33*	34	91	*+57*
8:1 Slope	72	100	*+28*	74	100	*+26*
Standard 2	51	86	*+35*	63	100	*+36*
2x DA	25	89	*+63*	40	99	*+60*
3:1 Slope	39	97	*+57*	55	99	*+44*
2:1 Slope	5	97	*+92*	31	98	*+67*

Grass cover data from both the greenhouse and field site were compared to specifications set in MD SHA 705 Turfgrass Establishment 705.03.10 Final Acceptance: “Final Acceptance will be granted after all operations have been completed, and when the seedlings of turfgrass species have grown at least 4 in. tall, exhibit dark green color, and are least 95 percent groundcover” (MDOT SHA 2020). Rainfall depth to 95% cover was used to directly compare between the greenhouse and field sites, since rainfall patterns differed between experiments (Figure 2-14). Images of field sites after vegetative establishment are also included in the Appendix. For both the greenhouse and field, 95% vegetative cover was achieved within the first 3 months, and rainfall depths were similar for all experiments with the exception of the 2.5-cm (1-in) depth greenhouse mesocosm and the 2x drainage area ratio mesocosm. For the shallower compost depth (2.5-cm (1-in)), vegetation that had already been established beneath the compost layer more quickly emerged through the compost than for the other mesocosms (7.6-cm (3-in)),

producing 95% cover more quickly. The 2x drainage area ratio mesocosm experienced a 10-cm/hr (4-in/hr) intensity storm event applied before full vegetation establishment, which resulted in erosion of compost and delayed full vegetative establishment.

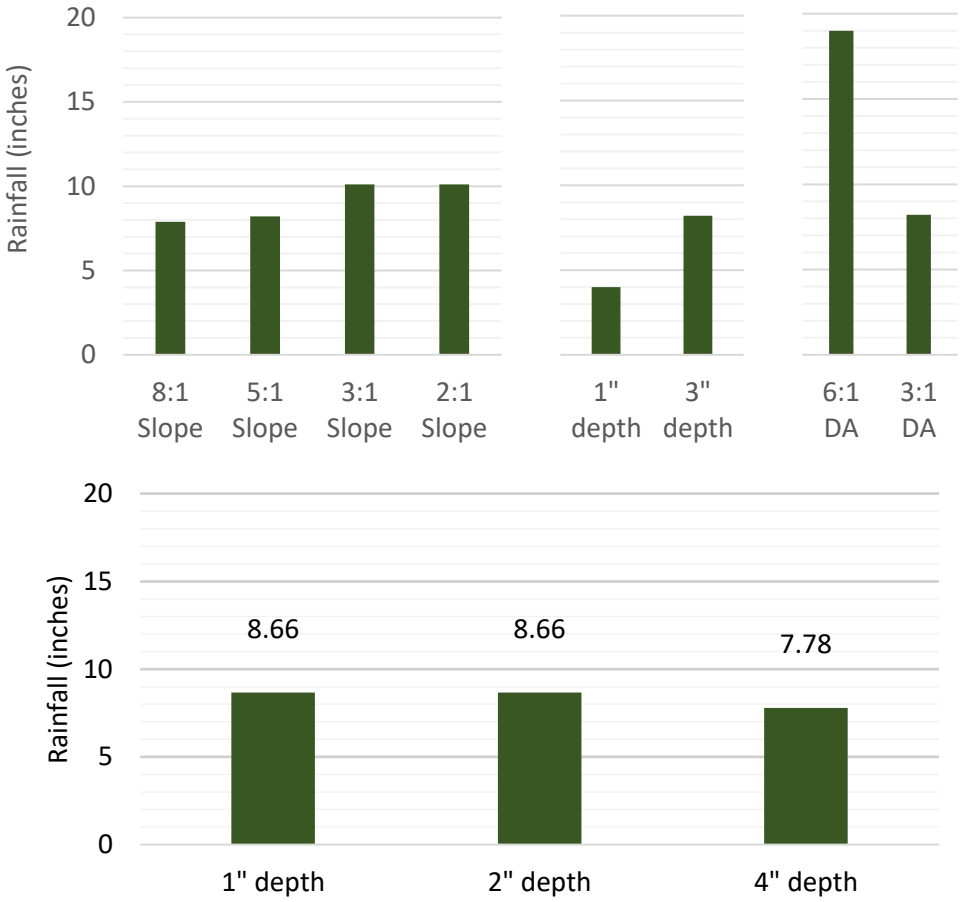


Figure 2-14: Rainfall Applied Until Vegetative Establishment for Field and Greenhouse. a) greenhouse mesocosms; b) field observational blanket: comparison of three sections with differing compost depths.

Improved vegetative cover can increase resistance to rainfall impact, improve infiltration, and slow flows through increased roughness (Abood et al. 2006; Pan and Shangguan 2006). The improvement of vegetative growth by compost treatments, which occurred over the first three months, therefore likely contributed significantly to improved hydraulic performance in VCB

systems. The results from this study mirror those for VCBs as erosion control measures, which have shown them to be successful in volume retention, dissipation of rainfall impact, soil structure improvement, and improvement of vegetative growth (AASHTO 2010; Bakr et al. 2012; Bhattarai et al. 2011; Faucette 2008; Faucette and Risse 2002; Faucette et al. 2007, 2009a; Fay et al. 2012; Mukhtar 2005).

Conclusions

Two field-scale VCBs experiencing real precipitation events were monitored over the course of 2.25 years at a highway median to evaluate their hydraulic and hydrologic performance as SCMs. Performance was evaluated as a combined system of a VCB overlaying the preexisting VFS. Differing lengths from edge-of-pavement were evaluated to assess the influence of flow path and potential storage volume with both discharge flows (hydrographs) and total event volumes being used in their evaluation. A range of greenhouse mesocosm studies were used to supplement field data through volume storage comparisons as well as evaluations of compost/soil hydraulic properties.

Due to highly compacted subsoils, infiltration was not a significant removal pathway for stormwater volumes, with storage being the main stormwater removal pathway. VCB application improved the hydraulic properties of VFS soil but did not have a significant impact on the highly compacted subsoils over the period of study (2.25 years). VCBs were found to improve site hydrology in comparison to highway runoff alone for both runoff flows and volumes. A large portion of smaller storm events (61%) were completely captured, and significant volume reductions were found for many larger storm events, resulting in 44% and 55% total volume removal over the full study period for the 3-m and 6-m VCBs, respectively. VCBs were shown to

mainly function as storage for small storms, at the beginning of larger storms, and between high intensity peaks of rainfall. At the highest flowrates and after saturation was reached, however, both VCB lengths were forced to mainly conveyance.

Event hydrographs were improved by VCB treatments, with evaluation of peak flows, time to peak, and event duration obtained from event hydrographs showing reductions of 39% and 43%, increases of 94% and 97%, and decreases of 10% and 9% for the 3-m and 6-m systems, respectively, in comparison to highway runoff based on the median. The 6-m VCB had a much improved performance over the 3-m VCB for both high flows and for overall flow reduction compared to the highway runoff, however both systems were unable to attenuate the highest flows. Comparisons of specific discharges (in mm/day) using observed VCB discharge flows from this study to drainage areas and forested streams from previous studies indicated a closer return to predevelopment performance for smaller flowrates; however little reduction was found for the largest observed flows. In most cases, the VCB/VFS system would be considered a pre-treatment likely to be uphill of a highway swale system. In this case many smaller storm events could be mitigated by the VCB/VFS alone while for larger storms significant reductions in flows and stormwater discharge volumes could be attained before discharge to the swale system for further treatment. However, for some events of high intensity and/or high antecedent moisture content, VCBs may have little to no effect, relying on downstream systems to mitigate stormwater impacts.

Because infiltration was found to be negligible, the most appropriate description of VCB/VFS volume retention performance was found to be a hockey-stick fit, where a representative average storage capacity is reached, after which no additional storage is provided by the system. For use of this method for design purposes, representative average storage

capacity can be estimated using estimated or measured values for saturated moisture content (Sat MC) and wilting point moisture content (WP MC) for both the VCB and VFS layer, since estimates of these parameters are widely available. Because curve numbers are often used in design guidelines, a CN of 84 was estimated for a VCB overlaying a VFS, which should provide a fair estimate of hydrologic performance if needed but is not considered the best representation of VCB functionality.

Greenhouse experiments used to evaluate a range of site characteristic variations showed that volume retention was not significantly changed with over a slope range of 20:1 to 2:1. Volume retention by a thinner VCB layer (2.5-cm vs 7.6-cm) was not found to be significantly different, indicating that not all available VCB storage was being utilized and significantly greater storage observed for a higher drainage area variation (6:1 vs 3:1) indicated that higher flowrates resulted in greater storage, but also higher net stormwater volume discharge. These observations highlighted a potential inefficiency in VCB implementation; since VCBs were applied above grade over the existing VFS, greater flowrates may be required to increase the highway runoff flow wetting front with the VCB layer. Greater drainage area ratios are not recommended due to the higher net discharge, but future designs may consider addressing the potential for increased storage capacity.

It is important to note that compost has been shown to release large amounts of nutrients immediately after application (see Chapter 3), making water quality performance of VCBs critical in decision-making. Overall performance evaluation and recommendations given here were considered through evaluation of hydrologic performance alone. Both hydrologic and pollutant removal improvements are important goals for SCMs, and further research on overall

water quality performance of VCBs will be essential to making appropriate design and implementation recommendations.

Acknowledgements

The authors acknowledge the support of the National Cooperative Highway Research Program (NCHRP 14-39), the Maryland Department of Transportation State Highway Administration (MDOT SHA), and the Low Impact Development (LID) Center.

Erica R. Forgione was supported by NRT-INFEWS: UMD Global STEWARDS (STEM Training at the Nexus of Energy, WAter Reuse and FooD Systems) that was awarded to the University of Maryland School of Public Health by the National Science Foundation National Research Traineeship Program, Grant number 1828910. Graduate student funding was also provided in part by the University of Maryland Graduate School Dean's Fellowship and COVID Delay Fellowship.

Mesocosm and field equipment design and construction support was provided by the University of Maryland Environmental Science and Technology (ENST) Project Development Center. Special thanks are also extended to Stancill's Inc. (Perryville, MD) for providing engineered soils and to Montgomery County Yard Trim Composting Facility (Dickerson, MD) for providing Leafgro yard waste compost.

CHAPTER 3: WATER QUALITY PERFORMANCE OF VEGETATED COMPOST BLANKETS FOR HIGHWAY STORMWATER MANAGEMENT

Erica R. Forgione[1], Gary K. Felton[2], Ahmet H. Aydilek[3], and Allen P. Davis[4]

[1] Graduate Research Assistant, Dept. of Civil and Environmental Engineering, Univ. of Maryland, College Park, MD 20742.
[2] Associate Professor, Dept. of Environmental Science and Technology, Univ. of Maryland, College Park, MD 20742,
[3] Professor, Dept. of Civil and Environmental Engineering, Univ. of Maryland, College Park, MD 20742, USA.
[4] Professor and Charles A. Irish, Sr. Chair in Civil Engineering, Dept. of Civil and Environmental Engineering, Univ. of Maryland, College Park, MD 20742, USA. (corresponding author). E-mail: apdavis@umd.edu USA.

Abstract

Urban stormwater poses serious risks to human and environmental health, including eutrophication caused by nutrient pollution and risk of toxicity to the aquatic environment caused by heavy metals. In an effort to improve the performance of existing highway Vegetated Filter Strips (VFS), which have limited performance in terms of volume reduction and pollutant removal, amendment of VFS with a Vegetated Compost Blanket (VCB), a layer of seeded compost placed on an established slope, has been proposed. Compost may improve water quality through increased volume retention through its high water holding capacity as well as immobilization of contaminants via its organic matter content. However, excess nutrient and heavy metal leaching may occur after application, which risks net beneficial performance. This research attempts to evaluate a novel VCB/VFS system primarily for water quality performance as a Stormwater Control Measure (SCM).

A large-scale field study of a 3-m and 6-m VCB as well as a greenhouse mesocosm study utilizing a synthetic stormwater were conducted and concentrations of Total Suspended Solids (TSS), Nitrate + Nitrite (NOx), Total Kjeldahl Nitrogen (TKN), Total Nitrogen (TN), Total Phosphorus (TP), filtered and total Copper, and total Zinc were analyzed. Exceedance

probability as well as calculated mass removals were used to evaluate VCB performance and concentrations were also compared to water quality criteria to quantify potential downstream effects. Speciation of nitrogen was used to evaluate nitrogen movement and partitioning of copper was used to evaluate heavy metal transport pathways.

Thirty-three representative field storm events, assessed by season and storm event size and duration, were sampled for water quality from the field site over a period of 2.25 years. Influent concentrations were much lower than expected, potentially due to biasing to larger storm events which produced outflow, as well as decreased pollutant loading caused by lower traffic volumes during the COVID-19 pandemic. Significant TSS removal was observed in both the field and greenhouse studies, with effluent TSS likely originating from the media itself rather than remaining influent particles, as evidenced by differences in metals partitioning between the influent and effluent. A large intensity (102 mm/hr (4 in/hr)) storm event in the greenhouse resulting in erosion prior to vegetative establishment supports use of an erosion control matting for VCB installation. Particulate metals were largely removed, while the initial compost copper content was likely influential in observations of dissolved copper leaching in the field experiment, which was not observed in the greenhouse. Highly elevated concentrations of nutrients (as high as 100 mg/L TN and 12 mg/L TP) were observed in the effluent of both field and greenhouse experiments, resulting in net nutrient leaching. Despite positive performance benefits for particulate pollutant removal and associated heavy metals from influent stormwater, compost nutrient leaching (and possibly copper) risks causing a net detriment to downstream water bodies, and compost composition and nutrient/metals release potential should be considered carefully before widespread implementation.

Introduction

During storm events, rain washes with it an array of pollutants from impervious surfaces, resulting in a highly variable and complex stormwater solution. This resulting urban stormwater runoff has become the focus of international efforts to reduce pollutant loading from urban areas to the surrounding environment, in the U.S. through the National Pollutant Discharge Elimination System (NPDES) (US EPA 2015b). This challenge has precipitated the use of novel green infrastructure systems called Stormwater Control Measures (SCMs), which are designed to reduce stormwater runoff volumes and decrease pollutant loadings, and are increasingly being utilized across the U.S. (National Research Council 2009). In the U.S., State Departments of Transportation (DOTs) are faced with both increasingly stringent environmental regulations for transportation infrastructure as well as sustainability objectives that include the use of recycled/repurposed materials. In addressing both of these challenges, the use of a novel SCM has been proposed, a Vegetated Compost Blanket (VCB), which would be used as an affordable, sustainable modification to an existing highway SCM, a Vegetated Filter Strip (VFS).

A VCB is a layer of compost loosely applied to an existing slope. VCBs have been used previously for erosion control (AASHTO 2010; US EPA 2012), and has been shown to successfully increase volume retention, infiltration, and vegetative growth (AASHTO 2010; Bakr et al. 2012; Bhattarai et al. 2011; Faucette 2008; Faucette and Risse 2002; Faucette et al. 2007, 2009b; Fay et al. 2012; Mukhtar 2005). In addition, compost has a large organic matter content, which may provide binding sites for certain pollutants (USCC 2001a). These benefits may improve on current highway VFS treatments, which have shown limited performance both hydrologically (Davis et al. 2012a) and for water quality (Barrett et al. 1998; Blanco-Canqui et

al. 2004; Boger et al. 2018; Deletic and Fletcher 2006; Knight et al. 2013; Magette et al. 1989; Stagge et al. 2012).

Particulates, nutrients, and heavy metals are all contaminants of concern which can be transported to critical waterbodies from urban and highway areas as non-point source pollution. Nutrients (nitrogen (N) and phosphorus (P)), while necessary to life in small amounts, in excess have threatened ecosystems by causing eutrophication, a phenomenon which leads to algal blooms (Carpenter et al. 1998; Conley et al. 2009; Harper 2012). Heavy metals are introduced to urban environments through vehicle wear and atmospheric deposition (Davis et al. 2001), and are harmful to humans and aquatic ecosystems due to toxicity and bioaccumulation (Ma et al. 2016; Zeitoun and Mehana 2014). Particulate matter negatively affects aquatic ecosystems by blocking light but can also be a major source of nutrients and heavy metals, which can sorb to the particle surface. Heavy metals in particular are often affiliated with the particulate phase of stormwater (Brown and Peake 2006; Djukić et al. 2016), and so removal of particulates should be important in assessment of metals removal.

One major challenge in the use of VCBs for improvement of stormwater quality is the potential for contaminants leaching from the compost itself. Compost is a nutrient-rich, microbially active material, which may leach large concentrations of N and P immediately after application, slowly decreasing over time, as has been previously reported (Ahmad et al. 2008; Brown et al. 2016; Butler and Coale 2005; Confesor Jr et al. 2009; Dietz 2007; Eghball 2003; Hurley et al. 2017; Iqbal et al. 2015; Li et al. 2011; Mullane et al. 2015; Reed et al. 2006). While SCMs containing compost have shown to be effective for metals removal through positively charged metals attaching to negatively charged organic matter (Seelsaen et al. 2007), compost also contains heavy metals including Cu and Zn (Finney et al. 2010; Khan et al. 2009; Lim et al.

2015), which are essential elements for plant life and so present in compost feedstocks as well as the resulting compost, and may be released with the dissolution of organic matter. Specifically, copper leaching has been observed previously in studies of bioretention media containing compost (Colton et al. 2014; Herrera Environmental Consultants, Inc. 2015; Mullane et al. 2015).

VCBs may offer improved water quality through increased stormwater retention, resulting in corresponding pollutant removal and as well as slowing of flow velocities and increased roughness caused by denser vegetation which can increase settling of particulate matter. When considering the overall performance of a VCB, both the VCB and underlying VFS layers should be considered. In the VCB layer, removal of smaller particles through filtration as well as adsorption of heavy metals and nutrients to the organic fraction of the compost may be influential. However, leaching of nutrients and possibly metals is also likely. In the VFS layer, soil may remove metals through adsorption to the organic matter fraction or iron and aluminum oxides (Davis et al. 2010). There is also potential for the VFS layer to adsorb the soluble, inorganic nutrient species (NH_4^+, PO_4-P) (Gérard 2016; Li and Davis 2014; Zhang et al. 2001). In both layers, microbiological transformations and plant uptake of nutrients and metals also play a role in transport and fates, especially since compost is highly microbially active.

The goal of this study is to evaluate the performance of VCBs as an amendment to existing VFSs on highway systems for improvement of stormwater quality. At a large-scale field site, 33 storm events were collected over 2.25 years, and in a mid-size greenhouse experiment 19 synthetic storm events were conducted between two sets of experiments for assessment of water quality performance. Total Suspended Solids (TSS), nitrite + nitrate (NO_x), Total Kjeldahl Nitrogen (TKN), Total Phosphorus (TP), total and filtered copper, and total zinc were collected

on a storm event basis as Event Mean Concentrations (EMC) and used to assess the overall performance of the VCB/VFS system. Additionally, assessment of VCB/VFS system performance under varying site (slope, drainage area ratio) and design (VCB depth, VCB length) conditions was completed through comparison of field and greenhouse data.

Materials and Methods

Field Site Description

A large-scale field study was conducted on a median on the eastbound side of Maryland Route 32 in Howard County, MD as described previously (Chapter 2). The site includes two VCBs directly adjacent to edge of pavement, both 7.6-cm (3-in) deep and 30.5-m (100-ft) along the highway. Widths differed with one VCB at 3-m (10-ft) wide perpendicular to the highway and the other 6-m (20-ft) wide perpendicular to the highway, both receiving runoff as sheet flow from the eastbound two-lane highway. Additionally, a 30.5-m (100-ft) section of a preexisting concrete channel was used to monitor influent highway stormwater runoff.

Field Sampling

Rainfall and flow data were collected using ISCO 6712 autosamplers as described previously (Chapter 2). Autosamplers were programmed to collect flow-weighted composite samples, and therefore the collected sample concentrations can be considered Event Mean Concentrations (EMCs). Only rainfall events large enough to produce effluent runoff from the VCBs were sampled for water quality analysis (approximately >0.25-in), therefore bias of the dataset to larger storm events was necessary. Prior to sample collection, field site maintenance was conducted, including cleaning collection pipes and the highway runoff channel, calibrating flow

meters, and connecting clean collection bottles. Due to equipment installation and troubleshooting immediately after installation on February 27, 2022, data collection was delayed by 21 days, during which time 12.7-cm (5-in) of rainfall was not monitored, as estimated by a nearby rain gauge. After collection, samples were prepared and transferred immediately to the Washington Suburban Sanitary Commission (WSSC, Silver Spring, MD) EPA Certified Laboratory for analysis.

Greenhouse Experiments

Both simulated rainfall and runoff were applied to two sets of mesocosm experiments (Studies 1 and 2) with a range of design variations, as described previously (Chapter 2). Mesocosms were 0.45-m wide by 1.8-m long (1.5-ft by 6-ft), so results can be compared to field results by length (3-m and 6-m (10-ft and 20-ft) length in field). Synthetic stormwater runoff emulating real field stormwater runoff was made by mixing pre-weighed chemicals into a measured volume of tap water, which was dechlorinated using sodium bisulfite. The chemical makeup of this synthetic stormwater recipe includes target contaminants TSS, nutrients, and heavy metals and background constituents and is based on national studies on runoff characteristics as well as highway runoff concentration data previously obtained from the field site (Collins et al. 2010; Liu and Davis 2014; Stagge et al. 2012). Synthetic stormwater composition is shown in Table 3-1.

Table 3-1: Chemical Composition of Synthetic Stormwater Used in Greenhouse Experiments.

Constituent	Value	Source
pH*	7.0	HCl or NaOH
Organic Carbon/COD	~10 mg/L COD	Aldrich Humic Acid
Hardness*	40 mg/L as $CaCO_3$ 15 mg/L as Ca^{2+}	$CaCl_2$
Dissolved Solids*	80 mg/L	$CaCl_2$
Suspended Solids	100 mg/L	Local sieved soil
Inorganic Nitrogen: NO3-	1 mg/L as N	$NaNO_3$
Organic N	2 mg/L as N	Glycine
Phosphorus	0.5 mg/L as P	Na_2HPO_4
Copper	0.06 mg/L	$CuCl_2$
Zinc	0.5 mg/L	$ZnCl_2$
Lead	0.04 mg/L	$PbCl_2$

** Already present in tap water*

Synthetic stormwater was mixed in a 600-L polypropylene tank with a Ryobi drill fitted with a stainless-steel pitched blade impeller rotated at 580 RPM. A sample was collected from the influent tank after mixing well to obtain a representative inflow composite sample. All mesocosm effluent from either the VFS or VCB layer was collected in a single container so that the total volume could be measured. After mixing well, a sample was taken from each effluent container. Because of this, influent and effluent samples from mesocosm experiments can be considered EMCs. After collection, greenhouse samples were also prepared and transferred immediately to WSSC through the same method.

Samples collected from the greenhouse experiment were either collected from the VCB layer (passing through compost only) or from the VFS layer (passing through compost and soil layers). Summary performance for Studies 1 and 2 in the greenhouse were separated because the first three storm events for Study 1 were not sent for water quality analysis. Results for greenhouse Studies 1 and 2 are summarized here (Table 3-4 and Table 3-6), with detailed EMC

and mass performance tables included in the Appendix. VCB effluent data was not able to be statistically evaluated for each mesocosm due to the small number of observations.

Water Quality Methods and Data Analysis

New plastic bottles were used for every sample collection, with preservation for metals analysis done with trace metal grade nitric acid and filtration for filtered (dissolved) metals done with a 0.22-µm filter. After preparation, samples were immediately transported and submitted along with a DI water sample as a field blank with a chain-of-custody form to a refrigerator at the WSSC. WSSC laboratory chemical analyses methods are shown in Table 3-2.

Table 3-2: WSSC Laboratory Methods.

Analytical Parameter		Method #	Equipment	Preservation Requirements	Detection Limit (mg/L)
Total Suspended Solids		SM 2540 D	Metlor Balance	Cool ≤6°C	1
Total Phosphorus		EPA 365.1	FIA	H_2SO_4 to pH <2, Cool ≤6°C	0.2
Total Nitrogen	Total Kjeldahl Nitrogen (TKN)	EPA 351.2	FIA	H_2SO_4 to pH <2, Cool ≤6°C	0.5
	Nitrate + Nitrite (NO_x)	EPA 353.2	FIA	H_2SO_4 to pH <2, Cool ≤6°C	0.2
Total Copper		EPA 200.8 Rev 5.4	ICP-MS	HNO_3 to pH <2	0.005
Filtered Copper*		EPA 200.8 Rev 5.4	ICP-MS	HNO_3 to pH <2	0.005
Total Zinc		EPA 200.8 Rev 5.4	ICP-MS	HNO_3 to pH <2	0.005

**Vacuum filtered with a 0.22 µm filter*

Data Handling and Statistical Analysis

All displayed concentration data for nitrogen is as equivalents of N (NO_x-N, TKN-N). Exceedance probability plots for comparisons of concentration data were created by ranking data in descending order, with probability of exceedance for each datapoint calculated as:

Equation 3-1

$$p = \frac{i - \alpha}{(n + 1 - 2\alpha)}$$

where i is rank and n is the total number of observations, with a value of 3/8 used for alpha for a normal distribution, as has been used previously (Davis 2007). Comparison of EMC data to water quality criteria was used to assess effectiveness of the system to protect downstream water quality. Concentrations for zinc were compared to criteria found in the US EPA National Recommended Water Quality Criteria (Aquatic Life Table) (US EPA 2015a). TN and TP concentrations were compared to Region IX (covers Maryland) criteria from the US EPA's Ecoregional Nutrient Criteria for Rivers and Streams (US EPA 2013). TSS and copper concentrations were compared to water quality criteria outlined in Davis and McCuen (Davis and McCuen 2005a; b). To calculate mass removal, the mass of pollutant (M) in the inflow and outflow for each storm event was calculated as:

Equation 3-2

$$M = V * EMC$$

where EMC is the event mean concentration (mg/L) and V is the volume (L). Weighted removal was calculated as the total pollutant percent removal (or release if negative) over the time period of the full experiment. It is calculated as:

Equation 3-3

$$Weighted\ Removal\ (\%) = 100 * \sum(M_{IN} - M_{OUT}) \ / \ \sum M_{IN}$$

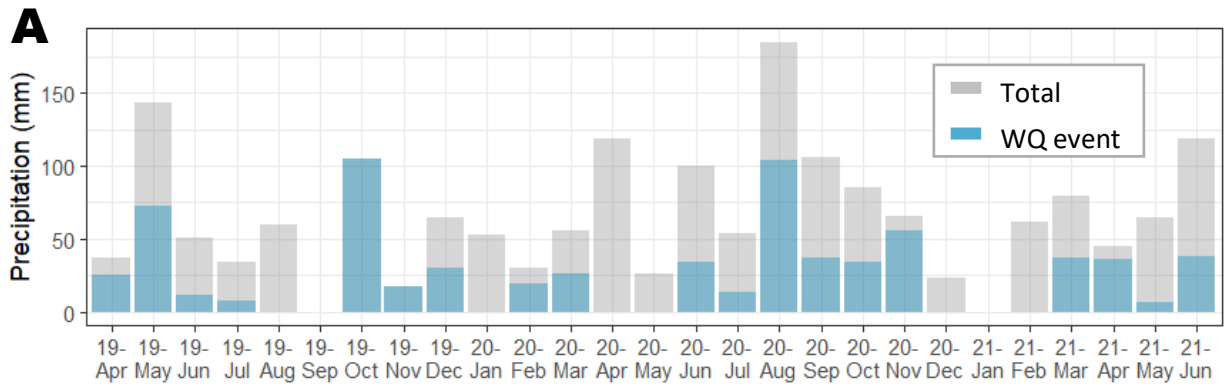
where M_{IN} and M_{OUT} are the total pollutant mass in and out for each event, as calculated by Equation 3-2. Any values below the detection limit were treated by replacement with half the detection limit, as recommended by USEPA (USEPA 2000). Student's t-test was used to make statistical comparisons based on mean and evaluated at a 5% significance level, though values of p are given as well. Kendall Tau test was used to detect statistically significant time series trends at a 5% significance level.

Results and Discussion

Water Quality Sampling Collection Characteristics

A monthly summary of all storm events sampled for water quality is shown in Figure 3-1B. Also included is a timeseries bar chart displaying the total rainfall resulting in VCB effluent (and therefore potentially large enough for data collection) for each month compared to the rainfall depth of collected storm events (Figure 3-1A). Gaps in data due to drought and COVID-19 lockdown restrictions are indicated. In addition, during winter months, freezing conditions at times necessitated pausing collection due to potential equipment damage, so less events were sampled in those months (Dec-Feb). Of the 33 water quality events, spring (Mar-May) constituted the most (12 events), followed by summer (Jun-Aug) (10 events), then fall (Sept-Nov) (8 events) and finally winter (3 events). Sample collection is approximately representative of precipitation in that spring rainfall constituted 32% of rainfall and 36% of sampled events; summer: 34% and 30%, fall: 20% and 24%, and winter: 14% and 9%.

A



B

Year	Month	# Observed Events	# Tested Events	Observed Rainfall (mm)	Tested Rainfall (mm)	% of Total Rainfall
2019	April	4	2	37	25	57%
	May	10	3	143	72	49%
	June	5	2	51	11	17%
	July	3	1	34	8	17%
	August	4	0*	60	0	0%
	September	0	0*	0	0	0%
	October	4	4	105	105	99%
	November	1	1	17	17	94%
	December	5	2	65	30	36%
2020	January	4	0	53	0	0%
	February	3	1	30	19	41%
	March	6	2	56	26	42%
	April	5	0**	119	0	0%
	May	4	0**	26	0	0%
	June	5	2	100	34	30%
	July	4	1	54	13	19%
	August	9	3	185	104	54%
	September	5	1	106	37	33%
	October	2	1	85	34	36%
	November	2	1	66	56	80%
	December	1	0	23	0	0%
2021	January	0	0	0	0	0%
	February	2	0	62	0	0%
	March	4	2	79	37	35%
	April	6	2	45	36	77%
	May	4	1	65	7	10%
	June	6	1	119	38	31%
	Total:	**108**	**33**	**1787**	**709**	**40%**

* *Drought* ** *Testing suspended due to coronavirus restrictions*

Figure 3-1: Rainfall Occurrence and Water Quality Testing Totals.

Storms were also representative of the range of rainfall events observed at the field site over the study period. When plotted as a range of rainfall depths and durations (Figure 3-2A), the rainfall-duration distribution for sampled storm events is similar to that of the full dataset (for storms producing VCB outflow), discussed in Chapter 2. When comparing distributions of precipitation (Figure 3-2B) and duration (Figure 3-2C), the sampled dataset has a slightly higher mean precipitation (21.5-mm (0.85-in) sampled, 16.5-mm (0.65-in) full) and duration (11.8 hr sampled, 8.4 hr full) than the full dataset. This is likely because sampling was biased towards storm events which would produce enough outflow from VCB systems to obtain a representative sample. Although collection prioritized events producing runoff from both VCB systems, not all samples were collected for all 33 storm events due to equipment errors, resulting in different size datasets for the highway runoff data (n = 28), 3-m outflow data (n = 27), and 6-m outflow data (n = 27).

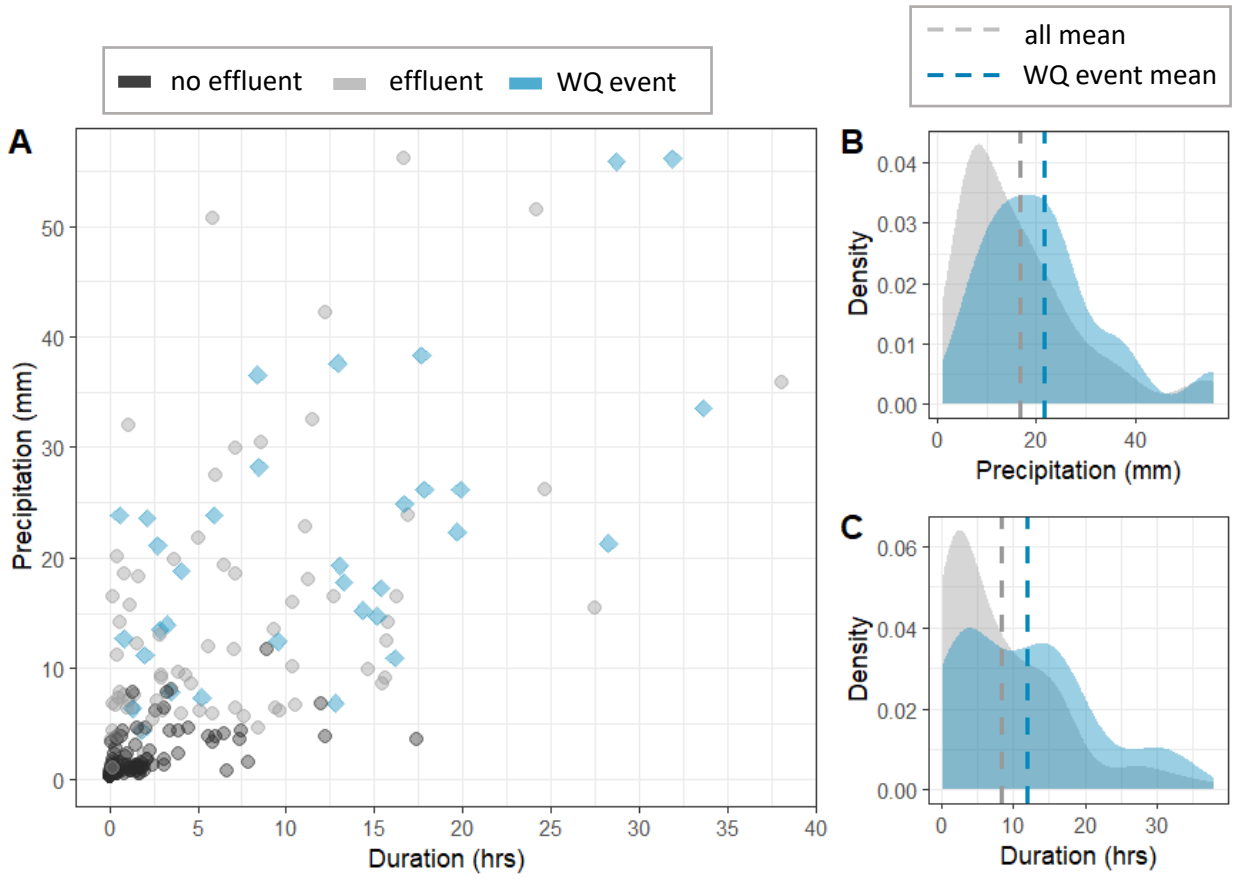
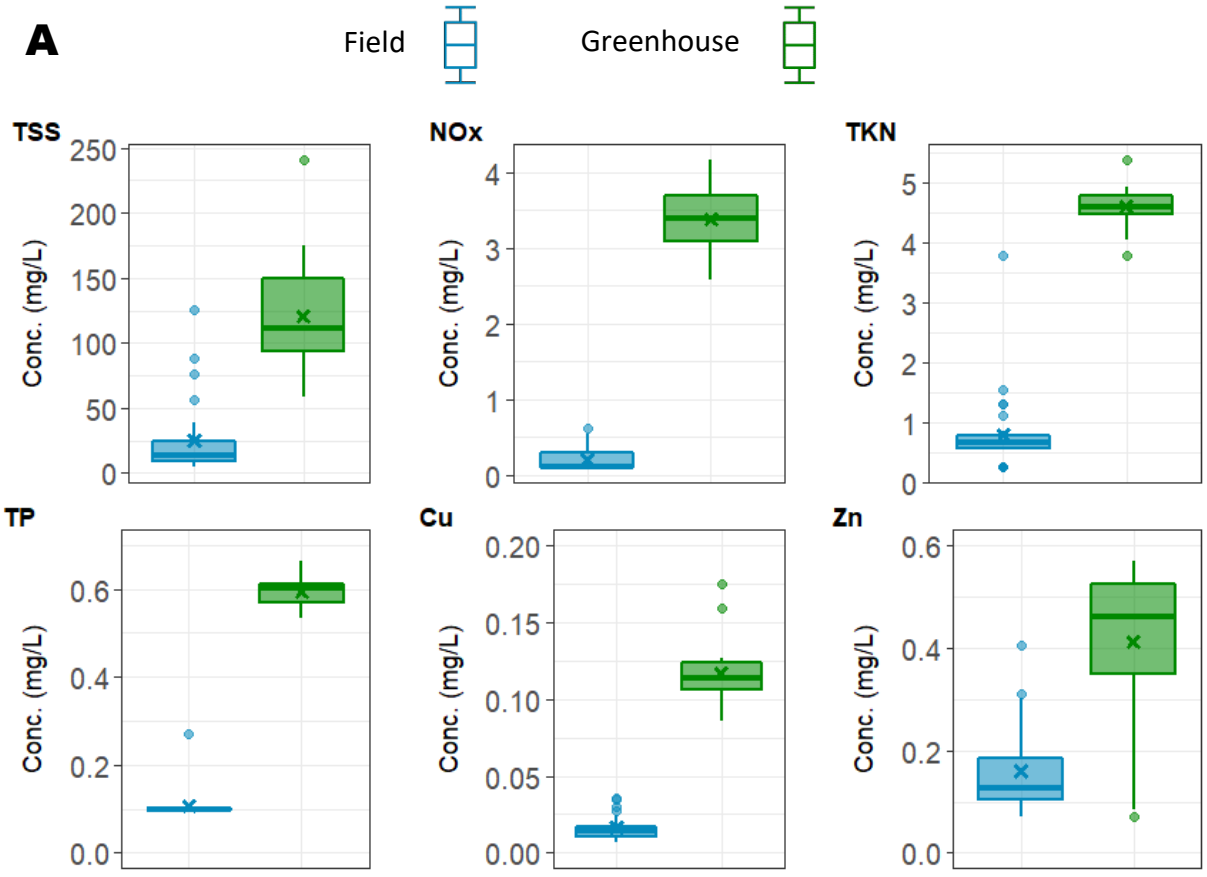


Figure 3-2: Water Quality Event Rainfall-Duration Distribution Compared to Full Dataset.

Runoff Characteristics

Highway stormwater runoff concentrations are expected to be highly variable (Pamuru et al. 2021; Pitt et al. 2018) and dependent on factors such as rainfall depth, storm intensity, antecedent dry period, drainage area, land use, and Annual Average Daily Traffic (AADT) (Kayhanian et al. 2007; Lee et al. 2011; Li and Barrett 2008). Actual highway stormwater runoff was collected at the highway runoff collection channel, while a synthetic stormwater was used in greenhouse experiments (Figure 3-3). The synthetic stormwater used in the greenhouse experiments matched well to the intended target values (some variation was expected as the base solution used was tap

water). Field concentrations, however, were much lower than expected over the 2.25-yr collection period in comparison to the previously measured data from 2012 (Stagge et al. 2012). There are two likely reasons for this discrepancy. First, concentrations observed in the highway stormwater runoff may trend lower due to dilution of contaminants by larger storm event volumes. In order to collect highway runoff and effluent from both VCB systems, selection of water quality sampling events required a bias toward larger storm events, with storms above ~6.35-mm (0.25-in) selected as targets, and a resulting mean precipitation of 21.5-mm (0.85-in) for all collected water quality events. Second, the study period spanned April 2019-June 2021, during which the COVID-19 pandemic hit, resulting in lower traffic volumes and potentially also reduced pollutant loadings. COVID-19 restrictions began in March 2020 in Maryland, resulting in 11 months of the 27 total in the pre-pandemic period and 16 in the post-pandemic period.



B

		TSS (mg/L)	NO_x-N (mg/L)	TKN-N (mg/L)	TP (mg/L)	Cu (mg/L)	Zn (mg/L)
Field Inflow (n = 31)	mean	16.5	0.159	0.627	0.104	0.0149	0.1454
	stdev	25.6	0.195	0.790	0.106	0.0165	0.1652
Greenhouse Inflow (n = 19)	mean	121	3.3868	4.6055	0.5951	0.1172	0.4124
	stdev	42.6	0.4506	0.3432	0.0344	0.0208	0.1511
Synthetic Stormwater*	target mean	100	2	4	0.5	0.06	0.5

**(From Stagge et al. 2012)*

Figure 3-3: Comparison of Greenhouse and Field Stormwater Influent Concentrations.

On highways, contaminants including TSS and heavy metals are expected to originate primarily from vehicles and pavement wear (Davis et al. 2001; Minnesota Stormwater Manual contributors 2021). Unexpectedly low pollutant concentrations are therefore likely in part due to lower traffic volumes experienced during the COVID-19 pandemic period, which were reduced by as much as 50% in the state of Maryland at the height of the pandemic and did not reach pre-pandemic levels until July 2021 (MDOT 2021). This is corroborated by Annual Average Daily Traffic (AADT) data for a selection of Maryland highways showing approximately 50% reduction at the beginning of the pandemic (RK&K 2020). The 2019 AADT (average annual daily traffic) for MD Rt. 32 was 77,881 in 2019 as per mapping provided by the Maryland Department of Transportation State Highway Administration (MD DOT SHA) (Data Services Division's Traffic Monitoring System (TMS) 2020), and so could be estimated as 38,940 for the early portion of the pandemic period. AADT was shown to have a significant effect on constituent concentrations when other effects (antecedent dry period, rainfall depth, rainfall intensity, land use etc.) were also accounted for (Kayhanian et al. 2003, 2007). In order to address the lower input concentrations, expected highway pollutant concentrations were included in plots and tables for comparison, and discussion includes contextualization for both the observed and expected input values.

Table 3-3: Summary EMC Statistics for Field Experiments.
a) highway runoff statistics; b) 3-m and 6-m VCB statistics; expected highway mass loading was calculated using mean concentrations expected in stormwater runoff; this comparison was made because field observed concentration were much lower than expected.

(a)

		Highway Runoff (n = 28)			
	Criteria	Expected Mean*	Measured Mean(Range)	Median	Criteria Exceed.
Parameter	mg/L	mg/L	mg/L	mg/L	%
TSS	25[a]	100	26 (4.3-126)	13.4	25
NO_x	0.2[a]	2	0.19 (0.1-0.614)	0.1	39
TKN	0.49[c]	4	0.77 (0.25-3.79)	0.677	75
TN	0.69[b]	6	0.98 (0.35-4.34)	0.856	61
TP	0.03565[b]	0.5	0.11 (0.1-0.272)	0.1	100
	µg/L	µg/L	µg/L	µg/L	%
Total Cu	13[a]	60	16 (6.9-36.1)	14.7	61
Filtered Cu	-	-	6 (2.5-14.5)	6.1	-
Filterable Cu	-	-	7.6 (2.5-27.8)	7.5	-
Total Zn	120[b]	500	165 (69.5-405)	128	61

** Approximate mean concentration from highway runoff collected at the same site previously (Stagge et al. 2012), and synthetic stormwater target*

a From Davis and McCuen (Davis and McCuen 2005b; a)

b From US EPA National Recommended Water Quality Criteria Aquatic Life Criteria Table or Ecoregional Nutrient Criteria Table (US EPA 2013, 2015a)

c Estimated as difference between TN and NO_x criteria

(b)

		3-m Effluent (n = 26)			6-m Effluent (n = 27)		
	Criteria	Mean (Range)	Median	Criteria Exceed.	Mean (Range)	Median	Criteria Exceed.
Parameter	mg/L	mg/L	mg/L	%	mg/L	mg/L	%
TSS	25[a]	22 (10.9-57.6)	18.6	31	17 (7-51.8)	13.7	15
NO_x	0.2[a]	4.4 (0.1-30)	0.809	65	10.2 (0.1-71.3)	1.3	78
TKN	0.49[c]	15 (2.29-49.1)	11.6	100	11 (2.1-38.9)	6.92	100
TN	0.69[b]	20 (2.39-60.4)	13	100	21 (2.2-95.8)	10.26	100
TP	0.03565[b]	6.41 (2.04-11.5)	6.44	100	2.91 (0.843-6.94)	2.78	100
	µg/L	µg/L	µg/L	%	µg/L	µg/L	%
Total Cu	13[a]	156 (31.7-409)	141	100	78 (25.4-141)	65	100
Filtered Cu	-	154 (30.8-396)	136	-	77 (22.5-146)	63	-
Filterable Cu	-	3.2 (2.5-25)	2.5	-	3.3 (2.5-8)	2.5	-
Total Zn	120[b]	117 (33.8-250)	112	42	50 (28.9-140)	46	4

** Approximate mean concentration from highway runoff collected at the same site previously (Stagge et al. 2012), and synthetic stormwater target*

a From Davis and McCuen (Davis and McCuen 2005b; a)

b From US EPA National Recommended Water Quality Criteria Aquatic Life Criteria Table or Ecoregional Nutrient Criteria Table (US EPA 2013, 2015a)

c Estimated as difference between TN and NO_x criteria

Table 3-4: Summary EMC Statistics for Greenhouse Experiments.
a) synthetic runoff statistics; b) greenhouse mesocosm VFS effluent statistics; c) greenhouse mesocosm VCB effluent statistics

(a)

		Synthetic Runoff (n = 19)		
	Criteria	Mean (Range)	Median	Criteria Exceed.
Parameter	mg/L	mg/L	mg/L	%
TSS	25[a]	121 (59-241)	111	100
NO_x	0.2[a]	3.39 (2.58-4.17)	3.39	100
TKN	0.49[c]	4.61 (3.8-5.39)	4.6	100
TN	0.69[b]	7.99 (6.88-8.95)	8.1	100
TP	0.03565[b]	0.60 (0.53-0.66)	0.6	100
	µg/L	µg/L	µg/L	%
Total Cu	13[a]	117 (85-175)	114	100
Filtered Cu	-	101 (50.8-166)	95	-
Filterable Cu	-	17 (2.5-42)	17	-
Total Zn	120[b]	412 (70-569)	461	89

** The first three storm events for Study 1 were not sent for water quality analysis.*
*** One storm event resulted in a large amount of compost erosion, resulting in high effluent concentrations from the VCB layer.*
a From Davis and McCuen (Davis and McCuen 2005b; a)
b From US EPA National Recommended Water Quality Criteria Aquatic Life Criteria Table or Ecoregional Nutrient Criteria Table (US EPA 2013, 2015a)
c Estimated as difference between TN and NO_x criteria

(b)

		Study 1 VFS Effluent (n = 27)*			Study 2 VFS Effluent (n = 29)		
	Criteria	Mean (Range)	Median	Criteria Exceed.	Mean (Range)	Median	Criteria Exceed.
Parameter	mg/L	mg/L	mg/L	%	mg/L	mg/L	%
TSS	25[a]	25.9 (11.8-47.3)	25.3	56	28 (5.7-70)	23.2	43
NO_x	0.2[a]	2.69 (1.97-3.37)	2.71	100	9.29 (1.84-61.5)	3.19	100
TKN	0.49[c]	5.98 (3.66-8.89)	5.88	100	13.86 (5.56-49.6)	9.21	100
TN	0.69[b]	8.67 (5.83-11.8)	8.18	100	23.15 (8.62-111)	13.1	100
TP	0.03565[b]	0.849 (0.406-1.67)	0.814	100	1.30 (0.1-3.97)	1.09	100
	µg/L	µg/L	µg/L	%	µg/L	µg/L	%
Total Cu	13[a]	27.6 (16-36)	28.6	100	43 (12.2-78.3)	45.5	93
Filtered Cu	-	25.8 (15.5-33.3)	27	-	45.1 (11.9-85.2)	45.6	-
Filterable Cu	-	2.6 (2.5-5.4)	2.5	-	2.7 (2.5-4.5)	2.5	-
Total Zn	120[b]	30.5 (14.7-53.8)	29.5	0	61.8 (17-13.1)	55.2	7

** The first three storm events for Study 1 were not sent for water quality analysis.*

*** One storm event resulted in a large amount of compost erosion, resulting in high effluent concentrations from the VCB layer.*

a From Davis and McCuen (Davis and McCuen 2005b; a)

b From US EPA National Recommended Water Quality Criteria Aquatic Life Criteria Table or Ecoregional Nutrient Criteria Table (US EPA 2013, 2015a)

c Estimated as difference between TN and NO_x criteria

(c)

		Study 1 VCB Effluent (n = 6)*			Study 2 VCB Effluent** (n = 7)		
	Criteria	Mean (Range)	Median	Criteria Exceed.	Mean (Range)	Median	Criteria Exceed.
Parameter	mg/L	mg/L	mg/L	%	mg/L	mg/L	%
TSS	25[a]	38 (14-62)	30	60	621 (22.5-2960)	140	71
NO_x	0.2[a]	1.99 (1.39-2.79)	1.9	100	23.9 (0.722-67.2)	14.1	100
TKN	0.49[c]	5.36 (4.14-7.86)	4.85	100	30.9 (5.34-63)	28.6	100
TN	0.69[b]	7.36 (5.88-9.25)	7.36	100	54.7 (7.78-130)	65.6	100
TP	0.03565[b]	1.31 (0.73-2.41)	1.05	100	5.09 (1-9)	5.78	100
	µg/L	µg/L	µg/L	%	µg/L	µg/L	%
Total Cu	13[a]	30.4 (22.4-43.6)	27.9	100	87.9 (26.1-200)	85.2	100
Filtered Cu	-	27.7 (20.3-40.2)	25	-	55.2 (26.3-83.6)	57.8	-
Filterable Cu	-	2.9 (2.5-3.4)	2.9	-	34.1 (2.5-138)	4.3	-
Total Zn	120[b]	59.7 (28.2-113)	48.3	0	335 (63.9-1240)	168	57

** The first three storm events for Study 1 were not sent for water quality analysis.*

*** One storm event resulted in a large amount of compost erosion, resulting in high effluent concentrations from the VCB layer.*

a From Davis and McCuen (Davis and McCuen 2005b; a)

b From US EPA National Recommended Water Quality Criteria Aquatic Life Criteria Table or Ecoregional Nutrient Criteria Table (US EPA 2013, 2015a)

c Estimated as difference between TN and NO_x criteria

Table 3-5: Summary Mass Statistics for Field Experiments.
a) observed mass statistics for field experiments; b) estimated mass statistics accounting for total volume removal; expected highway mass loading was calculated using mean concentrations expected in stormwater runoff; this comparison was made because field observed concentration were much lower than expected.

(a)

	3-m Observed Volume Removal = 27%				6-m Observed Volume Removal = 38%			
	Highway Runoff (n = 21)	3-m Effluent (n = 21)			Highway Runoff (n = 24)	6-m Effluent (n = 24)		
Parameter	Observed/ Expected g	g	Observed Removal (%)	Potential Expected Removal (%)	Observed/ Expected g	g	Observed Removal (%)	Potential Expected Removal (%)
TSS	4,131/27,670	3,192	23	88	6,555/41,992	4,349	34	90
NO_x	42.8/775	307	(-616)	60	59.4/1177	2,021	(-3304)	(-72)
TKN	135/1,054	2,049	(-1418)	(-94)	209/1600	1,869	(-796)	(-17)
TN	178/1,829	2,356	(-1225)	(-29)	268/2776	3,890	(-1352)	(-40)
TP	22.9/136	1,023	(-4369)	(-651)	34.7/207	630	(-1713)	(-205)
Total Cu	3.25/26.8	27.9	(-757)	(-4)	5.05/40.7	16.5	(-227)	59
Filtered Cu	1.33/23.2	27.5	(-1971)	(-19)	1.87/35.2	15.9	(-750)	55
Filterable Cu	1.88/3.87	0.882	53	77	3.14/5.88	1.13	64	81
Total Zn	33.9/94.4	19.7	42	79	52.8/143	10.5	80	93

(b)

	3-m Total Volume Removal = 44%		6-m Total Volume Removal = 55%	
	3-m Effluent (n = 21)		6-m Effluent (n = 24)	
Parameter	Total Removal (%)	Total Potential Expected Removal (%)	Total Removal (%)	Total Potential Expected Removal (%)
TSS	53	93	54	93
NO_x	(-339)	75	(-2252)	(-19)
TKN	(-832)	(-19)	(-519)	19
TN	(-713)	21	(-903)	3
TP	(-2642)	(-361)	(-1153)	(-111)
Total Cu	(-426)	36	(-126)	72
Filtered Cu	(-1171)	27	(-487)	69
Filterable Cu	71	86	75	87
Total Zn	64	87	86	95

Table 3-6: Summary Mass Statistics for Greenhouse Experiments.

	Overall Volume Removal = 30%			**Overall Volume Removal = 25%**		
Parameter	Study 1 OUT* Mass Removal (%) (n = 31)**			Study 2 OUT* Mass Removal (%) (n = 29)		
	Mass In (mg)	Mass Out (mg)	Weighted Removal	Mass In (mg)	Mass Out (mg)	Weighted Removal
TSS	180000	40000	78%	280000	58000	79%
NO_x	6018	4182	31%	12870	14392	(-12%)
TKN	7620	9448	(-24%)	10535	25374	(-141%)
TN	13668	13475	1%	17470	39765	(-128%)
TP	1020	1323	(-30%)	1360	2952	(-117%)
Total Cu	195	44	77%	280	90	68%
Filtered Cu	162	42	74%	265	92	65%
Filterable Cu	33	2.73	92%	25	5.37	79%
Total Zn	687	54	92%	1065	127	88%

** Study 1 and 2 OUT is the total mass for all mesocosm boxes in each setup.*

*** The first three storm events were not sent for water quality analysis for Study 1.*

Total Suspended Solids (TSS)

Greenhouse experiments significantly reduced TSS concentrations from highway runoff through assessment of effluent EMCs for both VFS and Study 1 VCB layers ($p < 0.001$ for all), while in the field there was no statistical significance between influent and effluent (Table 3-3 and Table 3-4). VCB effluent from Study 2 was not statistically evaluated, since a large intensity (10-cm/hr, 4-in/hr) event conducted before full vegetative establishment caused significant erosion and elevated effluent concentrations, preventing comparison. Mean effluent EMCs were 25.3 mg/L for greenhouse Study 1 and 23.2 mg/L for Study 2, reduced from the synthetic stormwater mean of 121 mg/L. At the field site, mean effluent EMCs were 22 mg/L for the 3-m VCBS and 17 mg/L for the 6-m VCB, in comparison to 26 mg/L for observed influent.

Particulate matter (as TSS) should be removed via particle filtration during stormwater infiltration and particle settling during surface flow (Davis et al. 2010). Removal of TSS should depend highly on filtration at the beginning of the storm event in the form of a first flush (Deletic 1998; Flint and Davis 2007; Lee et al. 2002), then could be dependent on both filtration and settling through the later part of the storm event if surface flow occurs. When surface flow occurs, vegetation can have a major impact on particle removal as the grass blades resist flow and increase channel roughness (Abood et al. 2006), which reduces flow velocity and increases particle settling. For the field dataset, the contribution of settling versus filtration cannot be directly identified due to the low observed influent concentrations. In the greenhouse, effluent collected from the VFS layer could only undergo filtration, while effluent collected from the VCB layer may have experienced both filtration and settling through surface flow.

Comparison of probability plots (Figure 3-4) for field and greenhouse show similar effluent EMCs (field range ~5-60 mg/L and median ~15 mg/L, greenhouse range ~5-70 mg/L and median ~24 mg/L) despite the disparity in median influent concentrations (13.4 mg/L field, 111 mg/L greenhouse), indicating both significant removal of TSS, but also that effluent TSS is likely originating mainly from the media itself rather than from remaining TSS in highway runoff. Greenhouse effluent in Figure 3-4 was collected from the VFS layer, meaning it had already infiltrated through both the compost and soil layers, further supporting this idea. Though field performance evaluation was limited by mostly low influent concentrations, for influent TSS concentrations greater than 20-30 mg/L (Figure 3-4), effluent concentrations for both the 3-m and 6-m VCBs remained lower, indicating TSS removal. Median effluent TSS EMCs are all at or below the criterion of 25 mg/L for excellent water quality in the Potomac River Basin (Davis and McCuen 2005a), with effluent EMCs exceeding this 15% of the sampled population for the 3-m field VCB, 11% for the 6-m field VCB, 43-56% for greenhouse VFS effluent and 60-71% for greenhouse VCB effluent (Table 3-3 and Table 3-4). Lower percent exceedance of criteria of the VFS effluent over VCB effluent indicates higher filtration as stormwater passes through both layers. Lower percent exceedance shown by the 6-m system over the 3-m, and better performance of both over the greenhouse experiments (1.8-m length), also indicates a better performance with longer flow path. For all experiments (except for greenhouse VCB effluent, which had a low number of observations), the majority of VCB discharges meet the TSS goal for water quality and VCBs provide significant protection against export of particulate matter to downstream waters.

Total weighted mass removals in the greenhouse experiment ranged from 78-79%, much larger than the 25-30% total stormwater volume removal, indicating improved performance over

volume retention alone (Table 3-5 and Table 3-6). However, field mass removals were found to be only 23% and 34% (in comparison to 27-38% observed volume removal) for the 3-m and 6-m VCBs, respectively, due to similarity in influent and effluent concentrations. In comparison to 100 mg/L for an expected influent mean EMC, field VCBs may potentially remove up to 88% for the 3-m field VCB, and 90% for the 6-m field VCB, though this is only an estimate since it was not directly measured. Accounting for the fraction of storm events which were fully captured by the field VCBs (~17% of total volume for each) an estimate of ~93% total mass removal is obtained for both VCBs. TSS reductions for VFSs of >75% for 8 to 20-m (Knight et al. 2013), 50-98% for 2.5 to 20-m (Gharabaghi et al. 2006), 51% for 7.6-m and 67% for 15.2-m (Winston et al. 2011), and >85% for 10-m (Han et al. 2005) have been observed previously, making VCB addition more effective than VFS alone in retaining TSS mass. In comparing to these previous studies on VFS by length, VCB addition attained higher TSS mass retention using a shorter flow path (~77% for 1.8-m, 88% for 3-m, and 90% for 6-m) than retention previously seen for VFSs (~8 to 20-m results in similarly high removals) (Gharabaghi et al. 2006; Han et al. 2005; Knight et al. 2013; Winston et al. 2011). Flow path length is a major factor in TSS removal for VFS systems (Gharabaghi et al. 2006; Yu et al. 2001), with length past the first 10 meters not having a significantly improved performance (Barrett et al. 1998; Gharabaghi et al. 2006; Han et al. 2005; Winston et al. 2017; Yu et al. 2001). In this study, lengths past 3 meters did not have a significantly better performance, further indicating the increased efficiency provided by the VCB layer to the VFS.

TSS export was observed for one storm event in the greenhouse (Figure 3-7). A 102 mm/hr (4 in/hr) event was conducted prior to full vegetative establishment 26 days after compost application and seeding which resulted in significant erosion from two of the four mesocosm

boxes. During this event, TSS effluent EMC values collected from the VCB layer (~200-3,000 mg/L) were much higher than for the influent (mean = 121 mg/L) while storm events conducted later in the experiment showed TSS removal in the VCB layer. No erosive events or significant TSS export was observed at the field site, likely because an erosion control straw matting was installed over the VCB. Protection of VCBs from high intensity storm events immediately after installation should be important, and these types of erosion control matting are recommended to avoid damage to the VCB and subsequent negative effects to downstream waterbodies.

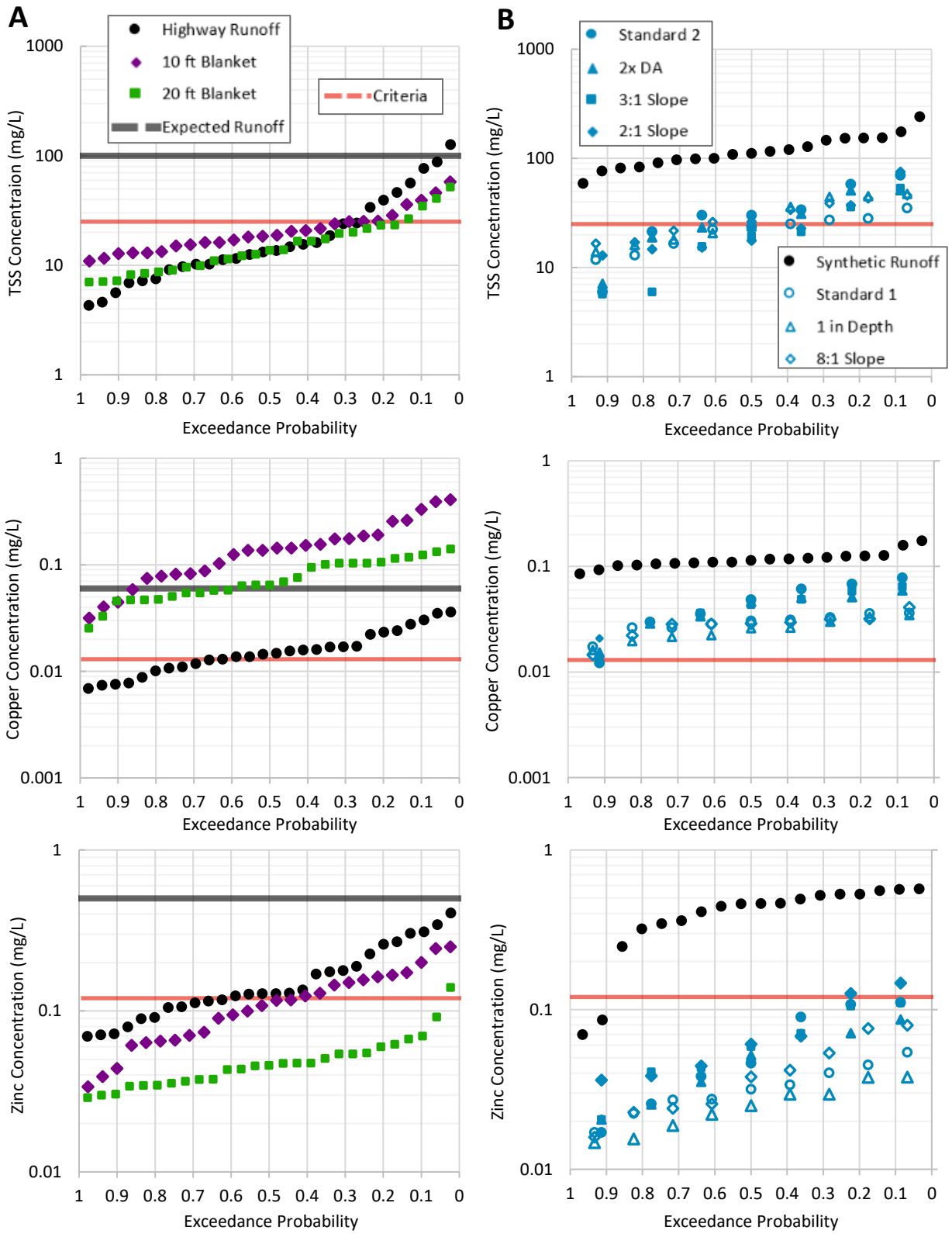


Figure 3-4: Field and Greenhouse Exceedance Probability for TSS, Total Cu, and Total Zn. A) field; B) greenhouse (VFS layer effluent only); detection limits are 1 mg/L for TSS, 0.005 mg/L for Cu, and 0.005 mg/L for Zn.

Heavy Metals

Consistent removal of both the dissolved and particulate copper fraction was observed in the greenhouse while copper leaching in the dissolved phase was observed in the field, likely in part due to differences in compost copper content (Table 3-7) for each site (field compost had 3.44 times higher copper content). Comparison of total copper probability plots (Figure 3-4) for field and greenhouse experiments also demonstrate net export of copper for field VCBs and net removal for greenhouse VCBs. Comparison of storm event EMCs (Table 3-3 and Table 3-4) outline these differences in metals performance. The field effluent has a median of 141 µg/L (range ~32-410 µg/L) for the 3-m VCB and 65 µg/L (range ~25-140 µg/L) for the 6-m VCB while the influent median is 14.7 µg/L, whereas the greenhouse has a median of ~35 µg/L (range ~12-80 µg/L) for VFS effluent and median of 27.9 µg/L (range ~22-44 µg/L) for the Study 1 VCB effluent, while the influent median is 114 µg/L. For field experiments, all effluent total copper EMCs exceed water quality criterion of 13 µg/L (Davis and McCuen 2005b), while for greenhouse experiments only ~30-40% exceed the criterion.

Table 3-7: Compost Composition and Potential Effect on Experiment Results.

		Compost				Experiment Effluent			
Parameter	units	Field Mean (n = 3)	GH Mean (n=3)	Field compared to GH*		Field 3-m mean EMC compared to GH*		Field 6-m mean EMC compared to GH*	
pH	--	5.2	6.8	-24%	a	-	-	-	-
C:N Ratio	--	10.9	13.2	-17%	a	-	-	-	-
Total Carbon	%	16.03	32.86	-51%	a	-	-	-	-
Total Nitrogen	%	1.469	2.492	-41%	-	-15%	-	-10%	-
P	%	0.951	0.273	+248%	b	+393%	a	+123%	a
Cu	mg/kg	253	57	+344%	a	+263%	a	+81%	a
Zn	mg/kg	451	173	+161%	a	+89%	a	-18%	-

** Compared to Study 2 in the greenhouse because Study 1 was missing data from the first 3 storm events*
a $p < 0.001$ b $p < 0.01$

Previous studies on compost blankets as erosion control measures focused on prevention of metals mass release in comparison to bare slopes (topsoil only) rather than on net removals (Chaganti and Crohn 2014; Glanville et al. 2003). Studies evaluating compost for heavy metals removal show varying results, with some observing modest (~30%) to high (>90%) metals removal, including for copper and zinc (Finney et al. 2010; Khan et al. 2009; Lim et al. 2015; Seelsaen et al. 2007), and others instead observing metals leaching, with the most commonly observed being copper (Chahal et al. 2016; Colton et al. 2014; Mullane et al. 2015).

Metals transport is heavily influenced by partitioning as particulate phase metals are expected to be removed concurrently with TSS through filtration and settling, while dissolved metals are affected by a more complex array of chemical and physical processes. Metals, often associated with the particulate phase in stormwater (Djukić et al. 2016; Han et al. 2006; Lange et al. 2020), should experience removal through retention of the first flush through filtration as well as settling and filtration if surface flows occur, the same as for TSS removal. In the dissolved phase, free positively charged metals may be removed through attachment to negatively charged humic substances in the VCB layer, as has been observed previously for Cu and Zn (Finney et al. 2010; Khan et al. 2009; Lim et al. 2015; Seelsaen et al. 2007). However, heavy metals have been shown to complex with Dissolved Organic Matter (DOM) in stormwater (Pamuru et al. 2021), making them more likely to remain in the aqueous phase and bypass potential removal pathways. This could partially explain the disparity in metals removal results between compost studies which used real stormwater runoff in the field which saw ~30% removal for Cu and Zn (Finney et al. 2010) and those using a synthetic stormwater not containing DOM in a lab setting which saw removals greater than ~85% (Lim et al. 2015; Seelsaen et al. 2007). In addition, because compost contains heavy metals, concurrent release of metals with the dissolution of organic

matter is also possible, or desorption may occur when influent copper concentrations are low. Release of dissolved copper from compost in SCMs has been observed previously (Colton et al. 2014; Mullane et al. 2015). DOM-complexed metals are less bioavailable than free metal ions, however, total removal is still important since metal export in all forms (particulate, free ionic, DOM-complexed) could still accumulate in the downstream environment and undergo further transformation to more bioavailable, toxic forms. In the VFS layer, metals removal may also occur through adsorption to organic matter or to minerals, especially iron and aluminum oxides (Davis et al. 2010), however VFSs have shown limited effectiveness for dissolved metals removal (Boger et al. 2018).

Evaluation of copper partitioning (Figure 3-5 and Figure 3-6) gives additional insight into removal pathways. Particulate copper in field influent made up ~55% of total copper based on the mean, while in the greenhouse it was only ~10%. Both sites show removal of particulate copper, with many effluent EMCs below the detection limit (0.005 mg/L) (represented as half the detection limit in plots, 0.0025 mg/L). Release of dissolved copper occurred in field VCBs with retention in greenhouse VCBs. This further supports the understanding that elevated effluent concentrations observed at the field site are due to leaching of copper from the compost itself, possibly in the form of DOM-metals complexes, as has been indicated previously (Chahal et al. 2016). Explanation for copper export at the field site as opposed to removal in the greenhouse may come from compost composition (Table 3-7). Compost used in the field experiment had significantly greater copper content ($p < 0.001$) by 344% than compost used in the greenhouse experiment. This parallels a significant increase in mean effluent concentrations of 263% for the 3-m VCB and 81% for the 6-m VCB over mean greenhouse effluent concentrations ($p < 0.001$ for both). Leaching may also have been exacerbated by low influent copper concentrations which

encouraged desorption of copper attached to compost as well as a significantly lower pH (5.2 field, 6.8 greenhouse, $p < 0.001$) (Table 3-7) in the field compost which may have encouraged higher copper release. Particulate copper mass (Table 3-5 and Table 3-6) was removed at both sites with mass reductions of ~79-92% for the greenhouse, 53% for field 3-m, and 64% for field 6-m (all higher than the observed volume removal) indicating effective performance for coincidental removal of heavy metals with TSS removal. The majority of leached effluent copper at the field site was in the dissolved phase (Figure 3-5). For dissolved copper, greenhouse removal ranged from 58-75% while field export was observed at -1,970% for the 3-m VCB and -750% for the 6-m VCB. When using expected influent concentrations, dissolved copper leaching for the 3-m system drops to -19% and net removal of 55% occurs for the 6-m system, however, this scenario was not directly observed, and should only be considered an estimate.

The theory that effluent TSS is likely flushing from the media layers through infiltration rather than being bypassed as surface flow is also further supported by differences in field site copper partitioning between the influent and effluent TSS (Figure 3-6). In addition to the particulate fraction of copper being higher in the field influent than the effluent (~55% vs 10%), the partitioning coefficient K_d (L/kg) was calculated for data above detection and shows significantly higher values ($p < 0.01$ for both) for particles in the influent (mean = 6.52x104 L/kg) than effluent (mean = 1.86x103 L/kg for 3-m VCB and mean = 6x103 L/kg for 6-m VCB). Influent K_d values are within range of those observed previously for copper in stormwater runoff (Maniquiz-Redillas and Kim 2014; Sansalone et al. 1996; Sansalone and Buchberger 1997). The differences in K_d indicate that the particles entering the VCBs are physically different from those exiting, strengthening evidence that influent particles are mostly or totally retained while particles exiting the system are flushed from the media itself.

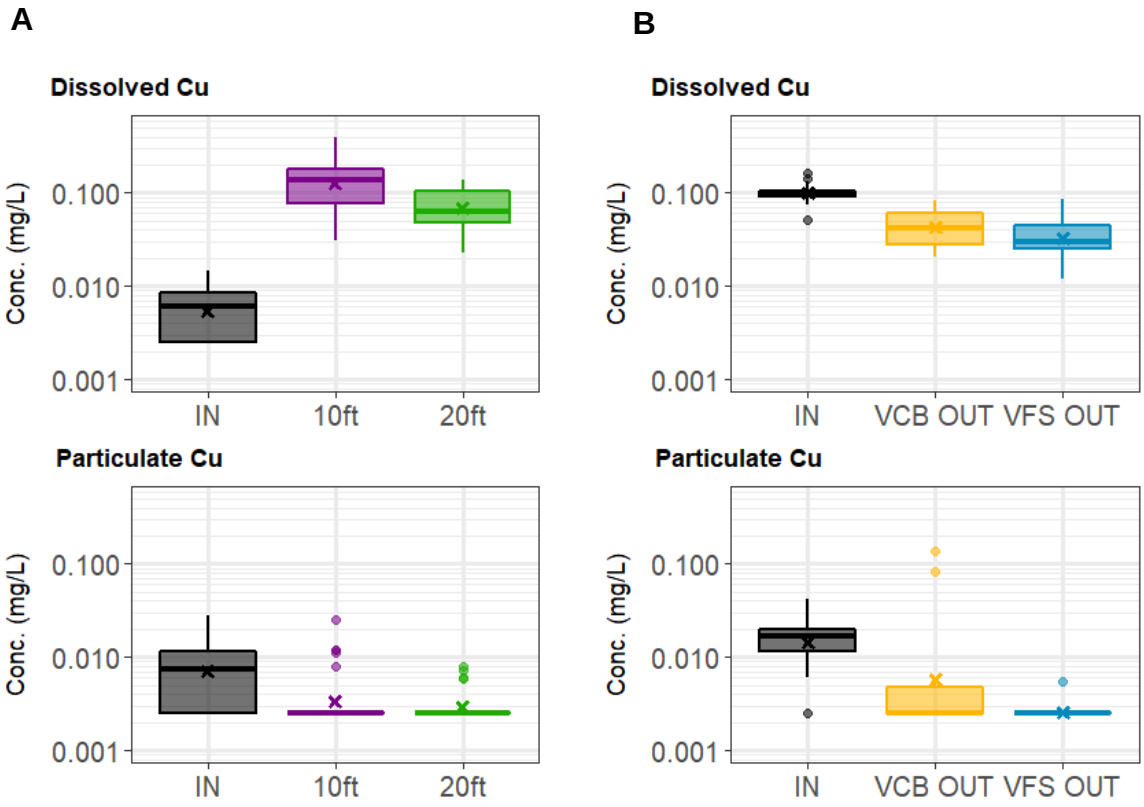


Figure 3-5: Copper Partitioning for Influent and Effluent.
A) Field Study; B) and Greenhouse Studies; detection limit for dissolved and particulate Cu is 0.005 mg/L.

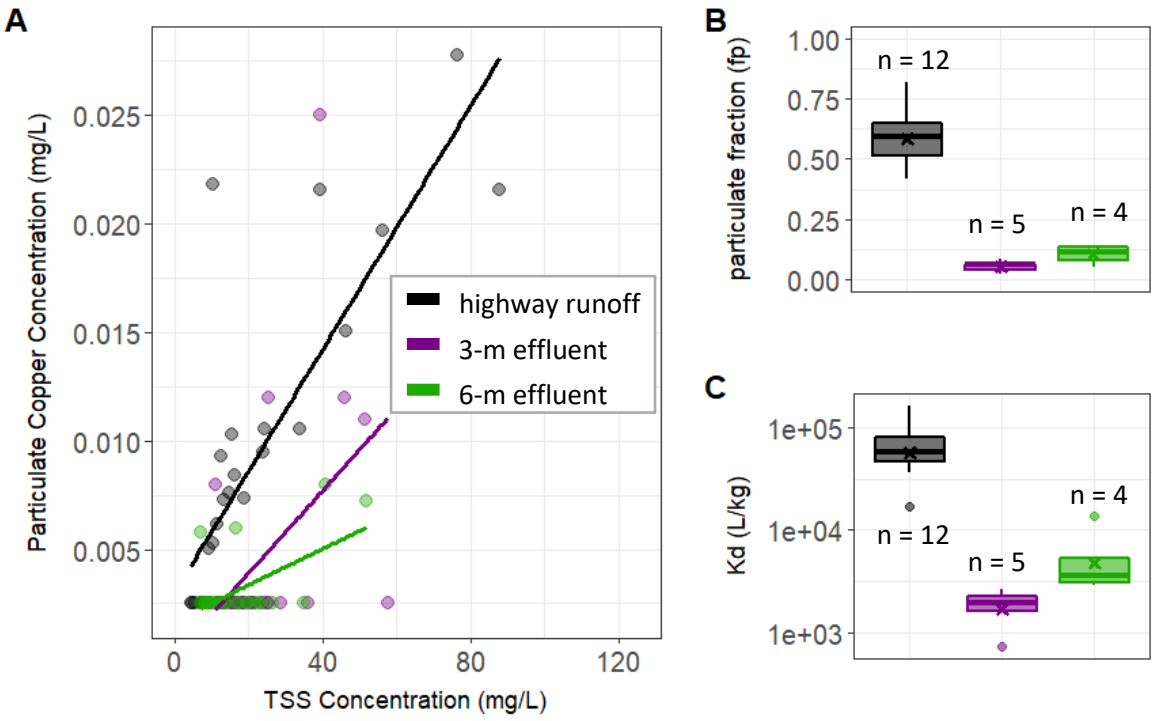
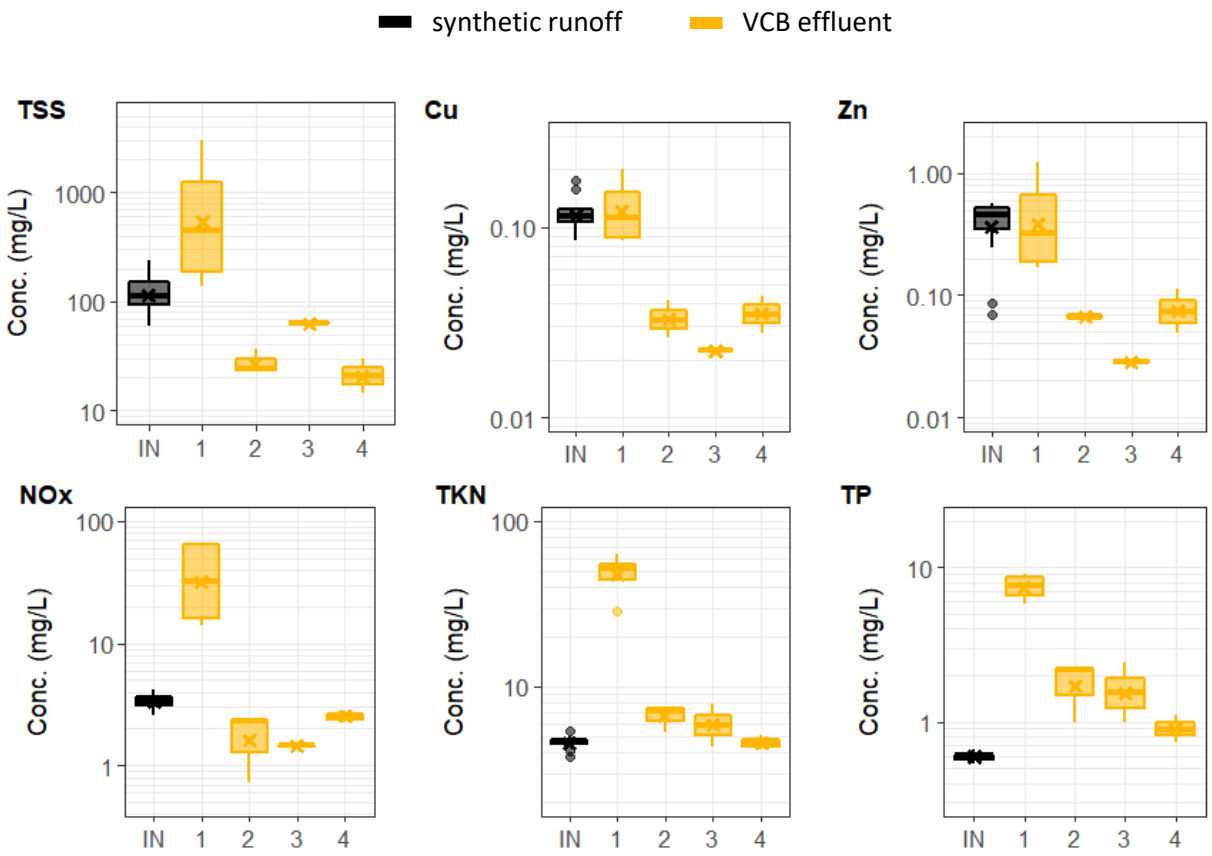


Figure 3-6: Copper Partitioning and K_d Values for Field Influent and Effluent. A) TSS Correlation; B) particulate fraction; C) partitioning coefficient K_d; detection limit for dissolved and particulate Cu is 0.005 mg/L.

For zinc, consistent total removal was observed at both sites, though evaluation of partitioning was not done. Mean EMCs (Table 3-3 and Table 3-4) were reduced from 412 µg/L in the influent to ~30-60 µg/L in VFS effluent and ~48 µg/L in Study 1 VCB effluent for greenhouse experiments and reduced to 117 µg/L for field 3-m and 50 µg/L for field 6-m in comparison to 165 µg/L for observed influent mean EMC. Additionally, probability plots for total zinc (Figure 3-4) indicate that both field and greenhouse experiments experienced removal of total zinc with field effluent having a range of ~30-250 µg/L and median of ~85 µg/L and an influent median of 128 µg/L, and the greenhouse VFS effluent having a range of ~15-55 µg/L and median of ~45 µg/L and an influent median of 461 µg/L. The water quality criterion of 120 µg/L (US EPA 2015a) was exceeded in the greenhouse experiment between 0-7% of storm

events for both VFS and VCB effluent, and in the field 42% for the 3-m and 4% for the 6-m system.

Unlike for dissolved copper, zinc export was not observed at the field site, despite a significantly larger Zn content (161%, $p < 0.001$) in the field compost (Table 3-7). For total zinc, both field and greenhouse showed significant mass removals higher than the observed volume removals (Table 3-5 and Table 3-6) of ~85-93% for greenhouse (25-30% volume removal), 42% for field 3-m (27% volume removal), and 80% for field 6-m (38% volume removal), indicating additional removal processes in addition to volume retention alone. The 6-m field VCB had increased retention of zinc over the 3-m VCB, indicating better performance overall for a longer flow path. Without partitioning data, specific removal processes cannot be determined. However, previous research on stormwater characterization has shown that the majority of Zn in stormwater was mainly in the particulate phase while Cu was mainly in the dissolved phase (Pamuru et al. 2021), which could indicate that much of the removal could be coincidental with TSS removals through settling and filtration. When comparing to the expected influent mass, a potential 79% mass retention was estimated for the field 3-m VCB, and 93% for the field 6-m VCB, though these were not directly measured.



Storm Event	Study	Days after start of experiment	Synthetic Storm Intensity (in/hr)	n
1*	2	26	4.00 (102 mm/hr)	4
2	2	183	2.00 (51 mm/hr)	3
3	1	296	4.00 (102 mm/hr)	3
4	1	441	6.00 (152 mm/hr)	3

**During Storm 1, two of four mesocosms experienced erosion, prior to full vegetative establishment*

Figure 3-7: Four Storm Events Resulting in VCB Effluent from Greenhouse.

Figure 3-8 outlines significant pathways for heavy metals transport and removal in a VCB/VFS system. Particulate-bound and dissolved forms of Cu and Zn enter the VCB/VFS in highway runoff, with dissolved forms likely associated with DOM. As the storm begins, the first flush of the particulate fraction is likely removed via filtration, with settling and filtration both contributing to particulate metals removal when flowrates are high, causing surface flow. Dissolved metals pass through the VCB and VFS layers, with potential for some removal through volume retention and via adsorption in the VFS, though attachment to DOM may keep metals in the dissolved phase. Cu leaching from compost has also been observed, likely released with the dissolution of organic matter, which may result in net Cu release from the VCB/VFS.

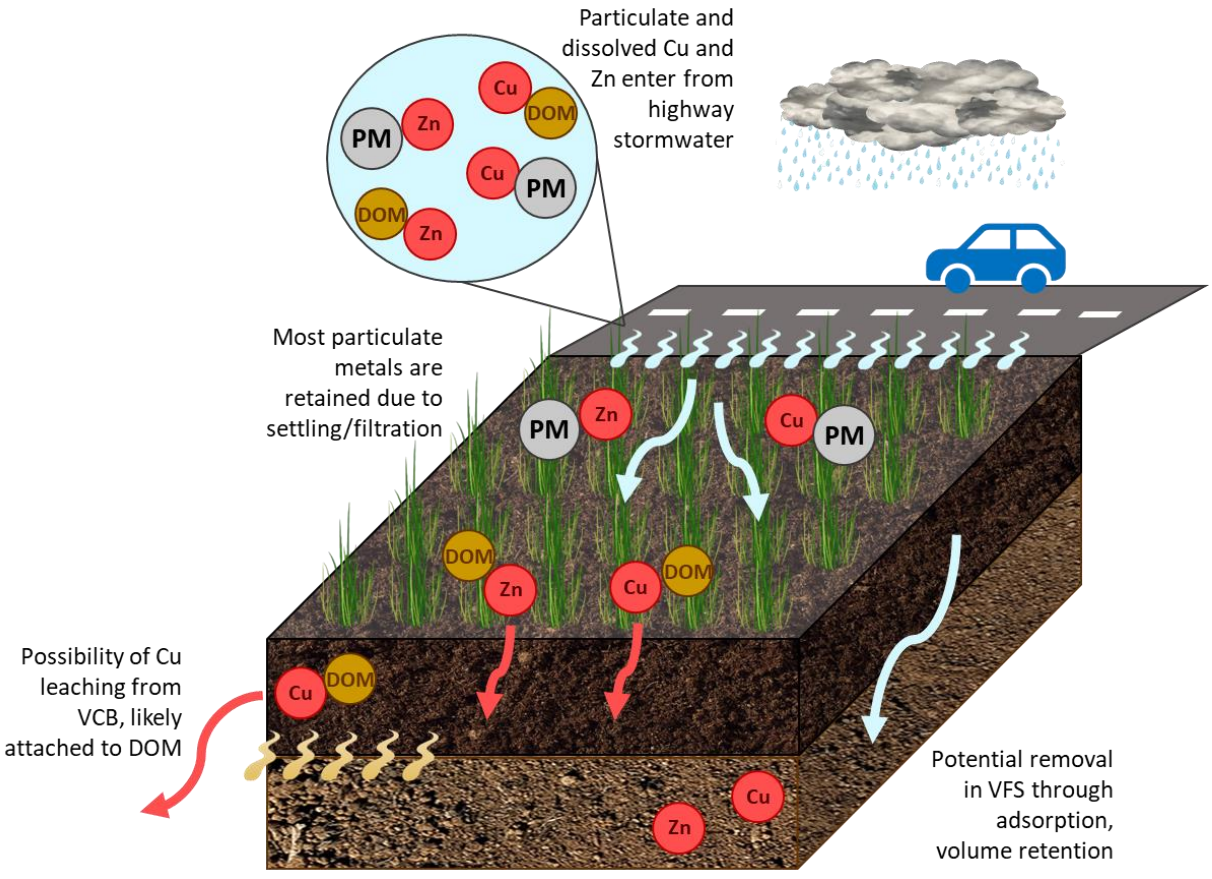


Figure 3-8: Influential Processes Affecting TSS and Metals Movement in a VCB/VFS.

Nutrients

In both experiments VCBs were observed to release, rather than remove, nutrients, as has been observed previously for compost treatments, including VCBs (Curtis et al. 2009; Faucette et al. 2004, 2005, 2007; Glanville et al. 2003). TN concentrations were significantly increased ($p < 0.01$) from influent (0.98 mg/L) to effluent (27.3 mg/L for 3-m and 20.8 mg/L for 6-m VCBs) for the field experiment based on the mean EMCs, as were TP concentrations ($p < 0.001$) from influent (0.11 mg/L) to effluent (6.42 mg/L for 3-m and 2.91 mg/L for 6-m VCBs). Evaluation of greenhouse mean TN EMCs were found to be significantly higher ($p < 0.01$) for Study 2 VFS (23.2 mg/L) and VCB (54.7 mg/L) layers in comparison to the influent (7.99 mg/L), but not for Study 1 (VFS mean EMC = 8.67 mg/L and VCB = 7.35 mg/L). This is likely because the first three storm events were not sent for water quality analysis, missing the highest effluent concentrations. For TP, greenhouse mean EMCs in effluent for VFS and VCB layers in both studies (ranging from 0.8-5 mg/L) were statistically significantly higher ($p < 0.01$ for all) than the influent (0.60 mg/L).

Exceedance probability plots (Figure 3-9) show the magnitude and range of nutrient release. TN effluent EMCs ranged from ~2-96 mg/L with a median of 10-13 mg/L for the field VCBs and from ~6-111 mg/L with a median of 7-13 mg/L for greenhouse VFS effluent and Study 1 VCB effluent. This is in contrast to median influent EMCs of 0.86 mg/L for the field and 8.1 mg/L for the greenhouse. For TP, effluent field EMCs ranged from ~0.8-12 mg/L with a median of 3-6 mg/L, while greenhouse EMCs ranged from ~0.1-4 mg/L with a median of 0.8-1 mg/L for VFS effluent and Study 1 VCB effluent; median influent EMCs were 0.1 mg/L for the field and 0.6 mg/L for the greenhouse. TN and TP water quality criteria of 0.69 mg/L for TN and 0.03656 mg/L for TP from the US EPA National Recommended Water Quality Criteria

Ecoregional Nutrient Criteria for Rivers and Streams (US EPA 2013) were both exceeded for all storm events in both the field and greenhouse. For the largest effluent EMCs at both sites (~60-130 mg/L for TN and 6-12 mg/L for TP), criteria were exceeded by two orders of magnitude for TN and by almost three orders of magnitude for TP. Similarly high concentrations of N and P have been observed previously for stormwater systems using compost (Chahal et al. 2016)

Large mass export of nitrogen and phosphorus were observed for both field and greenhouse experiments, based on mass comparisons of influent and effluent at each site (Table 3-5 and Table 3-6). Greenhouse experiments had net export of -128% for TN while field VCBs had net TN export of -1,225% for the 3-m VCB and -1,352% for the 6-m VCB. For TP, greenhouse VCBs had net export of -132% and field VCBs had net export of -4,369% for the 3-m VCB and -1713% for the 6-m VCB. Differences of an order of magnitude between greenhouse and field percent release is in part due to differences in influent concentrations observed in the field and greenhouse (Figure 3-3). When comparing effluent EMCs to expected influent concentrations, estimated TN removals drop to -29% and -40%, respectively, if comparing to expected influent concentrations and estimated TP removals drop to -651% and -205%, though these were not directly measured. TN concentrations observed at the field and greenhouse were not found to be significantly different from each other based on the mean EMC, while significantly larger TP mean EMCs (393% for 3-m and 123% for 6-m, $p < 0.001$ for both) observed at the field site in comparison to the greenhouse may be partly due to higher phosphorus content in compost used in the field experiment (field compost had 248% higher P content than greenhouse compost, $p < 0.01$) (Table 3-7).

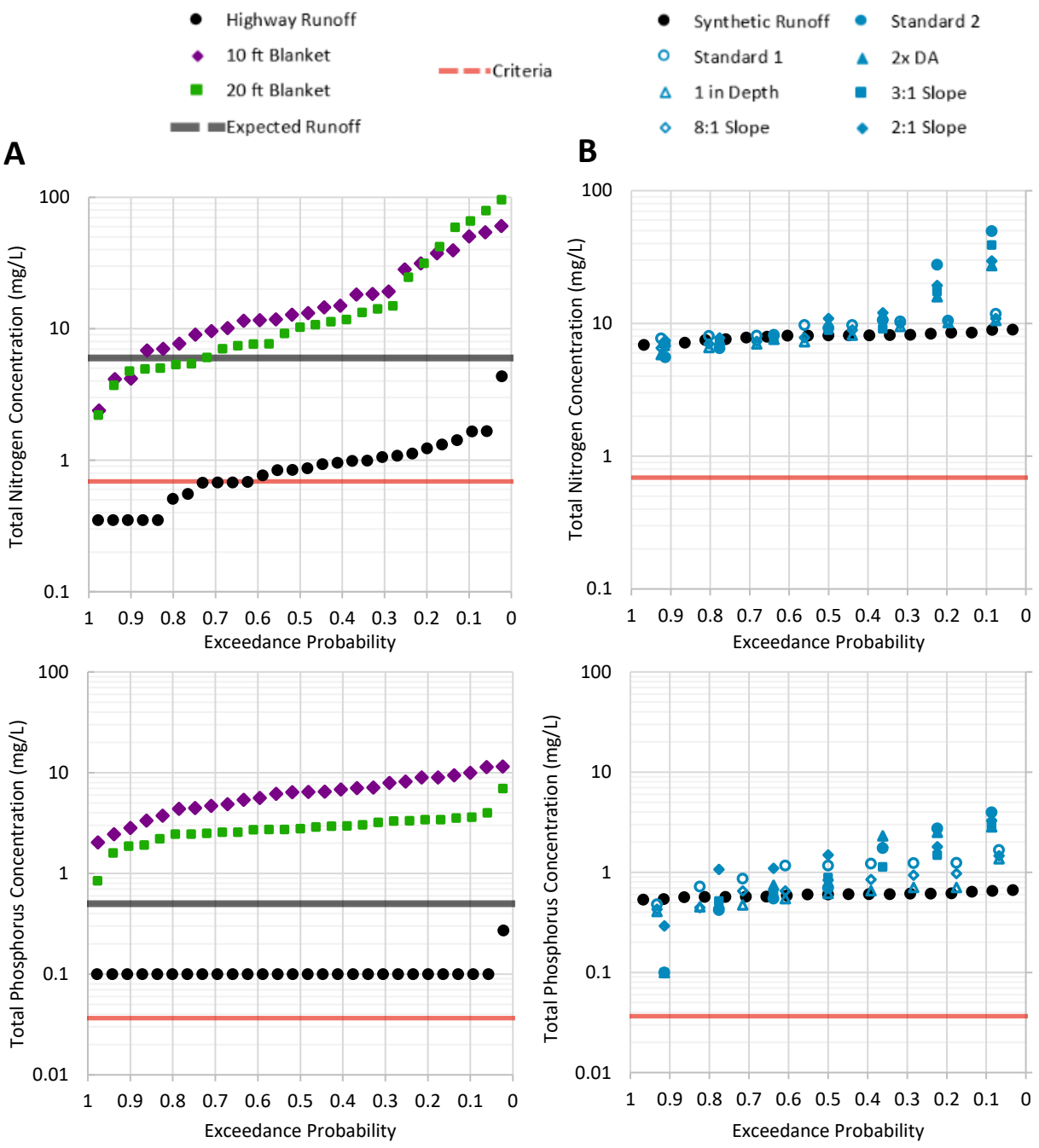


Figure 3-9: Field and Greenhouse Exceedance Probability for TN and TP. A) field; B) greenhouse (VFS layer effluent only); detection limits are 0.7 mg/L for TN (as sum of NO_x and TKN DLs (0.2 and 0.5 mg/L)) and 0.2 mg/L for TP.

Compost is primarily used as a fertilizer, being a nutrient-rich and microbially-active humus material that should provide nutrients to plants immediately after application and through a full growing season (USCC 2001b). Mineralization of compost is expected to occur, releasing the inorganic, soluble forms of nutrients (ammonium (NH_4^+) and orthophosphate (PO_4-P)), with high initial mass release that decreases over time. Because subsequent transformation of NH_4^+ to the oxidized forms of nitrogen (nitrate (NO_3^-) and nitrite (NO_2^-)) through the microbially-mediated process of nitrification also occurs, nitrogen mineralization is often referred to as the process by which organic forms of nitrogen are converted to the plant-available, inorganic forms, including both ammonium (NH_4^+) and nitrite/nitrate (NO_2^- and NO_3^-). The rate of mineralization varies with temperature, soluble carbon, moisture content, and the site-specific microbial community (Kraus et al. 2000; Strickland et al. 2009; Zaman and Chang 2004), with higher temperatures and moisture contents typically producing higher mineralization rates. Additionally, being an aerobic process, nitrification should increase at low water contents (Bouwman 1998), and so NO_x should increase when water content is low.

As compost leachate passes through the VFS layer, this may offer some opportunity for nutrient removal. Bioretention media may remove some ammonium (NH_4^+) via adsorption, while removal of dissolved organic nitrogen (DON) and nitrate (NO_3^-) are likely to be not significant (Li and Davis 2014). PO_4-P is likely to be removed to some extent in the VFS, since bioretention media has been well documented to remove phosphorus through adsorption (Hsieh et al. 2007; Komlos and Traver 2012; Li and Davis 2016; Liu 2014; Liu and Davis 2014; Yan et al. 2016, 2017, 2018). Additionally, uptake of the soluble, plant-available species (NO_3^-, NH_4^+, and PO_4-P) by turfgrasses should be influential to some extent as well. Specific mechanisms in the VCB

and VFS layers were not directly measured, but some discussion of potential transport factors will be made, with more detailed exploration provided in Chapter 4.

The highest observed concentrations for TN and TP in both the field and greenhouse occurred at the beginning of each experiment (Figure 3-10). TN concentrations at the field site were found to have a significant declining trend, according to a Kendall Tau test ($p < 0.001$ for both 3-m and 6-m VCBs), with no trend found for TP. Significant declining time series trends for N and P were only found for two mesocosms in the greenhouse experiment, but evaluations of greenhouse trends were complicated by separation of VCB and VFS effluent and smaller datasets (Study 1 n = 7, Study 2 n = 9). Additionally, a low intensity storm event (2-mm/hr, 0.08-in/hr) conducted at the beginning of Study 2 resulted in low effluent concentrations, likely due to less runoff contact with the compost layer, which contributed to the challenge of assessing a true time series trend. Decreasing concentrations of NO_x, TKN, and TP in VCB effluent over time can be observed in Figure 3-7, though statistical evaluation was not completed due to small sample size.

In greenhouse experiments effluent concentrations of TN later in the experiment (after ~180 days) decrease to the level of influent concentrations, while in the field this was not observed, mainly due to lower than expected influent concentrations; however, net nitrogen removal was never achieved at either site. TP concentrations observed at both the field and greenhouse sites remained elevated above influent concentrations for the entire study period. However, while greenhouse TP concentrations sometimes fall below influent concentrations (Figure 3-9), the same did not occur at the field site, which may be partially attributable to differences in compost composition (Table 3-7), with larger P content in the field resulting in larger release of P throughout the experiment.

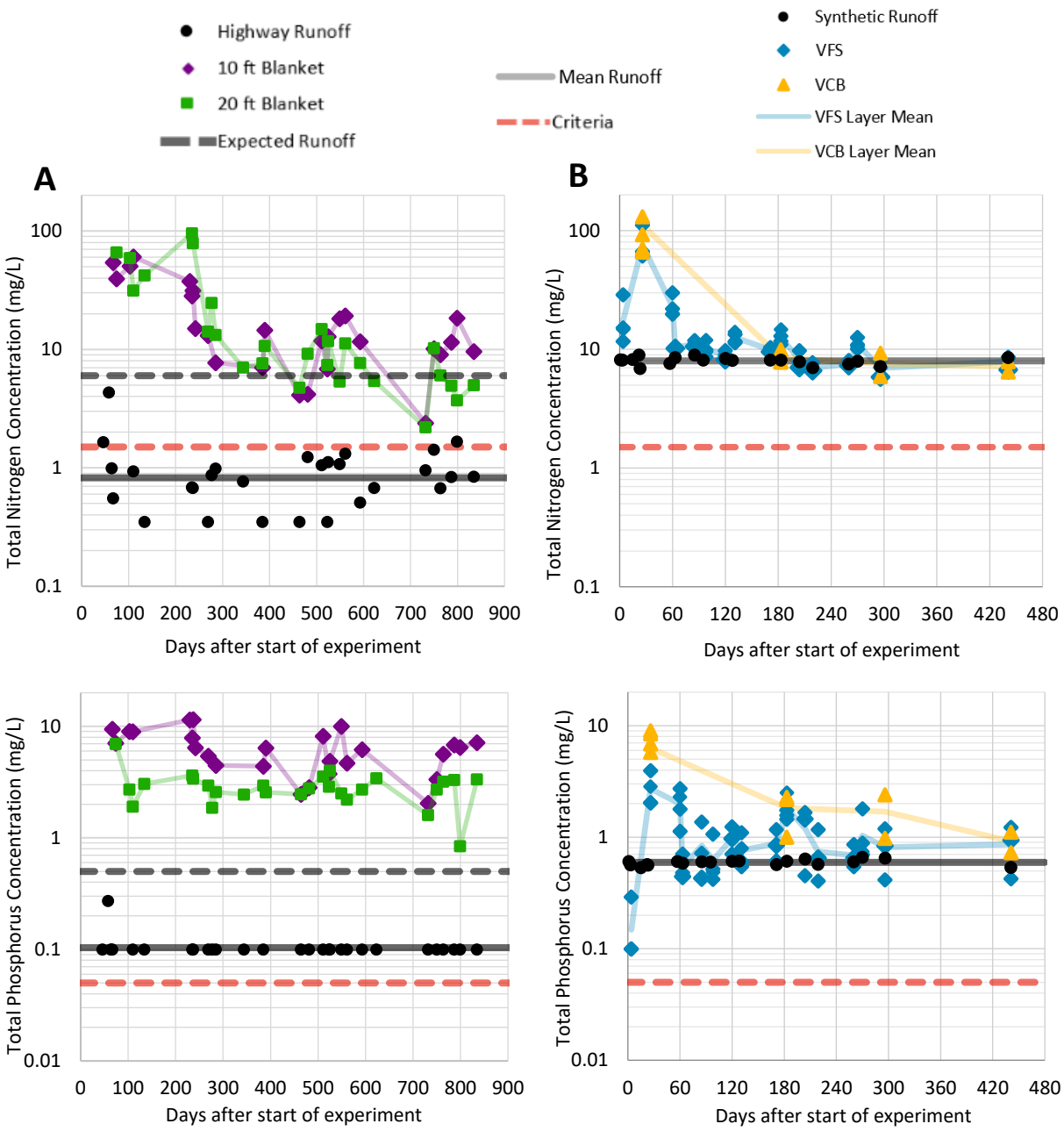


Figure 3-10: Timeseries of Nitrogen and Phosphorus EMCs in the Field and Greenhouse. A) field site; B) greenhouse experiment; for greenhouse experiments one low intensity storm event was conducted (2-mm/hr, 0.08-in/hr) at the beginning of the experiment; detection limits are 0.7 mg/L for TN (as sum of NO_x and TKN DLs (0.2 and 0.5 mg/L)) and 0.2 mg/L for TP.

NOx had a larger range in EMCs (~0.1-71 mg/L) than did TKN (~2-50 mg/L) at the field site as well as in the greenhouse (NOx range ~2-62 mg/L and TKN range ~4-50 mg/L) (Table 3-3 and Table 3-4), which is likely a result of changing moisture contents in the media over time. Differences between NOx and TKN ranges at both sites can also be observed in exceedance probability plots (Figure 3-11). The larger range of observed EMCs at the field site can likely be attributed to environmental conditions including larger fluctuations in temperature and moisture content than were experienced in the greenhouse, since greenhouse temperatures were maintained at ~22°C daytime temperature, 13°C nighttime temperature and were watered consistently on a Mon/Wed/Fri schedule. By mass, effluent NOx constituted 13% of TN for the 3-m field VCB, 52% of TN for the 6-m VCB, and 40% of TN on average for the greenhouse experiments. Evidence of higher nitrification with greater VCB length at the field site may be due to differences in moisture content caused by differences in volume retention. It is possible that because the 3-m VCB had a higher drainage area ratio than the 6-m VCB (3.5:1 and 2.5:1, respectively) (Chapter 2), moisture contents could have been higher due to the higher ratio of highway runoff volume entering the system, causing lower nitrification rates. However, this is only one factor in assessment of the fate of nitrogen in VCB/VFS systems, which could be affected by other microbial processes, including volatilization. Additionally, some removal of nitrogen in the VFS may have occurred through soil adsorption and plant uptake, further complicating explanations of nitrogen movement. Further discussion and analysis of nutrients in the VCB/VFS system are detailed in Chapter 4.

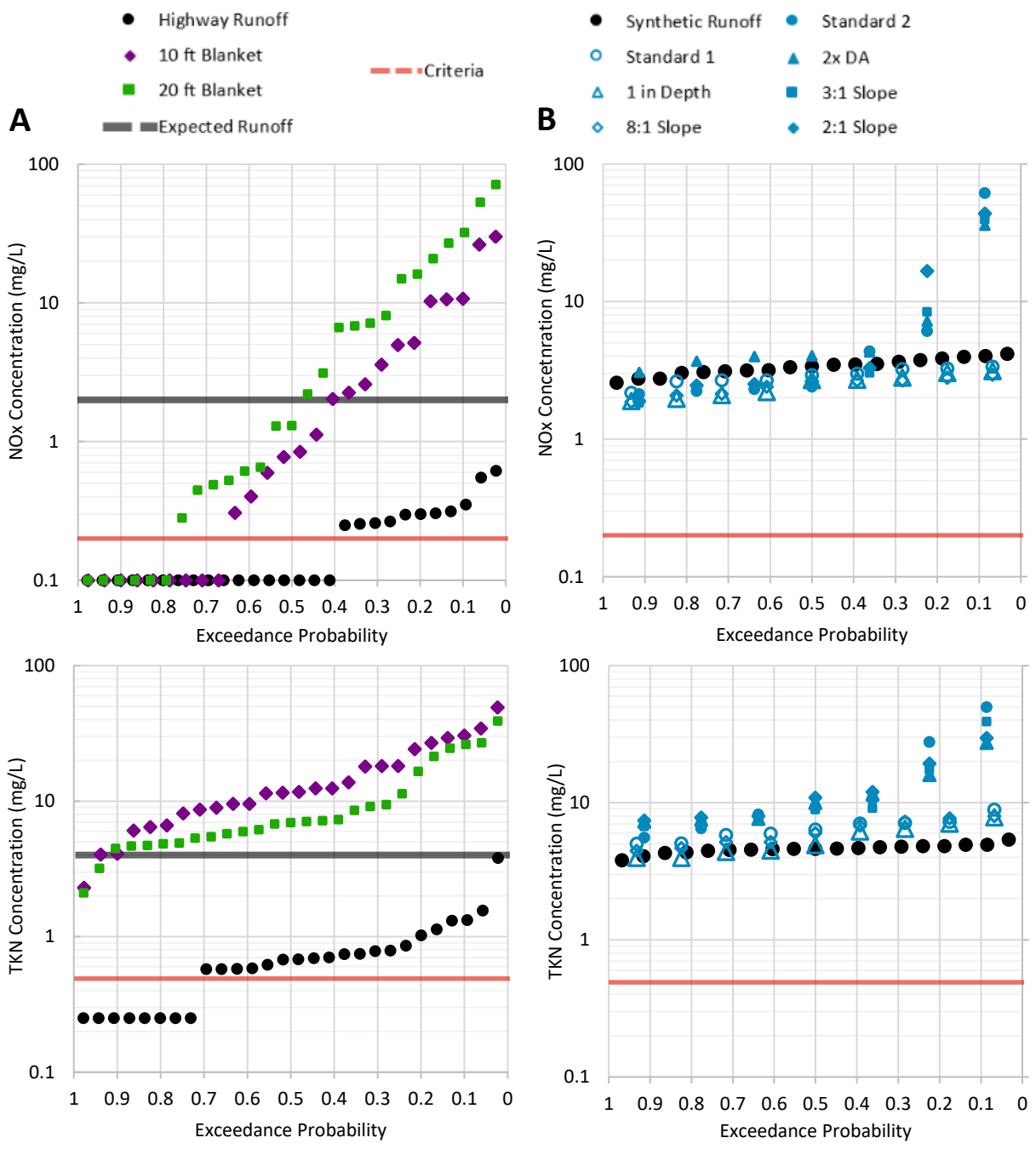


Figure 3-11: Field and Greenhouse Exceedance Probability for NO_x and TKN. A) field; B) greenhouse (VFS layer effluent only); detection limits are 0.2 mg/L for NO_x and 0.5 mg/L TKN.

Figure 3-12 shows the main transport processes affecting nutrient movement in a VCB/VFS system. Some N and P enters the VFS/VCB from highway runoff, (some of which may be particulate bound though this was not assessed in this research). Between storm events, organic forms of N in the VCB layer mineralize to NH_4^+, and organic forms of P to PO_4-P, with the degree of mineralization dependent on temperature and moisture content. Some DON and DOP may also be released. Nitrification occurs during periods of low saturation, with microbial transformation of NH_4^+ to NO_2^- and then to NO_3^-. During storm events, the mineralized mass of N and P is flushed from the VCB layer, with speciation of N dependent on moisture conditions between storm events. Some removal of NH_4^+ and PO_4-P should occur in the VFS layer, depending on soil properties and the amount of vegetative uptake, and some removal via volume retention should occur as well. Overall, net N and P release from the VCB/VFS is expected immediately after VCB installation and remain elevated after 1-2 years.

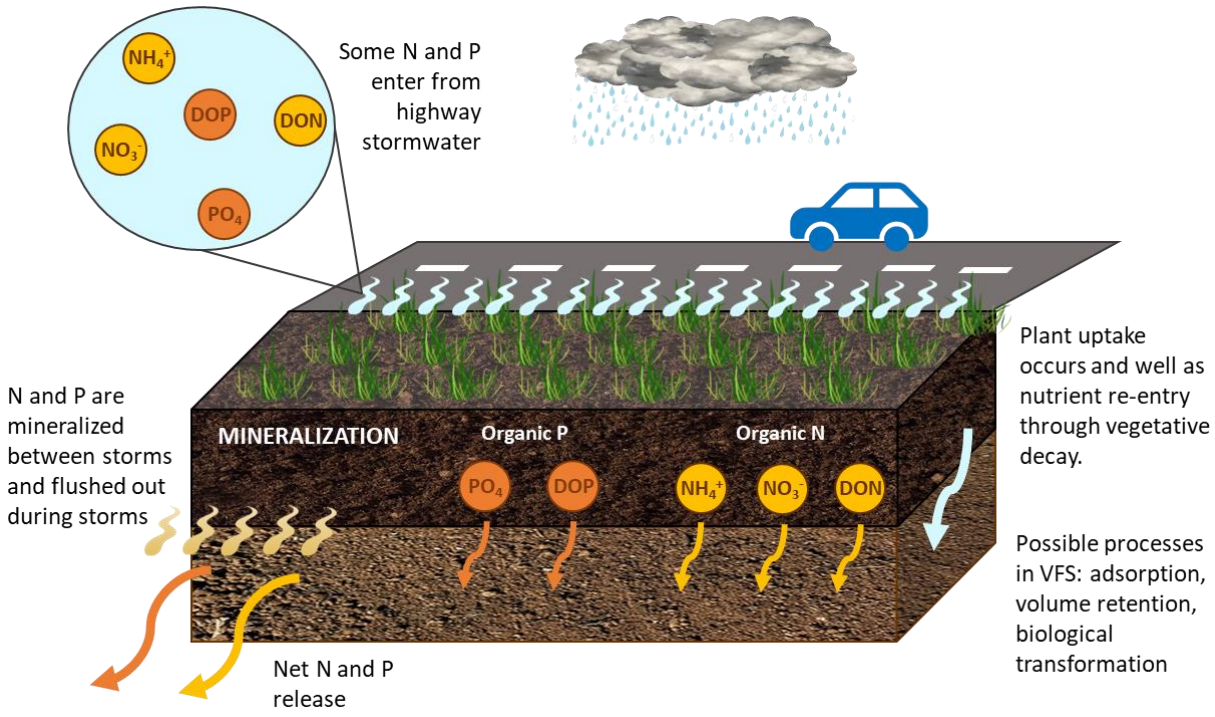


Figure 3-12: Influential Processes Affecting N and P Movement in a VCB/VFS.

Pollutant Loads

Comparison of pollutant concentrations to EPA aquatic criteria gives meaningful insight into instantaneous impacts on downstream water bodies, however overall performance can be evaluated through mass loadings (Table 3-8). Because observed influent stormwater concentrations were uncharacteristically low in this study, highway stormwater loads were also estimated using expected concentrations for comparison. Expected mean influent concentrations were obtained from a recent stormwater characterization study utilizing The National Stormwater Quality and The Best Management Practices databases (Pamuru et al. 2021), with influent stormwater EMCs of: TSS = 104 mg/L, NOx = 0.70 mg/L, TKN = 1.91 mg/L, TN mean = 2.08 mg/L, TP = 0.35 mg/L, total Cu = 0.0453 mg/L, filtered Cu = 0.0516 mg/L, and total Zn = 0.144 mg/L. Expected highway loads are not directly comparable, since this was not a tested scenario, but rather serve as a benchmark. Comparison of field mass loading rates for both the 3-m and 6-m VCBs to observed highway runoff loads show net reductions of TSS, particulate copper, and zinc, but net release of TN (both NO_x and TKN), TP, and dissolved copper, echoing results found through concentration data comparisons. It is possible that reductions may have been much greater had larger influent concentrations been observed. Additionally, expected influent highway loads for TN and TP (47.4 kg/ha/yr for TN and 3.53 kg/ha/yr for TP) are the same magnitude as VCB effluent loadings (33-41 kg/ha/yr for TN and 7-14 kg/ha/yr for TP). This could indicate that the relative contribution of nutrients by the VCB may have been lower had influent stormwater concentrations been high. However, these scenarios have not been directly tested, and specific conclusions cannot be made for this comparison.

Table 3-8: Mass Loads for Field Experiment Contaminants.

Field Experiment Mass Loading Rate				
Parameter	Observed Highway (kg/ac/yr) (n = 28)	Expected Highway* (kg/ac/yr) (n = 28)	10 ft (kg/ac/yr) (n = 21)	20 ft (kg/ac/yr) (n = 24)
TSS	84.1	716	44.6	46.1
NO_x	0.981	20.1	4.29	21.4
TKN	2.83	27.3	28.7	19.8
TN	3.81	47.4	33.0	41.3
TP	0.469	3.53	14.3	6.68
Total Cu	0.0685	0.695	0.390	0.175
Dissolved Cu	0.0299	0.600	0.384	0.168
Particulate Cu	0.0375	0.100	0.0123	0.0120
Total Zn	0.690	2.44	0.276	0.112

**Expected highway mass loading was calculated using mean concentrations expected in stormwater runoff; this comparison was made because field observed concentration were much lower than expected.*

Impact of Design Variations

Greenhouse experiment performance was summarized above, however some significant variations were found for the tested variations (which included slopes, compost depths, and drainage area ratios). Both EMC and mass data for greenhouse experiment mesocosm variations can be found in the Appendix. Effluent from the VCB layer was not statistically evaluated by variation due to the small sample size. For TSS, Cu (total, dissolved, and particulate), and Zn all VFS effluent concentrations were found to be statistically significantly lower than influent concentrations, based on the mean ($p < 0.001$ for all), and in comparison to the standard design (3:1 slope, 7.6-cm compost depth, 3:1 DA ratio), none of the design variations were found to be statistically significantly different, indicating that slopes between 8:1 and 2:1, VCB depths between 2.5-cm and 7.6-cm (1-in to 3-in), and drainage area ratio (3:1 to 6:1) did not significantly affect TSS or metals performance. Because VFS effluent passed through both the

compost and soil layers, filtration can be identified as the main retention pathway for TSS and particulate metals. For nutrients, comparison of Study 1 mesocosms was limited because the first three storm events were not sent for water quality analysis, likely missing the first flush of N and P from the compost layer. For Study 2, all mesocosms had statistically significantly ($p < 0.05$ for all) higher TKN, TN, and TP concentrations than the influent, based on the mean, showing that all mesocosm designs resulted in significant nutrient release. In comparison to the standard mesocosm (7.6-cm compost depth), the 2.5-cm compost depth mesocosm had statistically significantly lower mean TP concentration, indicating a better performance when less compost was applied, likely because less compost resulted in lower P mass release.

Conclusions

Water quality performance of a VCB overlaying a VFS on a highway median was assessed through field site monitoring and supplemental greenhouse investigations. Low influent stormwater concentrations observed at the field site presented a challenge to evaluating performance in a real scenario, so evaluations were supplemented with comparisons to expected influent stormwater mean concentrations as well as observed.

While VCBs were shown to be effective at removing TSS, mixed performance was found for metals removal, and consistent nutrient release was observed. Consistent TSS removal was observed for both field and greenhouse experiments, with effluent TSS likely originating from the media itself rather than remaining TSS from the influent, and the majority of effluent concentrations below the water quality criterion of 25 mg/L. For total zinc, both field and greenhouse showed significant mass removals, but while consistent removal of both the dissolved and particulate copper fraction was observed in the greenhouse, copper leaching in the

dissolved phase was observed in the field, likely in part due to differences in compost copper content for the composts used at each site. Large mass exports of nutrients (N and P) were observed at both sites, with all storm events exceeding the downstream water quality criteria of 0.69 mg/L for TN and 0.03656 mg/L for TP from the US EPA National Recommended Water Quality Criteria Ecoregional Nutrient Criteria for Rivers and Streams (US EPA 2013). The highest observed concentrations exceeded criteria up to two orders of magnitude for TN and almost three orders of magnitude for TP, echoing previous studies which have observed large amounts of nutrient loss from compost.

Greenhouse variations in slope, drainage area ratio, and compost depth had no significant effect on TSS, nitrogen, or metals performance, however a compost depth of 2.5-cm as opposed to 7.6-cm resulted in significantly less TP release. Increased VCB length resulted in increasing mass removals (or lower mass releases) for TSS, zinc, total, dissolved, and filtered copper, and TP, indicating increasing performance with a longer flow path due to increased retention of particulate pollutants and well as potential for additional pollutant removal in the VFS layer, though no difference for TN was found. Observed differences in nitrogen speciation were likely due to differing environmental conditions including temperature and moisture content.

A large intensity (102 mm/hr (4 in/hr)) storm event prior to vegetative establishment in the greenhouse resulted in erosion, with large releases of TSS, nutrients, and metals in the effluent. Similar erosive events were not observed at the field site, likely because erosion control matting was installed over the VCB during installation. This supports use of an erosion control matting during VCB installation to prevent loss of compost during vegetative establishment.

Despite improvements to the VFS system alone for particulate pollutant removal, the risk of nutrient and metals leaching makes VCB installation as an amendment to highway VFSs not

recommended without further research, especially for nutrient and metals sensitive watersheds. Differences in compost nutrient content resulted in differing magnitudes of nitrogen and phosphorus release. Additionally, copper release was observed for the field compost, which had a higher copper content, while for greenhouse compost, net copper removal was observed. These observations point toward compost composition as a major factor in nutrient and metal leaching and more research in this area could improve understanding and prediction of compost suitability for use as a VCB and as a component of SCMs in general.

Acknowledgements

The authors acknowledge the support of the National Cooperative Highway Research Program (NCHRP 14-39), the Maryland Department of Transportation State Highway Administration (MDOT SHA), and the Low Impact Development (LID) Center.

Erica R. Forgione was supported by NRT-INFEWS: UMD Global STEWARDS (STEM Training at the Nexus of Energy, WAter Reuse and FooD Systems) that was awarded to the University of Maryland School of Public Health by the National Science Foundation National Research Traineeship Program, Grant number 1828910. Graduate student funding was also provided in part by the University of Maryland Graduate School Dean's Fellowship and COVID Delay Fellowship.

Mesocosm and field equipment design and construction support was provided by the University of Maryland Environmental Science and Technology (ENST) Project Development Center. Special thanks are also extended to Stancill's Inc. (Perryville, MD) for providing engineered soils and to Montgomery County Yard Trim Composting Facility (Dickerson, MD) for providing Leafgro yard waste compost.

CHAPTER 4: NUTRIENT FATE AND TRANSPORT IN A VCB/VFS SYSTEM

Erica R. Forgione[1], Allen P. Davis[2], Ahmet H. Aydilek[3], Gary K. Felton[4], and Dr. Arash Massoudieh[5]

[1] Graduate Research Assistant, Dept. of Civil and Environmental Engineering, Univ. of Maryland, College Park, MD 20742.
[2] Professor and Charles A. Irish, Sr. Chair in Civil Engineering, Dept. of Civil and Environmental Engineering, Univ. of Maryland, College Park, MD 20742, USA. (corresponding author). E-mail: apdavis@umd.edu
[3] Professor, Dept. of Civil and Environmental Engineering, Univ. of Maryland, College Park, MD 20742, USA.
[4] Associate Professor, Dept. of Environmental Science and Technology, Univ. of Maryland, College Park, MD 20742, USA.
[5] Professor and Chair, Dept. of Civil and Environmental Engineering, The Catholic Univ. of America, Washington, DC 20064, USA.

Abstract

In pursuit of improving hydrologic and water quality performance of existing highway stormwater control systems, use of Vegetated Compost Blankets (VCBs) has been proposed. VCBs, loosely applied layers of compost which are then vegetated, would be applied over Vegetated Filter Strips (VFS) on highway slopes. Compost's high water holding capacity offers additional volume retention and the organic matter content may immobilize some contaminants of concern, however, the high nutrient content of compost poses a major threat to net beneficial performance due to excess nutrient leaching which occurs after application. This risk should be seriously considered before widespread implementation, since nutrient pollution contributes to eutrophication, the cause of algal blooms, which is a major threat to ecosystems. This research has posed the question: Can compost be used as a blanket amendment while avoiding excessive nutrient leaching?

Nitrogen (N) and phosphorus (P) in compost are naturally transformed from organic to inorganic, soluble forms through the microbially-mediated process of mineralization and there is a potential for nutrient removal through adsorption as compost leachate passes through the VFS

soil layer. Nutrient leaching from the VCB and potential nutrient removal through the VFS layer were assessed through lab-scale, greenhouse-scale, and field-scale experiments. Small scale laboratory experiments were completed to determine the N and P compost mineralization rates and potential soil adsorption capacities. Non-leached and leached composts were assessed to determine differences in nutrient mineralization based on compost age/exposure to stormwater. Greenhouse and field experiments were empirically evaluated using lab-obtained mineralization parameters and cumulative nutrient release, which was further supplemented by analysis of compost and soil composition. Additionally, nutrient release was simulated using a new open-source software, OpenHydroQual, which combines hydraulic and water quality modeling.

Composts from field and greenhouse experiments had similar C:N ratios but differed in total N and P content. Significant changes in compost composition over time were observed at the beginning and end of VCB experiments. N and P release rates differed between compost type and lower release rates and lower total mass releases were observed for leached composts in comparison to non-leached washed. Differences in release curves indicated that leached composts were likely mineralizing a less labile pool of N and P than the non-leached composts. Soils collected at the beginning and end of VCB experiments had significant changes in chemical characteristics, specifically, significantly higher P contents at the end of the experiments indicated a substantive pathway for P removal through the VFS layer. Adsorption experiments confirmed these observations, with P removal observed for all tested soils; increasing P adsorption was observed with increasing Al+Fe content. Comparison of nutrient mineralization curves from the laboratory to greenhouse and field experiments exhibited differences. For phosphorus this was likely due to removal of phosphate in the VFS layer, and for nitrogen, differences in moisture content and temperature likely resulted in differing amounts of

nitrification and volatilization. OpenHydroQual modeling showed modest results, with varying levels of accuracy for storm hydrograph simulation and mass release. Results indicate several ways nutrient leaching could be reduced when compost is applied as a surface layer.

Introduction

Rapid urbanization has resulted in worsening environmental and public safety issues due to the increased volume of stormwater runoff and its associated pollutant loadings (National Research Council 2009). This has led to the development of new green infrastructure systems (National Research Council 2009), commonly referred to as stormwater control measures (SCMs), an array of sustainable engineered alternatives to "gray" infrastructure. Green SCMs are designed to mimic the hydrologic behavior of the natural environment by retaining and infiltrating stormwater, removing pollutants via various remediation mechanisms. On highways, Vegetated Filter Strips (VFSs) and swales are commonly-used SCMs which have shown moderate performance for both hydrologic and water quality improvement and so have been identified for enhancement (TRB 2006). Compost is considered as a primary component in the design of a new type of SCM called a vegetated compost blanket (VCB), a layer of loosely laid compost that is placed on an existing hillside or embankment and seeded, which would be applied as an improvement to the VFS.

Compost is the product of a controlled aerobic process of biological decomposition in which raw organic materials are transformed into a relatively nutrient-rich and microbially active humus-like material that will provide nutrients to plants immediately upon application and through a full growing season (USCC 2001b; a). In addition to being a sustainable material, compost should improve soil structure, increase infiltration, increase water holding capacity, and

provide binding sites for certain pollutants (USCC 2001a), with overall goals to enhance vegetative growth (both above and below ground), reduce both stormwater flow volume and peak flow rate, and provide water quality improvement. Previous research has shown compost blankets to be effective for erosion control on steep slopes (AASHTO 2010; Bakr et al. 2012; Bhattarai et al. 2011; Faucette 2008; Faucette and Risse 2002; Faucette et al. 2007, 2009b; Fay et al. 2012; Mukhtar 2005), but little has been done to evaluate compost blankets as SCMs. However, compost itself has been used regularly in SCM designs throughout their short history, as both an amendment to improve vegetative growth as well as a potential material for pollutant binding. Early designs of bioretention basins incorporated compost as a large percentage of the media mix, which resulted in nutrient and metals leaching (Herrera Environmental Consultants, Inc. 2015). Other designs commonly call for a surface layer of compost or mulch.

While there is a potential for compost to bind and immobilize certain pollutants, one of the biggest challenges with compost treatments is that many compost types will release nutrients (nitrogen and phosphorus) in leachate, at least initially (Ahmad et al. 2008; Brown et al. 2016; Butler and Coale 2005; Chahal et al. 2016; Confesor Jr et al. 2009; Dietz 2007; Eghball 2003; Hurley et al. 2017; Iqbal et al. 2015; Li et al. 2011; Mullane et al. 2015; Reed et al. 2006; Storey et al. 2006). In large amounts, nutrients can become a serious threat to aquatic ecosystems (Carpenter et al. 1998). While nitrogen (N) and phosphorus (P) are necessary elements of life in small amounts, excess N and P in the environment can cause eutrophication (Harper 2012), wherein waters rich in N and P cause overgrowth of plant-life, often algae, that in turn removes oxygen from the water, killing aquatic life. While P is often the limiting nutrient in the environment, it has been shown that reducing concentrations of both N and P in water bodies may be vital to mitigating eutrophication (Conley et al. 2009).

Previous research conducted on field and greenhouse investigations of a VCB overlaying a VFS showed positive improvements for stormwater volume and flow attenuation and improved soil hydraulic properties (Chapter 2), however investigations of water quality performance showed large mass release of nutrients (both N and P) and copper in some cases (Chapter 3). These findings have further called into question the use of compost as the main component of an SCM due to the potential for net pollutant release. Additionally, previous investigations assessed the VCB and VFS as a combined system, therefore mechanisms occurring in each layer were not able to be separately evaluated.

Widespread VCB implementation risks the potential negative effects of large releases of N and P, presenting a need to examine the VCB and VFS layers separately and identify pathways of nutrient loss and removal. The goal of this study is to investigate nutrient loss through mineralization in VCBs and potential nutrient removal through adsorption in VFS soils to obtain a better mechanistic understanding of nutrient movement in a VCB/VFS system with the goal of reducing nutrient loss. Composts and soils used in large scale field and greenhouse experiments (Chapters 2 and 3) were evaluated through column compost mineralization studies conducted over the course of 12-17 weeks and soil batch adsorption experiments and results from laboratory scale experiments were compared to greenhouse and field data. Finally, a mechanistic model of the VCB/VFS system was created using the opensource software OpenHydroQual, which was selected due to its flexibility and combination of hydraulic and water quality modeling features. OpenHydroQual is a software whose predecessor is GIFMod (Green Infrastructure Flexible Model), which has been used previously in research for evaluation of green infrastructure systems (Alikhani et al. 2020; Almadani and Massoudieh 2018; Arash Massoudieh et al. 2017; Bacys et al. 2018). Findings from this research on compost leaching

combined with potential pathways of nutrient uptake should be expandable beyond the specific situation of VCBs on highway medians to other SCMs using compost as a surface layer.

Materials and Methods

Compost and Soil Composition

Field topsoil (VFS) and subsoil (underlying VFS) samples were collected from the site prior to VCB installation in summer 2018 and after the experiment was finished in summer 2021. Additionally, greenhouse experiment topsoil (VFS) was sampled before and after each experiment was completed. Soils were sent to the University of Delaware Soil Testing Program (UDel STP) for fertility analysis. Additionally, compost samples collected before application to the greenhouse and field experiments as well as compost samples collected after the end of each experiment were also sent to UDel STP for analysis of compost composition. Soil testing methods used by the UDel STP can be found at The University of Delaware's Cooperative Extension website (The Northeast Coordinating Committee for Soil Testing 2011). Methods from the US Composting Council's (USCC) Test Method for the Examination of Composting and Compost (TMECC) were used for compost analysis (USCC 2002).

Compost Mineralization Experiment

Composts used in field and greenhouse experiments (Chapters 2 and 3) were collected at the time of application and stored at room temperature to be tested as a "non-leached" sample (F and GH, respectively). Additionally, samples collected from the field (2.25 yr and ~110 bed volumes) and greenhouse (1 yr, ~35 bed volumes) experiments after they had been completed

were also tested in mineralization column experiments. Samples from the end of the experiments had been exposed to either real or synthetic stormwater runoff and so were considered “leached” (F-W and GH-W, respectively) and were tested as a comparison to evaluate how a leached and aged compost would compare to new. Mineralization experiments were conducted using a small rainfall simulation similar to the design of Al-Bataina et al. (2016). Compost was added at a height of 7.62-cm (3-in) to a 15.24-cm (6-in) polycarbonate column lined at the bottom with a fabric geotextile to allow effluent collection. Compost was added as to achieve a field bulk density by adding a third of the volume at a time, then tapping firmly three times on a hard surface between additions. The wet and dry mass added was measured and recorded. Synthetic stormwater using a recipe described previously (Chapter 3) was applied to the top of the columns intermittently using a Masterflex L/S Precision Variable-Speed Drive fitted with two Masterflex L/S Easy-Load® II 2-Channel Pump Heads. A spray nozzle was attached to the end of each tubing for uniform application at a flow rate equivalent to a 5.1-cm/hr (2-in/hr) intensity over 1 hour with a drainage area ratio of 3:1 (highway to VCB area), equivalent to a 5-year return period in Maryland, USA. Storm events were applied once per week for 11-17 weeks and samples were run in replicates of three. All effluent was collected in plastic containers below the columns to obtain the total volume. The experiments were conducted at room temperature (20°C). The experimental set-up is shown in Figure 4-1.



Figure 4-1: Laboratory Compost Mineralization Experiment Columns and Flow Apparatus.

Collected effluent samples and influent synthetic stormwater were each well mixed before collection of a representative sample, and then filtered using a 0.22-µm filter to prevent interference of the particulate fraction. Samples were analyzed for Total Dissolved Nitrogen (TDN) and Total Dissolved Phosphorus (TDP), as well as individual species. In addition, pH was measured for all influent and effluent samples.

The inorganic and organic fractions of dissolved N and P were calculated using the following equations:

Equation 4-1

$$\boldsymbol{DIN} = [NO_2^-] + [NO_3^-] + [NH_4^+]$$

Equation 4-2

$$\boldsymbol{DON} = TDN - DIN = TDN - ([NO_2^-] + [NO_3^-] + [NH_4^+])$$

Equation 4-3

$$\boldsymbol{DIP} = [PO_4 - P]$$

Equation 4-4

$$\boldsymbol{DOP} = TDP - DIP = TDP - [PO_4 - P]$$

where DIN refers to Dissolved Inorganic Nitrogen,
DON refers to Dissolved Organic Nitrogen,
DIP refers to Dissolved Inorganic Phosphorus,
and DOP refers to Dissolved Organic Phosphorus

The mineralization rate constants and nutrient release rate constants were found for N and P using the following first-order kinetic models, through identification of total mineralized or released mass, then minimizing the sum of squares of the residuals.

Equation 4-5

$$Y(t) = Y_o(1 - e^{-k_{min}t})$$

where Y(t) is the mass of mineralized nutrient (DIN or DIP) at time t,
Y_0 is the mass of potentially mineralizable nutrient (DIN or DIP),
k_{min} is the mineralization rate constant,
and t is time elapsed.

Equation 4-6

$$Z(t) = Z_o(1 - e^{-k_{release}t})$$

where Z(t) is the mass of total released nutrient (TDN or TDP) at time t,
Z_O is the mass of total released nutrient (TDN or TDP),
$k_{release}$ is the total release rate constant,
and t is time elapsed.

Nutrients Adsorption Experiment

A batch adsorption isotherm experiment was conducted by applying dilutions of compost leachate to a fixed mass of engineered soils. Soils align with Maryland State Highway Administration (SHA) highway topsoil specifications which were used at the greenhouse and

field sites. An engineered clayey soil and sandy soil fitting MDOT SHA specifications for topsoil (Section 920.01.02, (MDOT SHA 2020)) were obtained from Stancill's Inc., (Perryville, MD). The sandy mix consisted of 84.7% sand, 11.7% silt, 3.6% clay and the clayey mix consisted of 25.2% sand, 51.3% silt, 23.5% clay. Specifications for these soils can be found in the Appendix.

Compost leachate was made by adding a 76 g (dry basis) of compost per liter of dechlorinated (with sodium bisulfite) tap water, mixed thoroughly, then filtered to 0.22 µm to form a compost leachate stock solution. Dilutions of 60%, 50%, 25%, 20%, 15%, 10%, 5%, 1%, and 0.5% were made using deionized water with NaCl (65 m/L) and $CaCl_2$ (15 mg/L as Ca) added. Leachate was adjusted to pH 7 with 0.1M NaOH and 0.1M HCl and 50 mL of each dilution was added to 0.5 g of soil. Samples were observed and adjusted to pH 7 over the first 4 hours and containers were shaken end-over-end at 20◦C for 24-hrs.

After 24 hours the solution was filtered to 0.22-µm. Both the beginning leachate solutions and the final equilibrium solutions were analyzed for TDN, TDP, NO_2^-, NO_3^-, NH_4^+, and PO_4-P. The pH was measured at the end of the 24-hr period. The concentration of adsorbate (q_{eq}) was calculated through mass balance for each sample using the following equation:

Equation 4-7

$$q_{eq} = \frac{(C_0 - C_{eq})V}{m}$$

where: C_0 is the beginning concentration of the analyte,
C_{eq} is the equilibrium concentration of the analyte,
V is the volume of solution,
m is the mass of soil,
and q_{eq} is the equilibrium adsorbed concentration of analyte

q_{eq} was plotted against the equilibrium concentration (C_{eq}) to obtain an adsorption isotherm. All samples were assessed for best fit to either a Freundlich or Langmuir relationship through regression on the linear transformation of each equation. All samples best fit a Langmuir isotherm model through comparison of the proportion of explained variance (R^2) and were fit to the following equation through minimizing the sum of squares of the residuals:

Equation 4-8

$$q = \frac{Q K_L C}{1 + K_L C}$$

where: q is the equilibrium density of adsorbate on the surface (mg/g),
C is the equilibrium concentration of adsorbate in the solution (mg/L),
Q is a constant representing surface adsorption density for monolayer coverage (mg/g),
and K_L is a constant describing the shape of the curve.

Analytical Methods

TDN was analyzed through thermal decomposition followed by chemiluminescence using a Shimadzu TOC/TN Analyzer (ASTM D 8083). TDP was analyzed through persulfate digestion (Standard Methods 4500-P) then colorimetrically using a Seal AQ300 Discrete Analyzer (USEPA Method 365.1, Rev 2.0). Nitrite (NO_2^-) (USEPA Method 353.2 Rev. 2.0), ammonium (NH_4^+) (USEPA Method 350.1 Rev 2.0), and orthophosphate (PO_4-P) (USEPA Method 365.1, Rev 2.0) were tested colorimetrically using a Seal AQ300 Discrete Analyzer. Nitrate (NO_3^-) (USEPA Method 9056A) was analyzed for the mineralization experiment through ion chromatography using a Thermo Scientific Aquion IC System (using a Dionex™ IonPac™ AS22 column) and for the adsorption experiment colorimetrically using a Seal AQ300 Discrete Analyzer (USEPA Method 353.2 Rev. 2.0).

Biomass and Plant Tissue Nutrient Methods

Biomass measurements were collected at the field site over three periods of time (Fall 2020, Spring 2021, and Summer 2021) using a controlled mowing procedure (Lussem et al. 2019; University of Idaho College of Natural Resources 2009; Voelkel et al. 2018). At the beginning of the measurement period, turfgrasses were mowed to a height of 8.9-cm (3.5-in) and allowed to grow for 6-8 weeks, after which a small push mower with a collection bag was used to mow a 7.6-m (25-ft) section at the center of each testing area (a control area (no compost); each observational VCB area (compost depths of 2.5-cm (1-in), 5-cm (2-in), and 10-cm (4-in)); and the 6-m (20-ft) monitored VCB (7.6-cm (3 in)-depth)), with one pass in each direction. Biomass was collected, transferred to labeled paper bags, and weighed immediately before transportation to the UMD geotechnical engineering laboratory. Samples were dried in a 50°C oven until steady weight was recorded. Samples were then mixed thoroughly, and a representative sample was taken and mailed to the Penn State Agricultural Analytical Services Laboratory (https://agsci.psu.edu/aasl) for tissue analysis for N content through dry combustion analysis and P content through sample digestion and ICP analysis. Biomass collection dates are shown in Table 4-1. Collection during the first year after installation was prevented by unplanned mowing events.

Table 4-1: Field Site Biomass Sampling Collection Summary.

Season	Days from Start of Experiment	Biomass Growth Start Date	Biomass Collection Date	Growth Time (days)
Fall 2020	565	9/15/2020	10/28/2020	43
Spring 2021	761	3/30/2021	5/20/2021	51
Summer 2021	812	5/20/2021	7/6/2021	47

OpenHydroQual Model Development

OpenHydroQual utilizes user-selected modular blocks representing ponded water, unsaturated or saturated media, and impervious surfaces with a selection of connections between blocks which may be natural interfaces or user-defined connectors. Blocks have built-in equations for unsaturated flow (van Genutchten-Maulem equation (van Genuchten 1980; Mualem 1976)), saturated flow (Darcy equation), and surface water flow (diffusive wave equation (Govindaraju et al. 1985)), depending on the block's function and degree of saturation. Sources, such as precipitation and additional weather conditions can also be added to blocks to allow for input of specific environmental conditions. Evapotranspiration can be added using established models (e.g. Penman-Monteith Method (Zotarelli et al. 2009)).

A model of the VCB/VFS system described in Chapters 2 and 3 was created in OpenHydroQual, shown in Figure 4-2. The highway drainage area is represented by a catchment (far left catchment) and layers of compost (VCB), topsoil (VFS), and subsoil (compacted underlying layer) are each represented by a series of soil blocks overlaid with a catchment which allows rainfall to also be applied over the area. The subsoil layer was given an arbitrary depth of 0.9-m, much larger in comparison to the 7.62-cm VCB layer and 6.35-cm VFS layer, in order to represent a deep compacted soil layer as would be underlying a VCB/VFS in the field. Fixed head blocks function as outflow storage for flow exiting the system.

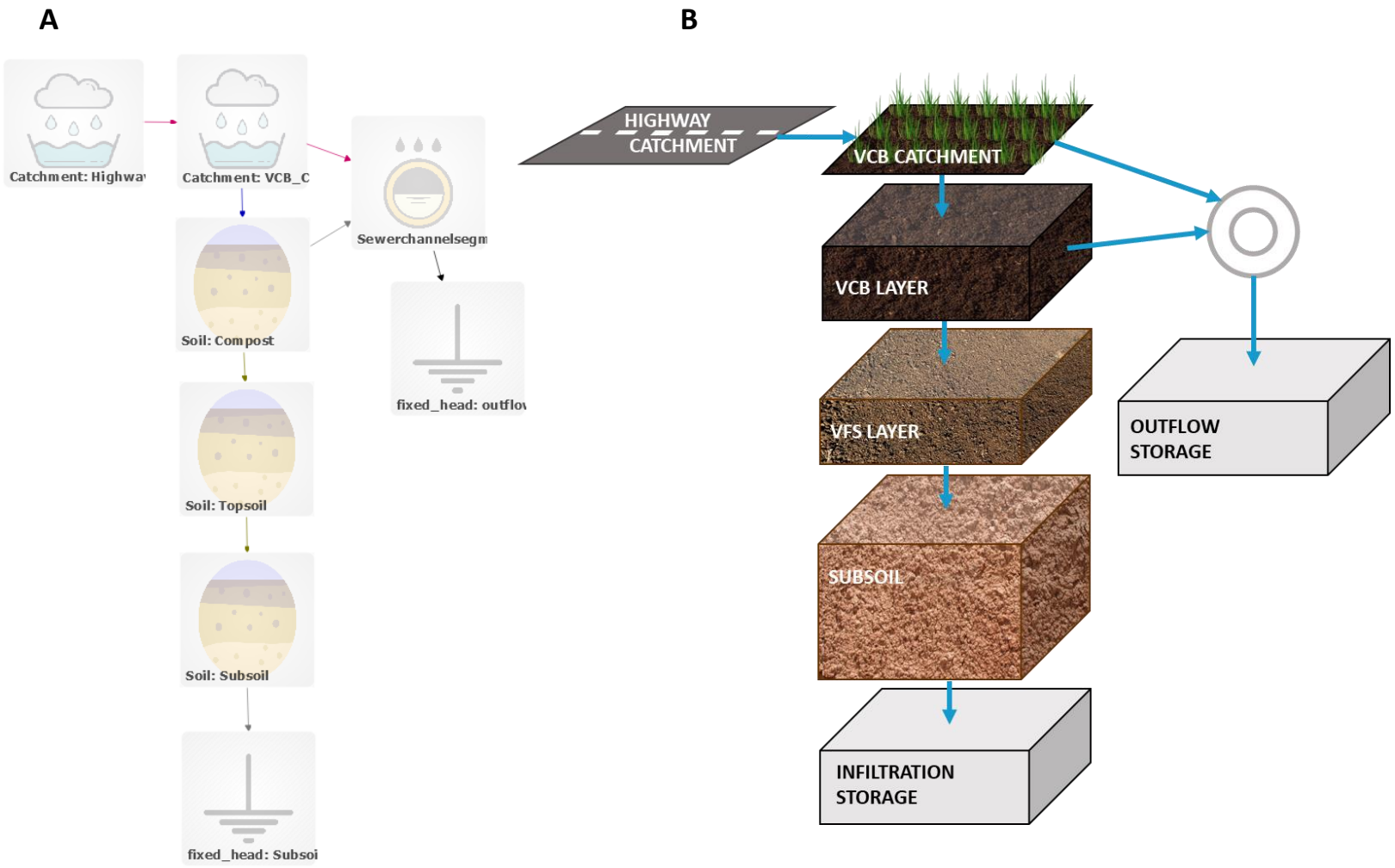


Figure 4-2: OpenHydroQual Model Structure for VCB/VFS System.
a) field VCB model structure created in OpenHydroQual using the Graphical User Interface (GUI); b) conceptualization of field VCB model structure as applied to the OpenHydroQual model.

As a test case for using OpenHydroQual to model nutrient movement, the 3-m (10-ft) length VCB at the field site was selected. Modeling the field site tests a real VCB/VFS implementation scenario where the underlying subsoil layer can also be included to best represent the real implementation scenario hydrology; additionally, weather data can easily be obtained and input. Physical parameter inputs for the highway drainage area and the soil blocks were chosen to describe the 3-m VCB/VFS for the model structure, shown in Table 4-2.

Table 4-2: Block Parameters for the OpenHydroQual System

Block	Parameter	Values	Obtained from
Highway and VCB Catchment	Geometry	100-m width VCB 10-m length VCB 4260 m^2 area Highway	Given by site
	Slope	0.1	Given by site
	Manning's n	0.016 Highway 0.030 VCB	Estimated (Chow 1959)
VCB VFS Subsoil	Geometry	100-m width for all 10-m length for all 7.6-cm depth VCB 6.4-cm depth VFS 0.9-m depth subsoil*	Given by site *Selected
	Slope	0.1	Given by site
	Saturated hydraulic conductivity (cm/s)	$7.87x10^{-2}$ VCB $1.62x10^{-2}$ VFS $2.53x10^{-6}$ Subsoil	Measured constant head permeameter (ASTM D5856)
	Initial moisture content (%)	70 VCB 40 VFS 30 Subsoil	Selected
	Residual moisture content (%)	1 VCB 17.9 VFS 4.3 Subsoil	Estimated (Duzgun et al. 2021)
	Saturated moisture content	75.50 VCB 44.38 VFS 35.40 Subsoil	Measured vacuum saturation (Klute 1965)
Sewer Channel	Geometry	6-in Diameter 50-ft Length	Selected
	Manning's n	0.010	Estimated (Chow 1959)

Precipitation timeseries consisted of 2-minute data collected at the field site supplemented with data from a nearby weather station in the case of missing data (e.g., autosampler batteries died). In these cases, data was supplemented with data from the Baltimore-Washington airport station (~13km distance) obtained from NOAA's National Centers for Environmental Information (NCEI) Climate Data Online (CDO) platform (https://www.ncdc.noaa.gov/cdo-web/). Temperature, humidity, and wind for use in estimation of potential evapotranspiration were also obtained from the same station dataset and solar radiation data was obtained from the National Solar Radiation Database (NSRDB) (https://nsrdb.nrel.gov/).

The mineralization process was added to the compost layer through the Desorption function from the Mass Transfer plug-in. (The name desorption is used as shorthand to denote a process which moves a constituent from the solid phase to the dissolved phase rather than directly representing desorption.) Constituents P_s and P_d were added, representing solid phase (unmineralized/unreleased) P and dissolved phase (mineralized/released) P. The release rate coefficients ($k_{release}$) were added to the model as a Reaction Parameter, P_release_rcoeff (for the example of modeling P release). Equation 4-5 models the cumulative mass released over time, but the model needs to use the non-cumulative mass released at each time for transformation to the dissolved phase. Because of this, a rearrangement of Equation 4-5 was used to model the first-order release (using P as the example):

Equation 4-9

$$rate\ expression\ = \frac{\Delta mass}{\Delta t} = P_release_rcoeff\ *\ P_s$$

where P_s is the solid (unmineralized) form of P,
P_d is the dissolved (mineralized) form of P,
P_release_rcoeff is the release rate coefficient ($k_{release}$),
t is time,
and the rate expression is the change of P mass over time, specifically the transformation of P_s to P_d over time.

P_s and P_d stoichiometry is given in the Reactions parameters, so input of -1 for P_s and 1 for P_d informs the model that for every 1 unit decrease in P_s results in a 1 unit increase in P_d. To introduce the mass of P that is available for release to the model, a starting P content (in g/m^3) for P_s was input in the VCB layer block, which is the total released mass found in column mineralization experiments. The same method was used for N release simulation, with only the values for the P_release_rcoeff and starting P_s (N_release_rcoeff and starting N_s) for the VCB layer changed.

Data Handling and Statistics

Previous chapters address data handling and QA/QC for hydrology (Chapter 2) and water quality (Chapter 3) data collected from greenhouse and field site experiments. For mineralization and adsorption laboratory experiments, calibration lines were run before every sample run and standard checks followed by a blank were run after every 10 samples. Blanks (and digestion blanks where applicable) were used in each run to confirm a low baseline. Student's t-test was used for statistical comparisons of datasets including soil and compost composition data and mineralization constants at a 5% significance level, but values of p are also provided.

Results and Discussion

Compost Mineralization

Composts used in field and greenhouse experiments were collected at the time of application and stored at room temperature to be tested as an "non-leached" sample (F and GH, respectively) for compost mineralization rate experiments. Additionally, aged and leached samples collected from the field (2.25 yr and ~110 bed volumes) and greenhouse (1 yr, ~35 bed volumes) experiments after they had been completed were also tested in mineralization column experiments. Samples from the end of the experiments had been exposed to either real or synthetic stormwater runoff and so were considered "leached" (F-W and GH-W, respectively) and were tested as a comparison to evaluate how a leached/aged compost would compare to new. Compost composition for non-leached and leached field and greenhouse samples are displayed in Table 4-3, serving as a comparison of both changes in compost over the course of each experiment as well as comparison of different compost characteristics for field and greenhouse at the beginning of the mineralization experiment.

Both composts had a pH below 7, with a pH of 5.2 for non-leached field compost and 6.8 for greenhouse compost. At the end of the experiment, leached field compost pH significantly increased to 6.6 ($p < 0.01$), closer approaching neutral pH. (After washing/aging in field and greenhouse experiments, both composts had 80-90% significantly lower electrical conductivity (EC) ($p < 0.001$), indicating a large amount of ionic constituents were released over the course of each experiment; high ECs in compost leachate that decreased over time has been observed previously for compost-amended media experiencing leaching (Chahal et al. 2016; Mullane et al. 2015; Xia et al. 2013). This is also supported by decreases in many ionic constituents over each

experiment, though not all were found to be statistically significant. Changes in moisture/solids content is mainly attributable to site conditions upon collection of leached samples (the antecedent moisture content was variable based on the day sampling was conducted). NH_4-N and NO_3-N content (what is immediately available for release) in non-leached composts were highly variable (877 ± 1296 mg/kg field and 190 ± 177 mg/kg greenhouse for NH_4-N; 1438 ± 1053 mg/kg field and 1744 ± 30 mg/kg greenhouse for NO_3-N), with the total mass and speciation of N likely attributable to both the natural high variability of compost and the specific moisture content and aeration in the collected samples. After leaching, aged composts had significantly lower NH_4-N and NO_3-N contents (all > 95% lower, $p < 0.05$ for all), except for the field NH_4-N content, which was not found statistically significant, likely due to the high standard deviation. The C:N ratio was not significantly changed for either compost, as expected since C:N ratio changes only slightly after maturation, though some significant decreases in total C, total N, and total P were found, which is expected due to loss through mineralization over the experiments. True differentiation of many compost parameters was made difficult by small sample size.

Table 4-3: *Compost Composition for Greenhouse and Field Experiments.*
All results are presented on a dry weight basis.

Parameter	units	FIELD (n=3) mean	FIELD (n=3) stdev	FIELD LEACHED (n=5) mean	FIELD LEACHED (n=5) stdev	% diff	stat. sig.	GREENHOUSE (n=3) mean	GREENHOUSE (n=3) stdev	GREEHOUSE LEACHED (n=24) mean	GREEHOUSE LEACHED (n=24) stdev	% diff	stat. sig.
pH	--	5.2	*0.7*	6.6	*0.3*	26%	b	6.8	*0.2*	7.0	*0.4*	3%	
EC	mmhos/cm	2.74	*0.53*	0.27	*0.10*	-90%	a	2.01	*0.13*	0.39	*0.28*	-81%	a
Solids	%	45	*1*	57	*11*	26%		38	*1*	73	*10*	90%	a
Moisture	%	55	*1*	43	*11*	-22%	a	62	*1*	27	*10*	-56%	a
Total Carbon	%	35.47	*0.87*	31.26	*2.58*	-12%	a	32.86	*0.58*	29.27	*2.32*	-11%	
Total Nitrogen	%	3.252	*0.262*	2.782	*0.235*	-14%		2.492	*0.024*	2.058	*0.193*	-17%	a
C:N Ratio	--	11.0	*0.6*	11.3	*0.8*	3%		13.2	*0.4*	14.3	*0.9*	8%	
NH4-N	mg/kg	877.4	*1295.6*	12.4	*3.9*	-99%		189.5	*176.6*	9.5	*12.9*	-95%	a
NO3-N	mg/kg	1438	*1053*	18	*13*	-99%	c	1744	*30*	72	*82*	-96%	a
P	%	2.105	*0.135*	2.144	*0.056*	2%		0.273	*0.006*	0.205	*0.034*	-25%	b
K	%	0.499	*0.012*	0.148	*0.056*	-70%	a	1.176	*0.057*	0.254	*0.112*	-78%	a
Ca	%	2.458	*0.036*	2.390	*0.065*	-3%		3.232	*0.041*	2.728	*0.291*	-16%	b
Mg	%	0.45	*0.01*	0.27	*0.04*	-39%	a	0.65	*0.02*	0.53	*0.10*	-17%	
Mn	mg/kg	987	*42*	934	*137*	-5%		1191	*65*	968	*141*	-19%	
Zn	mg/kg	997	*40*	1011	*9*	1%		173	*6*	157	*18*	-9%	
Cu	mg/kg	564	*19*	552	*20*	-2%		57	*1*	54	*6*	-5%	
Fe	mg/kg	25377	*3396*	34286	*488*	35%	a	12479	*59*	10468	*2133*	-16%	
B	mg/kg	36	*1*	11	*1*	-71%	a	50	*1*	21	*4*	-59%	a
S	mg/kg	10255	*675*	6692	*312*	-35%	a	2583	*81*	2081	*189*	-19%	a
Al	mg/kg	10617	*556*	8302	*302*	-22%	a	12115	*63*	5516	*1272*	-54%	a
Na	mg/kg	999	*66*	2282	*1152*	128%		395	*30*	139	*72*	-65%	a

**Differences in N and P content for field mineralization tests in comparison to this table is due to sample used for mineralization tests being collected from a different area. Results from that specific location were used in mineralization test comparisons for better accuracy.*

a $p < 0.001$ b $p < 0.01$ c $p < 0.05$

For a finished compost after the composting process, microbially mediated mineralization of organic forms of nitrogen to ammonium (NH_4^+) occurs, which may be followed by microbially mediated process of nitrification, where NH_4^+ is biologically oxidized to NO_2^- then to NO_3^- Because these steps in the nitrogen cycle are linked, mineralization is sometimes referred to as the process by which organic forms of nitrogen are converted to the plant-available, inorganic forms, including both ammonium (NH_4^+) and nitrate (NO_3^-) (Crohn 2004). In addition, several processes in the nitrogen cycle in which each of these soluble forms of nitrogen are transformed to the gaseous forms: ammonia (NH_3), nitrous oxide (N_2O), and nitrogen gas (N_2) should also be influential. The process of mineralization also occurs for phosphorus, which is microbially converted from organic forms of phosphorus to inorganic phosphates (PO4-P) (Hyland et al. 2005), specifically in the form of orthophosphates ($H_2PO_4^-$ or HPO_4^{2-}). However, unlike N, there is no volatilization pathway for P, making analysis somewhat easier for phosphorus, in that the mass balance will be closed. Because phosphorus mineralization is also a microbially mediated process, it will also be subject to variability based on temperature, moisture, and other environmental factors, however specific factors affecting phosphorus mineralization are not yet well understood (Spohn and Kuzyakov 2013).

Compost release of total nitrogen and phosphorus, presented as mg/g compost ((dry basis) (Figure 4-3 and Figure 4-4) were compared for compost used in the field and greenhouse experiments. The inorganic fractions represent the mineralized (DIN and DIP) fractions which were transformed from the organic to the inorganic, soluble forms which should give the mineralization rate (k_{min}). However, in this research, DON and DOP constituted a significant portion of released N and P (0-14% for N and 0-23% for P), and therefore the TDN and TDP release rates were also calculated. Results for mineralized N and P only (excluding the organic

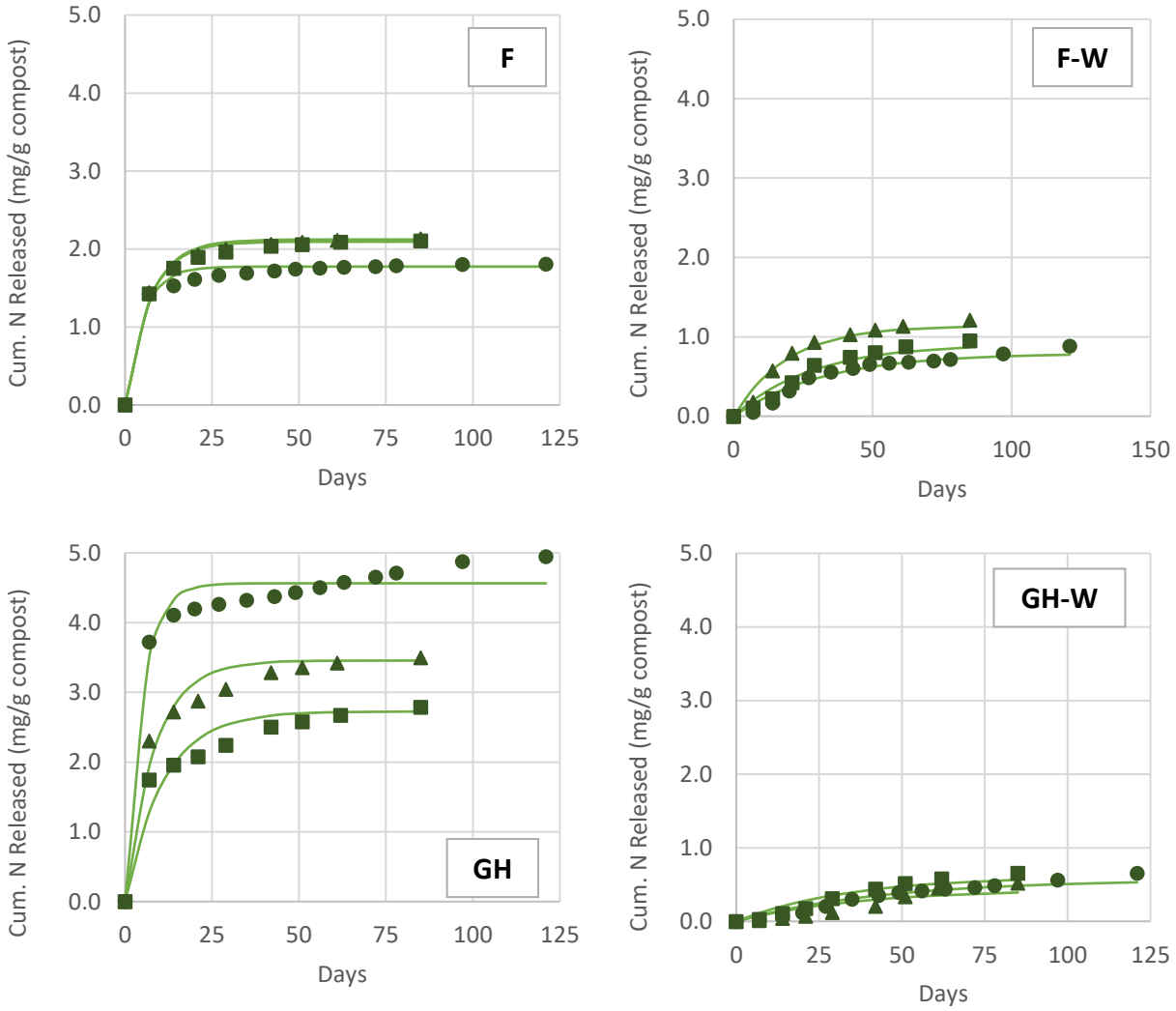
fractions) can be found in the appendix (Figure 5-6 and Figure 5-7). All mineralization tests were conducted in replicates of three.

Greenhouse and field composts demonstrated different trends in nitrogen release (Figure 4-3). Despite having a significantly higher total nitrogen content (33 ± 2.6 mg/g for F and 25 ± 0.2 mg/g for GH, $p < 0.01$), non-leached field compost released less total mass of nitrogen as well as less initial flush (first storm event mass release) (both ~1.8x less) than non-leached greenhouse compost, though not statistically significantly. This is also despite slightly lower C:N ratio in F compost (11.0 ± 0.6 for F, 13.2 ± 0.4 for GH, $p < 0.01$), since lower C:N ratios should promote greater mineralization, as well as non-statistically significantly different release rate constants ($k_{release}$ = 0.1587 day^{-1} for F and 0.1397 day^{-1} for GH, from Equation 4-6). The differences in total mass release may indicate differences in microbial communities as well as differences in compost composition related to different types of nitrogen pools.

After aging and leaching through repeated storm events, both the greenhouse and field composts had lower mean nitrogen release rate constants ($k_{release}$) (75%, $p < 0.01$ and 81%, $p < 0.05$, respectively) as well as lower mean initial flush (92%, $p < 0.001$ and 99%, $p < 0.05$, respectively) and mean total mass release (50%, $p < 0.001$ and 84%, < 0.01, respectively) (Figure 4-3). This difference was observed despite the minimal difference in initial total nitrogen content of the composts (24% less after leaching for field compost and 12% less after leaching for greenhouse compost on average). Non-leached composts released a much larger portion of total nitrogen mass (6.2% ± 0.6% for field and 15.0% ± 4.4% for greenhouse), while both leached composts released ~3-4% of total nitrogen mass (4.1% ± 0.7% for field and 2.9% ± 0.4% for greenhouse). This agrees with estimations of nitrogen release for yard waste and biowaste

compost of 5-15% release of total N in the first year, followed by 2-8% of the remaining total N mass in years following (Amlinger et al. 2003).

Nitrogen release curves for leached, aged composts (Figure 4-3) likely better fit an S-shaped curve (most evident in lower R^2 values, mean = 0.9473 and 0.7776 for F-W and GH-W, respectively, in comparison to F and GH, mean = 0.9860 and 0.9582, respectively), as has been observed previously in mineralization experiments on soils and plant residues (Chaves et al. 2004; Nosshi et al. 2007). The S-shape is caused by a lag phase at the beginning of the experiment when mineralization is limited until a fluctuation point. This is likely due to a smaller labile nitrogen pool (readily-available to microorganisms, nitrogen stored in carbohydrates, proteins) and a larger recalcitrant nitrogen pool (more resistant to microbial decomposition, nitrogen stored mainly in lignin) (Rovira and Vallejo 2002) in non-leached composts. Much of the readily available forms of nitrogen were likely already mineralized through aging/leaching in field and greenhouse experiments, leaving a much larger proportion of resistant forms of organic matter. Microbial biomass could have then experienced limited growth due to less nitrogen availability, causing a lag in mineralization. While this trend is important to note, an S-curve fit was not done in this research in order to 1) directly compare mineralization between compost types as well as to 2) maintain simpler equations for estimating net mineralization for use in further modeling.



	Compost N Content (mg/g)		$k_{release}$ (day^{-1})	R^2	Initial Flush N (mg/g)	Initial Flush N (%)	Total Released N Mass (mg/g)	Total Released N Mass (%)
F	32.523	**mean**	0.1587	0.9860	1.430	4.4%	2.013	6.2%
		stdev	0.0289	0.0077	0.009	0.03%	0.181	0.6%
F-W	24.685	**mean**	0.0393	0.9473	0.110	0.4%	1.013	4.1%
		stdev	0.0109	0.0176	0.065	0.3%	0.173	0.7%
GH	24.917	**mean**	0.1397	0.9582	2.586	10.4%	3.740	15.0%
		stdev	0.0624	0.0158	1.019	4.1%	1.102	4.4%
GH-W	21.290	**mean**	0.0261	0.7776	0.022	0.1%	0.610	2.9%
		stdev	0.0034	0.2491	0.008	0.04%	0.077	0.4%

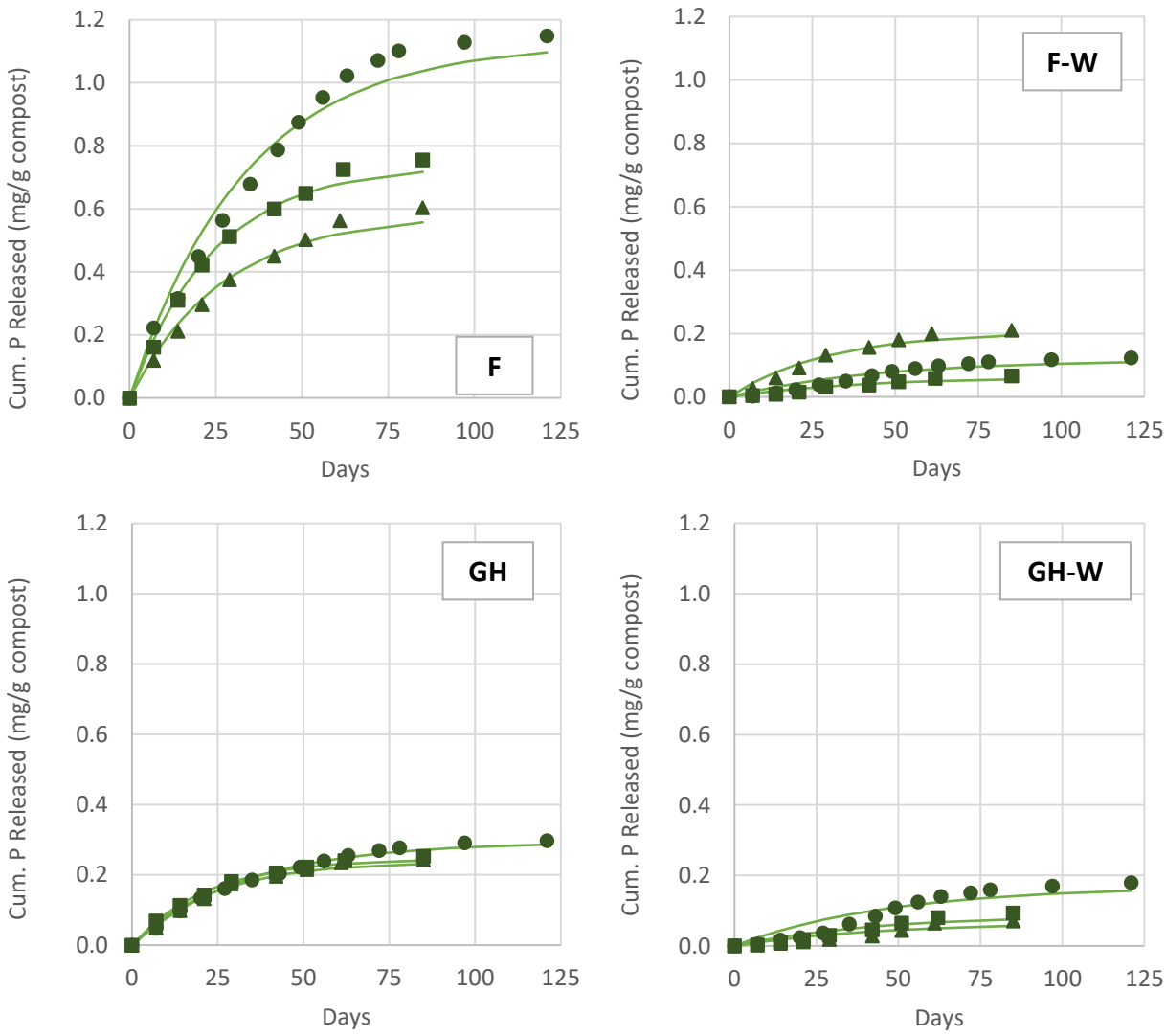
Figure 4-3: Total Nitrogen Release Curves and Best Fit Statistics.
$k_{release}$ and Total Released N Mass used in Equation 0-5; R^2 obtained from best fit; Compost N Content, Initial Flush N, and percentages are shown for comparison.

Greenhouse and field composts also showed different trends in total phosphorus release (Figure 4-3). With a 7.7x larger total phosphorus content (21 ± 1.4 mg/g for F and 2.7 ± 0.06 mg/g for GH, $p < 0.001$), non-leached field compost released a higher total mass of phosphorus as well as higher initial flush (both ~3x higher, $p < 0.05$ for both) than non-leached greenhouse compost. Despite this difference in mass release, the release rate constants ($k_{release}$ = 0.0358 day^{-1} for F and 0.0390 day^{-1} for GH) were similar (less than 10% difference, no statistical significance).

Similar to trends for nitrogen release, both greenhouse and field composts had lower mean phosphorus initial flush (first storm event mass release) (93%, $p < 0.01$ for both), and mean total mass release (84%, $p < 0.05$ and 57%, $p < 0.05$, respectively) for leached composts in comparison to non-leached (Figure 4-4). However, for release rate constants ($k_{release}$), aged field compost did not see a statistically significant decrease after leaching (22%), while there was a significant decrease found for aged greenhouse compost after leaching (43%, $p < 0.05$). The difference in initial total phosphorus content of the composts after leaching were similar, with 18% less total P after leaching for field compost and 19% less total P after leaching for greenhouse compost. Non-leached composts released a much larger portion of total phosphorus mass (4.0% for field and 9.6% for greenhouse, based on mean) in comparison to leached composts (0.8% for field and 5.1% for greenhouse, based on mean). The same trend observed for nitrogen release curves in leached composts was also observed for phosphorus, where likely an S-shaped curve would have more appropriately fit the dataset, evidenced by lower R^2 values for both F-W and GH-W, mean = 0.8755 and 0.7245, respectively, in comparison to non-leached (mean = 0.9821 and 0.9916 for F and GH, respectively). Phosphorus too seems to exhibit a lag phase for leached composts, indicating that a smaller labile pool of P may be present after

washing/aging. Similar to nitrogen, the first-order kinetic model was deemed an appropriate approximation of performance.

N release rate constants of non-leached composts were higher than for P (~0.14-0.16 day^{-1} for N and 0.036-0.039 day^{-1} for P), indicating that a higher mass of N is released earlier in the experiment than is P, though for leached composts these rate constants were more similar (~0.026-0.039 day^{-1} for N, ~0.022-0.028 day^{-1} for P). Leaching composts resulted in lower initial and total mass release of N and P for both of the composts in this study. The release rate constant was also lower after leaching for N for both composts, but not lower after leaching for P in the field compost. Significantly lower mass release and lower release rate constants indicates that a leached compost should release less mass immediately after application, less total mass, and may release mass more slowly over time. As discussed, this is likely due to a more labile pool of N and P being released through successive storm events in the leached compost, leaving a more recalcitrant pool which is more difficult for the microbial community to mineralize.



	Compost P Content (mg/g)		$k_{release}$ (day^{-1})	R^2	Initial Flush P (mg/g)	Initial Flush P (%)	Total Released P Mass (mg/g)	Total Released P Mass (%)
F	21.050	**mean**	0.0358	0.9821	0.167	0.8%	0.836	4.0%
		stdev	0.0055	0.0095	0.052	0.2%	0.282	1.3%
F-W	17.162	**mean**	0.0276	0.8755	0.011	0.1%	0.133	0.8%
		stdev	0.0061	0.0696	0.014	0.1%	0.073	0.4%
GH	2.733	**mean**	0.0390	0.9916	0.055	2.0%	0.264	9.6%
		stdev	0.0079	0.0037	0.012	0.4%	0.029	1.1%
GH-W	2.224	**mean**	0.0223	0.7245	0.004	0.2%	0.114	5.1%
		stdev	0.0013	0.0660	0.001	0.07%	0.058	2.6%

Figure 4-4: Total Phosphorus Release Curves and Best Fit Statistics. $k_{release}$ and Total Released P Mass used in Equation 0-5; R^2 obtained from best fit; Compost P Content, Initial Flush P, and percentages are shown for comparison.

Soil Adsorption

Comparisons of soil characteristics and composition before and after compost application (for the field ~2.25 yr and for the greenhouse ~1 yr) provide information about the compost's influence on soil chemical changes and possible influences on nutrient retention. Field soil characteristics before and after VCB installation are shown in Table 4-4. Organic matter content was not significantly increased over 2.25 years for either the VFS (topsoil) or subsoil layers, however, it often takes decades of consistent annual application for soil organic matter to increase by significant amounts (Termorshuizen et al. 2004). Soil pH was not changed significantly, however a significant increase in CEC by 80% was found for the VFS topsoil ($p < 0.001$), though significance was not found for the 30% increase in subsoil.

Base saturation was somewhat decreased for both soils (only significant for the subsoil, $p < 0.001$), which is likely most attributable to the increase in CEC, since the base saturation is calculated as the sum of Ca^+, K^+, and Mg^+ divided by the CEC. Most importantly, a significant increase in P content was observed for both soils (from 17.4 ± 6.8 to 249 ± 8.4 mg/kg ($p < 0.001$) for VFS topsoil and from 10.1 ± 12 to 64.8 ± 28 mg/kg ($p < 0.01$) for subsoil) as well as significant increases in the P saturation ratio (from 11.2 to 121% ($p < 0.001$) for VFS topsoil and from 8.1 to 22.6% ($p < 0.01$) for subsoil). A saturation greater than 100% for the VFS topsoil is likely because P saturation ratio is estimated as the ratio of P to Fe + Al content of the soil. Because the saturation ratio is so high, this P content is likely at or close to the maximum adsorption capacity for the VFS layer. For the subsoil, it is likely that the maximum capacity was not reached, but significant removal also occurred in this layer. Because the subsoil has a low hydraulic conductivity, mass flushing during a storm event will not infiltrate downward, which may partly explain why more adsorption capacity was left unfilled.

Table 4-4: Field Experiment Soil Characteristics Before and After Compost Application.
All results are presented on a dry weight basis.

		FIELD TOPSOIL (VFS)						FIELD SUBSOIL					
		Pre-Installation (n=7)		Post-Installation (n=4)				Pre-Installation (n=7)		Post-Installation (n=4)			
Parameter	**units**	**mean**	**stdev**	**mean**	**stdev**	**% diff**	**stat. sig.**	**mean**	**stdev**	**mean**	**stdev**	**% diff**	**stat. sig.**
pH	--	7.5	*0.3*	7.1	*0.4*	-6%		7.5	*0.3*	6.7	*0.7*	-11%	c
CEC	meq/100g	11.46	*2.02*	20.69	*1.10*	80%	a	8.53	*4.25*	11.14	*1.61*	31%	
OM	%	5.6	*1.7*	5.9	*1.4*	5%		2.5	*0.7*	2.6	*0.4*	2%	
P	mg/kg	17.40	*6.84*	248.72	*8.38*	1330%	a	10.09	*12.02*	64.79	*27.76*	542%	b
K	mg/kg	55.24	*8.37*	121.22	*105.06*	119%		30.57	*6.83*	82.26	*62.54*	169%	
Ca	mg/kg	1990.42	*415.51*	3349.59	*704.63*	68%	b	1473.18	*890.02*	1384.84	*330.13*	-6%	
Mg	mg/kg	164.33	*42.53*	284.53	*126.78*	73%	c	129.00	*33.81*	259.92	*121.97*	101%	c
Mn	mg/kg	124.41	*33.73*	65.39	*13.11*	-47%	b	164.09	*77.04*	175.74	*101.30*	7%	
Zn	mg/kg	35.11	*20.96*	39.85	*5.08*	14%		9.40	*11.78*	10.53	*1.16*	12%	
Cu	mg/kg	10.45	*4.59*	12.28	*3.21*	17%		5.31	*4.93*	5.82	*1.60*	10%	
Fe	mg/kg	203.22	*64.78*	289.55	*30.43*	42%	c	109.25	*35.19*	184.94	*38.70*	69%	b
B	mg/kg	1.40	*0.41*	1.78	*0.43*	27%		0.75	*0.38*	1.09	*0.37*	46%	
S	mg/kg	13.01	*2.31*	32.32	*0.63*	148%	a	13.07	*3.07*	35.73	*3.91*	173%	a
Al	mg/kg	378.07	*194.03*	376.26	*57.69*	0%		542.91	*214.41*	660.70	*59.14*	22%	
Na	mg/kg	443.54	*59.62*	582.70	*156.62*	31%		599.84	*126.29*	736.58	*284.72*	23%	
Base Sat.	%	100.0	*0.0*	92.9	*6.8*	-7%	c	99.7	*0.7*	82.2	*7.4*	-18%	a
P Sat.	Ratio	11.2	*2.4*	121.3	*9.6*	983%	a	8.1	*4.6*	22.6	*6.6*	179%	b
A-E Buffer	pH	8.08	*0.07*	7.84	*0.14*	-3%	b	8.09	*0.07*	7.77	*0.11*	-4%	a

a $p < 0.001$ b $p < 0.01$ c $p < 0.05$

Greenhouse soil characteristics before and after VCB installation are shown in Table 4-5, with a clayey topsoil included that was not used in greenhouse experiments but was used in adsorption experiments for comparison. Organic matter content was found to significantly decrease over ~1 year for the topsoil layer (from 2.7% ± 0.6% to 1.6% ± 0.4%, $p < 0.001$). This could be partially attributable to the small sample size for the pre-installation soil; however, it is possible that there was a loss of organic matter content in the soil layer through dissolution and/or mineralization, especially since greenhouse soil was an engineered soil not exposed to the elements, unlike at the field site where soils had a long period of time to reach steady-state conditions before the beginning of the experiment.

Soil pH increased significantly over the experiment (from 6.5 ± 0.0 to 7.1 ± 0.2, $p < 0.001$), as did CEC by 60% ($p < 0.001$), as was observed for the field topsoil, as well as a small increase in base saturation (99.3% ± 1.3% to 100% ± 0%, $p < 0.001$). As with the field soils, significant increase in P content was also observed (from 8.5 ± 1.0 to 23 ± 8.3 mg/kg ($p < 0.01$) as well as significant increases in the P saturation ratio (from 14.5% ± 0.7% to 27.1% ± 7.0% ($p < 0.001$). Unlike at the field site, saturation at or above 100% was not observed, indicating that the capacity for P removal via adsorption was not reached. This could be due to a shorter experiment as well as lower applied volumes in the greenhouse in comparison to the field (1 yr, ~35 bed volumes greenhouse, 2.25 yr and ~110 bed volumes field) as well as significantly lower P content in the greenhouse compost (7.7 times lower, $p < 0.001$) which resulted in significantly lower effluent P concentrations as well (Chapter 3).

Table 4-5: Greenhouse Experiment Soil Characteristics Before and After VCB Application. All results are presented on a dry weight basis.

		GH SANDY TOPSOIL (VFS) Pre-Installation (n=3)		GH SANDY TOPSOIL (VFS) Post-Installation (n=21)				GH CLAYEY TOPSOIL* (n=3)	
Parameter	**units**	**mean**	**stdev**	**mean**	**stdev**	**% diff**	**stat. sig.**	**mean**	**stdev**
pH	--	6.5	*0.0*	7.1	*0.2*	9%	a	6.7	*0.1*
CEC	meq/100g	3.18	*0.39*	5.09	*0.73*	60%	a	15.05	*0.13*
OM	%	2.7	*0.6*	1.6	*0.4*	-39%	a	3.8	*0.2*
P	mg/kg	8.53	*1.01*	23.07	*8.26*	170%	b	22.20	*2.16*
K	mg/kg	106.59	*6.79*	83.87	*54.10*	-21%		128.91	*3.27*
Ca	mg/kg	468.71	*52.83*	806.79	*112.42*	72%	a	1912.50	*24.88*
Mg	mg/kg	63.96	*7.45*	100.92	*18.74*	58%	b	397.73	*12.03*
Mn	mg/kg	19.09	*0.58*	17.17	*3.18*	-10%		94.92	*1.35*
Zn	mg/kg	1.20	*0.11*	1.77	*0.45*	48%	c	3.37	*0.19*
Cu	mg/kg	0.64	*0.09*	0.69	*0.09*	8%		2.01	*0.22*
Fe	mg/kg	127.39	*8.28*	142.96	*19.97*	12%		196.66	*16.56*
B	mg/kg	0.37	*0.03*	0.71	*0.15*	93%	a	1.27	*0.03*
S	mg/kg	4.82	*0.43*	5.28	*1.73*	10%		20.19	*3.09*
Al	mg/kg	115.51	*6.71*	139.88	*13.41*	21%	b	642.69	*8.39*
Na	mg/kg	15.96	*1.31*	9.86	*4.36*	-38%	c	16.61	*7.34*
Base Sat.	%	99.3	*1.3*	100.0	*0.0*	1%	b	87.8	*0.6*
P Sat.	Ratio	14.5	*0.7*	27.1	*7.0*	87%	b	10.8	*0.5*
A-E Buffer	pH	8.00	*0.01*	8.08	*0.03*	1%	a	7.77	*0.01*

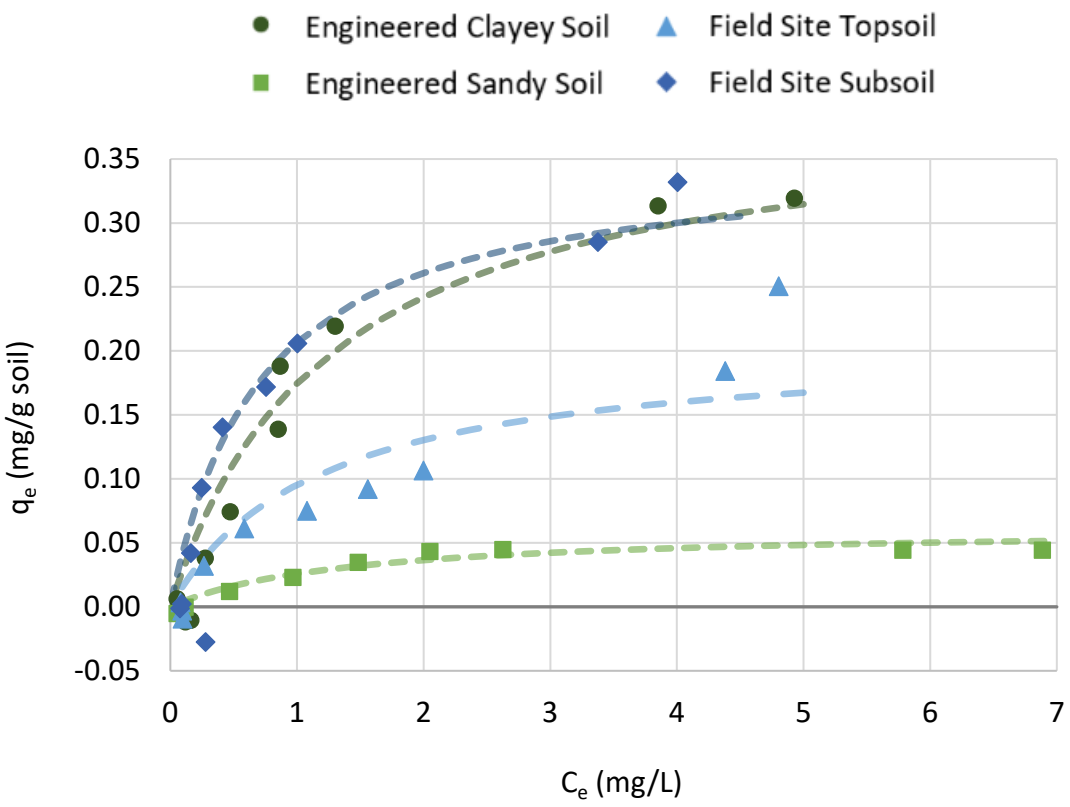
**Not used in greenhouse experiments; only used for comparison of soil types and in adsorption experiments.*

a $p < 0.001$ b $p < 0.01$ c $p < 0.05$

Some nutrient removal may occur in the VFS layer, though monitoring and understanding nitrogen movement should be made more difficult due to the complexity of the nitrogen cycle. Ammonium ($NH_4^{+)}$ has been shown to be removed via sorption by clays and several types of zeolite, a microporous aluminosilicate mineral (Khorsha et al. 2021; Khorsha and Davis 2016, 2017; Liu and Lo 2001a; Rožić et al. 2000; Wang et al. 2006) and DON adsorption was shown for soils in some situations (Bingham and Cotrufo 2016; Goyne et al. 2008; Kaiser and Zech 2000; Mariano et al. 2016). However, removal of NO_2^- and NO_3^- is not expected since these species are generally mobile and not easily removed by soils. For stormwater bioretention media, which is an engineered mix, it has been shown that removal of ammonium (NH_4^+) via sorption is likely to occur while removal of dissolved organic nitrogen (DON) and nitrate (NO_3^-) will not be significant, or may even be exported from the media (Li and Davis 2014). There have been numerous studies which have quantified and modeled sorption of phosphorus in bioretention systems and other SCMs (Hsieh et al. 2007; Komlos and Traver 2012; Li and Davis 2016; Liu 2014; Liu and Davis 2014; Yan et al. 2016, 2017, 2018). There is less complexity in observing phosphorus transformations because there is no pathway for loss of mass to the atmosphere, and sorption kinetics are better known and understood.

Soils used in field and greenhouse experiments were evaluated for their capacity for adsorption of nitrogen and phosphorus species. All soils demonstrated phosphorus adsorption in the form of orthophosphate (PO_4-P), with no discernable trend for DOP (all $R^2 < 0.1$). The only nitrogen species which showed some adsorption to the tested soils was NH_4^+, with no observable trend for NO_3^- or DON (all $R^2 < 0.1$). Adsorption of NH_4^+ but not NO_3^- or DON has been observed previously in engineered bioretention media (Li and Davis 2014). Adsorption isotherms for PO4-P are shown in Figure 4-5 and those for NH_4^+ are shown in Figure 4-6.

All tested soils showed some degree of phosphorus adsorption (Figure 4-5), with soils of higher clay content (engineered clayey soil and field site subsoil) having the highest theoretical adsorption capacities (Q) and therefore exhibiting the highest degree of PO4-P removal. Adsorption capacity Q increased with total Al+Fe content in the order engineered sandy soil (243 mg/kg Al+Fe) < field site topsoil (581 mg/kg Al+Fe) < field site subsoil (652 mg/kg Al+Fe) < engineered clayey soil (839 mg/kg Al+Fe). This is an expected result given that phosphorus adsorption by aluminum (Al) and iron (Fe) oxides has been well-documented (Zhang et al. 2001), including substantial PO_4-P sorption on clay minerals (Gérard 2016; Guedes et al. 2015). This result indicates significant phosphate removal from compost leachate despite the presence of dissolved organic matter, since humic acid has been shown to inhibit phosphorus adsorption (Fu et al. 2013; Maluf et al. 2018; Wang et al. 2016). The theoretical adsorption capacity Q for the field VFS (topsoil) was found to be 206.5 mg/kg which is within 17% of the 249 ± 8 mg/kg P content of topsoil measured 2.25 years after VCB application. This gives further evidence that field VFS topsoil had no additional P adsorption capacity. Differences in P adsorption values may be explained in part because adsorption capacity was tested in the lab with topsoil collected prior to VCB installation. Field VFS topsoil underwent significant chemical and physical changes due to compost application by the end of the experiment, including a mean 42% ($p < 0.05$) increase in Fe content (Table 4-4), may have somewhat increased P sorption capacity.



	Q (mg/g soil)	K_L (L/mg)	RMSE (mg/g soil)	R^2
Engineered Clayey Soil	0.3937	0.797	0.0226	0.94576
Engineered Sandy Soil	0.0617	0.723	0.0049	0.83497
Field Site Topsoil (VFS)	0.2065	0.855	0.0346	0.56280
Field Site Subsoil	0.3533	1.410	0.0162	0.96610

Figure 4-5: Phosphate Adsorption Isotherms and Langmuir Best Fit Statistics.

Previous research has quantified sorption of soluble nitrogen species from compost leachate, but they have mostly focused on specific adsorbents for advanced treatment rather than a soil matrix (Liu and Lo 2001a; b; Rožić et al. 2000; Theng 1972; Wang et al. 2006). In this research, adsorption isotherms were conducted for engineered soils from the greenhouse and field site experiments to test how compost leachate may interact with a VFS system. For NH_4^+,

adsorption isotherms were not able to provide good fits for adsorption but the results can be qualitatively described and related to nitrogen movement in field and greenhouse experiments (Figure 4-6). All soils exhibited some ability to remove NH_4^+ except the engineered clayey soil, which showed some level of desorption. This could be due to NH_4^+ release from the organic matter content in the soil itself or may also have been caused by interactions with competitor ions introduced by the compost leachate, specifically Ca^+, K^+, and Mg^+. Adsorption isotherms for the other soils demonstrated both adsorption as well as some "desorption" at lower leachate concentrations, indicated by values falling below the x-axis. For any soil, the challenge of monitoring nitrogen movement has been well known due to the complexity of the nitrogen cycle, and the observed "desorption" may be attributable to nitrogen transformations rather than sorption processes. Some portion of NH_4^+ may have been transformed through nitrification to NO_2^- and NO_3^-, making the mass balance used in calculating q_e incomplete, and giving the false impression of negative removal, or desorption. These results are also complicated by the potential influence of competitor cations, since adsorption of NH_4^+ has been shown to be mainly through cation exchange and to be correlated with clay content (Alshameri et al. 2018; Khorsha 2016; Khorsha et al. 2021; Khorsha and Davis 2017; Kothawala and Moore 2009; Liu and Lo 2001a; Rožić et al. 2000; Wang et al. 2006).

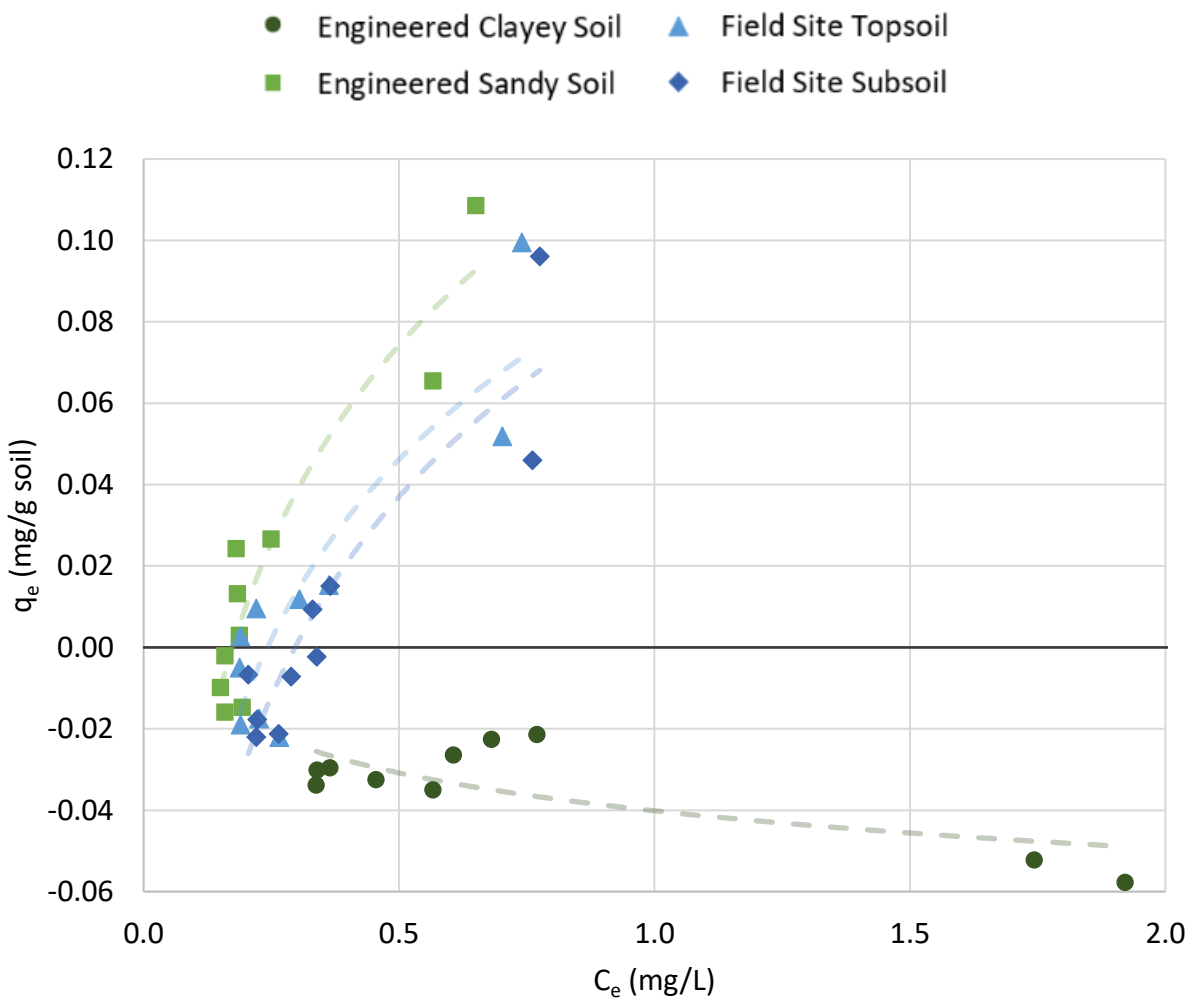
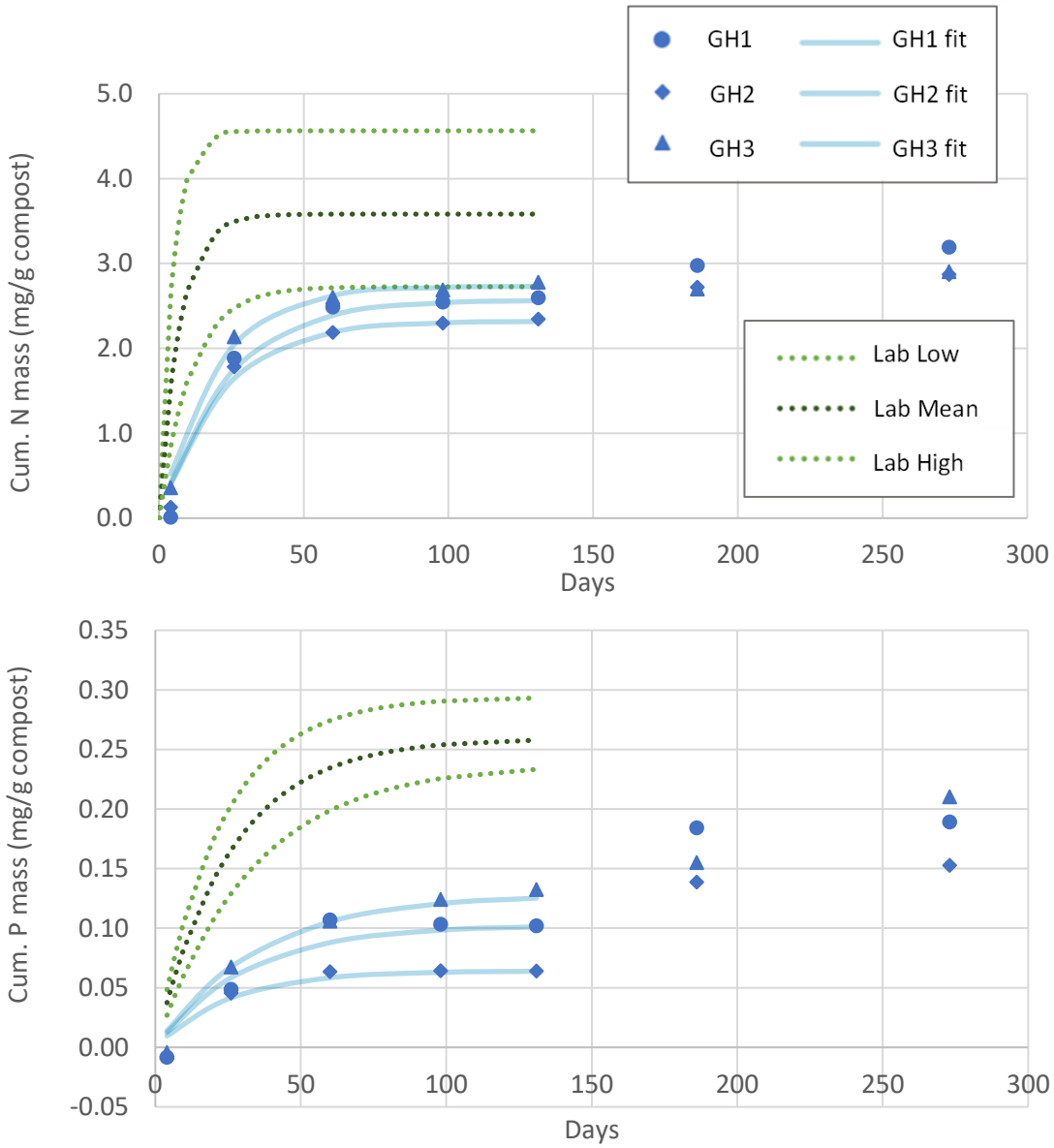


Figure 4-6: Results from Ammonium Adsorption Experiments.
Logarithmic fits are displayed to aid visualization but are not representative of true best fit.

Comparison to Large Scale Studies

Laboratory-obtained nitrogen and phosphorus release rates and total mass release were used to predict cumulative nutrient release (normalized by dry mass of compost) over time for the first 130 days of greenhouse experiments (Figure 4-7). This time period was chosen because lab experiments were run for approximately 120 days and greenhouse experiments had a sampling event at approximately 130 days, so total mass release should be approximately the same in this

time. Additional mass release observed after this timeframe are also displayed for comparison and the initial mass flush (mass release during first storm event) is also included with statistics for comparison. Both nitrogen and phosphorus laboratory predictions for mass release demonstrate higher mean mass release than what was observed in the greenhouse experiments, which is expected due to potential removals in the soil layer, since mineralization experiments only evaluated nutrient release from the compost alone while greenhouse experiments include both the VCB and VFS layers. For nitrogen, the greenhouse observation is within range of the laboratory prediction, being similar to the lowest mass release curve (greenhouse total mass releases ranges between 2.35 to 2.78 mg/g compost, lab estimations ranges between 2.73 to 4.56 mg/g compost). Based on the mean laboratory estimation, it is possible that some nitrogen removal was observed. However, the initial flush of nitrogen mass in laboratory studies was found to be highly variable and to have an outsize impact on the nitrogen release curve, with approximately 70% of total mass released during the first storm event, making this assessment less certain. For phosphorus, a reduction in mass release for all greenhouse experiments is found in comparison to the full range of laboratory predictions (greenhouse total mass release falls between 0.064 to 0.132 mg/g compost, lab estimations fall between 0.233 to 0.293 mg/g compost), indicating some removal through the soil layer, which is supported by net P content increase in greenhouse soils after VCB application (from 8.5 ± 1.0 to 23 ± 8.3 mg/kg ($p < 0.01$)).



	Nitrogen Release			Phosphorus Release		
	$k_{release}$	initial flush (mg/kg)	total release (mg/kg)	$k_{release}$	initial flush (mg/kg)	total release (mg/kg)
Lab 1	0.2100	3.718	4.944	0.0300	0.0474	0.2970
Lab 2	0.0910	1.741	2.783	0.0450	0.0686	0.2523
Lab 3	0.1180	2.300	3.493	0.0420	0.0492	0.2418
GH 1	0.0441	1.753	2.562	0.0324	0.0584	0.1011
GH 2	0.0475	1.646	2.317	0.0401	0.0416	0.0639
GH 3	0.0531	2.045	2.730	0.0288	0.0676	0.1252

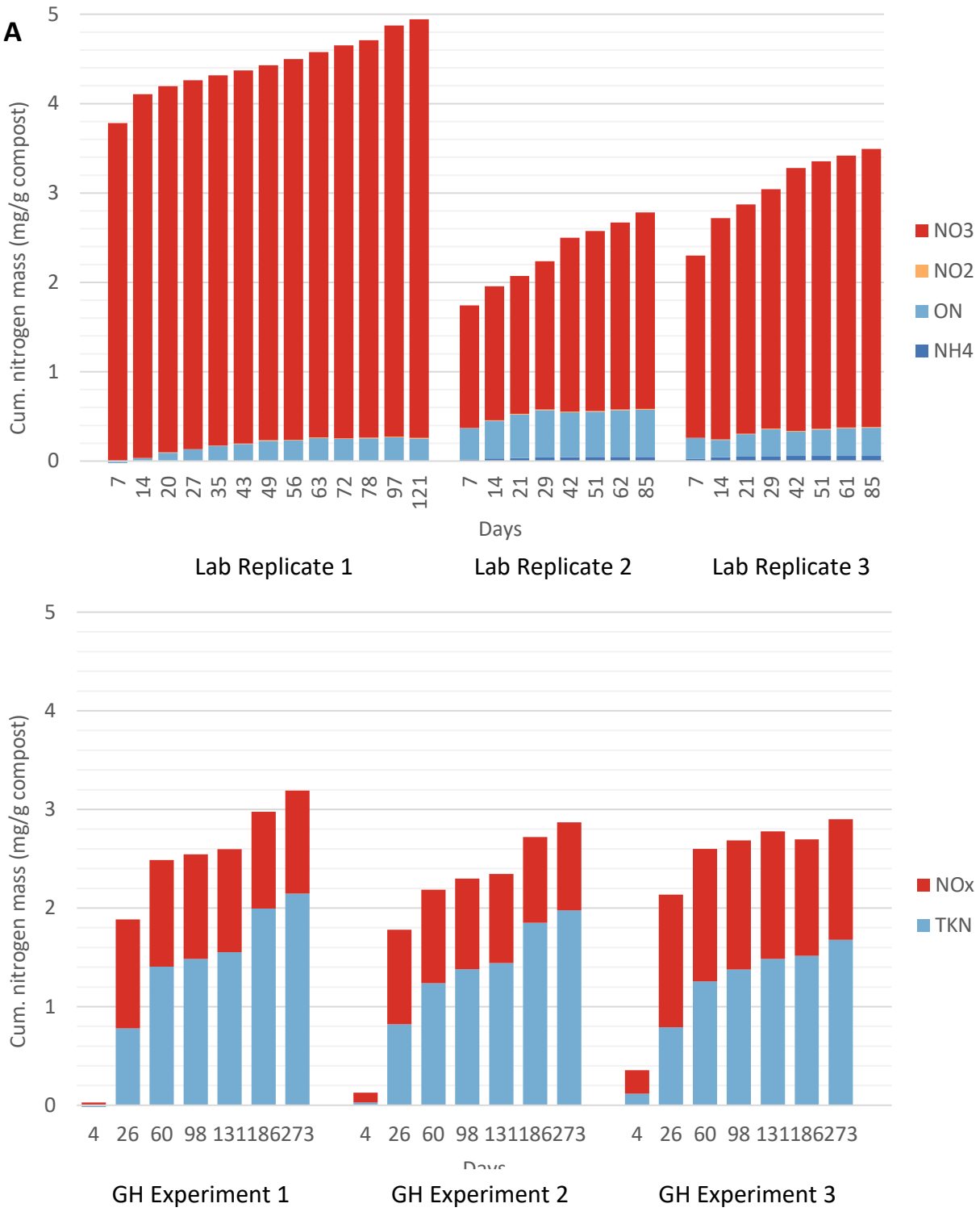
Figure 4-7: Comparison of Greenhouse and Mineralization Experiment Nutrient Release. comparison of greenhouse experiment nutrient release in stormwater effluent to release estimated by laboratory mineralization tests.

Mineralization experiments differed from greenhouse and field experiments in nitrogen speciation. Cumulative release curves were created for nitrogen species for each experiment with non-leached composts from both greenhouse and field mineralization laboratory experiments compared to observed data from greenhouse and field experiments (Figure 4-8). Greenhouse experiments can be directly compared to laboratory data since all applied storms were collected, however, field results are only partially comparable because some storm events were not captured.

For greenhouse experiments (Figure 4-8), a much larger proportion of TKN (sum of NH_4^+ and organic N) was released in comparison to laboratory tests, with total TKN release ranging from 5-21% in the laboratory and from 52-67% in the greenhouse). NO_3^- constituted the majority of remaining mass for both datasets, with negligible mass of NO_2^-. Additionally, the majority of laboratory column experiment TKN release was in the form of DON (84-99%) rather than NH_4^+. These results indicated potentially a higher degree of nitrification in laboratory studies than in the greenhouse, possibly attributable to differences in moisture content and temperature. Additionally, though temperatures were similar between laboratory and greenhouse (~20°C in laboratory and ~22°C daytime temperature in greenhouse), higher soil temperatures in the greenhouse likely increased the amount of nitrogen volatilization (transformation from NH_4^+ to $NH_3(g)$), which may also partially explain why mean total mass release was larger for the laboratory than the greenhouse.

In comparing laboratory experiment nitrogen speciation to field results (Figure 4-8), it is important to note that equipment installation and troubleshooting immediately after field installation delayed data collection by at least 21 days, during which time 12.7-cm (5-in) of rainfall was not monitored (as estimated by a nearby rain gauge), meaning that the initial mass release was not observed. A large spike in nitrogen was observed on day 238, soon after a drought period, with most of this mass being in the form of TKN for the 3-m VCB and in the form of NO_x for the 5-m VCB. These high mass releases had an outsize impact on the total release (totaling 42% of total TKN mass for 3-m and 83% of total NO_x mass for 6-m), so this storm event was excluded from the speciation comparison.

In the laboratory, the proportion of total nitrogen in the form of TKN was between 21-42%, while in the field, it was 86% for the 3-m VCB and 56% for the 6-m VCB, indicating a higher degree of nitrification for laboratory experiments. Additionally, higher seasonal temperatures likely encouraged higher amounts of nitrogen volatilization. In comparing the 3-m and 6-m VCBs, a higher proportion of NO_x was observed in the 6-m system, and though it is a partial sum, a lower mass of nitrogen release (per mass of compost) was observed. Because the 6-m system had a lower drainage area ratio (3.5:1 for 3-m and 2.5:1 for 6-m), moisture content was higher in this system, possibly reducing the degree of nitrification. Additionally, because this system experienced lower flowrates, this may have increased potential nitrogen retention in the underlying VFS layer.


A
Cum. nitrogen mass (mg/g compost)
5
4
3
2
1
0
7 14 20 27 35 43 49 56 63 72 78 97 121
7 14 21 29 42 51 62 85
7 14 21 29 42 51 61 85
Days
NO3
NO2
ON
NH4
Lab Replicate 1
Lab Replicate 2
Lab Replicate 3
Cum. nitrogen mass (mg/g compost)
5
4
3
2
1
0
4 26 60 98 131186273
4 26 60 98 131186273
4 26 60 98 131186273
NOx
TKN
GH Experiment 1
GH Experiment 2
GH Experiment 3

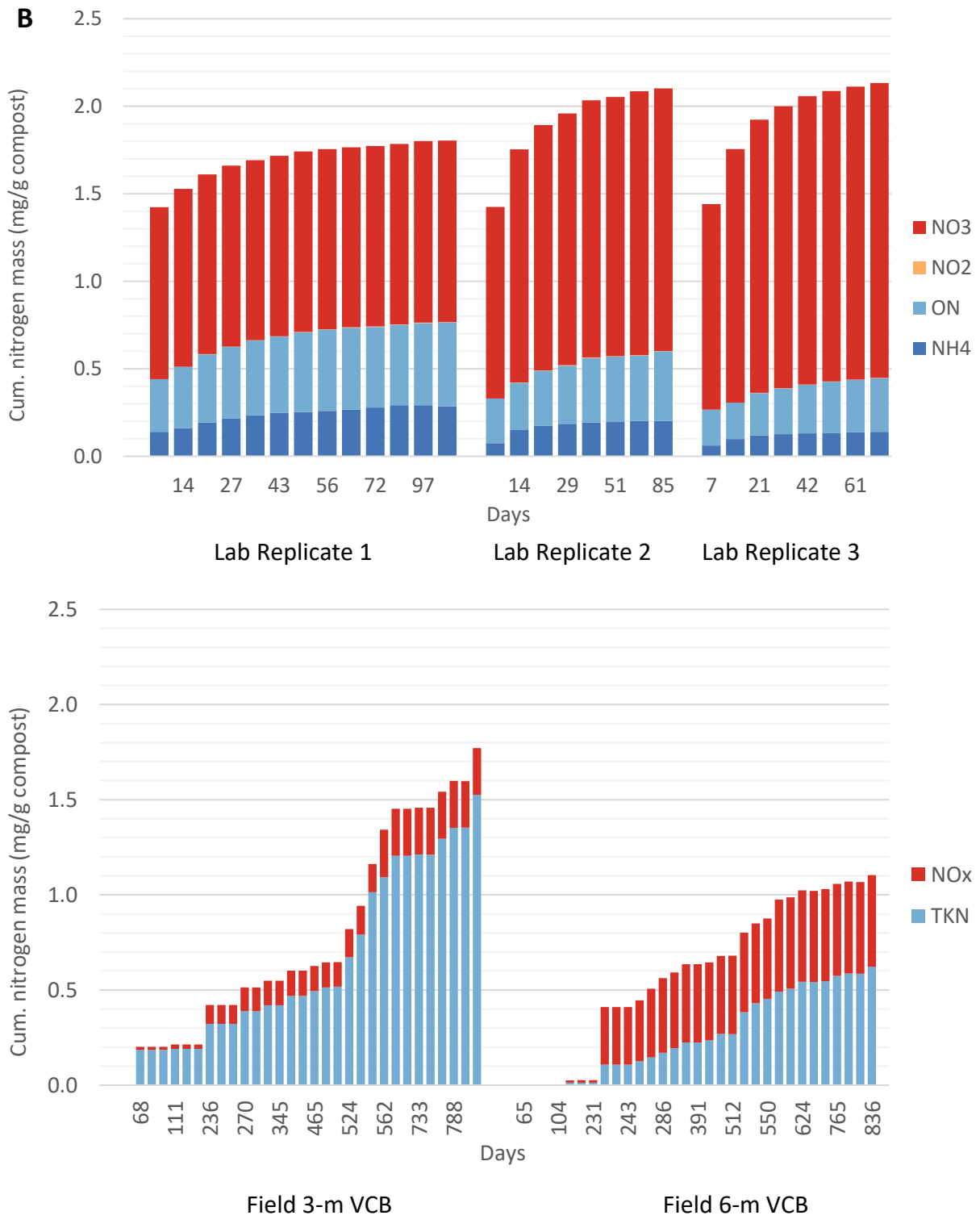


Figure 4-8: Laboratory and Field/Greenhouse N Speciation Comparison. A) non-leached greenhouse compost from laboratory mineralization studies compared to greenhouse observations; B) non-leached field compost from laboratory mineralization studies compared to field observations.

Nutrient Mass Balance

Biomass samples collected at the field site from areas of different compost depths as well as the associated nitrogen and phosphorus masses are shown in Figure 4-9, and biomass nutrients contents are shown in Table 4-6. Nitrogen tissue content for the sampling event in Fall 2020 were not collected due to human error and samples were not collected in the first growing season after installation due to unintended mowing of the site. Nitrogen and phosphorus tissue contents (%) were similar for locations with compost applications on average (within ~12% for N and ~20% for P) and were consistently higher than the control location (by ~25% for N and ~50% for P on average) (Table 4-6), though the small dataset size prevented statistical comparison, showing that all compost treatments resulted in some level of increased plant nutrient uptake.

Table 4-6: Biomass Plant Tissue Nutrient Content.
Control samples were taken from an area with no compost application; 2.5-, 5-, and 10-cm depth samples were collected from the observational VCB areas while the 7.6-cm depth samples were collected from the 6-m VCB area.

Nitrogen (%)	Control (0-cm depth)	2.5-cm depth	5-cm depth	7.6-cm depth	10-cm depth
Fall 2020	NA	NA	NA	NA	NA
Spring 2021	1.183	1.958	1.770	1.937	1.692
Summer 2021	1.806	1.867	2.263	2.439	2.129
Mean	1.495	1.913	2.017	2.188	1.911
STDEV	NA	NA	NA	NA	NA

Phosphorus (%)	Control (0-cm depth)	2.5-cm depth	5-cm depth	7.6-cm depth	10-cm depth
Fall 2020	0.32	0.45	0.65	0.54	0.74
Spring 2021	0.23	0.43	0.44	0.35	0.42
Summer 2021	0.25	0.51	0.61	0.47	0.56
Mean	0.27	0.46	0.57	0.45	0.57
STDEV	0.05	0.04	0.11	0.10	0.16

For Fall 2020, a positive linear correlation was found between biomass growth and compost depth (Pearson's $R^2 = 0.8307$), with between 30-90% increase in biomass in comparison to the control area. This performance is similar to results found for a study on sludge compost-amended soils which saw biomass increases of 30-120% with increasing amendment percent (Hua et al. 2008). However, sampling periods after this growth period showed weak correlations ($R^2 = 0.0006$ for Spring 2021 and $R^2 = 0.4225$ for Summer 2021). For spring, this is likely due to observed heterogeneous growth during the first growth period after winter dormancy and for both spring and summer 2021; a range of diverse plant species (many not grasses) were visually observed growing over the VCB areas during field site visits. This additional heterogeneity likely had an effect on increasing variability of biomass measurements between sampling locations. In summer months ~2 years after VCB installation, all depths of compost produced higher biomass (4-5 times higher) and also sequestered a greater mass of both nitrogen (5-6 times higher) and phosphorus (5-7 times higher) than the control.

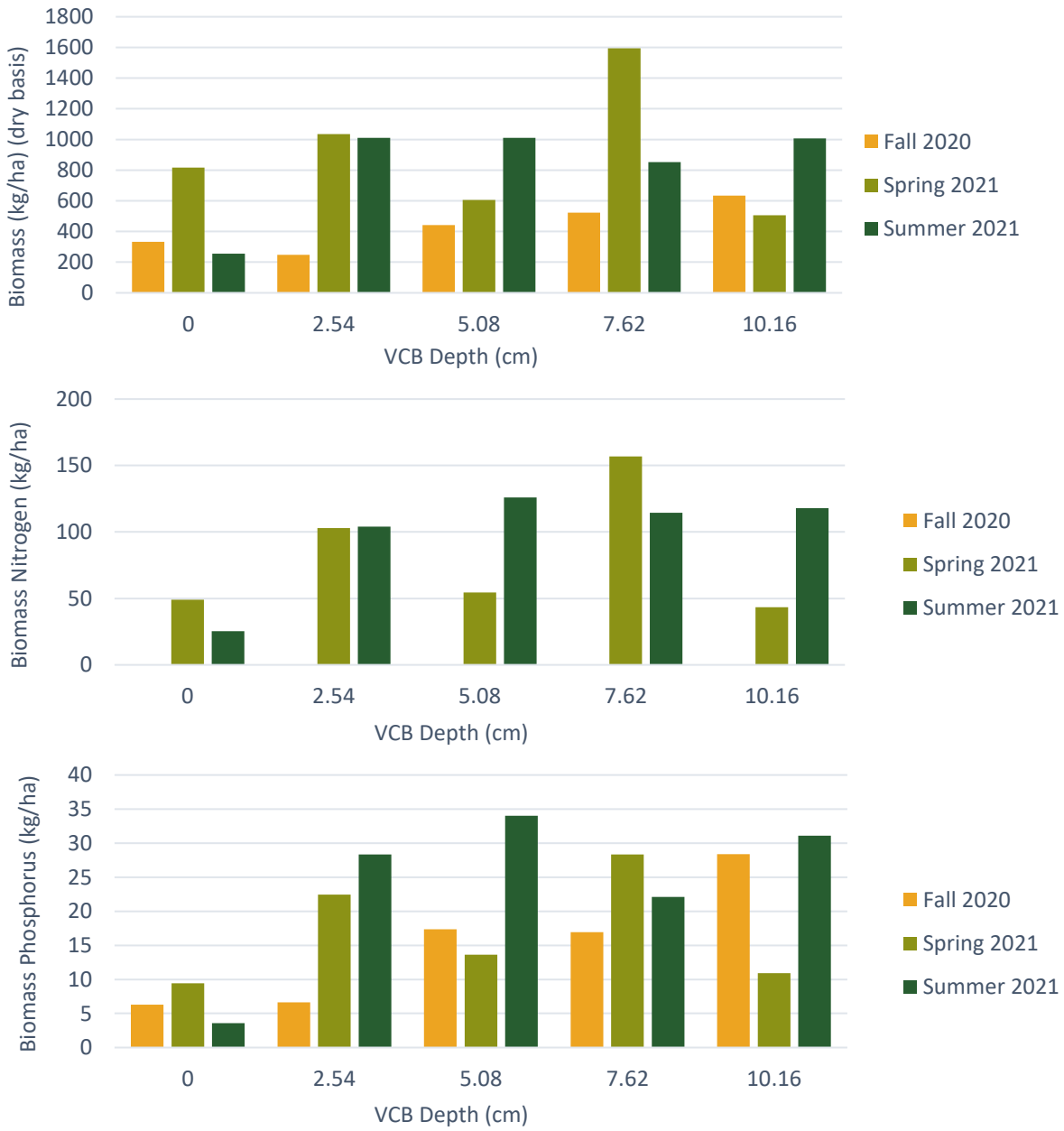


Figure 4-9: Field Biomass, Biomass Nitrogen, and Biomass Phosphorus.

Additionally, below-ground biomass, was not measured in this study, but has been shown to increase with increasing above-ground biomass (Liu et al. 2021). Additional benefits provided by below-ground biomass include additional carbon for soil microbiota; increased root density which leads to increased infiltration and reduced surface runoff; carbon sequestration; improved

drought resistance; increased resistance to erosion; and increased resistance to and recovery from stresses including insect stress, traffic stress, and disease stress.

A mass balance was estimated for the two field VCB/VFS systems, including inputs: N and P from highway runoff and N and P from the compost layer, outputs: N and P in outflow from the VCBs, and sinks: N and P collecting in the VFS layer and N and P collecting in vegetation (Table 4-7). Mass is presented as kg/ha for direct comparison between the 3-m and 6-m VCBs, and mass estimates were totaled over the 2.25 yr study period. Highway runoff and VCB outflow values were calculated using the mass loading rates presented in Chapter 3. VCB compost nutrient mass inputs was calculated using mineralization experiment results by taking the percent mass release of the un-leached field compost for the first year and the percent mass release of the leached compost for the remaining 1.25 yr and multiplying each by the total original N or P content in the field compost (this method was chosen to avoid the high variability in compost composition data). VFS nutrient mass removal for TP was obtained using results of soil composition data by subtracting the total P content from the soil prior to VCB installation from the total P content found at the end of the experiment. Vegetation nutrient mass uptake was estimated by averaging the nutrient uptake for collected biomass samples and assuming vegetative growth over 50% of the year, given that applied species are cool season turfgrasses (95% tall fescue and 5% Kentucky bluegrass (MDOT SHA 2020)). The mass balance gives an indication of the relative importance of each source and sink, however some factors were not able to be taken into account, such as vegetative decay in addition to uptake, and subsoil nutrient removal; however, the potential influence of these pathways are discussed.

Table 4-7: Field Site Nutrient Mass Balance.
Mass presented as kg/ha for direct comparison between 3-m and 6-m systems; % contribution to the total nutrient input is also presented to compare relative influence of each system component.

Total Nitrogen Mass Balance for 2.25 yr Field Study

	Inputs (kg/ha)		**Outputs (kg/ha)**	**Sinks (kg/ha)**	
Component	Highway Runoff*	VCB	3-m/6-m Outflow	VFS	Vegetation
Method	EMCs	compost composition	EMCs	soil composition	biomass tissue content
n	(n = 28)	(n = 6)	(n = 21)/(n = 24)	not measured	(n = 2)
value	8.57	1010	74.25/92.9	NA	153
Total	1019		74.25/92.9	153	

% Total Input	0.8%	99.2%	7%/9%	NA	15%
% Total Input			22% for 3-m and 24% for 6-m VCB/VFS System		

Total Phosphorus Mass Balance for 2.25 yr Field Study

	Inputs (kg/ha)		**Outputs (kg/ha)**	**Sinks (kg/ha)**	
Component	Highway Runoff*	VCB	3-m/6-m Outflow	VFS	Vegetation
Method	EMCs	compost composition	EMCs	soil composition	biomass tissue content
n	(n = 28)	(n = 6)	(n = 21)/(n = 24)	(n = 6)	(n = 3)
value	1.06	289	32.2/15.0	141	28
Total	290		32.2/15.0	169	

% Total Input	0.4%	99.6%	11%/5%	49%	10%
% Total Input			70% for 3-m and 64% for 6-m VCB/VFS System		

**Highway runoff mass presented is obtained from observed dataset. Expected highway runoff mass values are 107 kg/ha for TN and 7.94 kg/ha for TP.*

For nitrogen and phosphorus, highway runoff accounted for less than 1% of the total input to the system, with all other nutrient input attributed to that estimated to be released by the compost in the VCB. If expected highway influent concentrations had been observed, nitrogen contributed by highway runoff may have been as high as 9.6% of the total input and phosphorus 2.7%, and therefore the VCB is expected to have the majority of influence on nutrient

contribution to the system even in expected runoff conditions, making compost type and degree of nutrient release the most critical in mitigating nutrient release.

Only 22-24% of nitrogen was able to be accounted for through assessment of mass release in outflow (7% for 3-m and 9% for 6-m) and estimation of retention through plant uptake (~15%). However, nitrogen content was not assessed for the VFS layer, and total volume retention over the 2.25-yr experiment was calculated to be 44% for the 3-m VCB and 55% for the 6-m. This makes it likely that much of the nitrogen mass was retained through underlying soil layers. However, complexities of the nitrogen cycle, especially volatilization pathways, likely also played a large role and much of the nitrogen missing from the mass balance was likely also released to the atmosphere. Only 7-9% of total input N was released in effluent. Systems encouraging further removal of N and use of composts with lower N release (for example, leached composts) may therefore be able to reduce this mass to acceptable levels.

For phosphorus, 64-70% of phosphorus mass was identified through calculations of outflow mass (11% for 3-m and 5% for 6-m) and soil contents (49%) as well as estimations of vegetative uptake (~10%). For phosphorus, unaccounted mass is likely attributable to retention in the subsoil layer, since infiltration was not influential during storm events, but would be influential during long periods of time between storms. This is supported by soil composition data which showed a statistically significant 5.4x increase ($p < 0.01$) in P subsoil content (10.09 mg/kg to 65.79 mg/kg) at the top of the subsoil layer. Soil was highly impactful on P fate, with 49% removal of total P input in the VFS layer and was likely much higher due to additional adsorption in the subsoil. An estimated 10% was attributed to plant uptake, making this an additional substantial removal pathway. Overall, only 5-11% of total estimated P input was output in effluent, making the system efficient at removal of P relative to VCB release of P. This

also further supports potential use of leached composts rather than un-leached in VCB design, since soil and vegetative retention may further reduce effluent mass to more acceptable levels, making VCB installation more feasible.

OpenHydroQual Model

The 3-m field site VCB was selected as the test case for using OpenHydroQual to model nutrient movement. Geometries and media hydraulic properties were assigned to each block as described in Table 4-2, and timeseries datasets for precipitation and evapotranspiration parameters were uploaded as Sources. The Penman-Monteith Method (Zotarelli et al. 2009) was selected for evapotranspiration estimates and applied to the compost (VCB) and topsoil (VFS) layers, since these are in the root zone, but not to the subsoil layer. The sewer channel block was selected to serve as an open channel collection for VCB effluent to control flow moving into the fixed head storage block. The simulation time was selected as 2/27/2019 to 06/30/2019, from the time of VCB field application to approximately 100 days later, in order to confine the model to a timeframe where initial nutrient mineralization would occur (as this is the timeframe observed for column mineralization experiments). Flow outputs from the OpenHydroQual model were compared to those observed at the field site, and a selection of these is shown in Figure 4-10. The model was fairly accurate in peak timing and magnitude; however deviations can be observed. Being an idealized simulation of the test site, a smoothing effect can be observed in the modelled dataset. This is expected variation to observed data, since inherent heterogeneity at the field site will not be accounted for in the model (for example: inconsistencies in vegetative cover, soil permeability and compaction, uneven terrain, and preferential flows). At times modelled hydrograph peaks and peak timing is inconsistent with observed data, most evident in the peak in

the second storm event which reaches ~7.5-m^3/h in the observed dataset, but ~2.5-m^3/h in the modelled result. The short, high intensity events are more accurate than longer, smaller peak storms; which could be attributable to inaccuracies in estimation of soil hydraulic parameters.

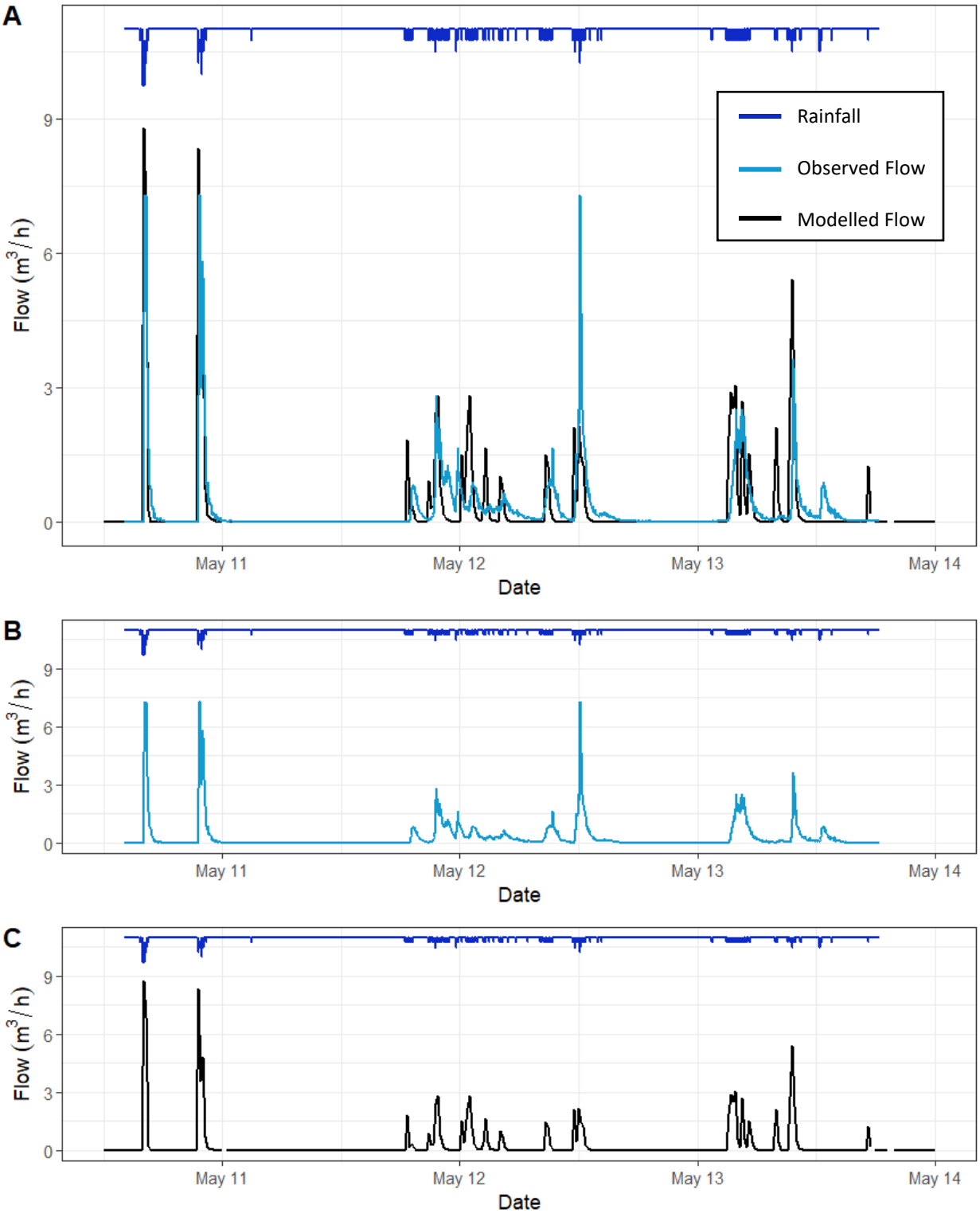


Figure 4-10: Comparison of Observed Field and Modelled OpenHydroQual Hydrographs. a) OpenHydroQual model outflow and field observed 3-m VCB outflow plotted together; b) field observation of 3-m VCB outflow; c) OpenHydroQual output flow timeseries data; for all: input rainfall data is displayed at the top for comparison.

All observed flow data for the simulation period (2/27/2019 to 06/30/2019) was compared to the model output at 2-minute timestep intervals since this was the timestep collected at the field site (Figure 4-11). The slope of the linear fit is close to 1 (0.8614), and a y-intercept close to 0 (0.6975), indicating a good overall trend close to 1:1. The R^2 is 0.5424, which indicates that more than half of variance can be explained by the simulation. However, errors in peak timing are likely responsible for the range of values falling on the y-axis when observed outflow is close to or equal to 0. Additionally, the field dataset was limited by a maximum observed flowrate (~170 m^3/day), which can be seen by the range of predicted values for a set of observations all sitting at x = 170 m^3/day.

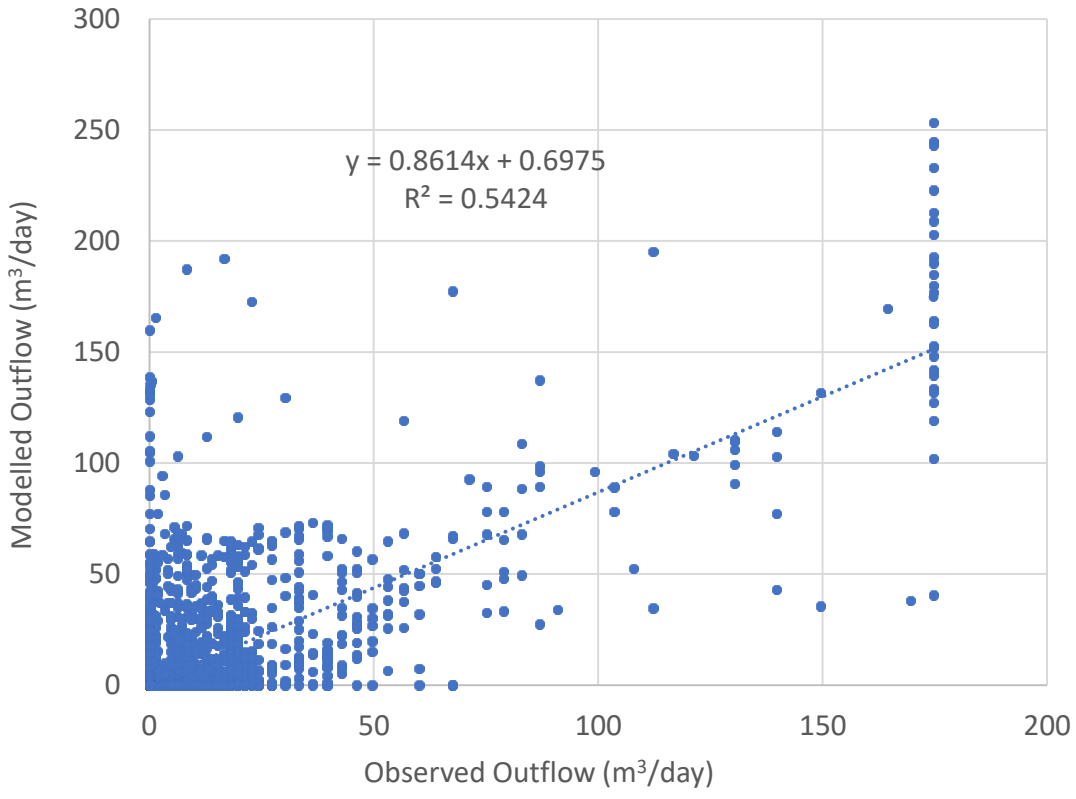


Figure 4-11: : Comparison of Modelled and Observed Outflow for Field 3-m VCB. The maximum limit for observed outflow as dictated by monitoring equipment can be observed at x = 170 m3/day; inaccuracies in peak timing can be observed by high values at x = 0.

Mass of phosphorus in the different control volumes (blocks) over time for the test period (2/27/2019-06/30/2019) are shown in Figure 4-12. The phase of P is indicated as either solid or dissolved. The applied precipitation inflow and the VCB outflow are displayed above both figures to connect storm events and outflow volumes to resulting P movement in the different blocks. Mass in the solid phase in the compost layer decreases exponentially over time, with the remaining mass approaching 0 around day 100. From the results obtained from laboratory experiments, this is expected and can be checked by plugging in the $k_{release}$ of 0.0358 day^{-1} and a time of 100 days to Equation 4-5, resulting in $Y(t) = Y_0*(1-0.028)$, indicating that the cumulative mass released at day 100 is 97.2% of the total mineralized mass. Mass released to the outflow only accounts for approximately half (~300 g) of the total mass released from the VCB by the end of the simulation due to volume retention. Only a relatively small amount (~40 g) was infiltrated to the fixed head storage block, however, infiltration is arbitrarily defined by the subsoil block at depth of 0.9-m, with much of the mass remaining in the pore space of the subsoil layer at the end of the simulation.

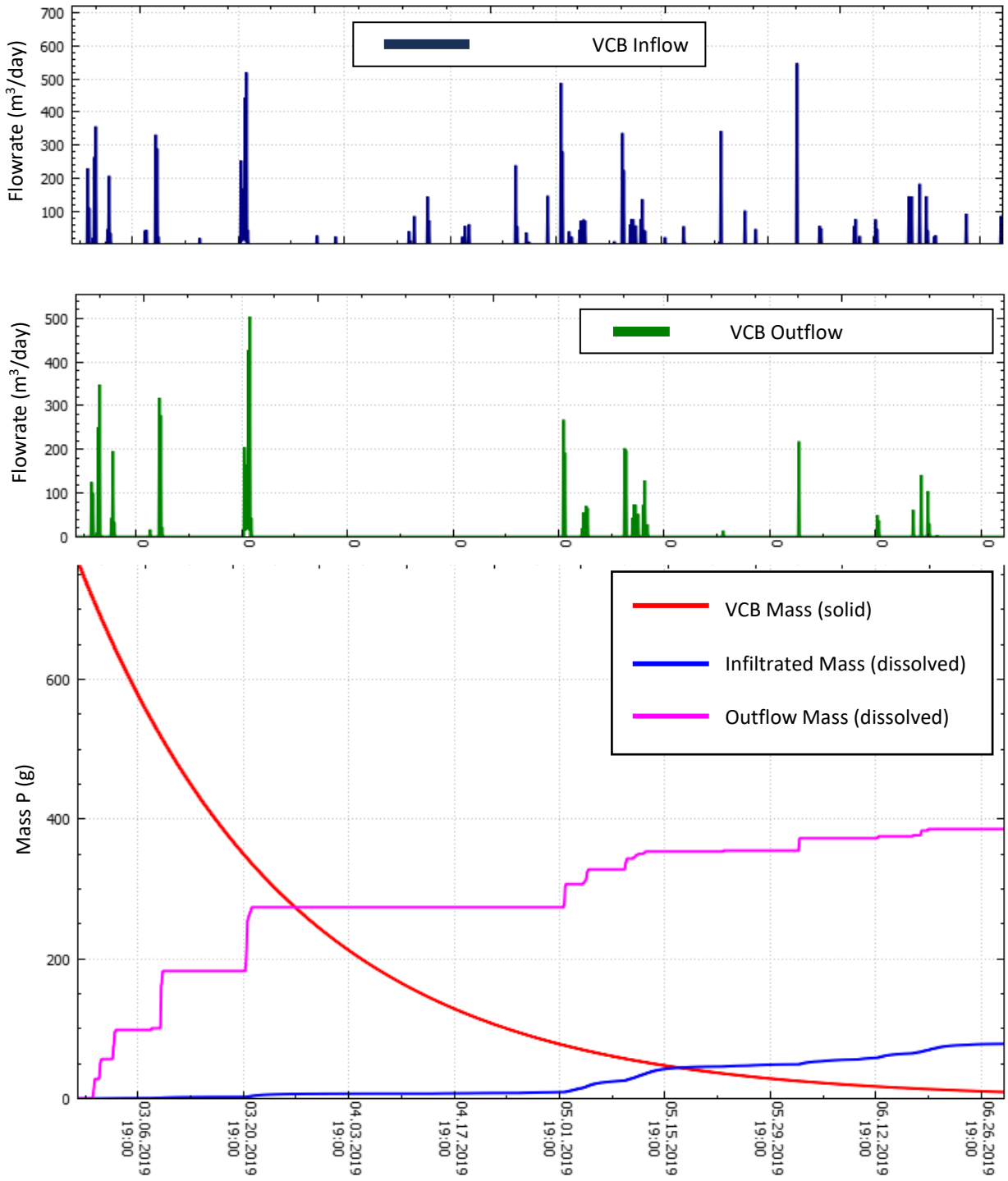


Figure 4-12: Total Phosphorus Mass Movement as Predicted by OpenHydroQual.

The same simulation was run for nitrogen release, with the mass of nitrogen in the different control volumes over time are shown in Figure 4-13, with the phase of N indicated as solid or dissolved, and the precipitation timeseries and the VCB outflow displayed above both figures. Similarly to the simulation for P, mass in the solid phase in the compost layer decreases exponentially over time, though a much larger proportion of mass is released at the beginning of the experiment as was observed in the mineralization experiments. Plugging in the $k_{release}$ of 0.1587 day^{-1} and a time of 100 days to Equation 4-5, results in $Y(t) = Y_0*(1-(1.28x10^{-7}))$, indicating that the cumulative mass released at day 100 is greater than 99.9% of the total mineralized mass and plugging in 20 days results in 95.8% cumulative mass release, which aligns with the model output. Mass released to the outflow accounts for approximately 75% (~1400 g) of the total mass released from the VCB by the end of the simulation, with the remaining removed via volume retention with ~100 g as infiltration in the fixed head storage block. This is a higher proportion of release to the outflow than what was predicted for phosphorus, likely because the majority of N mass was released early in the experiment while P was released more slowly over time (0.0358 day^{-1} rate constant for P, 0.1587 day^{-1} rate constant for N), making volume retention (to lower soil layers and to the infiltration storage) over the course of the experiment less impactful for N than P. While the total percent release is higher, smaller mass flushes for N are observed in comparison to P later in the experiment.

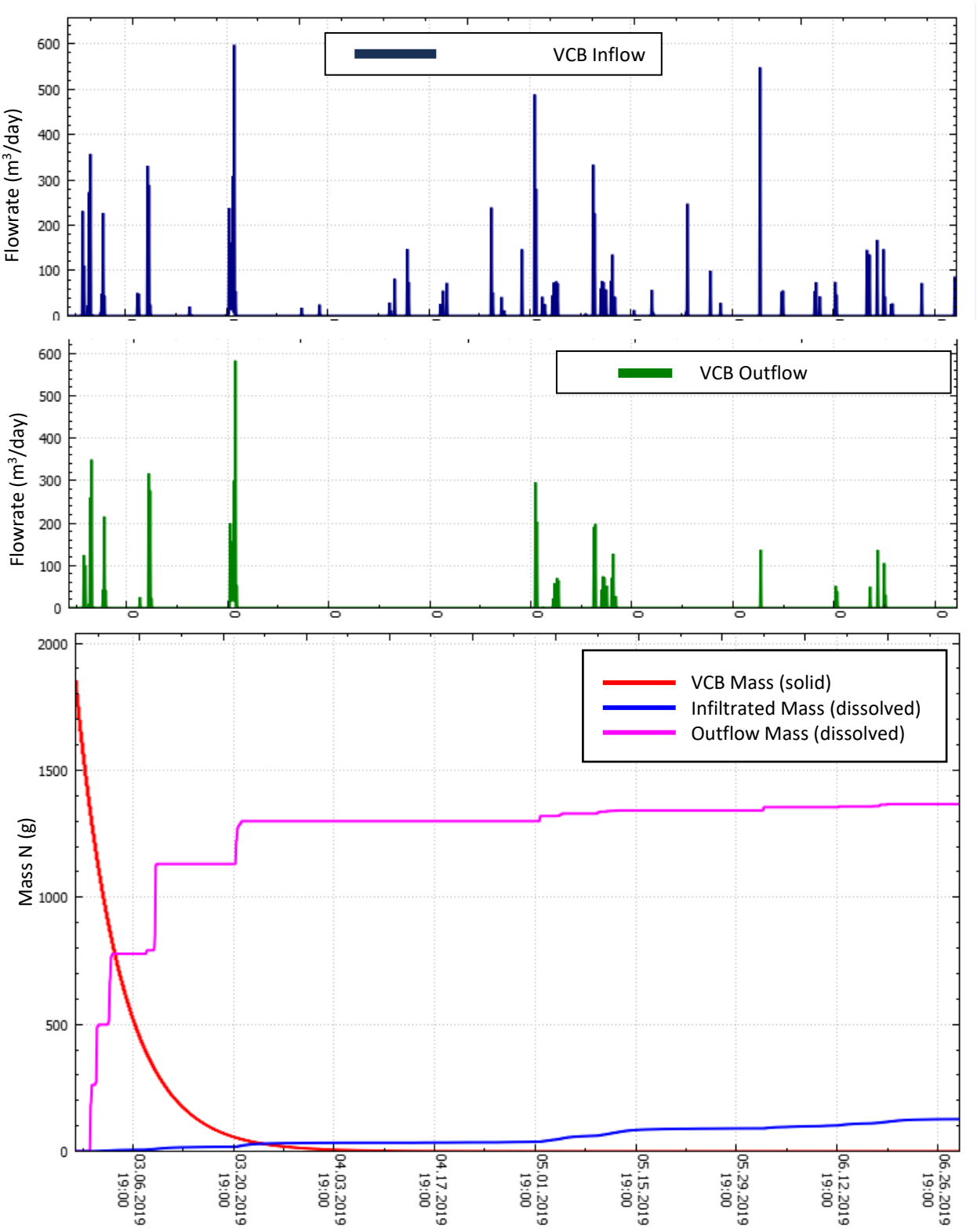
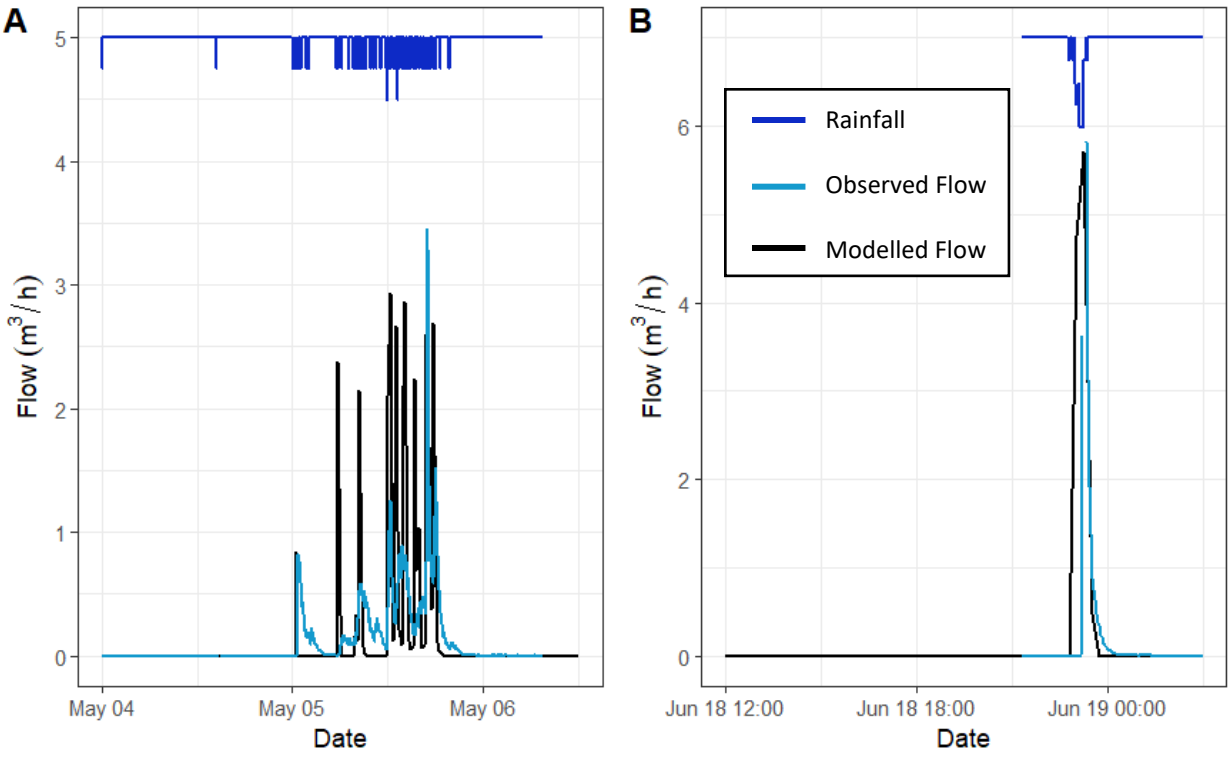


Figure 4-13: Total Nitrogen Mass Movement as Predicted by OpenHydroQual.

Two observed field storm events were used to compare the model output for total event volume and total event mass (Figure 4-14). The volume resulting from the modelled data for the first storm event (5/6/2019) was 150% greater than observed, and for the second storm event (6/18/2019) 50% greater. Many of the event peaks for the 5/6/19 event were overestimated by the model, resulting in higher total volume. Peak estimation for the 6/18/19 storm event where only one hydrograph peak was observed was much more accurate and resulted in a more similar volume estimation. Mass estimations for P were within the same magnitude (33 and 21 g for storm 1 and 1.9 and 6.4 g for storm 2, observed and predicted respectively), though large percent differences were observed (modelled mass was 36% lower for 5/6/19 and 239% higher for 6/18/19). For N, however, results were less accurate. For storm 1, the mass resulting from the model was an order of magnitude lower than the observed mass (95% lower, 9.5 g modelled, 191 g observed). For storm 2, the modelled mass was 55% lower than observed (5.6 g modelled, 12.6 g observed). Differences in mass release are likely attributable in large part to propagated errors in storm volume simulation. Additionally, differences in N total release and speciation (volatilization and nitrification) observed in greenhouse and field experiments likely also negatively impacted the accuracy of simulation results, which may partly explain why results for P release were found to be somewhat more accurate than for N. Additionally, changes in release rate due to temperature changes was not accounted for in the model, which would also decrease the accuracy of model.



	5/6/2019	6/18/2019
observed volume (L)	3539	1749
modelled volume (L)	8768	2623
observed P mass (g)	33.33	1.87
modelled P mass (g)	21.47	6.35
observed N mass (g)	191.29	12.62
modelled N mass (g)	9.46	5.62

Figure 4-14: Observed Storm Event Volumes and Mass Compared to Model Output.

A diagram showing the main pathways of nutrient movement in a VCB/VFS including results found in this chapter is shown in Figure 4-15. For phosphorus, mineralization occurs in the VCB layer, with P being mainly released as PO_4-P. As PO_4-P passes through the VFS layer, some removal via adsorption occurs, with increasing Al+Fe content resulting in increasing adsorption. (Not shown: Additional removal via adsorption is likely to occur in the subsoil layer as well, based on the adsorption isotherm obtained for field subsoil as well as significantly higher P content in subsoils collected after VCB installation. However any mass infiltrating below the VFS layer can be considered retained, since it should not be released in surface water and be removed as flow infiltrates to groundwater.) Despite removal via volume retention and adsorption, net release is still observed, since volume retention during storm events occurs only through VCB and VFS media storage (Chapter 2), resulting in effluent for larger storm events, which flushes out mineralized mass from VCB/VFS layers. Additionally, net mass release is higher than the mass removed even when adsorption capacity is filled.

For nitrogen, mineralization is the main process occurring in the VCB layer, with nitrification and volatilization also being influential pathways in both layers. Though laboratory mineralization experiments determined the net mineralization (with volatilization and nitrification also occurring during the experiment), greenhouse and field experiments indicated differences in the degree of nitrification and possibly volatilization in comparison to laboratory results. The moisture content and temperature should be influential in the release of N from the VCB layer as well as movement in the VFS layer. Some adsorption via cation exchange should occur for NH_4^+, however specific factors were not found due to other biological transformation of N in the VFS layer, making predictions of N movement more difficult.

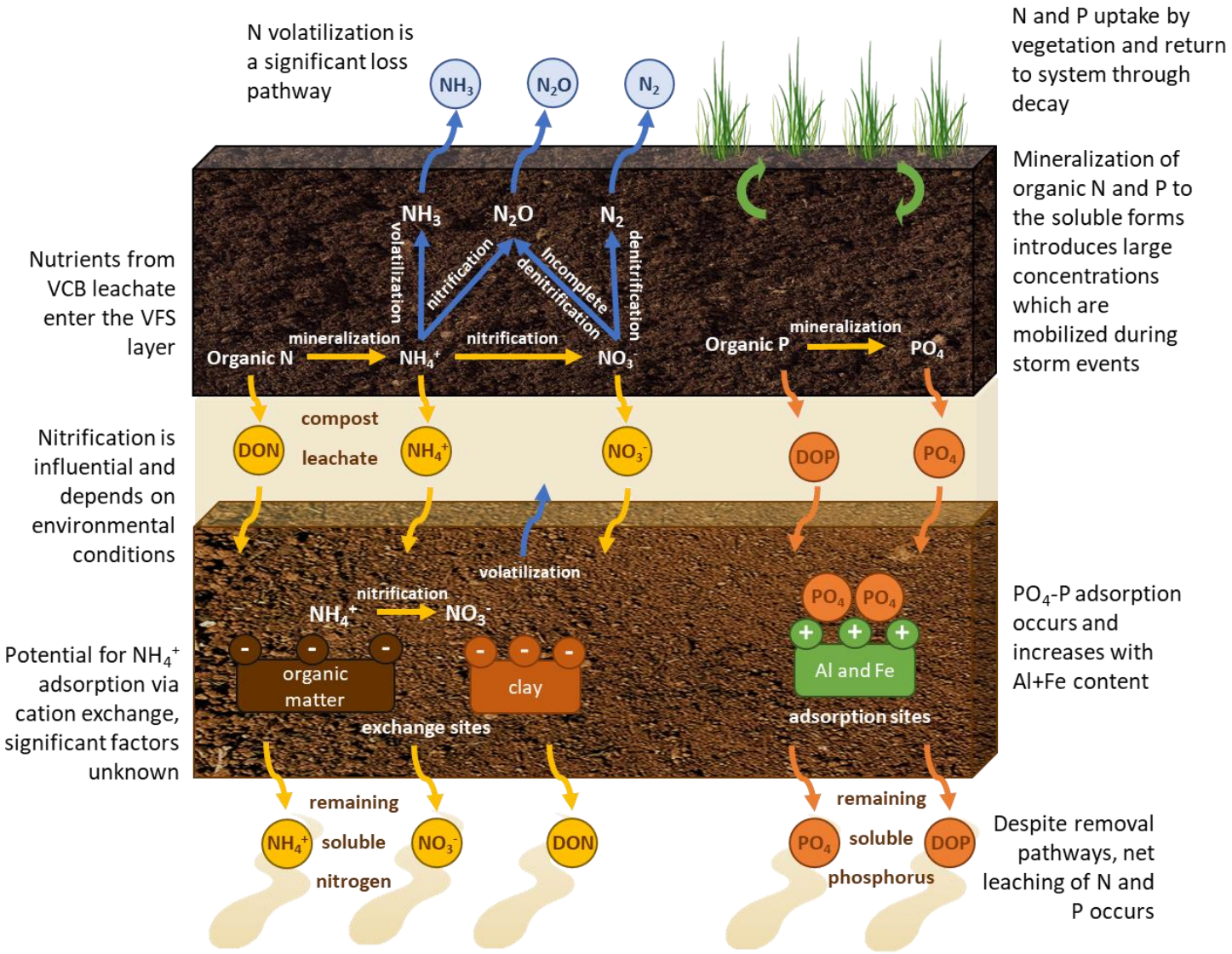


Figure 4-15: Processes Affecting Nutrient Movement and Transport in a VCB/VFS.

Conclusions

Large release of N and P from non-leached composts was observed during mineralization experiments, with large variations in total mass release in some cases. After aging and leaching through storm events, both the greenhouse and field composts had lower mean nitrogen release rate constants ($k_{release}$), lower mean initial flush (first mass release),and total mass release. Differences in nutrient release of non-leached composts are likely mainly due to mineralization occurring from the more recalcitrant N and P pools left after significant washing/leaching during experiments released the labile pool. Because nutrient release can be a detriment to downstream waterbodies, this indicates that using more matured and/or more leached composts could be preferred as they result in lower amounts of N and P release. Additionally, assessment of composts for labile and recalcitrant pool contents could also improve compost selection.

Soils showed significant adsorption removal of phosphates from compost leachate, with increasing Al+Fe content resulting in higher adsorption capacity (Q). Greenhouse and field experiment data supported this finding, with statistically significantly higher P contents in soils at the end of the experiment. Some potential for ammonium adsorption was identified, but true assessment was not possible due to co-occurring transformation processes. While some amount of nitrogen removal through adsorption may be possible for some soil types, microbial transformations should be much more influential to nitrogen fate and transport in the VCB/VFS system. Compost application over soils with higher Al+Fe content should result in less net P release since the soil layer offers a removal pathway through adsorption. Additionally, this has implications for other stormwater systems using compost as a surface layer, since P released in compost leachate may take up adsorption sites in the lower media layers. Because stormwater

engineered media is usually designed to remove P from influent stormwater, this may potentially decrease the efficiency of the system for P removal.

Both composts and soils demonstrated significant chemical composition changes after VCB application to a VFS in field and greenhouse experiments. After exposure to either real or synthetic stormwater over long periods of time (1-2 years) compost released a large portion of ionic constituents, and had somewhat lower N and P contents, though C:N ratio did not significantly change. After washing, composts also had more than 95% less mass of the immediately available N species (NH_4-N and NO_3-N), indicating that leached composts should have much lower nutrient release immediately after application, which was confirmed through assessments of initial flush in the mineralization experiments. Soils showed an associated increase for some ionic constituents, with increasing cation exchange capacity and also significant increases in P content. For the field topsoil, the VFS soil was found to have reached adsorption capacity, through comparison of the P saturation ratio to the theoretical adsorption capacity (Q) found in the adsorption experiments).

Comparison of theoretical nutrient release curves from laboratory column studies to nutrient release observed in the greenhouse and field sites showed differences between lab-obtained values and experimental observations. N speciation differed, with higher nitrification observed in the lab than in field or greenhouse, likely due to differences in saturation and temperature. Lower P release in the greenhouse experiment than that predicted by the column experiments was likely due to P adsorption through the soil layer.

OpenHydroQual modeling indicated varying levels of accuracy with regard to simulation of storm event hydrographs and release estimations of N and P in comparison to field data. Simulations showed significant mass reduction through volume retention in underlying subsoil,

which reduced mass loss to effluent. Goodness of fit explained more than 50% of the variance for outflow data, however, errors in peak flow timing and magnitude were identified. Estimations of P may be more accurate than for N since N biological transformations were found to be highly influential, however, for both nutrients, lack of release rate adjustment due to temperature changes limited the success of model performance.

Results indicate several pathways for reducing nutrient release by compost when applied as a blanket. Leaching of compost resulted in significantly lower mass release and a significantly lower initial mass flush for both N and P. Leached composts actually showed evidence of a small lag phase in nutrient mineralization for both N and P, while release rates significantly decreased for N and for P in the greenhouse compost. This could make aging or leaching compost before application a way to reduce the impact of excess nutrient release immediately after application and over time through reduction in mass release and slowing of nutrient release rates. Additionally, because volume retention is a major mass loss pathway, designs can be adjusted to increase infiltration, thereby increasing nutrient removal as well. Finally, compost leachate used in adsorption experiments showed that removal of PO_4-P by Al+Fe, so future designs may increase the use of soils or amendments containing these elements to increase removal of P in layers underlying the compost layer.

Acknowledgements

The authors acknowledge the support of the National Cooperative Highway Research Program (NCHRP 14-39), the Maryland Department of Transportation State Highway Administration (MDOT SHA), and the Low Impact Development (LID) Center.

Erica R. Forgione was supported by NRT-INFEWS: UMD Global STEWARDS (STEM Training at the Nexus of Energy, WAter Reuse and FooD Systems) that was awarded to the University of Maryland School of Public Health by the National Science Foundation National Research Traineeship Program, Grant number 1828910. Graduate student funding was also provided in part by the University of Maryland Graduate School Dean's Fellowship and COVID Delay Fellowship.

Mesocosm and field equipment design and construction support was provided by the University of Maryland Environmental Science and Technology (ENST) Project Development Center. Special thanks are also extended to Stancill's Inc. (Perryville, MD) for providing engineered soils and to Montgomery County Yard Trim Composting Facility (Dickerson, MD) for providing Leafgro yard waste compost.

CHAPTER 5: CONCLUSIONS AND NEW RESEARCH QUESTIONS

Conclusions

The addition of a Vegetated Compost Blanket (VCB) to a Vegetated Filter Strip (VFS) on a highway median offered water quantity benefits as a Stormwater Control Measure (SCM). Significant volume and flow reductions were observed for VCB/VFS systems over the highway runoff alone. Though infiltration was not found to be a significant loss pathway during the duration of a storm event, many smaller storm events (61%) were completely captured, with significant volume reductions during larger storm events. Additionally, the system functioned mainly as conveyance during high intensity peaks and after saturation was reached. Total volume removal over the full study period was found to be 44% and 55% for a 3-m and a 6-m field VCB, respectively. VCBs were able to bring the site closer to a pre-urbanized condition in comparison to specific discharges from forested watershed streams, and comparisons to studies on VFSs alone showed improved performance through addition of the VCB. A hockey-stick relationship using an average design storage was determined for the relationship between influent and effluent volume and a simple estimation for the average design storage was given using easily obtained moisture content parameters.

VCB performance for water quality had mixed results, with good performance for particulate pollutants observed, but high releases of nutrients, and in the case of the field site, copper as well. TSS, particulate copper, and total zinc removal was observed in both the field and greenhouse experiments, with TSS likely originating from the media itself rather than being remaining TSS from the influent stormwater matrix. A large intensity storm event in the greenhouse resulted in erosion of compost prior to vegetative establishment, which resulted in

elevated pollutant concentrations in the effluent, leading to a recommendation for use of an erosion control blanket as was used in the field site VCB installation. Dissolved copper leaching was observed at the field site, which is likely due to a higher copper content in the compost used in field experiments. Large mass export of N and P was observed in both field and greenhouse studies, with the highest concentrations exceeding criteria by two orders of magnitude for TN and three orders of magnitude for TP, with concentrations at the end of each experiment still exceeding both inflow concentrations and water quality criteria. Due to high nutrient release observed in both experiments, and the potential for metals leaching as well (specifically, copper), use of VCBs for stormwater management on highway systems is not currently recommended due to the risks of eutrophication and heavy metals toxicity in surrounding aquatic environments.

Assessment of nutrient release in laboratory scale experiments showed that leached composts (those applied to field (2.25 yr) and greenhouse (1 yr) experiments and exposed to either real or synthetic stormwater) had lower initial mass flush, total mass release, and release rate constants for both N and P. This observation is likely due to most of the labile (readily available) N and P pools being mineralized and subsequently leached out during experiment storm events, leaving the recalcitrant (resistant) pools, which are more slowly released through microbially-mediated mineralization. Soils from the greenhouse and field experiments were tested in batch adsorption experiments and showed significant P adsorption removal from compost leachate, with an increased capacity for P removal with increasing Al+Fe content. This was further supported by chemical analyses of soils taken before and after experiments showing significant P content increases after compost installation. Comparison of greenhouse and field experiment nutrient release to laboratory-obtained release curves indicated significant differences. For phosphorus, based on adsorption studies and soils composition, this is likely due

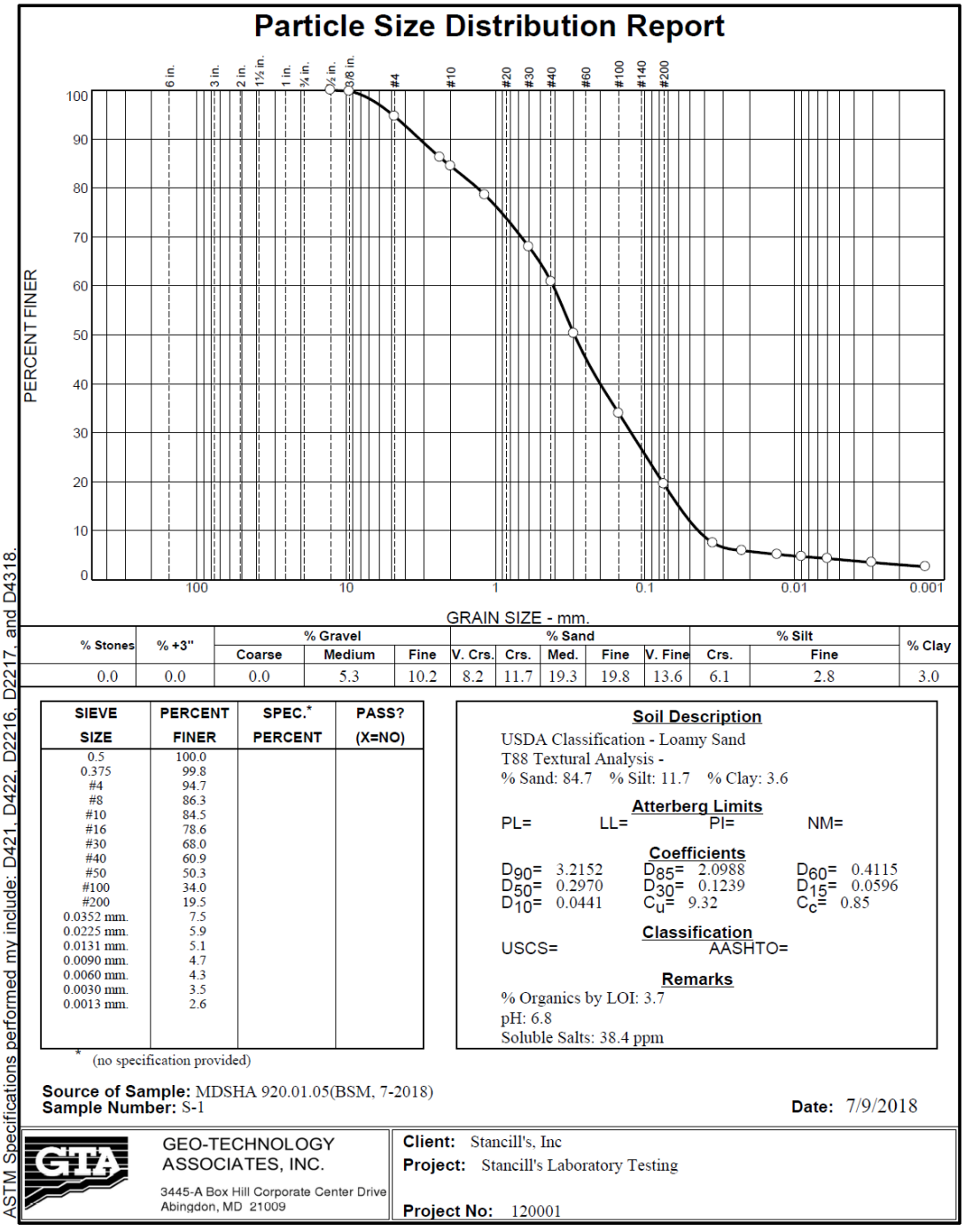
to removal of phosphate in the soil (VFS) layer. For nitrogen, differences in moisture content and temperature between the laboratory setting and greenhouse/field sites likely resulted in differing amounts of volatilization. Differences in nitrogen speciation as observed in the laboratory also differed from greenhouse and field studies, which is likely due to differences in the amount of nitrification caused by differences in temperature and moisture content conditions. Modeling in OpenHydroQual showed differences between model output for both hydrology and N and P mass release, with some modest accuracy for hydrology, but highly varied results for N and P mass release simulation.

Results indicate several ways to minimize nutrient release from a VCB, which may be implemented in other situations such as for erosion control and in bioretention systems as well. Lower compost depth resulted in lower P release in greenhouse experiments, so less compost application may decrease P in effluent. Additionally, increased volume retention should increase nutrient removal. Leached composts resulted in significantly lower total mass release and initial mass flush for both N and P, and in some cases lower release rate constants; therefore washing/aging composts so that the labile pool of N and P is mostly leached away before application might make use of compost more viable in stormwater systems. Because P adsorption was observed with increasing Al+Fe content, additional P removal might be achieved through selection of the underlying media, or addition of amendments. Finally, compost composition was found to be important in N, P, and Cu release. Further assessment of the labile and recalcitrant pools of N and P in the compost may help better predict nutrient release, additionally, the total N, P, and metals content may be restricted to minimize net release.

New Research Questions

Additional research on compost composition and its effects on nutrient and metals release is needed, given the complexity of a leachate matrix as well as the high variability in compost based on source, time of year, feedstocks, and composting procedures. Specifically, additional research on N and P pools could provide a better estimation of nutrient release in the long-term, since this research focused on the initial nutrient release after application. Further exploration of aged (leached) composts could also further support use of an aged/leached compost for engineered applications such as use in a VCB, since lower mass release was observed for leached composts in this research. Additionally, assessment of compost leachate including dissolved organic matter, both quantity and type (ex. humic vs fulvic acids), in relation to compost leachate and the contaminants of concern is also recommended. This parameter should have a significant impact on both nutrient and metal fate and transport, affecting both contaminant mobility and removal processes. Commonly on highway medians, a VFS system flows into a swale for further treatment and conveyance. Assessment of a full highway treatment system, including a swale, could provide a better assessment of overall performance, since runoff from the VCB/VFS will likely often flow downstream to a secondary swale treatment system.

APPENDIX



% Stones	% +3"	% Gravel			% Sand					% Silt		% Clay
		Coarse	Medium	Fine	V. Crs.	Crs.	Med.	Fine	V. Fine	Crs.	Fine	
0.0	0.0	0.0	5.3	10.2	8.2	11.7	19.3	19.8	13.6	6.1	2.8	3.0

SIEVE SIZE	PERCENT FINER	SPEC.* PERCENT	PASS? (X=NO)
0.5	100.0		
0.375	99.8		
#4	94.7		
#8	86.3		
#10	84.5		
#16	78.6		
#30	68.0		
#40	60.9		
#50	50.3		
#100	34.0		
#200	19.5		
0.0352 mm.	7.5		
0.0225 mm.	5.9		
0.0131 mm.	5.1		
0.0090 mm.	4.7		
0.0060 mm.	4.3		
0.0030 mm.	3.5		
0.0013 mm.	2.6		

* (no specification provided)

Soil Description

USDA Classification - Loamy Sand
T88 Textural Analysis -
% Sand: 84.7 % Silt: 11.7 % Clay: 3.6

Atterberg Limits

PL= LL= PI= NM=

Coefficients

D_{90}= 3.2152 D_{85}= 2.0988 D_{60}= 0.4115
D_{50}= 0.2970 D_{30}= 0.1239 D_{15}= 0.0596
D_{10}= 0.0441 C_u= 9.32 C_c= 0.85

Classification

USCS= AASHTO=

Remarks

% Organics by LOI: 3.7
pH: 6.8
Soluble Salts: 38.4 ppm

Source of Sample: MDSHA 920.01.05(BSM, 7-2018)
Sample Number: S-1

Date: 7/9/2018

GEO-TECHNOLOGY ASSOCIATES, INC.
3445-A Box Hill Corporate Center Drive
Abingdon, MD 21009

Client: Stancill's, Inc
Project: Stancill's Laboratory Testing
Project No: 120001

Tested By: J. Watkins **Checked By:** T. Wirth

Figure 5-1: Laboratory-Scale Sandy Topsoil Mix Description and Textural Parameters.

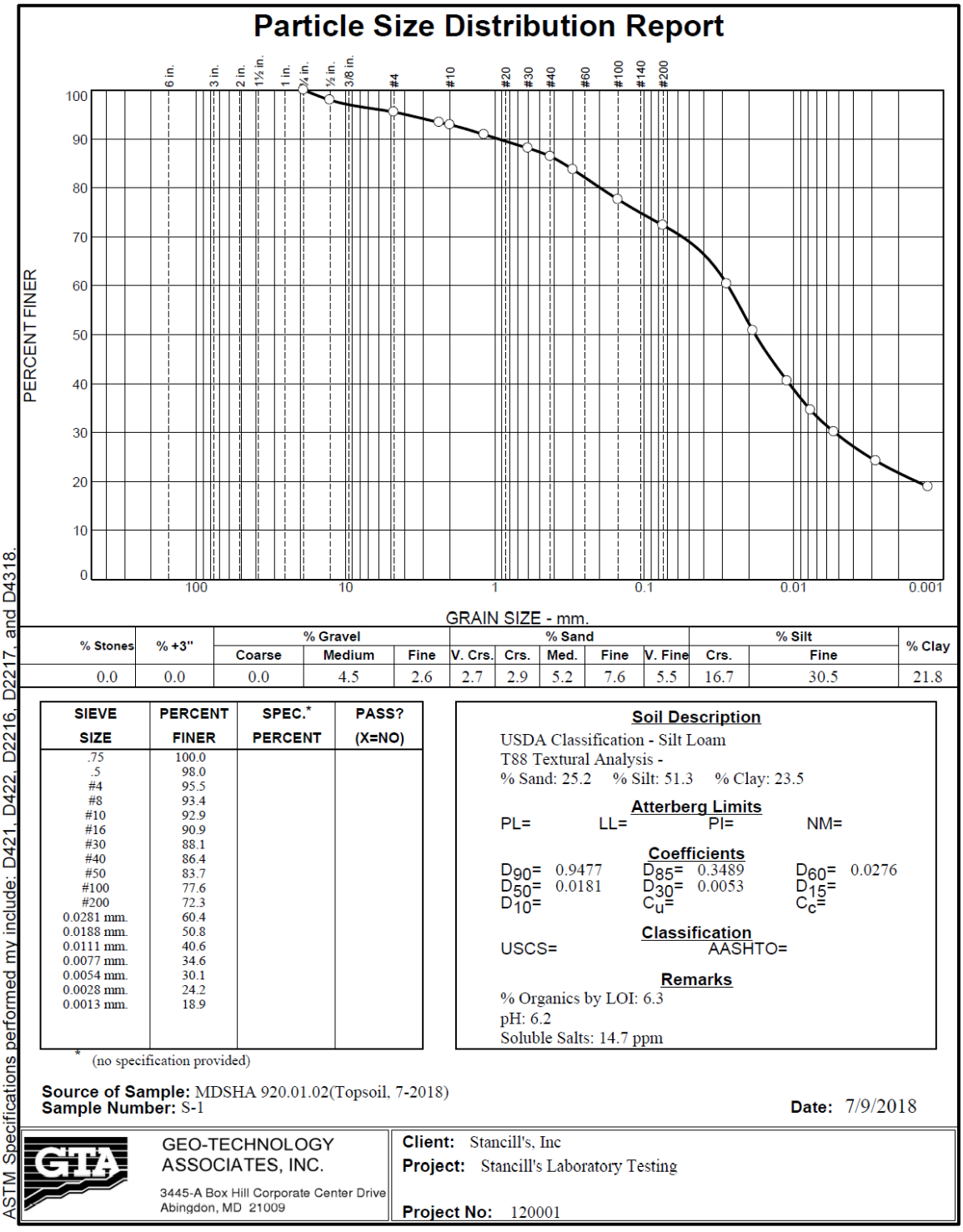


Figure 5-2: Laboratory-Scale Clayey Topsoil Mix Description and Textural Parameters.

CONTROL 1 1” DEPTH CLAYEY TOPSOIL 8:1 SLOPE

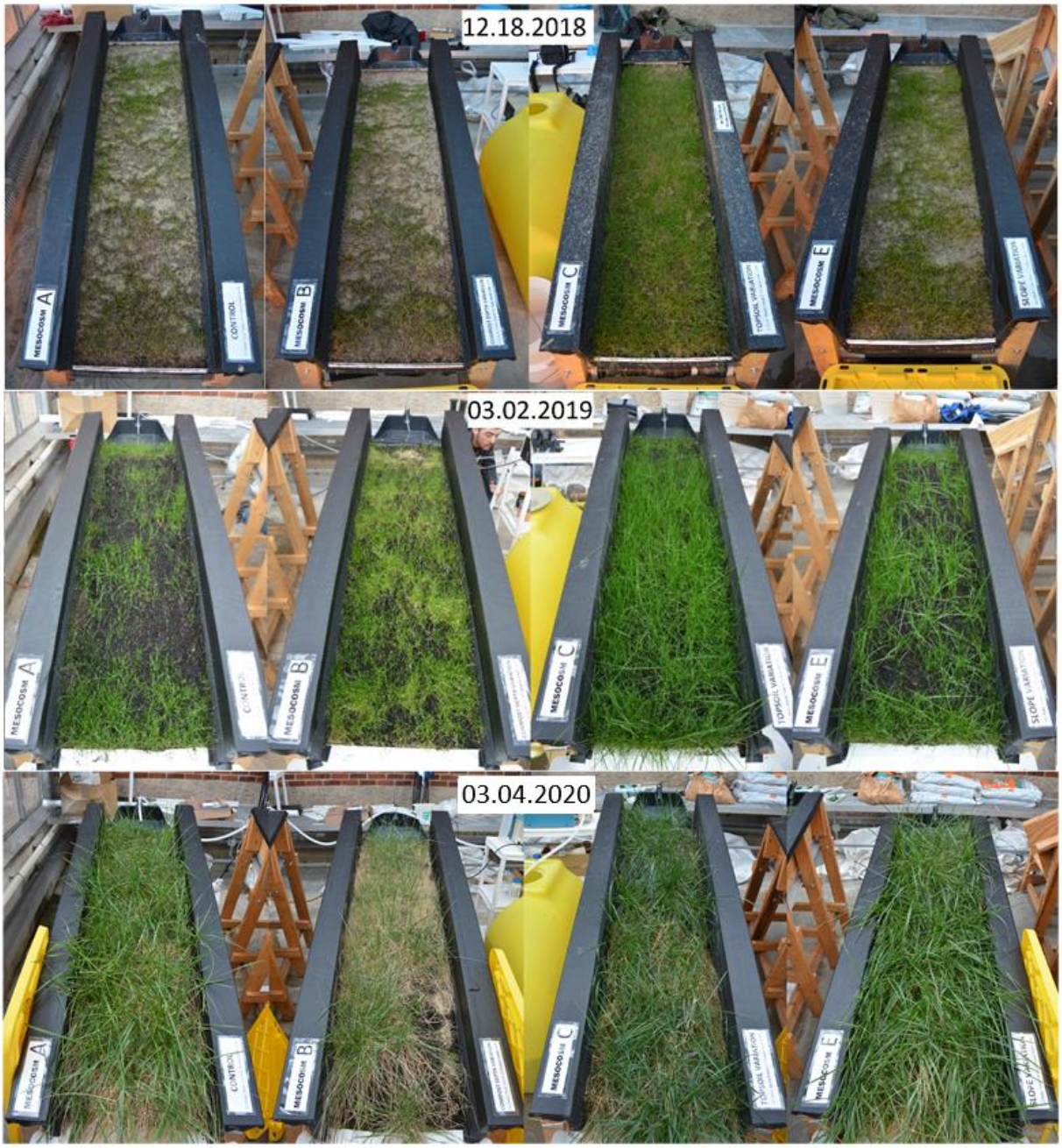


Figure 5-3: Photos of the Four Mesocosms in Study 1.
Before compost application on 12/18/18 (top), after grass establishment on 3/2/20 (middle), and at the end of the experiment on 3/3/20 (bottom).

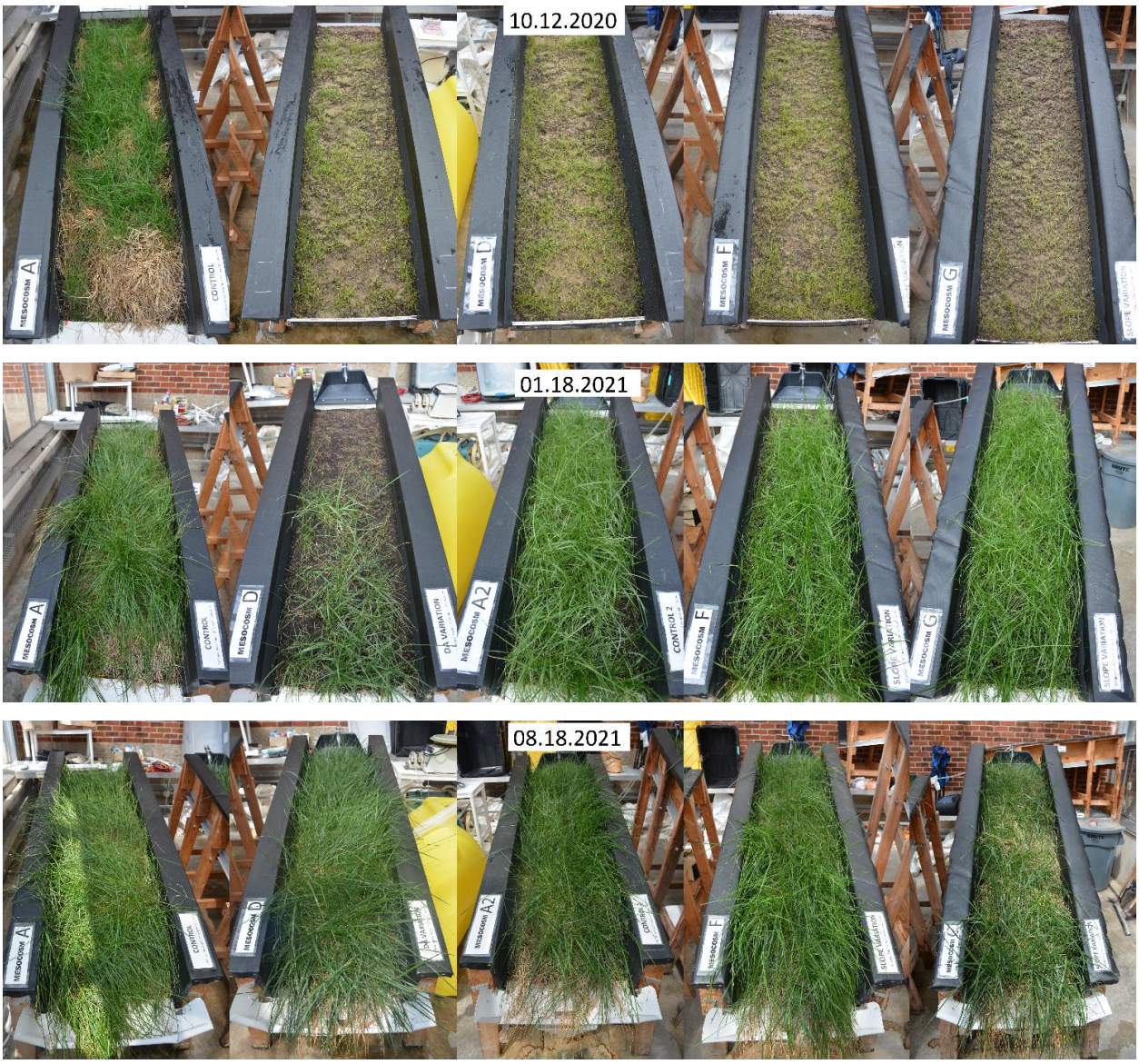


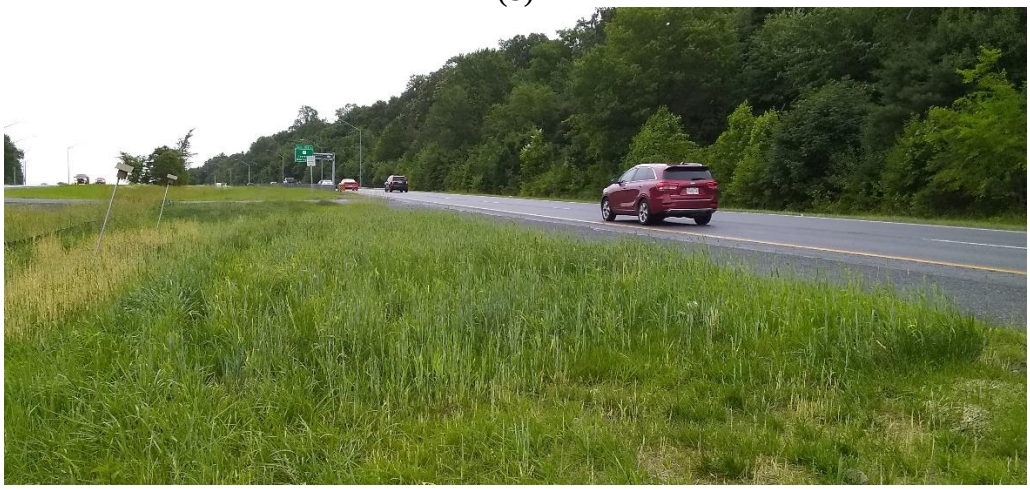
Figure 5-4: Photos of the Four Mesocosms in Study 2 and Standard from Study 1. Before compost application on 10.12.2020 (top), after grass establishment on 1.18.2021 (middle), and at the end of the experiment on 6.7.2021 (bottom).



(a)

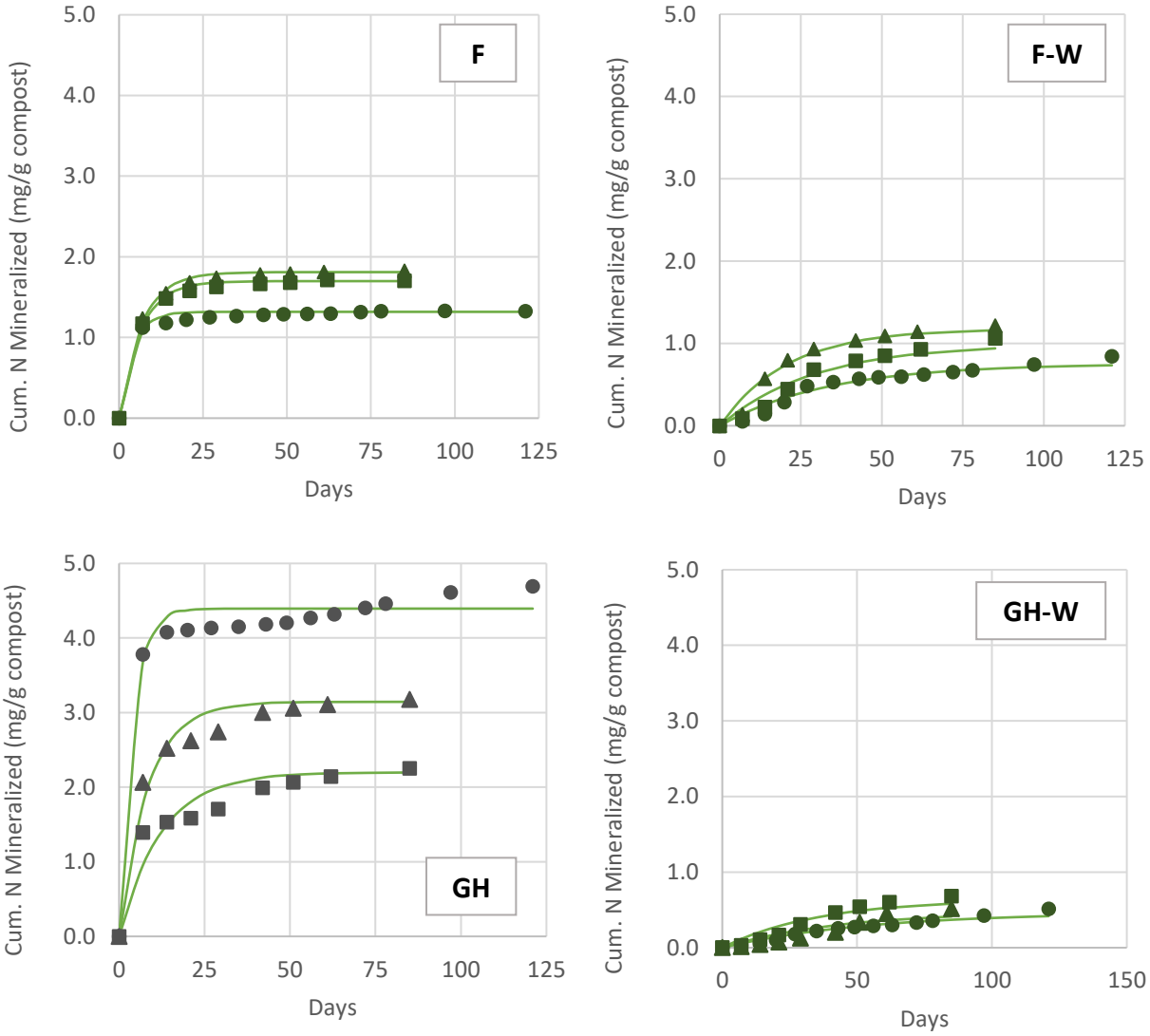


(b)



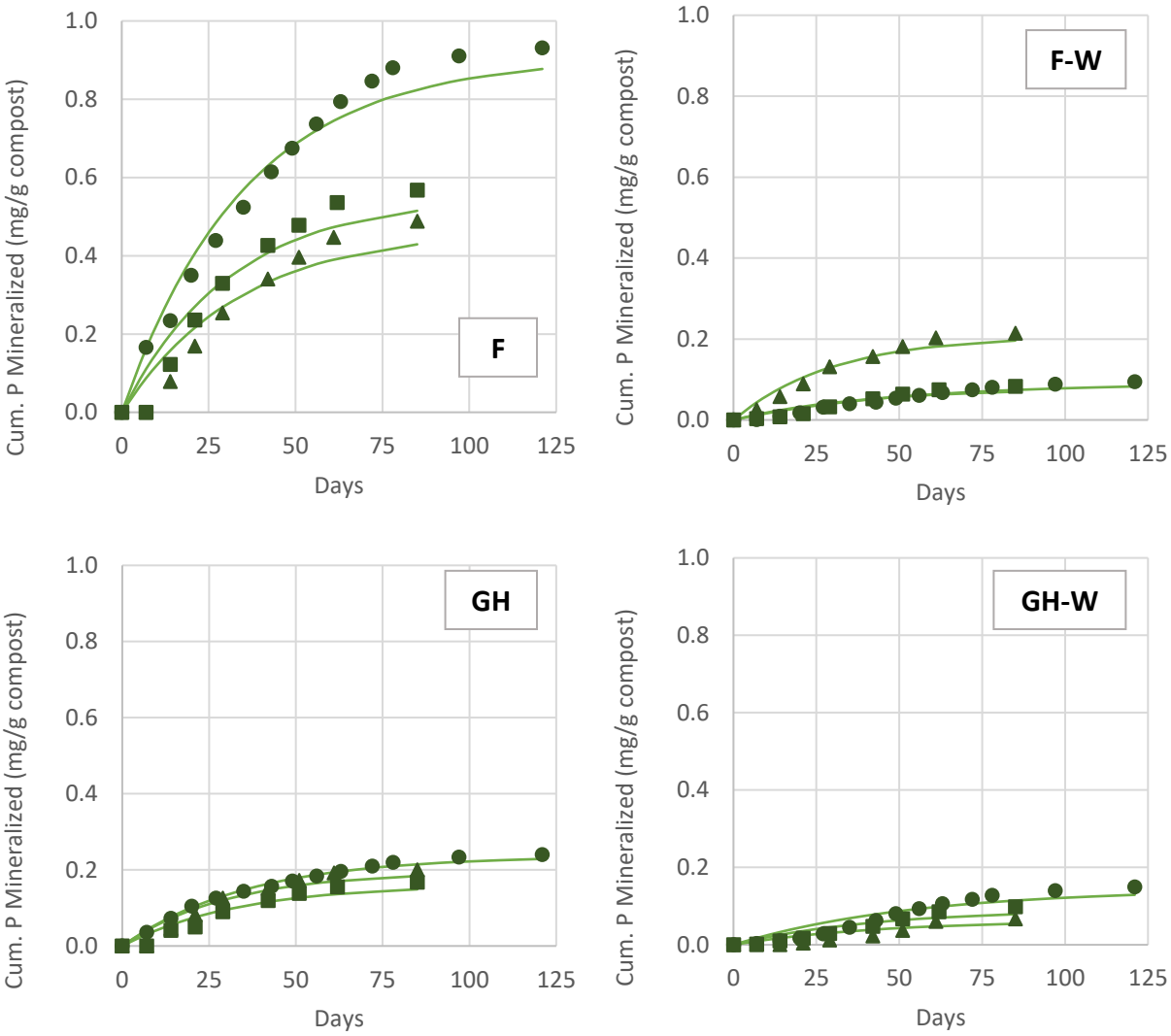
(c)

Figure 5-5: Field Site Vegetated Compost Blankets After Establishment.
a) 3-m VCB: 30.5-m (100-ft) along highway, 3-m (10-ft) perpendicular to highway; b) 6-m VCB: 30.5-m (100-ft) along highway, 6-m (20-ft) perpendicular to highway; c) observational VCB: 30.5-m (100-ft) along highway, 6-m (20-ft) perpendicular to highway; images of VCBs taken on June 09, 2019, 102 days after installation.



	Total Mass (mg/g)		k_{min} (day^{-1})	R^2	Initial Flush (mg/g)	Initial Flush (%)	Total Mineralized Mass (mg/g)	Total Mineralized Mass (%)
F	32.523	**mean**	0.1823	0.9912	1.176	3.6%	1.618	4.4%
		stdev	0.0509	0.0085	0.056	0.2%	0.260	0.8%
F-W	24.685	**mean**	0.0373	0.9396	0.094	0.4%	1.042	4.2%
		stdev	0.0096	0.0205	0.042	0.2%	0.188	0.8%
GH	24.917	**mean**	0.1539	0.9546	2.414	9.7%	3.375	13.5%
		stdev	0.0946	0.0293	1.232	4.9%	1.232	4.9%
GH-W	21.290	**mean**	0.0229	0.7930	0.025	0.1%	0.571	2.7%
		stdev	0.0049	0.1564	0.008	0.04%	0.097	0.5%

Figure 5-6: Nitrogen Mineralization Curves.



	Total Mass (mg/g)		k_{min} (day^{-1})	R^2	Initial Flush (mg/g)	Initial Flush (%)	Total Mineralized Mass (mg/g)	Total Mineralized Mass (%)
F	21.050	**mean**	0.0299	0.9038	0.055	0.3%	0.662	3.1%
		stdev	0.0019	0.0601	0.096	0.5%	0.236	1.1%
F-W	17.162	**mean**	0.0263	0.8656	0.010	0.1%	0.130	0.8%
		stdev	0.0068	0.0962	0.014	0.1%	0.073	0.4%
GH	2.733	**mean**	0.0302	0.9119	0.012	0.4%	0.203	7.4%
		stdev	0.0026	0.0690	0.021	0.8%	0.036	1.3%
GH-W	2.224	**mean**	0.0214	0.6472	0.002	0.1%	0.105	4.7%
		stdev	0.0027	0.1864	0.002	0.1%	0.042	1.9%

Figure 5-7: Phosphorus Mineralization Curves.

Table 5-1: Summary of Nitrogen Mineralization.

	Compost N Content (%)	Replicate	k_{min} (day^{-1})	RMSE (mg/g)	R^2	Total Mass (mg/g)	Initial Flush (mg/g)	Initial Flush (%)	Total Mineralized Mass (mg/g)	Total Mineralized Mass (%)
Field Compost	3.2523	1	0.2410	0.0465	0.9813	32.523	1.124	3.5%	1.326	4.1%
		2	0.1560	0.0332	0.9961		1.170	3.6%	1.704	5.2%
		3	0.1500	0.0351	0.9962		1.235	3.8%	1.825	3.8%
		mean	0.1823	0.0383	0.9912		1.176	3.6%	1.618	4.4%
		stdev	0.0509	0.0072	0.0085		0.056	0.2%	0.260	0.8%
Field Compost - Leached	2.4685	1	0.0297	0.0557	0.9351	24.685	0.054	0.2%	0.845	3.4%
		2	0.0341	0.0847	0.9217		0.089	0.4%	1.062	4.3%
		3	0.0480	0.0732	0.9619		0.139	0.6%	1.220	4.9%
		mean	0.0373	0.0712	0.9396		0.094	0.4%	1.042	4.2%
		stdev	0.0096	0.0146	0.0205		0.042	0.2%	0.188	0.8%
Greenhouse Compost	2.4917	1	0.2610	0.1856	0.9731	24.917	3.782	15.2%	4.693	18.8%
		2	0.0816	0.1980	0.9208		1.393	5.6%	2.253	9.0%
		3	0.1190	0.1724	0.9698		2.066	8.3%	3.178	12.8%
		mean	0.1539	0.1853	0.9546		2.414	9.7%	3.375	13.5%
		stdev	0.0946	0.0128	0.0293		1.232	4.9%	1.232	4.9%
Greenhouse Compost - Leached	2.1290	1	0.0182	0.0337	0.9250	21.290	0.029	0.1%	0.513	2.4%
		2	0.0279	0.0763	0.8336		0.030	0.1%	0.682	3.2%
		3	0.0226	0.0828	0.6202		0.016	0.1%	0.517	2.4%
		mean	0.0229	0.0643	0.7930		0.025	0.1%	0.571	2.7%
		stdev	0.0049	0.0267	0.1564		0.008	0.04%	0.097	0.5%

Table 5-2: Summary of Phosphorus Mineralization.

	Compost P Content (%)	Replicate	k_{min} (day^{-1})	RMSE (mg/g)	R^2	Total Mass (mg/g)	Initial Flush (mg/g)	Initial Flush (%)	Total Mineralized Mass (mg/g)	Total Mineralized Mass (%)
Field Compost	2.1050	1	0.0282	0.0444	0.9710	21.050	0.166	0.8%	0.931	4.4%
		2	0.0320	0.0562	0.8851		0.000	0.0%	0.567	2.7%
		3	0.0295	0.0524	0.8554		0.000	0.0%	0.488	2.3%
		mean	0.0299	0.0510	0.9038		0.055	0.3%	0.662	3.1%
		stdev	0.0019	0.0060	0.0601		0.096	0.5%	0.236	1.1%
Field Compost - Leached	1.7162	1	0.0197	0.0081	0.8893	17.162	0.001	0.01%	0.094	0.5%
		2	0.0259	0.0110	0.7598		0.003	0.02%	0.083	0.5%
		3	0.0333	0.0144	0.9478		0.026	0.1%	0.214	1.2%
		mean	0.0263	0.0112	0.8656		0.010	0.1%	0.130	0.8%
		stdev	0.0068	0.0031	0.0962		0.014	0.1%	0.073	0.4%
Greenhouse Compost	0.2733	1	0.0278	0.0066	0.9906	2.733	0.036	1.3%	0.240	8.8%
		2	0.0299	0.0178	0.8616		0.000	0.0%	0.168	6.1%
		3	0.0330	0.0202	0.8836		0.000	0.0%	0.200	7.3%
		mean	0.0302	0.0149	0.9119		0.012	0.4%	0.203	7.4%
		stdev	0.0026	0.0072	0.0690		0.021	0.8%	0.036	1.3%
Greenhouse Compost - Leached	0.2224	1	0.0183	0.0176	0.7885	2.224	0.004	0.2%	0.150	6.7%
		2	0.0234	0.0136	0.7173		0.002	0.1%	0.098	4.4%
		3	0.0226	0.0140	0.4359		0.000	0.0%	0.067	3.0%
		mean	0.0214	0.0151	0.6472		0.002	0.1%	0.105	4.7%
		stdev	0.0027	0.0022	0.1864		0.002	0.1%	0.042	1.9%

Table 5-3: Summary of Nitrogen Release.

	Compost N Content (%)	Replicate	K_{min} (day^{-1})	RMSE (mg/g)	R^2	Total Mass (mg/g)	Initial Flush (mg/g)	Initial Flush (%)	Total Released Mass (mg/g)	Total Released Mass (%)
Field Compost	3.2523	1	0.1920	0.0698	0.9771	32.523	1.424	4.4%	1.805	5.5%
		2	0.1430	0.0646	0.9903		1.425	4.4%	2.102	6.5%
		3	0.1410	0.0641	0.9907		1.440	4.4%	2.133	6.6%
		mean	0.1587	0.0662	0.9860		1.430	4.4%	2.013	6.2%
		stdev	0.0289	0.0031	0.0077		0.009	0.03%	0.181	0.6%
Field Compost - Leached	2.4685	1	0.0307	0.0545	0.9442	24.685	0.050	0.2%	0.882	3.6%
		2	0.0355	0.0732	0.9315		0.102	0.4%	0.949	3.8%
		3	0.0516	0.0669	0.9662		0.179	0.7%	1.209	4.9%
		mean	0.0393	0.0649	0.9473		0.110	0.4%	1.013	4.1%
		stdev	0.0109	0.0095	0.0176		0.065	0.3%	0.173	0.7%
Greenhouse Compost	2.4917	1	0.2100	0.2153	0.9667	24.917	3.718	14.9%	4.944	19.8%
		2	0.0910	0.2129	0.9400		1.741	7.0%	2.783	11.2%
		3	0.1180	0.1956	0.9679		2.300	9.2%	3.493	14.0%
		mean	0.1397	0.2079	0.9582		2.586	10.4%	3.740	15.0%
		stdev	0.0624	0.0108	0.0158		1.019	4.1%	1.102	4.4%
Greenhouse Compost - Leached	2.1290	1	0.0224	0.0544	0.8803	21.290	0.025	0.1%	0.655	3.1%
		2	0.0291	0.0691	0.9589		0.029	0.1%	0.654	3.1%
		3	0.0268	0.0911	0.4936		0.013	0.1%	0.521	2.4%
		mean	0.0261	0.0715	0.7776		0.022	0.1%	0.610	2.9%
		stdev	0.0034	0.0185	0.2491		0.008	0.04%	0.077	0.4%

Table 5-4: Summary of Phosphorus Release.

	Compost P Content (%)	Replicate	K_{min} (day^{-1})	RMSE (mg/g)	R^2	Total Mass (mg/g)	Initial Flush (mg/g)	Initial Flush (%)	Total Released Mass (mg/g)	Total Released Mass (%)
Field Compost	2.1050	1	0.0300	0.0543	0.9724	21.050	0.223	1.1%	1.149	5.5%
		2	0.0409	0.0215	0.9914		0.161	0.8%	0.755	3.6%
		3	0.0366	0.0237	0.9826		0.119	0.6%	0.603	2.9%
		mean	0.0358	0.0331	0.9821		0.167	0.8%	0.836	4.0%
		stdev	0.0055	0.0184	0.0095		0.052	0.2%	0.282	1.3%
Field Compost - Leached	1.7162	1	0.0225	0.0126	0.8486	17.162	0.002	0.01%	0.124	0.7%
		2	0.0260	0.0074	0.8233		0.004	0.02%	0.066	0.4%
		3	0.0343	0.0133	0.9546		0.026	0.2%	0.211	1.2%
		mean	0.0276	0.0111	0.8755		0.011	0.1%	0.133	0.8%
		stdev	0.0061	0.0032	0.0696		0.014	0.1%	0.073	0.4%
Greenhouse Compost	0.2733	1	0.0300	0.0073	0.9927	2.733	0.047	1.7%	0.297	10.9%
		2	0.0450	0.0057	0.9946		0.069	2.5%	0.252	9.2%
		3	0.0420	0.0083	0.9875		0.049	1.8%	0.242	8.8%
		mean	0.0390	0.0071	0.9916		0.055	2.0%	0.264	9.6%
		stdev	0.0079	0.0013	0.0037		0.012	0.4%	0.029	1.1%
Greenhouse Compost - Leached	0.2224	1	0.0211	0.0219	0.7777	2.224	0.005	0.2%	0.180	8.1%
		2	0.0237	0.0122	0.7453		0.003	0.1%	0.093	4.2%
		3	0.0222	0.0109	0.6506		0.003	0.1%	0.070	3.2%
		mean	0.0223	0.0150	0.7245		0.004	0.2%	0.114	5.1%
		stdev	0.0013	0.0060	0.0660		0.001	0.07%	0.058	2.6%

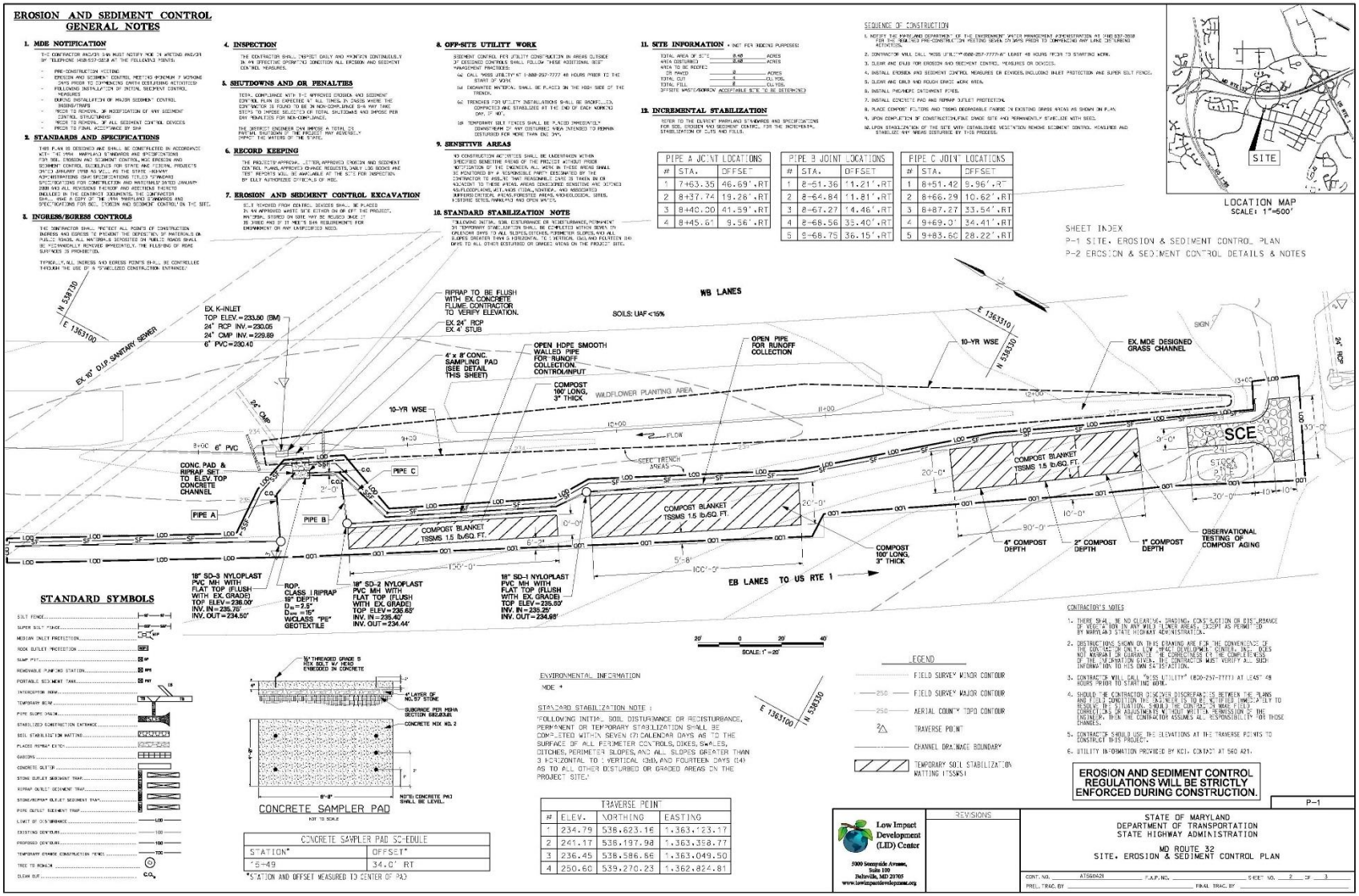


Figure 5-8: Field Site VCB Design Plan Page 1.

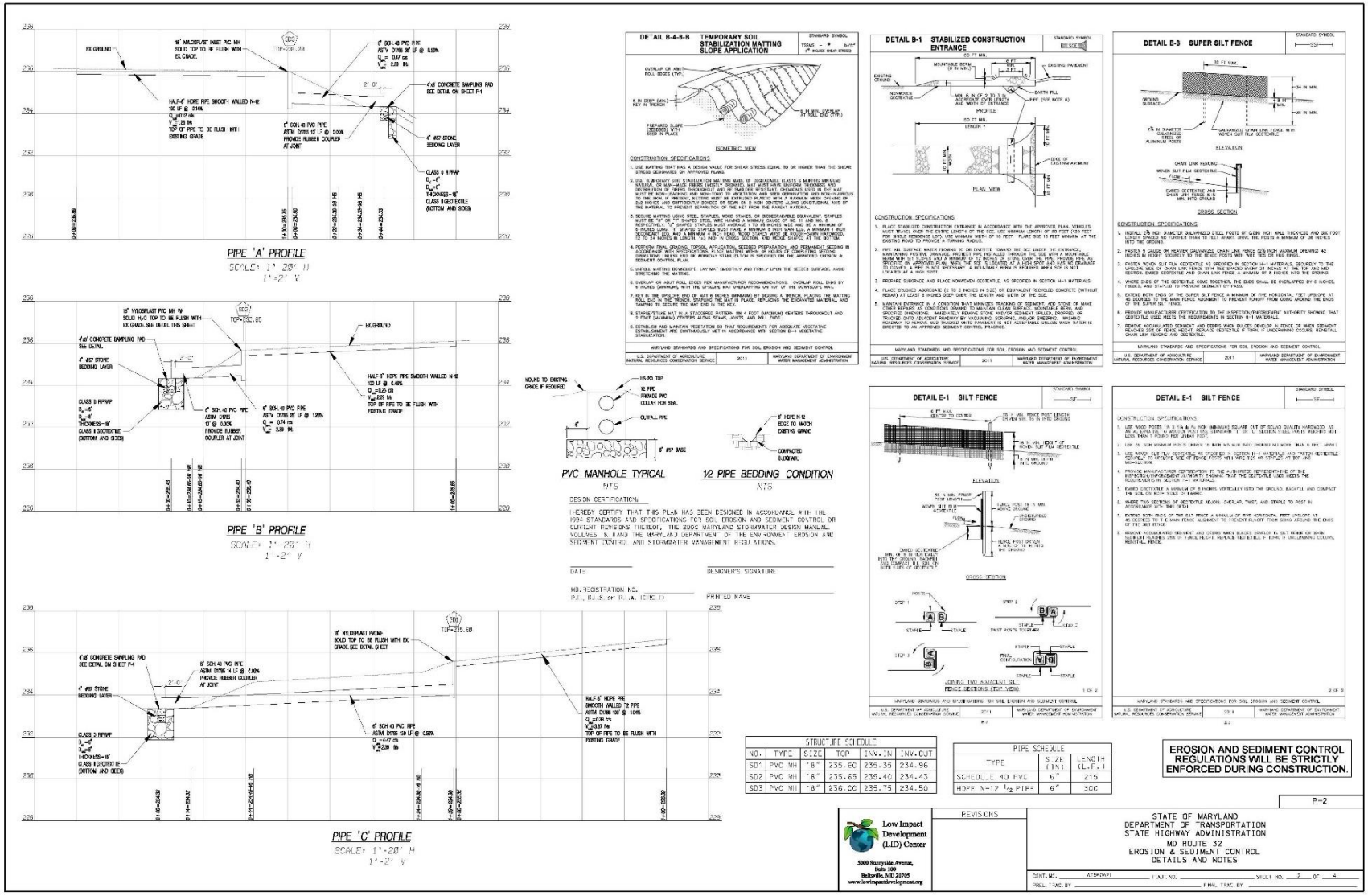


Figure 5-9: Field Site VCB Design Plan Page 2.

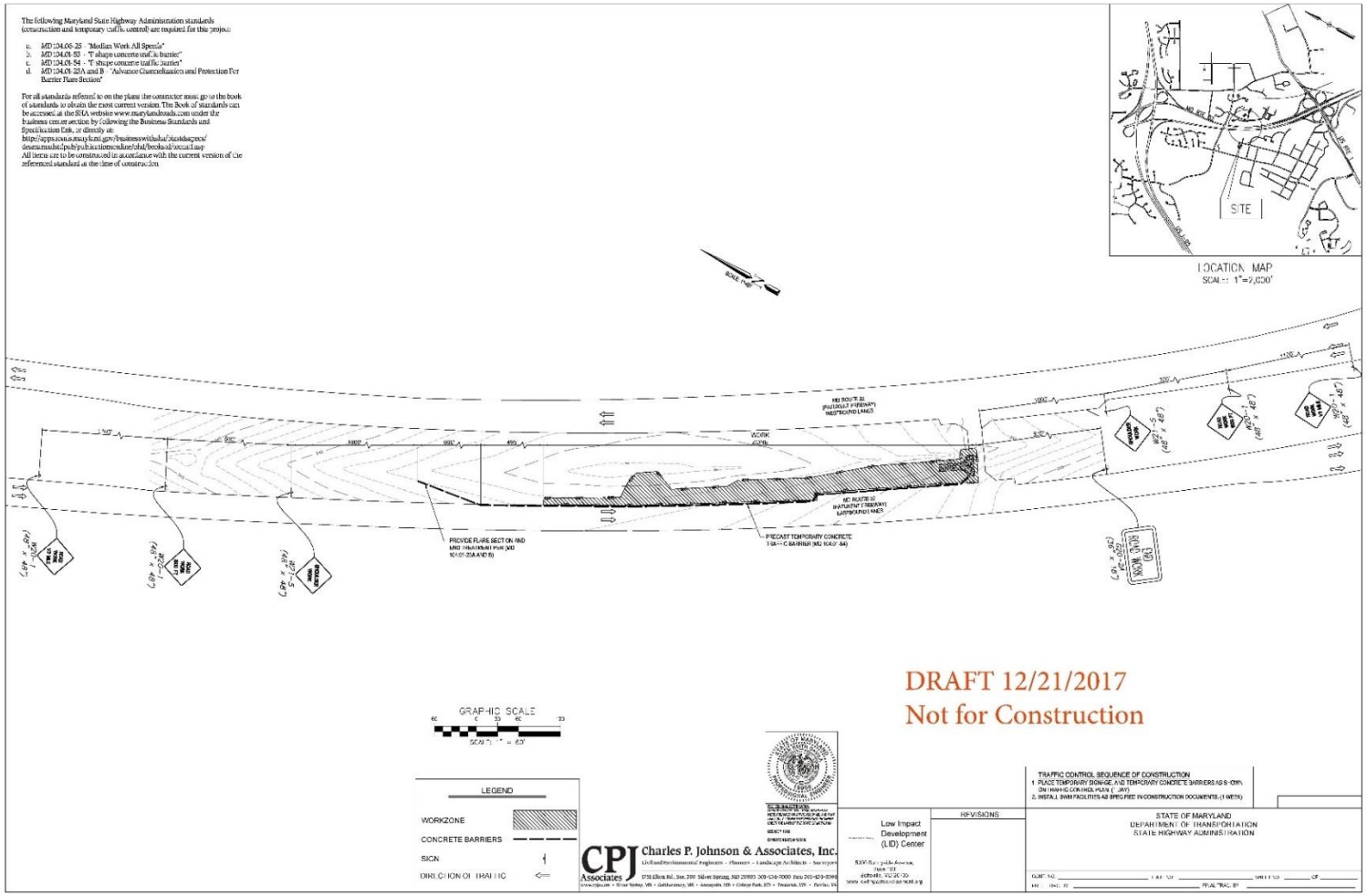


Figure 5-10: Field Site VCB Design Plan Page 3.

REFERENCES

AASHTO. 2010. “Standard Practice for Compost for Erosion/Sediment Control (Compost Blankets) AASHTO Designation: R 52-10.” American Association of State Highway and Transportation Officials (AASHTO).

Abood, M. M., B. Yusuf, T. A. Mohammed, and H. Ghazali. 2006. “Manning Roughness Coefficient for Grass-Lined Channel.” 13 (4): 14.

Ahmad, Z., S. Yamamoto, and T. Honna. 2008. “Leachability and Phytoavailability of Nitrogen, Phosphorus, and Potassium from Different Bio-Composts Under Chloride- and Sulfate-Dominated Irrigation Water.” *J. Environ. Qual.*, 37 (3): 1288–1298. https://doi.org/10.2134/jeq2007.0414.

Al-Bataina, B. B., T. M. Young, and E. Ranieri. 2016. “Effects of Compost Age on the Release of Nutrients.” *International Soil and Water Conservation Research*, 4 (3): 230–236. https://doi.org/10.1016/j.iswcr.2016.07.003.

Alikhani, J., C. Nietch, S. Jacobs, B. Shuster, and A. Massoudieh. 2020. “Modeling and Design Scenario Analysis of Long-Term Monitored Bioretention System for Rainfall-Runoff Reduction to Combined Sewer in Cincinnati, OH.” *Journal of Sustainable Water in the Built Environment*, 6 (2): 04019016. American Society of Civil Engineers. https://doi.org/10.1061/JSWBAY.0000903.

Almadani, M., and A. Massoudieh. 2018. “Evaluation of Catchment-Scale Efficiency of Green Infrastructure in an Urban Watershed through Process-Based Modeling.” *AGU Fall Meeting Abstracts*, 51.

Alshameri, A., H. He, J. Zhu, Y. Xi, R. Zhu, L. Ma, and Q. Tao. 2018. “Adsorption of ammonium by different natural clay minerals: Characterization, kinetics and adsorption isotherms.” *Applied Clay Science*, Small Size – Big Science: The 3rd Asian Clay Conference, 159: 83–93. https://doi.org/10.1016/j.clay.2017.11.007.

Amlinger, F., B. Götz, P. Dreher, J. Geszti, and C. Weissteiner. 2003. “Nitrogen in biowaste and yard waste compost: dynamics of mobilisation and availability—a review.” *European Journal of Soil Biology*, A collection of application-related papers from the conference “Microbiology of Composting,” 39 (3): 107–116. https://doi.org/10.1016/S1164-5563(03)00026-8.

Arash Massoudieh, M. Maghrebi, B. Kamrani, C. Nietch, M. Tryby, S. Aflaki, and S. Panguluri. 2017. “A flexible modeling framework for hydraulic and water quality performance assessment of stormwater green infrastructure.” *Environmental Modelling & Software*, 92: 57–73. https://doi.org/10.1016/j.envsoft.2017.02.013.

Bacys, M., U. Khan, J. Sharma, and T. R. Bentzen. 2018. “An evaluation of global bioretention cell design guidelines.” 20: 17987.

Bakr, N., D. C. Weindorf, Y. Zhu, A. E. Arceneaux, and H. M. Selim. 2012. “Evaluation of compost/mulch as highway embankment erosion control in Louisiana at the plot-scale.” *Journal of Hydrology*, 468–469 (Supplement C): 257–267. https://doi.org/10.1016/j.jhydrol.2012.08.040.

Barrett, M. E., P. M. Freeze, J. F. Malina, and R. J. Charbeneau. 1998. “Performance of Vegetative Controls for Treating Highway Runoff.” *Journal of Environmental Engineering*, 124 (11): 1121–1128. https://doi.org/10.1061/(ASCE)0733-9372(1998)124:11(1121).

Beighley, R. E., B. Scholl, L. B. Faucette, and J. Governo. 2010. “Runoff Characteristics for Construction Site Erosion Control Practices.” *J. Irrig. Drain Eng.*, 136 (6): 405–413. https://doi.org/10.1061/(ASCE)IR.1943-4774.0000202.

Bhattarai, R., P. K. Kalita, S. Yatsu, H. R. Howard, and N. G. Svendsen. 2011. “Evaluation of compost blankets for erosion control from disturbed lands.” *Journal of Environmental Management*, 92 (3): 803–812.

Bilotta, G. S., and R. E. Brazier. 2008. “Understanding the influence of suspended solids on water quality and aquatic biota.” *Water Research*, 42 (12): 2849–2861. https://doi.org/10.1016/j.watres.2008.03.018.

Bingham, A. H., and M. F. Cotrufo. 2016. “Organic nitrogen storage in mineral soil: Implications for policy and management.” *Science of The Total Environment*, 551–552: 116–126. https://doi.org/10.1016/j.scitotenv.2016.02.020.

Blanco-Canqui, H., C. J. Gantzer, S. H. Anderson, E. E. Alberts, and A. L. Thompson. 2004. “Grass Barrier and Vegetative Filter Strip Effectiveness in Reducing Runoff, Sediment, Nitrogen, and Phosphorus Loss.” *Soil Sci. Soc. Am. J.*, 68 (5): 1670–1678. https://doi.org/10.2136/sssaj2004.1670.

Boger, A. R., L. Ahiablame, E. Mosase, and D. Beck. 2018. “Effectiveness of roadside vegetated filter strips and swales at treating roadway runoff: a tutorial review.” *Environmental Science: Water Research & Technology*, 4 (4): 478–486. Royal Society of Chemistry. https://doi.org/10.1039/C7EW00230K.

Bouwman, A. F. 1998. “Nitrogen oxides and tropical agriculture.” *Nature*, 392 (6679): 866–867. https://doi.org/10.1038/31809.

Brown, J. N., and B. M. Peake. 2006. “Sources of heavy metals and polycyclic aromatic hydrocarbons in urban stormwater runoff.” *Science of The Total Environment*, 359 (1): 145–155. https://doi.org/10.1016/j.scitotenv.2005.05.016.

Brown, S., A. Corfman, K. Mendrey, K. Kurtz, and F. Grothkopp. 2016. “Stormwater Bioretention Systems: Testing the Phosphorus Saturation Index and Compost Feedstocks as Predictive Tools for System Performance.” *J. Environ. Qual.*, 45 (1): 98–106. https://doi.org/10.2134/jeq2014.10.0414.

Butler, J. S., and F. J. Coale. 2005. “Phosphorus Leaching in Manure-Amended Atlantic Coastal Plain Soils.” *J. Environ. Qual.*, 34 (1): 370–381.

Caltrans. 2012. *Stormwater Infiltration Relative to Hydrologic Soil Group, Compost, and Vegetation*. Roadside Erosion Control and Management Study. Final Report. The State of California, Department of Transportation (Caltrans).

Carpenter, S. R., N. F. Caraco, D. L. Correll, R. W. Howarth, A. N. Sharpley, and V. H. Smith. 1998. “Nonpoint Pollution of Surface Waters with Phosphorus and Nitrogen.” *Ecological Applications*, 8 (3): 559–568. https://doi.org/10.1890/1051-0761(1998)008[0559:NPOSWW]2.0.CO;2.

Chaganti, V. N., and D. M. Crohn. 2014. “Evaluation of compost blankets for erosion control and runoff water quality on a constructed hillslope in Southern California.” *Transactions of the ASABE, American Society of Agricultural and Biological Engineer*, 57: 403–416. https://doi.org/10.13031/trans.57.10199.

Chahal, M. K., Z. Shi, and M. Flury. 2016. “Nutrient leaching and copper speciation in compost-amended bioretention systems.” *Science of The Total Environment*, 556: 302–309. https://doi.org/10.1016/j.scitotenv.2016.02.125.

Chaves, B., S. De Neve, G. Hofman, P. Boeckx, and O. Van Cleemput. 2004. “Nitrogen mineralization of vegetable root residues and green manures as related to their (bio)chemical composition.” *European Journal of Agronomy*, 21 (2): 161–170. https://doi.org/10.1016/j.eja.2003.07.001.

Chow, V. T. 1959. *Open-channel Hydraulics*. Blackburn Press.

Coduto, D., M. Yeung, and W. Kitch. 2011. *Geotechnical Engineering: Principles and Practices*.

Collins, K. A., T. J. Lawrence, E. K. Stander, R. J. Jontos, S. S. Kaushal, T. A. Newcomer, N. B. Grimm, and M. L. Cole Ekberg. 2010. “Opportunities and challenges for managing nitrogen in urban stormwater: A review and synthesis.” *Ecological Engineering*, Managing Denitrification in Human Dominated Landscapes, 36 (11): 1507–1519. https://doi.org/10.1016/j.ecoleng.2010.03.015.

Colton, J., C. Greyall, R. Jack, and D. Lester. 2014. *Metals Release Related to Compost Use in Bioretention Technologies: Summary of Preliminary Literature Review*. 41. King County Science and Technical Support Section. Seattle WA: King County Department of Natural Resources and Parks.

Confesor Jr, R. B., J. M. Hamlett, R. D. Shannon, and R. E. Graves. 2009. “Potential Pollutants from Farm, Food and Yard Waste Composts at Differing Ages: Leaching Potential of Nutrients Under Column Experiments. Part II.” *Compost Science & Utilization*, 17 (1): 6–17. https://doi.org/10.1080/1065657X.2009.10702394.

Conley, D. J., H. W. Paerl, R. W. Howarth, D. F. Boesch, S. P. Seitzinger, K. E. Havens, C. Lancelot, and G. E. Likens. 2009. “Controlling Eutrophication: Nitrogen and Phosphorus.” *Science*, 323 (5917): 1014–1015. American Association for the Advancement of Science. https://doi.org/10.1126/science.1167755.

Cook, L. M., S. McGinnis, and C. Samaras. 2020. “The effect of modeling choices on updating intensity-duration-frequency curves and stormwater infrastructure designs for climate change.” *Climatic Change*, 159 (2): 289–308. https://doi.org/10.1007/s10584-019-02649-6.

Copeland, C. 2016. *Green Infrastructure and Issues in Managing Urban Stormwater*. 29. CRS Report, Prepared for Members and Committees of Congress. Washington D.C.: Congressional Research Service.

Coutts, C., and M. Hahn. 2015. “Green Infrastructure, Ecosystem Services, and Human Health.” *International Journal of Environmental Research and Public Health*, 12 (8): 9768–9798. Multidisciplinary Digital Publishing Institute. https://doi.org/10.3390/ijerph120809768.

Crohn, D. 2004. “Nitrogen Mineralization and its Importance in Organic Waste Recycling.” *Proceedings, National Alfalfa Symposium*. San Diego, CA: UC Cooperative Extension, University of California, Davis 95616.

Curtis, M. J., D. E. Rider, A. Fristensky, and V. P. Claassen. 2009. “Cumulative Sediment, Nitrogen and Phosphorus Losses From Bare And Compost Amended Fill Slopes.” *Compost Science & Utilization*, 17 (1): 25–30. https://doi.org/10.1080/1065657X.2009.10702396.

CVC and TRCA. 2010. “Low Impact Development Stormwater Management Planning and Design Guide 4.6 Vegetated Filter Strips.” Credit Valley Conservation (CVC) and Toronto and Region Conservation Authority (TRCA).

Data Services Division’s Traffic Monitoring System (TMS). 2020. “Traffic Volume Maps.” Traffic Volume Maps. Howard County, MD: MD DOT SHA.

Davis, A. P. 2007. “Field Performance of Bioretention: Water Quality.” *Environmental Engineering Science*, 24 (8): 1048–1064. https://doi.org/10.1089/ees.2006.0190.
Davis, A. P., and R. H. McCuen (Eds.). 2005a. “Water Quality Parameters.” *Stormwater Management for Smart Growth*, 12–36. Boston, MA: Springer US.
Davis, A. P., and R. H. McCuen (Eds.). 2005b. “Stormwater Quality.” *Stormwater Management for Smart Growth*, 131–173. Boston, MA: Springer US.
Davis, A. P., M. Shokouhian, and S. Ni. 2001. “Loading Estimates of Lead, Copper, Cadmium, and Zinc in Urban Runoff from Specific Sources.” *Chemosphere*, 44 (5): 997–1009. https://doi.org/10.1016/S0045-6535(00)00561-0.
Davis, A. P., J. H. Stagge, E. Jamil, and H. Kim. 2012a. “Hydraulic performance of grass swales for managing highway runoff.” *Water Research*, Special Issue on Stormwater in urban areas, 46 (20): 6775–6786. https://doi.org/10.1016/j.watres.2011.10.017.
Davis, A. P., R. G. Traver, and W. F. Hunt. 2010. “Improving Urban Stormwater Quality: Applying Fundamental Principles.” *Journal of Contemporary Water Research & Education*, 146 (1): 3–10. https://doi.org/10.1111/j.1936-704X.2010.00387.x.
Davis, A. P., R. G. Traver, W. F. Hunt, R. Lee, R. A. Brown, and J. M. Olszewski. 2012b. “Hydrologic Performance of Bioretention Storm-Water Control Measures.” *Journal of Hydrologic Engineering*, 17 (5): 604–614. https://doi.org/10.1061/(ASCE)HE.1943-5584.0000467.
Deletic, A. 1998. “The first flush load of urban surface runoff.” *Water Research*, 32 (8): 2462–2470. https://doi.org/10.1016/S0043-1354(97)00470-3.
Deletic, A., and T. D. Fletcher. 2006. “Performance of grass filters used for stormwater treatment—a field and modelling study.” *Journal of Hydrology*, 317 (3): 261–275. https://doi.org/10.1016/j.jhydrol.2005.05.021.
Diaz, L. F., M. de Bertoldi, and W. Bidlingmaier. 2007. *Compost Science and Technology*. Elsevier.
Dietz, M. E. 2007. “Low Impact Development Practices: A Review of Current Research and Recommendations for Future Directions.” *Water Air Soil Pollut*, 186: 351–363. https://doi.org/10.1007/s11270-007-9484-z.
Djukić, A., B. Lekić, V. Rajaković-Ognjanović, D. Veljović, T. Vulić, M. Djolić, Z. Naunovic, J. Despotović, and D. Prodanović. 2016. “Further insight into the mechanism of heavy metals partitioning in stormwater runoff.” *Journal of Environmental Management*, 168: 104–110. https://doi.org/10.1016/j.jenvman.2015.11.035.
Dunne, N. (Ed.). 2013. *Easy Compost*. Brooklyn, NY: Brooklyn Botanic Garden.
Duzgun, A. O., M. Hatipoglu, and A. H. Aydilek. 2021. “Shear and Hydraulic Properties of Compost-Amended Topsoils for Use on Highway Slopes.” *Journal of Materials in Civil Engineering*, 33 (8): 04021192. American Society of Civil Engineers. https://doi.org/10.1061/(ASCE)MT.1943-5533.0003797.
Eghball, B. 2003. “Leaching of Phosphorus Fractions Following Manure or Compost Application.” *COMMUN SOIL SCI PLANT ANAL*, 34 (19 & 20): 2803–2815. https://doi.org/DOI: 10.1081/CSS-120025207.
van Es, H. M., C. B. Ogden, R. L. Hill, R. R. Schindelbeck, and T. Tsegaye. 1999. “Integrated Assessment of Space, Time, and Management-Related Variability of Soil Hydraulic Properties.” *Soil Science Society of America Journal*, 63 (6): 1599–1608. https://doi.org/10.2136/sssaj1999.6361599x.

Fassman-Beck, E., W. Hunt, R. Berghage, D. Carpenter, T. Kurtz, V. Stovin, and B. Wadzuk. 2016. "Curve Number and Runoff Coefficients for Extensive Living Roofs." *Journal of Hydrologic Engineering*, 21 (3): 04015073. American Society of Civil Engineers. https://doi.org/10.1061/(ASCE)HE.1943-5584.0001318.

Faucette, B. 2008. "Performance and Design for Compost Erosion Control and Compost Storm Water Blankets." *Proceedings of the EC-08*. Orlando, FL.

Faucette, B., and M. Risse. 2002. "Controlling Erosion with Compost and Mulch." *BioCycle*, June 2002.

Faucette, L. B., J. Governo, C. F. Jordan, B. G. Lockaby, H. F. Carino, and R. Governo. 2007. "Erosion control and storm water quality from straw with PAM, mulch, and compost blankets of varying particle sizes." *Journal of Soil and Water Conservation*, 62 (6): 404–413.

Faucette, L. B., J. Governo, R. Tyler, C. F. Gigley, and B. G. Lockaby. 2009a. "Performance of Compost Filter Socks and Conventional Sediment Control Barriers Used for Perimeter Control on Construction Sites." *Journal of Soil and Water Conservation*, 64 (1): 81–88. https://doi.org/10.2489/jswc.64.1.81.

Faucette, L. B., C. F. Jordan, L. M. Risse, M. Cabrera, D. C. Coleman, and L. T. West. 2005. "Evaluation of stormwater from compost and conventional erosion control practices in construction activities." *Journal of Soil and Water Conservation*, 60 (6): 288–297.

Faucette, L. B., L. M. Risse, M. A. Nearing, J. W. Gaskin, and L. T. West. 2004. "Runoff, erosion, and nutrient losses from compost and mulch blankets under simulated rainfall." *Journal of Soil and Water Conservation*, 59 (4): 154–160.

Faucette, L. B., B. Scholl, R. E. Beighley, and J. Governo. 2009b. "Large-scale performance and design for construction activity erosion control best management practices." *J. Environ. Qual.*, 38 (3): 1248–1254. https://doi.org/10.2134/jeq2008.0415.

Fay, L., M. Akin, and X. Shi. 2012. *Cost-Effective and Sustainable Road Slope Stabilization and Erosion Control*. Washington, D.C.: Transportation Research Board of the National Academies.

FHWA. 2014. "Office of Highway Policy Information - Highway Finance Data Collection." *U.S. Department of Transportation Federal Highway Administration*. Accessed March 17, 2020. https://www.fhwa.dot.gov/policyinformation/pubs/hf/pl11028/chapter1.cfm.

Finney, K. A., B. Gharabaghi, E. McBean, R. P. Rudra, and G. MacMillan. 2010. "Compost Biofilters For Highway Stormwater Runoff Treatment." *Water Quality Research Journal of Canada*, 45 (4): 391–402.

Flint, K. R., and A. P. Davis. 2007. "Pollutant Mass Flushing Characterization of Highway Stormwater Runoff from an Ultra-Urban Area." *Journal of Environmental Engineering*, 133 (6): 616–626. https://doi.org/10.1061/(ASCE)0733-9372(2007)133:6(616).

Foster, J., A. Lowe, and S. Winkelman. 2011. *The Value of Green Infrastructure for Urban Climate Adaptation*. 1–52. The Center for Clean Air Policy.

Fu, Z., F. Wu, K. Song, Y. Lin, Y. Bai, Y. Zhu, and J. P. Giesy. 2013. "Competitive interaction between soil-derived humic acid and phosphate on goethite." *Applied Geochemistry*, 36: 125–131. https://doi.org/10.1016/j.apgeochem.2013.05.015.

van Genuchten, M. Th. 1980. "A Closed-form Equation for Predicting the Hydraulic Conductivity of Unsaturated Soils." *Soil Science Society of America Journal*, 44 (5): 892–898. https://doi.org/10.2136/sssaj1980.03615995004400050002x.

Gérard, F. 2016. “Clay minerals, iron/aluminum oxides, and their contribution to phosphate sorption in soils — A myth revisited.” *Geoderma*, 262: 213–226. https://doi.org/10.1016/j.geoderma.2015.08.036.

Gharabaghi, B., R. Rudra, and P. Goel. 2006. “Effectiveness of Vegetative Filter Strips in Removal of Sediments from Overland Flow.” *Water Quality Research Journal of Canada*, 41. https://doi.org/10.2166/wqrj.2006.031.

Glanville, T. D., T. L. Richard, and R. A. Persyn. 2003. “Impacts of Compost Blankets on Erosion Control, Revegetation, and Water Quality at Highway Construction Sites in Iowa.” Agricultural and Biosystems Engineering Technical Reports and White Papers.

Govindaraju, R. S., S. E. Jones, and M. L. Kavvas. 1985. “Modeling of Overland Flow by the Diffusion Wave Approach.” Kentucky Water Resources Research Institute, University of Kentucky. https://doi.org/10.13023/KWRRI.RR.159.

Goyne, K. W., H.-J. Jun, S. H. Anderson, and P. P. Motavalli. 2008. “Phosphorus and Nitrogen Sorption to Soils in the Presence of Poultry Litter-Derived Dissolved Organic Matter.” *Journal of Environmental Quality; Madison*, 37 (1): 154–63.

Guedes, R. S., A. R. Fernandes, E. S. de Souza, and J. R. R. e Silva. 2015. “Maximum Phosphorus Adsorption Capacity Adjusted to Isotherm Models in Representative Soils of Eastern Amazon.” *Communications in Soil Science and Plant Analysis*, 46 (20): 2615–2627. Taylor & Francis. https://doi.org/10.1080/00103624.2015.1089264.

Han, J., J. S. Wu, and C. Allan. 2005. “Suspended Sediment Removal by Vegetative Filter Strip Treating Highway Runoff.” *Journal of Environmental Science and Health, Part A*, 40 (8): 1637–1649. Taylor & Francis. https://doi.org/10.1081/ESE-200060683.

Han, Y. H., S. L. Lau, M. Kayhanian, and M. K. Stenstrom. 2006. “Correlation analysis among highway stormwater pollutants and characteristics.” *Water Science and Technology*, 53 (2): 235–243. https://doi.org/10.2166/wst.2006.057.

Harper, D. 2012. *Eutrophication of Freshwaters: Principles, problems and restoration*. Springer Science & Business Media.

Hendricks, M. D. 2017. “The Infrastructures of Equity and Environmental Justice.” Thesis.

Hendricks, M. D., and S. Van Zandt. 2021. “Unequal Protection Revisited: Planning for Environmental Justice, Hazard Vulnerability, and Critical Infrastructure in Communities of Color.” *Environmental Justice*, 14 (2): 87–97. Mary Ann Liebert, Inc., publishers. https://doi.org/10.1089/env.2020.0054.

Herrera Environmental Consultants, Inc. 2015. *City of Redmond Six Swales Bioretention Monitoring*. 1122. Final Report. Redmond, WA: City of Redmond Public Works Natural Resources Division.

Higgins, C., Z. Liu, R. Stewart, R. Kelley, and S. Drake. 2016. *Design Guide For Roadside Infiltration Strips In Western Oregon*. Final Report. Oregon State University: Oregon Department of Transportation and Federal Highway Administration.

Hsieh, C., A. P. Davis, and B. A. Needelman. 2007. “Bioretention Column Studies of Phosphorus Removal from Urban Stormwater Runoff.” *Water Environment Research*, 79 (2): 177–184. https://doi.org/10.2175/106143006X111745.

Hua, L., Y. Wang, W. Wu, M. B. McBride, and Y. Chen. 2008. “Biomass and Cu and Zn Uptake of Two Turfgrass Species Grown in Sludge Compost–soil Mixtures.” *Water Air Soil Pollut*, 188 (1): 225–234. https://doi.org/10.1007/s11270-007-9539-1.

Hurley, S., P. Shrestha, and A. Cording. 2017. “Nutrient Leaching from Compost: Implications for Bioretention and Other Green Stormwater Infrastructure.” *Journal of Sustainable*

Water in the Built Environment, 3 (3): 04017006. https://doi.org/10.1061/JSWBAY.0000821.

Hyland, C., Q. Ketterings, D. Dewing, K. Stockin, K. Czymmek, G. Albrecht, and L. Geohring. 2005. "Agronomy Fact Sheet Series Fact Sheet 12: Phosphorus Basics - The Phosphorus Cycle." Cornell University Cooperative Extension.

Iqbal, H., M. Garcia-Perez, and M. Flury. 2015. "Effect of Biochar on Leaching of Organic Carbon, Nitrogen, and Phosphorus from Compost in Bioretention Systems." *Science of The Total Environment*, 521–522 (Supplement C): 37–45. https://doi.org/10.1016/j.scitotenv.2015.03.060.

Jaffe, M., M. Zellner, E. Minor, M. Gonzalez-Meler, L. Bucci Cotner, D. Massey, H. Ahmed, M. Elberts, H. Sprague, S. Wise, and B. Miller. 2010. *The Illinois Green Infrastructure Study*. A Report to the Illinois Environmental Protecton Agency on the Criteria in Section 15 of Public Act 96-0026, The Illinois Green Infrastructure for Clean Water Act of 2009. Illinois: University of Illinois at Chicago, Chicago Metropolitan Agency for Planning, Center for Neighborhood Technology, University of Illinois at Urbana-Champaign.

Kaiser, K., and W. Zech. 2000. "Sorption of dissolved organic nitrogen by acid subsoil horizons and individual mineral phases." *European Journal of Soil Science*, 51 (3): 403–411. https://doi.org/10.1046/j.1365-2389.2000.00320.x.

Kayhanian, M., A. Singh, C. Suverkropp, and S. Borroum. 2003. "Impact of Annual Average Daily Traffic on Highway Runoff Pollutant Concentrations." *Journal of Environmental Engineering-asce - J ENVIRON ENG-ASCE*, 129. https://doi.org/10.1061/(ASCE)0733-9372(2003)129:11(975).

Kayhanian, M., C. Suverkropp, A. Ruby, and K. Tsay. 2007. "Characterization and Prediction of Highway Runoff Constituent Event Mean Concentration." *Journal of Environmental Management*, 85: 279–295. https://doi.org/10.1016/j.jenvman.2006.09.024.

Khaleel, R., K. Reddy, and M. Overcash. 1981. "Changes in Soil Physical Properties Due to Organic Waste Applications: A Review." *J ENVIRON QUAL*, 10: 133–141. https://doi.org/10.2134/jeq1981.00472425001000020002x.

Khan, E., S. Khaodhir, and D. Ruangrote. 2009. "Effects of moisture content and initial pH in composting process on heavy metal removal characteristics of grass clipping compost used for stormwater filtration." *Bioresource Technology*, 100 (19): 4454–4461. https://doi.org/10.1016/j.biortech.2008.12.062.

Khorsha, G. 2016. "Management of Ammoniacal Nitrogen in Stormwater Runoff." https://doi.org/10.13016/M2M533.

Khorsha, G., and A. Davis. 2016. "Characterizing Clinoptilolite Zeolite and Hydroaluminosilicate Aggregates for Ammonium Removal from Stormwater Runoff." *Journal of Environmental Engineering*, 143: 04016082. https://doi.org/10.1061/(ASCE)EE.1943-7870.0001167.

Khorsha, G., and A. Davis. 2017. "Ammonium Removal from Synthetic Stormwater using Clinoptilolite and Hydroaluminosilicate Columns."

Khorsha, G., B. Kjellerup, and A. Davis. 2021. "Characterizing Laboratory-Scale Clinoptilolite bio-columns for Removal and Nitrification of Ammoniacal Nitrogen in Simulated Stormwater." *Water environment research : a research publication of the Water Environment Federation*. https://doi.org/10.1002/wer.1589.

Kirchhoff, C. J., J. F. Malina, and M. Barrett. 2003. *Characteristics of Composts : Moisture Holding and Water Quality Improvement*. 159. Research Report. Austin, TX: Texas Department of Transportation.

Klute, A. 1965. "Water Capacity." *Methods of Soil Analysis*, 273–278. John Wiley & Sons, Ltd.

Knight, E. M. P., W. F. Hunt, and R. J. Winston. 2013. "Side-by-side evaluation of four level spreader–vegetated filter strips and a swale in eastern North Carolina." *Journal of Soil and Water Conservation*, 68 (1): 60–72. Soil and Water Conservation Society. https://doi.org/10.2489/jswc.68.1.60.

Komlos, J., and R. G. Traver. 2012. "Long-Term Orthophosphate Removal in a Field-Scale Storm-Water Bioinfiltration Rain Garden." *Journal of Environmental Engineering*, 138 (10): 991–998. https://doi.org/10.1061/(ASCE)EE.1943-7870.0000566.

Konrad, C. P. 2003. "USGS Fact Sheet FS-076-03 Effects of Urban Development on Floods." U.S. Geological Survey - Water Resources.

Kothawala, D. N., and T. R. Moore. 2009. "Adsorption of dissolved nitrogen by forest mineral soils." *Canadian Journal of Forest Research*, 39 (12): 2381–2390. Canadian Science Publishing. https://doi.org/10.1139/X09-147.

Kraus, H. T., R. L. Mikkelsen, and S. L. Warren. 2000. "Container Substrate Temperatures Affect Mineralization of Composts." *HortScience*, 35 (1): 16–18. American Society for Horticultural Science. https://doi.org/10.21273/HORTSCI.35.1.16.

Kreeb, L. B. 2003. "Hydrologic efficiency and design sensitivity of bioretention facilities." Honor's Research. University of Maryland (College Park, Md.).

Lange, K., H. Österlund, M. Viklander, and G.-T. Blecken. 2020. "Metal speciation in stormwater bioretention: Removal of particulate, colloidal and truly dissolved metals." *Science of The Total Environment*, 724: 138121. https://doi.org/10.1016/j.scitotenv.2020.138121.

Lee, J. H., K. W. Bang, L. H. Ketchum, J. S. Choe, and M. J. Yu. 2002. "First flush analysis of urban storm runoff." *Science of The Total Environment*, 293 (1): 163–175. https://doi.org/10.1016/S0048-9697(02)00006-2.

Lee, J. Y., H. Kim, Y. Kim, and M. Y. Han. 2011. "Characteristics of the Event Mean Concentration (EMC) from Rainfall Runoff on an Urban Highway." *Environmental Pollution*, 159 (4): 884–888. https://doi.org/10.1016/j.envpol.2010.12.022.

Li, J., and A. P. Davis. 2016. "A unified look at phosphorus treatment using bioretention." *Water Research*, 90: 141–155. https://doi.org/10.1016/j.watres.2015.12.015.

Li, L., and A. P. Davis. 2014. "Urban Stormwater Runoff Nitrogen Composition and Fate in Bioretention Systems." *Environ. Sci. Technol.*, 48 (6): 3403–3410. https://doi.org/10.1021/es4055302.

Li, M.-H., and M. E. Barrett. 2008. "Relationship Between Antecedent Dry Period and Highway Pollutant: Conceptual Models of Buildup and Removal Processes." *Water Environment Research*, 80 (8): 740–747. https://doi.org/10.2175/106143008X296451.

Li, M.-H., C. Sung, M. Kim, and K.-H. Chu. 2011. "Assessing Performance of Bioretention Boxes in Hot and Semiarid Regions." *Transportation Research Record: Journal of the Transportation Research Board*, 2262: 155–163. https://doi.org/10.3141/2262-15.

Lim, H. S., W. Lim, J. Y. Hu, A. Ziegler, and S. L. Ong. 2015. "Comparison of filter media materials for heavy metal removal from urban stormwater runoff using biofiltration systems." *Journal of Environmental Management*, 147: 24–33. https://doi.org/10.1016/j.jenvman.2014.04.042.

Liu, C., and K. Lo. 2001a. “Ammonia Removal from Compost Leachate Using Zeolite. II. a Study Using Continuous Flow Packed Columns.” *Journal of Environmental Science & Health, Part B -- Pesticides, Food Contaminants, & Agricultural Wastes*, 36 (5): 667–675. https://doi.org/10.1081/PFC-100106193.

Liu, C.-H., and K. V. Lo. 2001b. “Ammonia Removal from Composting Leachate Using Zeolite. I. Characterization of the Zeolite.” *Journal of Environmental Science and Health, Part A*, 36 (9): 1671–1688. Taylor & Francis. https://doi.org/10.1081/ESE-100106251.

Liu, J. 2014. “Field Evaluation of Enhanced Phosphorus and Nitrogen Removal in Stormwater Control Measures.” https://doi.org/10.13016/M2PP61.

Liu, J., and A. P. Davis. 2014. “Phosphorus Speciation and Treatment Using Enhanced Phosphorus Removal Bioretention.” *Environ. Sci. Technol.*, 48 (1): 607–614. https://doi.org/10.1021/es404022b.

Liu, Y., M. Xu, G. Li, M. Wang, Z. Li, and H. J. De Boeck. 2021. “Changes of Aboveground and Belowground Biomass Allocation in Four Dominant Grassland Species Across a Precipitation Gradient.” *Frontiers in Plant Science*, 12: 609. https://doi.org/10.3389/fpls.2021.650802.

Lussem, U., A. Bolten, J. Menne, M. L. Gnyp, J. Schellberg, and G. Bareth. 2019. “Estimating biomass in temperate grassland with high resolution canopy surface models from UAV-based RGB images and vegetation indices.” *JARS*, 13 (3): 034525. SPIE. https://doi.org/10.1117/1.JRS.13.034525.

Ma, Y., P. Egodawatta, J. McGree, A. Liu, and A. Goonetilleke. 2016. “Human health risk assessment of heavy metals in urban stormwater.” *Science of The Total Environment*, 557–558: 764–772. https://doi.org/10.1016/j.scitotenv.2016.03.067.

Magette, W., R. Brinsfield, R. Palmer, and J. D. Wood. 1989. “Nutrient and Sediment Removal by Vegetated Filter Strips.” https://doi.org/10.13031/2013.31054.

Maluf, H. J. G. M., C. A. Silva, N. Curi, L. D. Norton, S. D. Rosa, H. J. G. M. Maluf, C. A. Silva, N. Curi, L. D. Norton, and S. D. Rosa. 2018. “Adsorption and availability of phosphorus in response to humic acid rates in soils limed with CaCO3 or MgCO3.” *Ciência e Agrotecnologia*, 42 (1): 7–20. Editora UFLA. https://doi.org/10.1590/1413-70542018421014518.

Maniquiz-Redillas, M., and L.-H. Kim. 2014. “Fractionation of heavy metals in runoff and discharge of a stormwater management system and its implications for treatment.” *Journal of Environmental Sciences*, 26 (6): 1214–1222. https://doi.org/10.1016/S1001-0742(13)60591-4.

Mariano, E., D. L. Jones, P. W. Hill, and P. C. O. Trivelin. 2016. “Mineralisation and sorption of dissolved organic nitrogen compounds in litter and soil from sugarcane fields.” *Soil Biology and Biochemistry*, 103: 522–532. https://doi.org/10.1016/j.soilbio.2016.10.004.

MDOT. 2021. “Maryland Hits Milestones Across Transportation Network as Highway, Airport and Port Numbers Approach Pre-Pandemic Levels - MDOT.” Accessed October 29, 2021. https://mdot.maryland.gov/tso/pages/newsroomdetails.aspx?newsId=543&PageId=38.

MDOT SHA. 2020. “Standard Specifications for Construction and Materials.” Maryland Department of Transportation (MDOT).

Minnesota Stormwater Manual contributors. 2021. “Total Suspended Solids (TSS) in stormwater - Minnesota Stormwater Manual.” Accessed October 31, 2021.

https://stormwater.pca.state.mn.us/index.php/Total_Suspended_Solids_(TSS)_in_stormwater.
Miranda, L. S., B. Wijesiri, G. A. Ayoko, P. Egodawatta, and A. Goonetilleke. 2021. "Water-sediment interactions and mobility of heavy metals in aquatic environments." *Water Research*, 202: 117386. https://doi.org/10.1016/j.watres.2021.117386.
Moore, T. L., J. S. Gulliver, L. Stack, and M. H. Simpson. 2016. "Stormwater management and climate change: vulnerability and capacity for adaptation in urban and suburban contexts." *Climatic Change*, 138 (3): 491–504. https://doi.org/10.1007/s10584-016-1766-2.
Mualem, Y. 1976. "A new model for predicting the hydraulic conductivity of unsaturated porous media." *Water Resources Research*, 12 (3): 513–522. https://doi.org/10.1029/WR012i003p00513.
Mukhtar, S. 2005. "Using Compost for Erosion Control and Revegetation." Texas A&M AgriLife Communications.
Mukhtar, S., M. L. McFarland, and C. A. Wagner. 2008. "Runoff and Water Quality from Inorganic Fertilizer and Erosion Control Compost Treatments on Roadway Sideslopes." *Transactions of the ASABE, American Society of Agricultural and Biological Engineer*, 51: 927–936. https://doi.org/10.13031/2013.24531.
Mullane, J. M., M. Flury, H. Iqbal, P. M. Freeze, C. Hinman, C. G. Cogger, and Z. Shi. 2015. "Intermittent Rainstorms Cause Pulses of Nitrogen, Phosphorus, and Copper in Leachate from Compost in Bioretention Systems." *Sci. Total Environ.*, 537: 294–303. https://doi.org/10.1016/j.scitotenv.2015.07.157.
National Research Council. 2009. *Urban Stormwater Management in the United States*. Washington, D.C.: National Academies Press (U.S.).
Nosshi, M. I., J. Butler, and M. J. Trlica. 2007. "Soil nitrogen mineralization not affected by grass species traits." *Soil Biology and Biochemistry*, 39 (5): 1031–1039. https://doi.org/10.1016/j.soilbio.2006.11.013.
NRCS. 1986. "Urban Hydrology for Small Watersheds."
O'Driscoll, M., S. Clinton, A. Jefferson, A. Manda, and S. McMillan. 2010. "Urbanization Effects on Watershed Hydrology and In-Stream Processes in the Southern United States." *Water*, 2 (3): 605–648. Molecular Diversity Preservation International. https://doi.org/10.3390/w2030605.
Ogden, C. B., H. M. van Es, and R. R. Schindelbeck. 1997. "Miniature Rain Simulator for Field Measurement of Soil Infiltration." *Soil Science Society of America Journal*, 61 (4): 1041–1043. https://doi.org/10.2136/sssaj1997.03615995006100040008x.
Olszewski, J., and A. Davis. 2012. "Comparing the Hydrologic Performance of a Bioretention Cell with Predevelopment Values." *Journal of Irrigation and Drainage Engineering*, 139: 124–130. https://doi.org/10.1061/(ASCE)IR.1943-4774.0000504.
Owen, D. C., M. T. Bensi, A. P. Davis, and A. H. Aydilek. 2020. "Measuring soil coverage using image feature descriptors and the decision tree learning algorithm." *Biosystems Engineering*, 196: 112–126. https://doi.org/10.1016/j.biosystemseng.2020.06.002.
Pamuru, S. T., E. Forgione, K. Croft, B. V. Kjellerup, and A. P. Davis. 2021. "Chemical characterization of urban stormwater: Traditional and emerging contaminants." *Sci Total Environ*, 151887. https://doi.org/10.1016/j.scitotenv.2021.151887.
Pan, C., and Z. Shangguan. 2006. "Runoff hydraulic characteristics and sediment generation in sloped grassplots under simulated rainfall conditions." *Journal of Hydrology*, Water

Resources in Regional Development: The Okavango River, 331 (1): 178–185. https://doi.org/10.1016/j.jhydrol.2006.05.011.
Persyn, R., T. Glanville, T. Richard, J. Laflen, and P. Dixon. 2004. "Environmental Effects of Applying Composted Organics to New Highway Embankments: Part 1. Interrill Runoff and Erosion." *Agricultural and Biosystems Engineering Publications*, 47 (2): 463–469.
Persyn, R., T. Richard, T. Glanville, J. Laflen, and P. Dixon. 2007. "Evaluation of Revegetation from Blanket Applied Composts on a Highway Construction Site." *Agricultural and Biosystems Engineering Publications*, 23 (5): 631–635.
Pitt, R., A. Maestre, and J. Clary. 2018. "The National Stormwater Quality Database (NSQD), Version 4.02." bmpdatabase.org.
Reed, S., D. Shinde, K. Konomi, K. Jayachandran, P. Nkedi-Kizza, and M. Reza Savabi. 2006. "Phosphorus Leaching Potential from Compost Amendments in a Carbonatic Soil." *Soil Science*, 171: 865–873. https://doi.org/10.1097/01.ss.0000228057.00463.48.
RK&K. 2020. "COVID-19 Traffic Impacts Observations and Considerations for a Path Forward." PDH Presentation.
Rovira, P., and V. R. Vallejo. 2002. "Labile and recalcitrant pools of carbon and nitrogen in organic matter decomposing at different depths in soil: an acid hydrolysis approach." *Geoderma*, 107 (1): 109–141. https://doi.org/10.1016/S0016-7061(01)00143-4.
Rožić, M., Š. Cerjan-Stefanović, S. Kurajica, V. Vančina, and E. Hodžić. 2000. "Ammoniacal nitrogen removal from water by treatment with clays and zeolites." *Water Research*, 34 (14): 3675–3681. https://doi.org/10.1016/S0043-1354(00)00113-5.
Rynk, R. 1992. *On-Farm Composting Handbook*. NRAES. Ithaca, N.Y.: Northeast Regional Agricultural Engineering Service, Cooperative Extension.
Sansalone, J. J., and S. G. Buchberger. 1997. "Partitioning and First Flush of Metals in Urban Roadway Storm Water." *Journal of Environmental Engineering*, 123 (2): 134–143. American Society of Civil Engineers. https://doi.org/10.1061/(ASCE)0733-9372(1997)123:2(134).
Sansalone, J. J., S. G. Buchberger, and S. R. Al-Abed. 1996. "Fractionation of heavy metals in pavement runoff." *Science of The Total Environment*, 189–190: 371–378. https://doi.org/10.1016/0048-9697(96)05233-3.
Seelsaen, N., R. McLaughlan, S. Moore, and R. M. Stuetz. 2007. "Influence of compost characteristics on heavy metal sorption from synthetic stormwater." *Water Sci. Technol.*, 55 (4): 219–226.
Spohn, M., and Y. Kuzyakov. 2013. "Phosphorus mineralization can be driven by microbial need for carbon." *Soil Biology and Biochemistry*, 61: 69–75. https://doi.org/10.1016/j.soilbio.2013.02.013.
Stagge, J. H., A. P. Davis, E. Jamil, and H. Kim. 2012. "Performance of grass swales for improving water quality from highway runoff." *Water Research*, Special Issue on Stormwater in urban areas, 46 (20): 6731–6742. https://doi.org/10.1016/j.watres.2012.02.037.
Storey, B. B., A. B. R. Desai, M.-H. Li, H. C. Landphair, and T. Kramer. 2006. *Water Quality Characteristics and Performance of Compost Filter Berms*. Technical Report. Texas Transportation Institute.
Strickland, M. S., C. Lauber, N. Fierer, and M. A. Bradford. 2009. "Testing the functional significance of microbial community composition." *Ecology*, 90 (2): 441–451. https://doi.org/10.1890/08-0296.1.

Taylor, K. G., and P. N. Owens. 2009. “Sediments in urban river basins: a review of sediment–contaminant dynamics in an environmental system conditioned by human activities.” *J Soils Sediments*, 9 (4): 281–303. https://doi.org/10.1007/s11368-009-0103-z.

Termorshuizen, A., S. Moolenaar, A. Veeken, and W. J. Blok. 2004. “The value of compost.” *Re-views in Environmental Science & Bio-technology 3 (2004) 4*, 3. https://doi.org/10.1007/s11157-004-2333-2.

The Northeast Coordinating Committee for Soil Testing. 2011. “Recommended Soil Testing Procedures for the Northeastern United States | Cooperative Extension | University of Delaware.” *Recommended Soil Testing Procedures for the Northeastern United States*. Accessed August 9, 2022. https://www.udel.edu/academics/colleges/canr/cooperative-extension/fact-sheets/soil-testing-procedures-northeastern-US/.

Theng, B. K. G. 1972. “Adsorption of Ammonium and Some Primary n -Alkylammonium Cations by Soil Allophane.” *Nature*, 238 (5360): 150–151. https://doi.org/10.1038/238150a0.

Trautmann, N., and M. Krasny. 2014. “Composting in the Classroom: Scientific Inquiry for High School Students.”

TRB. 2006. *Evaluation of Best Management Practices for Highway Runoff Control*. National Cooperative Highway Research Program. Washington, D.C.: Transportation Research Board of the National Academies of Science.

Trimble, S. W. 1997. “Contribution of Stream Channel Erosion to Sediment Yield from an Urbanizing Watershed.” *Science*, 278 (5342): 1442–1444. American Association for the Advancement of Science. https://doi.org/10.1126/science.278.5342.1442.

University of Idaho College of Natural Resources. 2009. “Principles of Vegetation Measurement & Assessment and Ecological Monitoring & Analysis: Direct Measures of Biomass.” *Principles of Vegetation Measurement & Assessment and Ecological Monitoring & Analysis*. Accessed November 29, 2021. https://www.webpages.uidaho.edu/veg_measure/Modules/Lessons/Module%207(Biomass&Utilization)/7_3_Direct%20Methods.htm.

US EPA. 2012. “Stormwater Best Management Practice: Compost Blankets.” *EPA: Office of Water: NPDES*. Accessed December 8, 2017. https://www3.epa.gov/npdes/pubs/compostblankets.pdf.

US EPA. 2013. “Ecoregional Nutrient Criteria for Rivers and Streams.” Data and Tools. Accessed December 19, 2021. https://www.epa.gov/nutrient-policy-data/ecoregional-nutrient-criteria-rivers-and-streams.

US EPA. 2015a. “National Recommended Water Quality Criteria - Aquatic Life Criteria Table.” Data and Tools. Accessed December 22, 2021. https://www.epa.gov/wqc/national-recommended-water-quality-criteria-aquatic-life-criteria-table.

US EPA. 2015b. “NPDES Stormwater Program.” *US EPA*. Overviews and Factsheets. Accessed February 20, 2020. https://www.epa.gov/npdes/npdes-stormwater-program.

USCC. 2001a. “USCC Factsheet: Compost & Its Benefits.” The United States Composting Council.

USCC. 2001b. “Field Guide to Compost Use.” The US Composting Council.

USCC. 2002. “The Test Method for the Examination of Composting and Compost (TMECC).” US Composting Council, Bethesda, MD.

USEPA. 2000. “Guidance for Data Quality Assessment EPA QA/G-9.” United States Environmental Protection Agency, Office of Water.

Voelkel, B., M. Marshall, A. Lund, A. Gobeli, and R. Lopez. 2018. *A Simple Method for Estimating Plant Biomass Used in Grazing Management*. College Station, TX: Texas A&M AgrilLife Research Extension with Texas A&M Natural Resources Institute.

Wang, H., J. Zhu, Q. Fu, C. Hong, H. Hu, and A. Violante. 2016. "Phosphate adsorption on uncoated and humic acid-coated iron oxides." *J Soils Sediments*, 16 (7): 1911–1920. https://doi.org/10.1007/s11368-016-1383-8.

Wang, Y., S. Liu, Z. Xu, T. Han, S. Chuan, and T. Zhu. 2006. "Ammonia removal from leachate solution using natural Chinese clinoptilolite." *Journal of Hazardous Materials*, 136 (3): 735–740. https://doi.org/10.1016/j.jhazmat.2006.01.002.

Winston, R. J., A. R. Anderson, and W. F. Hunt. 2017. "Modeling Sediment Reduction in Grass Swales and Vegetated Filter Strips Using Particle Settling Theory." *Journal of Environmental Engineering*, 143 (1): 04016075. American Society of Civil Engineers. https://doi.org/10.1061/(ASCE)EE.1943-7870.0001162.

Winston, R. J., W. F. Hunt, D. L. Osmond, W. G. Lord, and M. D. Woodward. 2011. "Field Evaluation of Four Level Spreader–Vegetative Filter Strips to Improve Urban Storm-Water Quality." *Journal of Irrigation and Drainage Engineering-ASCE*, 137 (3): 170–182. https://doi.org/10.1061/(ASCE)IR.1943-4774.0000173.

Xia, Y. P., P. J. Stoffella, Z. He, M. K. Zhang, D. V. Calvert, X. Yang, and S. B. Wilson. 2013. "Leaching Potential of Heavy Metals, Nitrogen, and Phosphate from Compost-Amended Media." *Compost Science & Utilization*, 15: 29–33. https://doi.org/10.1080/1065657X.2007.10702307.

Yan, Q., J. R. Bruce, and A. P. Allen. 2017. "Lab-Scale Column Studies for Enhanced Phosphorus Sorption from Synthetic Urban Stormwater Using Modified Bioretention Media." *Journal of Environmental Engineering*, 143 (1): 04016073. https://doi.org/10.1061/(ASCE)EE.1943-7870.0001159.

Yan, Q., A. P. Davis, and B. R. James. 2016. "Enhanced Organic Phosphorus Sorption from Urban Stormwater Using Modified Bioretention Media: Batch Studies." *Journal of Environmental Engineering*, 142 (4): 04016001. American Society of Civil Engineers. https://doi.org/10.1061/(ASCE)EE.1943-7870.0001073.

Yan, Q., B. R. James, and A. P. Davis. 2018. "Bioretention Media for Enhanced Permeability and Phosphorus Sorption from Synthetic Urban Stormwater." *Journal of Sustainable Water in the Built Environment*, 4 (1): 04017013. https://doi.org/10.1061/JSWBAY.0000836.

Yu, S. L., J.-T. Kuo, E. A. Fassman, and H. Pan. 2001. "Field Test of Grassed-Swale Performance in Removing Runoff Pollution." *Journal of Water Resources Planning and Management*, 127 (3): 168–171. American Society of Civil Engineers. https://doi.org/10.1061/(ASCE)0733-9496(2001)127:3(168).

Zaman, M., and S. X. Chang. 2004. "Substrate type, temperature, and moisture content affect gross and net N mineralization and nitrification rates in agroforestry systems." *Biol Fertil Soils*, 39 (4): 269–279. https://doi.org/10.1007/s00374-003-0716-0.

Zeitoun, M. M., and E.-S. E. Mehana. 2014. "Impact of Water Pollution with Heavy Metals on Fish Health: Overview and Updates." 14.

Zhang, M., A. Kumar, Y. Li, and D. Calvert. 2001. "Aluminum and Iron Fractions Affecting Phosphorus Solubility and Reactions in Selected Sandy Soils." *Soil Science*, 166: 940–948. https://doi.org/10.1097/00010694-200112000-00008.

Zotarelli, L., M. D. Dukes, C. C. Romero, and K. W. Migliaccio. 2009. “Step by Step Calculation of the Penman-Monteith Evapotranspiration (FAO-56 Method).” 10.